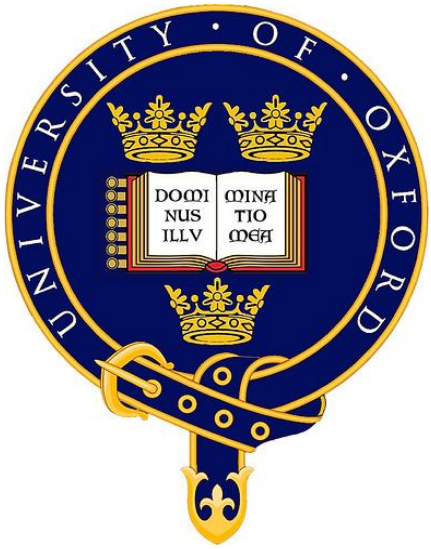

DEVELOPMENT AND ASSESSMENT OF PARTICULATE TRANSMISSION-BLOCKING MALARIA VACCINES

Thesis submitted for the degree of Doctor of Philosophy

Trinity Term 2014

Yuanyuan Li

Kellogg College

Word count: ~37,000 (excl. Abstract, Bibliography, Tables and Diagrams)

Development and assessment of particulate transmission-blocking malaria vaccines

Yuanyuan Li, Kellogg College, University of Oxford

Thesis submitted for the degree of Doctor of Philosophy, Trinity Term 2014

Abstract

Transmission-blocking vaccines (TBVs) target *Plasmodium* parasite sexual stages, aiming to block further development of the parasite within the mosquito host. *Plasmodium falciparum* zygote/ookinete surface protein Pfs25 is one of the leading TBV candidate antigens and antibodies against Pfs25 have been shown to exhibit complete transmission-blocking activity in pre-clinical studies. Phase 1 human clinical trials have revealed that Pfs25 was a poor immunogen in humans in the formulations tested and high titers of anti-Pfs25 antibodies are required to achieve good transmission-blocking activity in the *ex vivo* standard membrane feeding assay which measures the functional activity of the antibodies induced. Work in this thesis describes the production of recombinant monomeric Pfs25 protein, Pfs25 based particulate vaccines (Pfs25-IMX313 nanoparticle, Pfs25-HBsAg VLP and Pfs25-Qβ VLP) and a Pfs25-Pfs28 multivalent protein vaccine in the *Pichia pastoris* protein expression system. These proteins were tested in mice using protein-in-adjuvant formulations and their immunogenicity was assessed. Pfs25-IMX313 nanoparticle induced significantly higher anti-Pfs25 antibodies than monomeric Pfs25 and the antibodies had higher avidity and transmission-blocking activity. All of the candidate vaccines generated, except for Pfs25-HBsAg VLP, were immunogenic. The Pfs25-IMX313 nanoparticle induced the highest antibody response in mice followed by the Pfs25-Pfs28 multivalent protein and Pfs25-Qβ VLP.

Acknowledgements

Firstly, I would like to thank my supervisor Dr Sumi Biswas for her guidance, support and friendship throughout my DPhil study. Without her guidance and advices this thesis would not have been possible.

I would like to thank Prof. Adrian Hill for giving me the opportunity to work at the Jenner Institute under his co-supervision. His scientific inputs throughout my DPhil study have been greatly valued.

I would like to thank Dr Fergal Hill, Dr. Kazutoyo Miura, Prof Martin Bachmann and Dr Simon Draper for their collaboration and support in my research. Their advice has been invaluable.

A special thank you to the Jenner Institute transmission-blocking vaccine group members: Daria Nikolaeva, Darren Leneghan, Sara Zakutansky and Alex Fyfe for their constant advice and support (both scientific and emotional).

I would like to thank all the other members of the Jenner Institute for their help, in particular: Julie Furze, Jing Jin, Katharine Collins, Anita Milicic, Paulo Bettencourt, Federica Cappuccini, Pawan Dulal and Matthew Dicks.

Finally, I would like to thank my family for their support (both emotional and financial) to me (an international student) for this DPhil study in the University of Oxford. Without my family, I would not be where I am today.

Statements

Standard membrane feeding assay (SMFA) in this study was done in collaboration with the Malaria Vaccine Initiative (MVI) SMFA reference laboratory at the National Institute of Health, USA. The assay was performed by Dr. Kazutoyo Miura and his colleagues.

Conjugation of monomeric Pfs25 protein to bacterial phage Qβ virus-like particle (VLP) was done in collaboration with Prof. Martin Bachman's group in Zurich, Switzerland. Martin Bachman's group provided the Qβ –VLP and the chemical conjugation was performed by Dr Franziska Zabel.

Table of Contents

Abbreviations

aa	Amino acids
ACK	Ammonium chloride potassium
ADCI	Antibody-dependent cellular inhibition
AdHu5	Human adenovirus serotype 5
AF488	Alexa Fluor 488
AM	Adenoviral prime MVA boost regime
AP	Adenoviral prime protein boost regime
APC	Antigen presenting cells
BCG	Bacillus Calmette–Guérin
BCR	B cell receptor
C4bp	C4 binding protein
ChAd63	Chimpanzee adenovirus serotype 63
CSP	Circumsporozoite surface protein
CXCR	Chemokine receptor
DC	Dendritic cell
DLN	Draining lymph node
EBA	Erythrocyte-binding antigen
EBA175	Erythrocyte-binding antigen–175
E. coli	*Escherichia coli*
DFA	Direct feeding assay
DMFA	Direct membrane feeding assay
EGF	Epidermal growth factor
ELISA	Enzyme-linked immunosorbant assay
EPA	Exoprotein A
FasL	Fas ligand
FcR	Fc Receptor
FDC	Follicular dendritic cell
GC	Germinal Centre
GLMM	Generalized linear mixed models
GLURP	Glutamate-rich protein

GM-CSF	Granulocyte-macrophage colony-stimulating factor
GSK	Glaxo Smith Kline
HBV	Hepatitis B virus
HBcAg	Hepatitis B core antigen
HBsAg	Hepatitis B surface antigen
Hc4bp	Human C4bp
HIV	Human immunodeficiency virus
His-tag	Histidine-tag
HPV	Human papilloma virus
IRBC	Infected red blood cell
ID	Intra-dermal
IM	Intra-muscular
IV	Intra-venous
IFN	Interferon
Ig	Immunoglobulin
IL	Interleukin
Iu	Infectious units
kDa	Kilodalton
LN	Lymph node
LPS	Lipopolysaccharide
mAb	Monoclonal antibody
MHC	Major histocompatibility complex
MPL	Monophosphoryl lipid A
MSP	Merozoite surface protein
MVA	Modified vaccinia virus Ankara
NLR	NOD-like receptors
OD	Optical density
OMPC	Outer-membrane protein complex
OVA	Ovalbumin
PAMP	Pathogen associated molecular patterns
PBS	Phosphate buffered saline

PCR	Polymerase chain reaction
Pfu	Plaque forming units
PMA	phorbol-12-myristate-13-acetate
PRR	Pattern recognition receptors
PP	Protein prime-boost regime
RBC	Red blood cell
RESA	Ring-infected erythrocyte surface antigen
RLR	Rig-I-like receptor
SEC	Size-exclusion chromatography
SHM	Somatic hyper mutation
SMFA	Standard membrane feeding assay
TB	Tuberculosis
TCR	T-cell Receptor
T_{FH}	T-follicular helper cell
TBV	Transmission-blocking vaccine
Th	T helper cell
TLR	Toll-like receptor
TNF	Tumour necrosis factor
VLP	Virus-like particle
v/v	Volume to volume
WGCF	Wheat germ cell-free

Chapter 1

Introduction

1. Introduction

1.1 Vaccine

Vaccines have been developed to prevent and control many infectious diseases and are one of the most cost effective interventions for public health. Introduction of a vaccine has successfully contributed to the elimination of smallpox [1]. Vaccines are also used to control infectious diseases such as polio [2], measles [3] and tetanus [4]. A full list of vaccines licensed for immunization and distribution in the US is summarised in table 1.1 below. Although vaccines have been successfully developed for many diseases as showed in table 1.1, there is still an urgent need for highly effective vaccines against several other diseases such as human immunodeficiency virus (HIV), Tuberculosis (TB) and malaria all of which still cause major global morbidity and mortality.

Disease (vaccine target)	**Vaccine trade name**	**Vaccine contents**
Adenovirus associated acute respiratory disease	Not available (NA)	Live adenovirus type 4 and type 7
Anthrax	Biothrax	*Bacillus anthracis* antigen (PA) adsorbed on alum
Diphtheria and tetanus	DECAVAC, TENIVAC	Diphtheria and tetanus toxoids adsorbed on alum
Diphtheria, tetanus and pertussis	Infanrix, DAPTACEL, Adacel and Boostrix	Diphtheria and tetanus toxoids and pertussis antigens adsorbed on alum
Diphtheria, tetanus, pertussis and poliomyelitis	KINRIX	Diphtheria and tetanus toxoids, pertussis antigens and inactivated poliovirus adsorbed on alum
Diphtheria, tetanus, pertussis, hepatitis B and poliomyelitis	Pediarix	Diphtheria and tetanus toxoids, pertussis antigens, hepatitis B surface antigen (HBsAg) virus-like-particle (VLP) and inactivated

		poliovirus adsorbed on alum
Haemophilus influenza type b	PedvaxHIB	Capsular polysaccharide of *Haemophilus influenza* type b conjugated to an outer membrane protein complex (OMPC) of *Neisseria meningitidis* serogroup B
Haemophilus influenza type b	ActHIB, Hiberix	Capsular polysaccharide of *Haemophilus influenza* type b conjugated to tetanus toxoid
Haemophilus influenza type b and Hepatitis B	Comvax	Components from PedvaxHIB plus Recombivax HB
Hepatitis A	Havrix, VAQTA	In activated hepatitis A virus
Hepatitis A and Hepatitis B	Twinrix	Components from Havrix plus Engerix-B
Hepatits B	Recombivax HB, Engerix-B	HBsAg VLP
Human Papillomavirus	Gardasil	VLP of recombinant major capsid (L1) from Human Papillomavirus (HPV) types 6, 11, 16 and 18
Human Papillomavirus	Cervarix	VLP of recombinant L1 from HPV types 16 and 18
Influenza A H1N1 (2009)	NA	Inactivated, split viron of influenza A H1N1
Influenza A H5N1	NA	Inactivated, split viron of influenza A H5N1
Influenza A and B	Afluria, FluLaval, Fluarix, Fluvirin, Agriflu, Fluzone, Flucelvax, Flublok, Fluarix Quadrivalent, Fluzone Quadrivalent, FluLaval Quadrivalent	Inactivated, split viron of selected influenza A and influenza B strains
Influenza A and B	FluMist, FluMist Quadrivalent	Live, attenuated influenza A and influenza B virus of selected strains
Japanese Encephalitis Virus	Ixiaro, JE-Vax	Inactivated whole virus
Measles and mumps	M-M-Vax	Live, attenuated virus
Measles, mumps and rubella	M-M-R II, ProQuad	Live, attenuated virus
Meningococcal (Groups A, C, Y, and W-135)	Menveo	Oligosaccharides from *N. meningitidis* serogroup A, C, Y and

		W-135 conjugated to *Corynebacterium diphtheriae* CRM197 protein
Meningococcal (Groups A, C, Y, and W-135)	Menactra	Polysaccharides from *N. meningitidis* serogroup A, C, Y and W-135 conjugated to diphtheria toxoid
Meningococcal (Groups A, C, Y, and W-135)	Menomune-A/C/Y/W-135	Soluble polysaccharides from *N. meningitidis* serogroup A, C, Y and W-135
Meningococcal (Groups C and Y) and *Haemophilus influenza* type b	MenHibrix	Polysaccharides from *N. meningitidis* serogroup C and Y plus Capsular polysaccharide of Haemophilus influenza type b conjugated to tetanus toxoid
Pneumococcal infection	Pneumovax 23, Prevnar, Prevnar 13	Saccharides from capsular antigens of different *Streptococcus pneumoniae* serotypes conjugated to diphtheria CRM_{197} protein
Poliovirus	Poliovax, IPOL	Inactivated poliovirus
Rabies	Imovax, RabAvert	In activated virus
Rotavirus	ROTARIX, RotaTeq	Live, attenuated virus
Smallpox	ACAM2000	Live vaccinia virus
Tetanus	NA	Tetanus toxoids adsorbed on alum
Typhoid	Vivotif	Live, attenuated *Salmonella typhi* Ty21a
Typhoid	TYPHIM Vi	Capsular polysaccharide from *Salmonella enterica* serovar *Typhi, S typhi* Ty2 strain
Tuberculosis	BCG vaccine	Live attenuated *Mycobacterium bovis*
Varicella virus	Varivax	Live, attenuated varicella virus
Yellow fever	YF-Vax	Live, attenuated 17D-204 strain of yellow fever virus
Herpes zoster	Zostavax	Live, attenuated varicella-zoster virus

Table 1.1 List of vaccines licensed for immunization and distribution in the US. Adapted from [5].

1.2 Vaccine types

Early vaccines were mostly whole-organism vaccines which consisted of live attenuated and inactivated/killed microbes. These whole-organism vaccines resemble natural infectious microbes and thus induce the desired immune response. They have contributed to the elimination of smallpox, as well as the control of many other infectious diseases listed in table 1.1. The disadvantages of whole-organism vaccines are that: for live attenuated vaccine, it requires special storage conditions to keep organisms alive and there are concerns of attenuated pathogen mutating inside the host into a virulent strain; inactivated/killed vaccine on the other hand stimulates a weaker immune response and often requires boosters to create long-term immunity. Another type of vaccine that is well known is the toxoid vaccines such as diphtheria and tetanus vaccines. Toxoid vaccines target certain bacterial secreted toxins and the vaccine formulation is detoxified bacterial toxins that are purified from supernatants of culture medium.

As genomic sequencing and molecular technology advances, subunit vaccines have become a new focus. Unlike the whole-organism vaccines, subunit vaccines contain only purified antigenic parts of a pathogen such as essential protein(s) or polysaccharide(s), and as a result, are able to induce strong and specific host immune responses. These specific antigens can be directly isolated from pathogens such as the acellular pertussis vaccine which contains bacterial protein components including detoxified pertussis toxin, filamentous hemagglutinin, pertactin and fimbriae types 2 and 3 directly extracted and purified from cells and supernatants of culture medium [6]. For all polysaccharide based subunit vaccines, the polysaccharide antigens are directly isolated from bacterial culture medium. For most protein-based subunit vaccines, the protein antigens are manufactured

using recombinant DNA technology. Basically, a gene coding for the protein of interest is inserted into a producer cell. The target protein is expressed (either intracellularly or secreted) and the protein produced by this method is termed a recombinant protein. More and more vaccines under pre-clinical development utilize this method and are known as recombinant subunit vaccines; successful commercial recombinant subunit vaccines include recombinant hepatitis B vaccine [7] and human papillomavirus (HPV) vaccine [8] [9]. Instead of producing recombinant proteins, genetically engineered viruses carrying the genes coding for the antigen of interest can be used to deliver the coding sequence to the host cells where the antigen protein is expressed and displayed to host immune system. This type of vaccine is termed viral vectored subunit vaccines and several of these vaccines are now being tested in clinical trials [10]. Similarly, protein antigen sequences can be incorporated into a genetically engineered DNA plasmid with a strong viral promoter and used to vaccinate directly to host. This is known as a DNA subunit vaccine and several clinical trials have been conducted using this antigen delivery method [11].

1.3 Vaccine Immunology

In order for the host immune system to react to a vaccine and generate a vaccine-mediated immune response, both innate and adaptive immune systems need to be activated. Most of the vaccines that are licensed today mediate protection through the induction of immunoglobulin (Ig) G antibodies. Some diseases such as malaria, HIV and TB also require additional cellular immune response of T cells to mediate the clearance of the pathogen. Thus, depending on the disease, the aim is to induce the appropriate humoral and/or cellular immune response.

1.3.1 Innate immune system

The innate immune system is the first line of defence against invading pathogens, and it is also the first point of contact with the vaccine. Therefore, understanding the innate immune system is important for vaccine development.

One important role played by the innate immune system is pathogen clearance. This can be achieved either directly or indirectly by innate immune cells such as macrophages, natural killer (NK) cells, γδ T cells, mast cells, basophils and eosinophils. Macrophages can be found residing in most tissues. They phagocytose to clear potential bacterial pathogens and secrete cytokines to induce local inflammatory responses during which recruitment of other lymphocytes occurs. Mast cells, eosinophils and basophils protect the epithelial surfaces of the human body. These cells release histamine upon pathogen encounter, and are involved in the inflammatory response as well as the defence against parasites. NK cells are involved in cytotoxic killing of host cells that have their major histocompatibility complex (MHC) class 1 down-regulated due to viral infection [12]. γδ T cells are a subset of T cells that have more recently been well defined. Unlike most T cells that express the T-cell receptor (TCR) composed of αβ heterodimers, this subset of T cells express γδ composed TCR and shows very little TCR diversity. γδ T cells are particularly enriched at epithelial surfaces and some subsets of γδ T cells were shown to be antimicrobial via phagocytosis [13] while other subsets were shown to exhibit antitumor activity and respond to cellular stress [14]. The complement system forms part of the innate immune response and is involved in the clearance of pathogens. The complement system is present in most tissues of the human body and consists of a number of plasma proteins that initially exist as inactive precursors. When these inactivated plasma proteins encounter pathogens, they can be activated via

three pathways (the classical pathway (antibody binding to pathogen), the lectin pathway (mannose-binding lectin recognising pathogen's carbohydrate) and the alternative pathway (directly acting on microbial surfaces)) all of which trigger proteolytic reactions generating active forms of complement proteins. The activated complement system can induce an inflammatory response, promote phagocytosis via opsonisation as well as form a membrane attack complex leading to pathogen lysis and death [15].

Another important role of the innate immune system is antigen recognition and antigen presentation. Professional antigen presenting cells (APCs) such as dendritic cells (DCs) not only provide innate defence against invading pathogens by phagocytosis, but also display fragments of the internalised antigen on its MHC molecules and migrate to secondary lymphoid organs where they activate the adaptive immune response by presenting antigen to naïve T cells. The recognition of antigen by APC is through the interaction between the pathogen-associated molecular patterns (PAMPs) displayed on the surface of a pathogen and the pattern-recognition receptors (PRRs) expressed on APCs. To date, several PRRs expressed by DCs such as Toll-like receptors (TLRs), NOD-like receptors (NLRs), C-type lectin-like receptors (CLRs) and RIG-I-like receptors (RLRs) are well documented [16].

1.3.2 Adaptive immune system

During an infection, if the innate immune system fails to clear the pathogen, the adaptive immune system will be activated and create an antigen-specific, long lasting immune response. All vaccines purposely target the adaptive immune system.

B cells are responsible for producing antibodies which are a secreted form of B-cell receptor (BCR). Antibodies are able to circulate throughout the body in the blood and provide systemic humoral immunity. Naïve B cells can in general be divided into 3 subclasses: B-1 B

cells, marginal zone (MZ) B cells and follicular B cells. Both B-1 B cells and MZ B cells are non-circulating B cells resident in peritoneal and pleural cavities [17] or MZ of the spleen [18] respectively. They both spontaneously secrete natural antibodies with extensive polyreactivity and provide important protection in the early immune response [19]. Upon activation after encountering the antigen, both B-1 B cells and MZ B cells produce antibodies with low affinity and act in a T cell independent manner. In contrast, follicular B cells reside in primary lymphoid follicles of secondary lymphoid organs including lymph node (LN) and spleen. Activation of follicular B cells requires helps from follicular helper T (Tfh) cells [20] resulting in a follicular B cell clonal expansion and formation of germinal centres (GCs) at the edge of the T cell zone. In the GC, activated follicular B cells undergo somatic hyper mutation (SHM) with the help from Tfh cells (providing survival signals) and follicular dendritic cell (FDC) (sequestering antigens in the form of immune complexes for follicular B cell activation [21]) resulting in antibody affinity maturation and antibody isotype switch. After the GC reaction, follicular B cells differentiate into plasma B cells capable of producing class-switched antibody with high antigen affinity, and affinity matured memory B cells capable of mediating immune responses in the case of re-infection.

T cells, on the other hand, play a central role in cell-mediated immunity. T cells in general can be divided into 2 subclasses: CD4+ T cells and CD8+ T cells. CD4+ T cells do not usually exhibit cytotoxic effects but rather function to activate other cell types and produce cytokines to modulate host immune responses. CD4+ T cells can be further divided into T helper cell (Th) type 1, type 2, type 17 and T regulatory cells (Treg). Naïve CD4+ T cells differentiate into Th1 cells in the presence of interleukin (IL) 12 and interferon gamma (IFN-γ). Th1 cells are responsible for targeting intracellular infections such as viruses and

intracellular bacteria. Th1 cells function by producing interferon-γ, IL-2 and tumor necrosis factor (TNF-α), recruiting as well as activating macrophages and natural killer cells, promoting antibody isotype switching to IgG2a and IgG3 [22]. Differentiation into Th2 cells is stimulated by the presence of IL-4. Th2 T cells are believed to be responsible for targeting extracellular pathogens. Th2 cells function by secreting Interleukin (IL)-4, IL-5, IL-9 and IL-13 and recruit histamine-releasing cells as well as promoting antibody isotype switching to IgG1, IgG2b, IgA and IgE [22]. Th17 cells are differentiated in response to transforming growth factor beta (TGF-β), IL-6, IL-22 and IL-23 [23]. Th17 cells produce IL-17 which in turn induces the production of other cytokines including IL-6, granulocyte colony-stimulating factor (G-CSF), granulocyte macrophage colony-stimulating factor (GM-CSF), IL-1β, TGF-β, Tumor necrosis factor alpha (TNF-α) and several chemokines from host epithelial and stromal cells [24]. Through the production of cytokines and chemokines, the main immunological function of Th17 cells is believed to induce bone marrow expansion and local inflammatory response resulting in recruitment of mononuclear cells to sites of infection [24]. In addition, Th17 cells were shown to mediate the regression of tumors in mice [25] and were also known to associate with autoimmune pathologies [26]. Treg cells are a subset of CD4+ T cells that act as suppressors by producing the immunosuppressive cytokine TGF-β and IL-10. This suppressive function is important to maintain immune tolerance to self-antigens and prevent autoimmune diseases [27]. CD8+ T cells are cytotoxic effecter cells. They recognize virus-infected host cells via interaction between TCR and MHC class 1. After recognition, CD8+ T cells secrete pro-inflammatory cytokines IFN-γ and TNF-α and induce target cell death by releasing perforin and granzyme as well as through the activation of Fas ligand (FasL) which binds to the death receptor (Fas) on target cells [28].

1.4 Malaria

Malaria is caused by a protozoan parasite of the genus Plasmodium. It is a mosquito-borne disease endemic to the tropical and subtropical countries. The greatest burden of malaria is in Africa. It was estimated, in 2012, 3.4 billion of people were at risk of malaria. The estimated global cases of malaria were 207 million (80% of these malaria cases were from the Africa region) and the worldwide mortality from malaria in 2012 was estimated to be 627,000 according to the World Malaria Report [29]. Of the estimated global deaths, most occur in sub-Saharan Africa (90%) and in children under 5 years (77%). Malaria not only has an impact on the health of affected community, but also has a negative socioeconomic impact. In addition to the death toll, annual clinical malaria attacks create more than 800 million days of illness in Africa [30] which lead to a substantial slow down of economic growth in affected countries [31].

1.4.1 Malaria pathology

Malaria in humans can be caused by five *Plasmodium* species: *falciparum*, *vivax*, *ovale*, *malariae* and *knowlesi*. Among them, *Plasmodium falciparum* and *Plasmodium vivax* are the most common causes of human malaria. The common clinical sign of a malaria clinical attack involves a cyclical pattern of fevers and chills which synchronizes with the erythrocytic cycle of schizont rupture and release of a new generation of merozoites [32]. *P. falciparum* is the most deadly species. It is estimated that 90% of global malaria mortality is caused by *P. falciparum* [29]. *P. falciparum* is deadly because only *P. falciparum* infected red blood cells (iRBCs) can adhere to endothelial cells in small capillaries and post-capillary venules of specific organs such as the brain and lungs [33]. In addition, *P. falciparum* iRBCs can also bind to non-infected RBCs causing further blockage. This sequestration will cause

mechanical obstruction of blood flow and is associated with severe disease and complications (often leading to death in children) such as severe anaemia, respiratory distress or cerebral malaria and even multiple organ failure [34].

1.4.2 Life cycle of malaria

The malaria parasite life cycle involves two hosts: the human and the mosquito. The human is the host in which malaria spends the asexual stages (pre-erythrocytic stage and erythrocytic stage) of its life cycle; however, the mosquito is malaria's definitive host in which the parasite undergoes sexual reproduction. In general, the malaria life cycle can be divided into three stages.

Pre-erythrocytic stage (liver-stage): Malaria infection begins with the bite of an infected female *Anopheles* mosquito. Haploid sporozoites are released from the salivary glands of the mosquito when it takes a blood meal. The parasites quickly gains access to the host bloodstream during mosquito feeding, and are carried through the blood to the liver where they invade liver cells (hepatocytes). During the next 7-14 days, the sporozoites undergo differentiation and asexual replication within hepatocytes, resulting in tens of thousands of merozoites which are released at the end of hepatic development. For *P. vivax* and *P.ovale*, hypnozoites (latent stage of liver-stage parasite) can develop at this stage.

Erythrocytic stage (blood-stage): The merozoites released from infected hepatocytes invade red blood cells (RBCs). After invasion, the intracellular parasite undergoes morphological changes and develops first into a trophozoite, followed by a mature trophozoite and finally into a schizont. Each schizont stage parasite contains 16-32 newly formed merozoites which will eventually be released into the bloodstream to invade new RBCs. The length of the

erythrocytic cycle of invasion, replication and rupture varies between parasite species (usually 48 hours for *P.falciparum*). This stage is associated with malaria pathology.

Sexual stage (mosquito stage): During the erythrocytic stage, a subset of merozoites terminally differentiates into male and female gametocytes. These sexual forms of the parasite are taken up by a female *Anopheles* mosquito during a blood meal. These gametocytes fertilise to form a zygote inside the mosquito mid-gut. The zygote undergoes further differentiation into a mobile ookinete which traverses the mid-gut wall and encysts as an oocyst on the exterior of the gut wall. Within the oocyst, haploid sporozoites are formed via meiosis. Eventually, sporozoites are released and travel to the mosquito's salivary glands ready to infect a new host.

1.4.3 Natural acquired immunity against malaria

Residents of malaria endemic regions can develop naturally acquired immunity (NAI) against the parasite. The development of NAI is generally believed to be due to repeated exposure to malaria. As reviewed in [35], in area of intense transmission, this NAI can reduce the frequency of severe clinical attacks or mortality caused by *P.falciparum* in any age group beyond early childhood (defined as children under age of 5). Children under age of 5, especially those under 1 year of age, lack most NAI-mediated protection. The failure of younger children to develop strong NAI is likely due to lack of repeated exposure to the parasite. It could also be due to an innate difference in the way their acquired immune system handles malaria compared to other age groups. This age-dependant effect has been observed when following malaria-naïve Javanese migrants to Papua, where malaria is hyper- to holoendemic. The prevalence of *P. falciparum* parasitaemia was initially the same across different age groups; however after 18 to 24 months of residence, an age-dependent

pattern emerged. The prevalence of parasitemia decreased markedly with increasing age beyond 6-10 years [36]. This increasing protection as a function of age observed in Javanese migrants was quantitatively parallel to those found in local residents [37]. Although the underlying mechanism is unclear, NAI is strongly related to age. NAI also seems not to be the cumulative product of many years continuous exposure. In fact, a study following the same group of migrants identified four infections within a 24 month period as the threshold for developing NAI in adults [38].

NAI associated protection is believed to be mediated by antibodies against blood stage antigens such as the variant surface antigens (VSAs) that are present on the surface of infected red blood cells (iRBCs) [39]. *P. falciparum* erythrocyte membrane protein 1 (PfEMP1), as one of the most well documented VSAs, has been implicated as the key target of NAI induced antibodies [40]. PfEMP1 is known to be responsible for the adherence of iRBCs to host endothelial receptors as well as non-infected erythrocytes. Other VSAs including rifin [41] and STEVOR [42] are also documented and believed to be the target of NAI. In addition to VSAs, antigens expressed on merozoites are also targeted by NAI. Such antigens include apical membrane antigen (AMA-1) [43], merozoite surface protein 1 (MSP-1) [44], merozoite surface protein 3 (MSP-3) [45] and glutamate-rich protein (GLURP) [46].

1.4.4 Current malaria prevention and treatment

Anti-malaria drugs have long been in use (i.e. chloroquine); other malaria counter measures such as insecticide treated mosquito nets (ITN) (protective nets impregnated with insecticides for covering beds, living quarters, or even water containers), indoor residual spraying (IRS) (a process of spraying the inside of places of residence with insecticide to kill mosquitoes) have been introduced in some malaria affected regions. The rise of drug

resistant malaria [47] is becoming a serious issue. Although artemisinin-based combination therapies (ACTs) have been introduced to provide adequate cure rates and delay development of resistance, there have been many reports of the emergence of artemisinin resistance in *Plasmodium falciparum* [48]. In addition, there are still millions of people at risk of malaria who do not have access to ACTs or interventions such as ITN or IRS [29]. Other measures of controlling malaria are urgently needed and a malaria vaccine would provide a cost-effective way to control the disease.

1.5 *Plasmodium* vaccines

Candidate vaccines against *P. falciparum* have been extensively studied and tested in recent decades. Because of the complexity of the malaria parasite, vaccine development is a difficult task. According to World Health Organization (WHO) [14], there are over 20 subunit vaccine constructs currently being evaluated in clinical trials or are in advanced preclinical development. Most of these vaccines were developed to target *P. falciparum*.

Most *P. falciparum* vaccines are designed to target a specific parasite stage. Candidate vaccines are mainly directed towards preventing parasite initial invasion and/or reducing *P. falciparum* associated morbidity and mortality [49]. As a result, pre-erythrocytic and asexual blood stages malaria vaccines have received great attention as these vaccines can protect the individual from getting infected or experiencing severe disease symptoms. The concept of transmission-blocking vaccines (TBVs) has been introduced and has become of much greater interest recently with new long term goals of global malaria eradication. TBV target antigens expressed during the sexual stage of malaria life cycle and aim to block parasite transmission.

1.5.1 Pre-erythrocytic Vaccines

Pre-erythrocytic vaccines aim to induce sterile protection by targeting either sporozoites and/or infected hepatocytes.

It has been known for 40 years that protective immunity against the pre-erythrocytic stages could be induced by vaccinating volunteers with radiation-attenuated *P. falciparum* sporozoites [50]. Early studies demonstrated that multiple immunizations with a thousand infectious bites from mosquitoes carrying radiation-attenuated sporozoites were needed to achieve complete protection in 93% of volunteers against challenges; while this protection persisted for at least 42 weeks [51, 52]. This protection was achieved by vaccinating via infectious mosquito bites; however this method is not feasible for field vaccinations. An injectable metabolically active, non-replicating sporozoite vaccine (named PfSPZ) that meets the regulatory standards has been produced recently by a company called Sanaria [53]. The first clinical trial of PfSPZ was conducted in 80 adults [54]. In this trial, volunteers received up to 6 doses of PfSPZ vaccine (containing up to 1.35 $x10^5$ PfSPZ /dose) subcutaneously (SC) or Intradermally (ID). The vaccine was proved to be safe, and induced sporozoite-specific B cell and cytokine producing CD4+ T cell response. Interestingly no antigen-specific CD8+ T cell response was detected. Furthermore, only 2 out of 44 volunteers who received complete dose of vaccination were protected. It was later demonstrated, by comparing Intravenous (IV) and SC immunisation of PfSPZ in non-human primates, that IV immunisation induced significantly higher antigen specific CD4+ and CD8+ T cell responses suggesting that the route of administration plays a key role in the immune response PfSPZ induced. In the second clinical trial [55] in which 40 adults received 4 to 6 doses of PfSPZ via the IV route, PfSPZ induced higher level, but dose dependent immune responses. 12 of the

15 subjects who received the highest vaccine dose (1.35 x10^5 PfSPZ/dose) 4 to 6 times over many months were protected.

The RTS,S vaccine is the most advanced malaria vaccine, and has reached Phase 3 clinical trials. This subunit particle vaccine is based on *P. falciparum* circumsporozoite protein (CSP), an antigen expressed on sporozoites and within infected hepatocytes [56]. RTS,S consists of hepatitis B surface antigen (HBsAg) particles with HBsAg fused to the central repeat and the entire C-terminal region of the *P. falciparum* CSP mixed with non-recombinant HBsAg at a molar ratio of 1:4 [57]. In series of Phase 2 clinical trials [58-63], RTS,S was tested with several adjuvants (including GSK's AS adjuvant platform) and overall 30%-50% of naïve adults were protected against homologous *P. falciparum* challenges. Both AS01 and AS02 adjuvant have been shown to be safe and immunogenic [63]. In Phase 2 field trials, RTS/S formulated in AS01/02 gave approximately 30% to 35% protection in adults [64] [65]. Similar results were observed in children, approximately 30%-50% of children and infants immunized with RTS,S in AS01/02 were protected from clinical malaria [66-70]. The Phase 3 trial of RTS,S/AS01 began in May 2009 and had completed enrolment in 2011 with 15,460 children from seven countries in sub-Saharan Africa: Burkina Faso, Gabon, Ghana, Kenya, Malawi, Mozambique, and the United Republic of Tanzania. Children were divided into two age categories: 6 to 12 weeks of age and 5 to 17 month of age. RTS,S/AS01 conferred 55.8% protection against clinical malaria and 47.3% protection against severe malaria in children in the older age category [71]. The protection was only 31.3% and 36.6% respectively in younger children [72].

Another partially successful pre-erythrocytic stage malaria vaccine that has advanced to clinical trial is a viral vectored vaccine (administrated using ChAd63 prime followed by MVA

boost) based on the liver stage antigen thrombospondin-related adhesion protein (TRAP) fused with a string of defined cytotoxic T lymphocyte epitopes (ME) [73]. A Phase 1 Trial conducted in UK adults [74] as well as in African adults [75] revealed this vaccine is safe and highly immunogenic with some sterile efficacy induced. Phase 2 trials of this vaccine are now being conducted.

1.5.2 Blood-stage Vaccines

Passive transfer of IgGs from adults carrying NAI to children with severe malaria rapidly reduced the parasitemia and fever [76] [77]. These clinically effective IgGs showed no detectable inhibitory effect on invasion or intra-erythrocytic development of the parasites *in vitro*, however they demonstrated the ability to kill parasites in an antibody-dependent, cellular inhibitory (ADCI) fashion [78]. These antibodies were also shown to prevent the binding of infected erythrocytes to endothelial cells [79] [80], as well as promoting opsonisation resulting in destruction of merozoites and infected erythrocytes [81] [82]. As mentioned in section 1.4.3, the mechanism of NAI mediated protection is through production of antibodies targeting VSAs expressed on iRBCs and several surface antigens expressed on merozoite. This led to the development of malaria blood-stage vaccine which aims to prevent and control malaria associated symptoms by targeting the erythrocytic life cycle of the parasite.

Most malaria blood-stage vaccine candidates are based on the two well-studied antigens: merozoite surface protein-1 (MSP-1) and apical membrane antigen-1 (AMA-1). However, in recent Phase 2 trials [83] [84], vaccines based on these two antigens failed to demonstrate efficacy in African children. Studies to enhance the AMA-1 vaccine efficacy with the more potent adjuvant AS02 [85] have shown a 64.3% efficacy against the vaccine parasite strain,

even though the efficacy against the primary end point (one clinical episode caused by any strain of malaria) was only 17.4% [86]. Other studies to increase vaccine immunogenicity with viral vector prime-boost regime [87] [88] [89] as well as with combination of MSP-1 and AMA-1 [90] have been ongoing. The problem with vaccines targeting MSP-1 or AMA-1 is that there is great genetic polymorphism resulting from selective pressure [91]. This genetic polymorphism presents a major hurdle for blood-stage malaria vaccine development. Subsequently, identification of other blood-stage candidates has become more important in this field.

Combination B is a vaccine consisting of 3 recombinant proteins: ring-infected erythrocyte surface antigen (RESA), MSP-1 and MSP-2 formulated in Montanide ISA720 adjuvant [92]. In Phase 2 trial in Papua New Guinea, this vaccine demonstrated a 62% efficacy in reduction of parasite density; however this vaccine effect appeared specific to parasites with the vaccine's MSP-2 genotype [93].

GMZ2 is a MSP-3 and GLURP fusion protein vaccine formulated in aluminium hydroxide [94]. Two Phase 1 trials demonstrated GMZ2 to be safe and induced higher anti-GMZ2 antibodies than the rabies control group [95] [96]. GMZ2 is currently being tested in a large Phase 2b clinical trial.

The MSP-3 long synthetic peptide (MSP3-LSP) consists of synthetic peptides covering the fully conserved region (amino acid sequence 186-276) of MSP-3 [97]. This vaccine was formulated with aluminium hydroxide and demonstrated safety and immunogenicity in both adults [98] [99] and children [100] [101]. MSP3-LSP is currently being tested in a Phase 2 clinical trial in Mali.

Erythrocyte-binding antigen–175 (EBA175) is a conserved antigen of *P. falciparum* which is involved in binding of the parasite to erythrocytes [102]. Recombinant EBA175 formulated in aluminium phosphate has been developed as blood-stage malaria vaccine target. This vaccine has been tested in Phase 1 clinical trial which demonstrated not only the safety of the vaccine but also the ability of vaccine to generate significant level of antibodies after 3 doses that inhibited parasite growth *in vitro* [103].

P. falciparum reticulocyte-binding protein homologue 5 (PfRH5) is a very conserved antigen involved in merozoite invasion with only five non-synonymous single nucleotide polymorphisms [104]. Preclinical studies using viral vectored vaccine expressing PfRH5 demonstrated that it was highly immunogenic and out-performed several other blood stage antigens in terms of the growth inhibitory activity of the antiserum delivered by the same vaccine platform. Anti-PfRH5 vaccine also induced cross-strain neutralizing antibodies [105]. Currently, a Phase 1a clinical trial is being conducted in Oxford using viral vectors (ChAd63-MVA) expressing PfRH5.

1.5.3 Transmission-blocking vaccines

The sexual, mosquito stage of the malaria life cycle involves the transmission of the parasite from an infected person to a female mosquito where the parasite undergoes sexual reproduction and prepares to invade a new human host. Vaccines developed to target antigens expressed during the sexual, mosquito stage of the parasite are believed to interrupt malaria transmission from infected mosquitoes to human hosts and this type of vaccine is termed a malaria transmission-blocking vaccines. This vaccine strategy is not a novel concept, as it dates from the 1970s (see below), and was published as a WHO meeting report in 2000 and was described as “an ideal public good” [106]. Today, TBV have become

a focus as WHO updated the Malaria Vaccine Technology Roadmap in 2013 and introduced a new strategic goal: “The development of malaria vaccines that reduce transmission of the parasite and thereby substantially reduce the incidence of human malaria (parasite) infection” [107]

1.5.3.1 Proof of concept

The first evidence to show that malaria transmission from infected hosts to mosquitoes could be blocked come from two studies published in 1976 [108, 109]. Both studies used an avian malaria model. Chickens immunized with the avian malaria parasite *Plasmodium gallinaceum* gametocytes generated antibodies that recognized antigens on gametocytes. Vaccinated chickens were then infected with the parasite of the same species, and mosquitoes were fed on blood from vaccinated and infected chickens. The existence of vaccine-induced antibodies in the blood completely prevented subsequent infection in the mosquito. Interestingly, the antibodies had no effect on gametocytes when they remained in the blood of vaccinated chicken. The antibodies only worked in the mosquito midgut after being taken up in the blood meal from vaccinated and infected chickens. Subsequent studies have revealed the major antigens involved in this immunity and their orthologs in *P. falciparum* (Pfs48/45 and Pfs230). Pfs25 and Pfs28 which are expressed in later phase of parasite sexual stage cycle (zygotes and ookinetes) have also been discovered and studied.

Unlike vaccines that target pre-erythrocytic stages and asexual blood stage parasites, which will combat malaria once they enter the human host, vaccines targeting the sexual stage of the parasite will prevent infection of mosquito host hence preventing the spread of the parasite. Although such vaccines would be of great benefit to the public, it is at present of the least interest to today’s pharmaceutical industry, possibly because of ethical reasons as

the vaccine does not protect the individual leading to concerns about the feasibility of licensure, as well as the fact that its relevance is only to poor countries where malaria is endemic. However, if the final goal is to achieve local elimination and global eradication of malaria, interventions that prevent parasite transmission from infected host to vector will be required. The overall objective of the TBV is to reduce and prevent the transmission of the parasite from an infected individual and reduce secondary infections and new cases of malaria [110].

1.5.3.2 Mathematical model of malaria TBV in human population

Malaria transmission is believed to be local. This is because malaria transmission is strictly limited to mosquito breeding sites. According to Carter *et al* [111] in order for malaria transmission to take place, humans need to be or live within 1 km radius of such a breeding site. This situation makes TBV application more feasible.

The relationship between the basic reproduction number (Ro, number of new cases of malaria generated per existing case) of malaria and TBV vaccine coverage (c, proportion of the community with effective TBV coverage in a human population) was determined and summarised by WHO malaria report 2000 [112]. Basically, if Ro_{TBV} is the Ro with a specific level of TBV coverage, Ro_I is the Ro before deploying the TBV, then:

$$\mathbf{Ro_{TBV} = Ro_I (1 - c)}$$

According to this equation, the relationship between above values are calculated and are as presented in Table 1.1 below:

		Ro_{TBV}														
c	Ro_I	2	3	4	5	8	10	15	20	25	30	50	100	200	500	1000
0.2		1.6	2.4	3.2	4	6.4	8	12	16	20	24	40	80	160	400	800
0.3		1.4	2.1	2.8	3.5	5.6	7	10.5	14	17.5	21	35	70	140	350	700
0.4		1.2	1.8	2.4	3	4.8	6	9	12	15	18	30	60	120	300	600
0.5		1	1.5	2	2.5	4	5	7.5	10	12.5	15	25	50	100	250	500
0.6		0.8	1.2	1.6	2	3.2	4	6	8	10	12	20	40	80	200	400
0.7		0.6	0.9	1.2	1.5	2.4	3	4.5	6	7.5	9	15	30	60	150	300
0.8		0.4	0.6	0.8	1	1.6	2	3	4	5	6	10	20	40	100	200
0.9		0.2	0.3	0.4	0.5	0.8	1	1.5	2	2.5	3	5	10	20	50	100
0.95		0.1	0.15	0.2	0.25	0.4	0.5	0.75	1	1.25	1.5	2.5	5	10	25	50
0.98		0.04	0.06	0.08	0.1	0.16	0.2	0.3	0.4	0.5	0.6	1	2	4	10	20
0.99		0.02	0.03	0.04	0.05	0.08	0.1	0.15	0.2	0.25	0.3	0.5	1	2	5	10

Table 1.1 Numerical values for Ro_{TBV} (malaria basic reproduction number) in a human community under various levels of TBV vaccine coverage. Ro_{TBV} values below the line are equal or less than 1, in which case the malaria transmission stops. Adapted from [112].

In this model, in order to cease malaria transmission, Ro_{TBV} needs to fall below 1. As indicated in Table 1.1, effective TBV coverage that will result in Ro_{TBV} below 1 increase as Ro_I increase. In low endemic areas where Ro_I is less than 10 [112], a TBV coverage of 90% or less could eliminate local malaria. And vaccine coverage of 90% or less is usually considered achievable, on the other hand, vaccine coverage of above 90% is generally considered unattainable [113]. In high endemic areas where Ro_I is greater than 10 [112], TBV alone will not stop the malaria transmission completely. However other interventions such as mosquito control or personal protection could be deployed at the same time, and such interventions are able to reduce the Ro by 3 to 5 folds [112]. As a result, TBV and other interventions together could have a huge impact on malaria transmission in high endemic

areas. This effect of reducing malaria inoculation rates will be great benefit to public health as reduction in disease and also mortality would be expected [113].

1.5.3.3 Evaluating vaccine induced transmission blocking immunity

A TBV targets the sexual development of the parasite inside the mosquito, therefore to determine the TBV vaccine efficacy in preclinical and clinical vaccine development, test sera or antibodies from vaccinated individuals must be tested together with parasites inside the mosquito. Novel assays have been developed to analyze such vaccine induced transmission blocking immunity. The standard membrane feeding assay (SMFA) and direct membrane feeding assay (DMFA) have been developed for such a purpose. In the SMFA, *in vitro* cultured gametocytes are mixed with either test serum, or test antibodies and then placed in an artificial membrane feeder from which laboratory raised *Anopheles* mosquito are fed through a membrane. A week after the feed, the mosquito midgut is dissected and the number of oocysts is counted. DMFA uses blood from gametocyte carriers as the source of parasite instead of laboratory cultured parasites in SMFA. SMFA is easy to perform in any lab whereas DMFA is more restricted because of the source of the parasite. However DMFA will show important TBV efficacy data against circulating strains of the parasite. The membrane feeding assay's readouts are: transmission reducing activity (TRA) and transmission blocking activity (TBA). TRA measures the reduction in the mean number of oocysts in infected mosquitoes (oocyst intensity) and the TBA measures the reduction in the proportion of infected mosquitoes (oocyst prevalence). TRA is calculated based on the ratio of the number of oocyst developed in the midgut, comparing the test and the control group [114]. TRA=100* (1 - mean oocyst number with immune plasma/ mean oocyst number in control group). TBA is calculated based on the ratio of the overall number of infected

mosquito in the test group compared to the control group. TBA=100* (1 - prevalence of infection for mosquitoes fed with immune plasma/ prevalence of infection for control group).

Field scientists prefer to measure TBV efficacy by using TBA. The number of oocysts inside a mosquito is not thought to influence the mosquito's infectivity. A mosquito is infectious if there are sporozoites in its salivary glands [115] and it has been shown that a single oocyst can generate a large number of sporozoites [116]. Laboratory scientists prefer to use TRA to assess efficacy because TRA shows more discriminatory results since it is in general easier to achieve a reduction in oocyst numbers than a complete clearance. It is difficult to predict TBV field efficacy based on laboratory TRA or TBA data. Over the years the membrane feeding assays have been refined to maximise transmission. As a result, oocyst density in the control group is very high whereas in malaria endemic areas (with moderate to high incidence) wild-caught mosquitoes have very low oocyst numbers (<5) [117]. Despite this, two measurements (TBA and TRA) are clearly correlated [118]. TBA is highly influenced by the degree of parasite exposure (as measured by oocyst intensity in the control group). The relationship between TBA and TRA under different parasite exposures are non-linear [119]. In highly infected mosquitoes (high parasite exposure) small changes in oocyst prevalence can mask large differences in oocyst intensity. According to this relationship, if the control group has a mean oocyst intensity of 100, a reduction in oocyst prevalence of 20% may equal a reduction in oocyst intensity by 90% [119]. As a result, it is important to understand the meanings behind TRA and TBA. It is true that it is difficult to predict the field efficacy based on the laboratory data. However, membrane feeding assays remain one of the few biological assays widely utilized to test the functional activity of antibodies both in

preclinical and clinical TBV vaccine development [120]. For the purpose of this study, we use the both TRA and TBA as the readouts.

1.5.3.4 Transmission-blocking vaccine candidate antigens

Malaria TBV targets antigens that are expressed on the surface of the mosquito stage parasite. The details of the mosquito stage malaria cycle are illustrated in the figure 1.1 below. During the blood meal, malaria gametocytes are ingested by the mosquito. Inside the mosquito midgut, gametocytes emerge from iRBCs and within minutes differentiate into male and female gametes. Each female gametocyte develops into a single immotile female (macro) gamete and each male gametocyte give rise to up to eight flagellated male (micro) gametes. During fertilization, the male and female gametes fuse to form a zygote. The zygote further develops into an ookinete followed by migration through the wall of the midgut and development into an oocyst. Oocyst stage parasites are located on the outside of the midgut. During this stage, sporozoites develop inside each oocyst before rupture, when they will be released and migrate to enter the mosquito salivary glands [121]. Among all the transmission-blocking vaccine antigens (Reviewed [110], [113], [122], [123], [124], [125]), five antigens have attracted the most attention recently and are regarded as the leading transmission-blocking vaccine candidates. As indicated in Figure 1.1, these antigens can be divided into two groups: 1) HAP2, Pfs48/45 and Pfs230 which are expressed on the gametocyte and gamete stages of malaria parasite life cycle. These antigens are also expressed in the human host and as a result, exposed to the human immune system. One clear advantage with such antigens is that vaccine-induced immunity could potentially be boosted by natural infection. 2) Antigens such as Pfs25 and Pfs28 are expressed in the later

stages (zygote and ookinete stage) of the life cycle and as a result, these antigens are not exposed to human immune system.

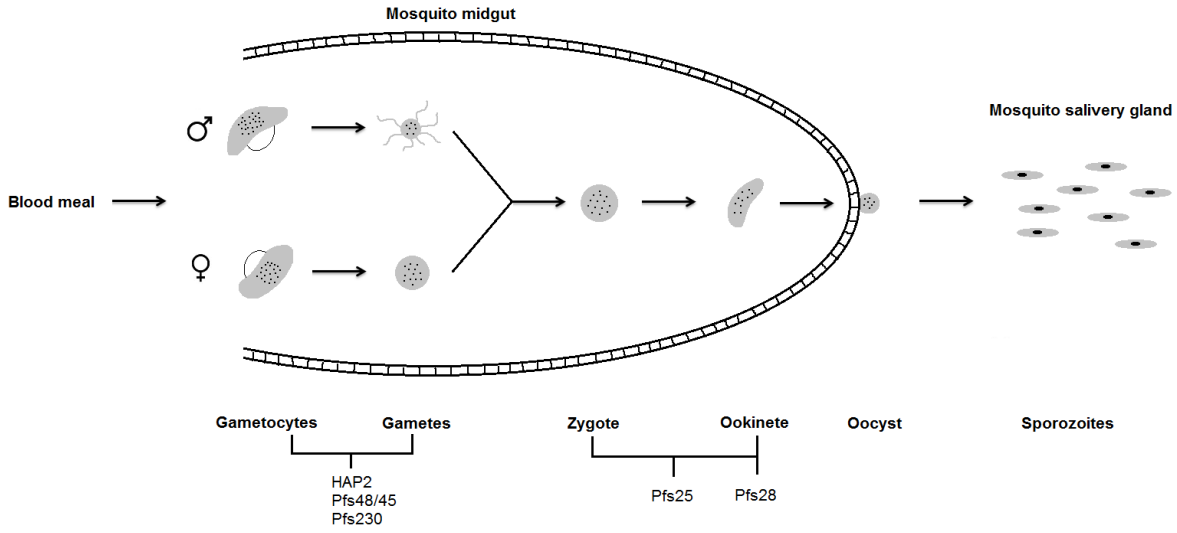

Figure 1.1. Mosquito stage of *P. falciparum* development. Leading TBV candidate antigens are labelled with their corresponding expression stages.

1.5.3.4.1 HAP2

HAP2 is a male specific sterility gene which was originally identified in *Arabidopsis thaliana*. Later study [126] has revealed that in *Plasmodium*, HAP2 is expressed on male gametocytes and gametes and is essential for fusion of the gamete surface membrane during fertilization. A recent study [127] using gene disruption has demonstrated that HAP2 disruption in *Plasmodium* blocks fertilization and thereby mosquito transmission of malaria, suggesting that HAP2 is a good target for TBV. The first study to test HAP2 as a TBV antigen candidate used the *Plasmodium berghei* model [128]. In this study, a fragment of *P. berghei* HAP2

protein was successfully produced using *Escherichia coli* (*E. coli*). Rabbits vaccinated with this protein generated HAP2 specific anti-sera which not only inhibited ookinete conversion *in vitro*, but also significantly inhibited oocyst development *in vivo* using the standard SMFA. A more recent study [129] has produced *P. falciparum* HAP2 using the wheat germ cell-free (WGCF) expression system. The protein was immunogenic and total IgGs were purified from vaccinated mice and tested in a SFMA. At a total IgG concentration of 0.75 mg/mL, HAP2 anti-sera showed significant inhibition of oocyst development. The level of inhibition observed was similar to other TBV leading antigens (Pfs25 and Pfs230C) tested in the same study.

1.5.3.4.2 Pfs48/45

P. falciparum gamete fertilization requires the surface protein Pfs48/45. This surface protein is expressed by both male and female gametocytes and gametes. A gene disruption study showed both Pfs48/45 and Pbs48/45 (the Pfs48/45 ortholog from *P. berghei*) knockout parasites failed to form zygotes [130]. Although P48/45 is expressed on both male and female gametes, gene knockout studies only affected the male gametes resulting in its inability to penetrate fertile female gametes [130]. In addition, studies with Pfs48/45 and Pfs230 double knockout parasites demonstrated that Pfs48/45 is required to retain Pfs230 on the gamete surface [131]. Monoclonal antibodies against Pfs48/45 prevented zygote development and subsequent mosquito infection [132] and anti-Pfs48/45 antibodies found in human serum in endemic areas after natural infection correlated with transmission reducing activity (TRA) in the field [133]. Several attempts have been made to produce Pfs48/45 protein. Both fragments [134] and full-length [135] Pfs48/45 have been successfully produced in *E. coli.* In both studies, protein produced in *E. coli* was

immunogenic and significantly inhibited oocyst development in SMFA assays. In the Jenner Institute, Pfs48/45 has been successfully expressed in viral vectors: Chimpanzee adenovirus serotype 63 (ChAd63) and modified vaccinia virus Ankara (MVA). Mice immunised with a ChAd63 prime and MVA boost vaccination regime generated high levels of anti-Pfs48/45 antibody and subsequent SMFA proved such antibodies inhibited oocyst development (Kapulu *et al*. submitted).

1.5.3.4.3 Pfs230

Similar to Pfs48/45, Pfs230 is a pre-fertilisation antigen which is expressed on both male and female gametocytes and gametes. The role of Pfs230 in parasite development is not clear. Disrupting Pfs230 significantly inhibits oocyst production and mosquito infectivity. Interestingly, Pfs230 disrupted male gametocytes successfully emerge from RBCs and exflagellate to produce microgametes. However, Pfs230 disrupted male gametes failed to interact with RBCs to form exflagellation centres [131]. The purpose of such erythrocyte adhesion is not known, however it is believed to carry out an important function since microgametes of the human malaria *P. falciparum* can bind human erythrocytes but not chicken erythrocytes, whereas avian host *Plasmodium gallinaceum* microgametes bind chicken but not human erythrocytes [136]. An early study showed anti-Pfs230 mAb blocked malaria transmission [137]. Anti-Pfs230 antibodies are present in individuals living in malaria endemic areas and a correlation between anti-Pfs230 antibody and TRA in the field was observed [133]. Full-length Pfs230 is a 363-kDa protein and consists of 3135 amino acids (aa) and contains 70 cysteine residues [138]. Due to its size and complexity, full length recombinant Pfs230 has not been successfully produced. An initial study divided this antigen into 6 different regions (region A: aa 304-378; region B: aa 375-452; region C: aa 443-1132;

region D: aa 1166-1541; region E: aa 1727-2397; region F: aa 2398-3135). Only the antisera induced by region C recombinant protein generated significant TRA [139]. Hence, attempts have concentrated on making vaccines based on Pfs230 region C (termed Pfs230C). Pfs230C recombinant protein has been successfully produced by various expression systems including *E.coli* [139] [140], WGCF [129] [141] and *Nicotiana benthamiana* plants [142]. Such recombinant Pfs230C proteins all induced antibodies with significant TBA and/or TRA. Other vaccination delivery system such as Pfs230C DNA vaccine [143] were attempted, however the DNA vaccine did not induce as strong TRA as recombinant protein vaccine did. In the Jenner Institute, Pfs230C was successfully expressed in viral vectors. Using ChAd63 prime followed by MVA boost, strong TRA and TBA was achieved in SMFA (Kapulu *et al*. submitted).

1.5.3.4.4 Pfs25

Unlike HAP2, Pfs48/45 and Pfs230 which are pre-fertilization antigens, Pfs25 is a 25kDa *Plasmodium falciparum* sexual stage outer membrane protein which is expressed mainly on the surface of zygotes and ookinetes [144]. Pfs25 contains four tandem epidermal growth factor-like (EGF) domains and these have been proposed to be involved in a receptor-ligand interaction required for parasite invasion of mosquito midgut epithelium [145]. Anti-Pfs25 monoclonal antibodies (mAbs) completely block transmission of the parasite from humans to the mosquito host [146] and Pfs25 is the most extensively studied and the most promising TBV candidate. Various animal studies have demonstrated that a Pfs25-based vaccine exhibited very high, and in some cases complete, TBA [147-152]. In a recent comparative study [129], Pfs25 was compared head-to-head with two other leading TBV antigen candidates, Pfs230C and PfHAP2. Using protein-in-adjuvant vaccination in mice and SMFA to assess the IgG functionality, anti-Pfs25 IgG showed significantly higher inhibition of

parasite development (TBA and TRA) than anti-Pfs230C and anti-HAP2 IgGs. In the Jenner Institute, Pfs25 has also been compared head-to-head with TBV antigen candidates Pfs230C, Pfs48/45 and AnAPN1 using viral vectored vaccines in mice. Similar results were observed, anti-Pfs25 IgG showed complete blockade in both SMFA and DMFA (Kapulu *et al*, comparative assessment of transmission-blocking vaccine candidates against plasmodium falciparum, submitted). Another advantage of using Pfs25 as a TBV antigen is that Pfs25 is known to have very limited sequence polymorphism unlike Pfs230 and Pfs48/45 [153].

Pfs25 and Pvs25 (the P. vivax orthologue) are the only *Plasmodium* TBV candidates that have entered human clinical trials [154, 155]. A Phase 1 clinical trial using protein-in-adjuvant (Montanide ISA 51) formulation was discontinued due to side effects of the adjuvant. It was observed in this clinical trial that Pfs25 protein formulated with ISA 51 was not strongly immunogenic. Among 5 volunteers who completed 2 scheduled vaccinations, only 1 elicited a strong IgG response which resulted in a >90% TRA in SMFA. This inhibition was directly correlated with the level of the anti-Pfs25 IgGs [154]. This result suggested the feasibility of inducing transmission-blocking immunity in human using Pfs25-based vaccines, but there is a need for more immunogenic formulations as high antibody titres are required to get potent transmission-blocking immunity. To increase Pfs25's immunogenicity in human, two different approaches were attempted: conjugating recombinant Pfs25 protein to a detoxified *Pseudomonae aeruginosa* exoprotein A (EPA) [156] and expressing recombinant Pfs25 on the surface of a virus-like particle (VLP) consisting of Alfafa mosaic virus coat proteins [157]. Both vaccines are highly immunogenic compared to monomeric Pfs25 and are currently being tested in Phase 1 trials.

1.5.3.4.5 Pfs28

Pfs28 is another structurally complex outer membrane protein. It has structural similarities to Pfs25, as both of them contain four EGF domains and is genetically linked on chromosome 10 [158]. It is a 28 kDa sized protein and is expressed on the surface of late stage ookinete [158]. The function of Pfs28 was not fully understood, however functional redundancy between Pfs25 and Pfs28 was suggested [159]. After successful Pfs28 protein expression in yeast, although poor immunogenicity was observed, anti-Pfs28 sera were found to exhibit TBA [158]. In addition, there was a synergistic effect in TBA after mixing antibodies to Pfs25 and Pfs28 in an SMFA [158, 160]. This finding led to development of Pfs25-Pfs28 fusion protein vaccine which induced a better TBA immunity in mice [160].

1.5.3.5 Transmission-blocking vaccine development

As mentioned in previous sections, many studies have been done to test for different TBV candidate antigens. So far, Pfs48/45, Pfs230C and Pfs25 have received the most attention. Very few studies have been done to compare these leading antigens head to head. In one recent study [129], PfHAP2, Pfs230C and Pfs25 were expressed using the WGCF system and formulated with Montanide ISA720. Antibodies from Pfs25 vaccinated mice exhibited more TRA and TBA than other antigens in SMFA. Another study performed in the Jenner Institute by Kapulu *et al* (submitted) has compared Pfs48/45, Pfs230C and Pfs25 using viral vectored vaccines. In this study, Pfs25 and Pfs230C antibodies exhibited higher transmission-blocking and transmission-reducing activity when tested in SMFA and DMFA. In addition, Pfs25 is the only TBV candidate that has been tested in human clinical trials. As mentioned earlier, Pfs25 formulated in Montanide ISA 51 demonstrated that a recombinant Pfs25 protein, although relatively poor in overall immunogenicity, could generate functional antibodies in some

human vaccinees and the TRA observed was strongly correlated with the anti-Pfs25 antibody level [154]. Now several technologies are being developed to improve Pfs25 immunogenicity, including conjugating Pfs25 to a carrier protein or expressing Pfs25 in a VLP system.

Another problem TBV will face is that the vaccine has no direct benefit to the vaccinee, but only to the vaccinated community. To overcome this problem, the combination of TBV with a pre-erythrocytic vaccine, which can introduce some degree of protection, is considered to be a good vaccine strategy. Additionally, recent regulatory advice from the US Food and Drugs Administration to the malaria vaccine development community is that these regulators see no problem in principle with the development of a stand-alone transmission-blocking vaccine that offers community-level protection against malaria transmission.

1.5.3.6 Improving Pfs25 immunogenicity

1.5.3.6.1 Use of potent adjuvant

Adjuvants are used to enhance and modulate the immunogenicity of a vaccine antigen or immunogen. The host immune system can react to natural pathogens and mount an immune response because the pathogen contains PAMPs [161] which can be recognized by PRRs on host immune cells and activate the innate immune system. Unlike live-attenuated or inactivated whole organism vaccines which still exhibit PAMPs, recombinant proteins are highly purified antigens which lack PAMPs and as a result, cannot trigger a desired immune response on their own.

The first adjuvant aluminium salt (alum) was used in humans in the 1920s. As summarised by Garçon *et al* [162], to date, there are only 6 adjuvants have been licensed for use in

human vaccines: alum, liposomes (artificial vesicles consisting of lipid layers), MF59 (an oil in water emulsion), Montanide ISA51 (a water-in-oil emulsion), AS04 (based on lipopolysaccharide (LPS) derivative, monophosphoryl lipid A (MPL) and alum) and AS03 (based on α-tocopherol (vitamin E) and squalene in an oil-in-water emulsion). Other adjuvants such as AS01 and AS15 are currently in late-stage development. Adjuvants vary in their modes of action. Some adjuvants such as alum and MF59 mainly function as a delivery system by creating antigen depots at the injection site. These antigen depots provide slow release of the antigen resulting in prolonged immune stimulation and increase in APC recruitment as well as activation [163] [164]. Other adjuvants such as AS04 contain ligands for PRRs which directly target APCs inducing prompt innate immune response.

Because different adjuvants induce different immune activation pathways, it is necessary to test the antigen of interest (Pfs25 in this case) with different available adjuvants to compare their immunogenicity. Potent adjuvants are most likely to be reactogenic like Montanide ISA 51 in the Pfs25 human trial study [154]. Such adjuvants may be difficult to include in a vaccine that has an indirect effect on the person being vaccinated. Another problem with adjuvants is that the handful of adjuvants with a good safety profile are all owned by pharmaceutical companies (e.g. AS adjuvant system are owned by GSK) and often difficult to access. Therefore, developing technologies to improve immunogenicity of Pfs25 recombinant protein without the need for potent adjuvants is important.

1.5.3.6.2 Conjugated protein vaccine

An antigen with poor immunogenicity can be coupled to an immunogenic carrier protein (mostly by chemical conjugation) to enhance the antigen's immunogenicity. This approach was developed in the 1980s mainly to overcome the lack of immunogenicity of

polysaccharide vaccines in infants. Infants lack the ability to mount an immune response to polysaccharide vaccines because their T-cell independent B cell response is not well developed. By chemically linking polysaccharide to a carrier protein with T cell epitopes (e.g. tetanus toxoid or diphtheria toxoid) the conjugated vaccine changes the immune response from T-cell independent to T-cell dependent, leading to increased immunogenicity in infants. Today, conjugated vaccines have been widely used in humans; successful examples include the licensed *Haemophilus influenzae* Type b vaccine conjugated to tetanus toxoid [107] and *pneumococcal* vaccine conjugated to diphtheria toxoid [106].

Pfs25 has been conjugated and tested with different protein carriers. Recombinant exoprotein A (EPA) from *Pseudomonas aeruginosa* are expressed from *E. coli* [165]. Conjugation of this recombinant EPA to the capsular polysaccharide of *Salmonella enterica serovar* Typhi increased the antigen immunogenicity and showed more than 90% efficacy (of typhoid fever reduction) in young children [166, 167]. Pfs25 was conjugated to recombinant EPA (termed Pfs25-EPA) and tested as a TBV candidate [156, 168, 169]. This conjugation significantly increased the Pfs25 antibody response in mice and is currently being tested in human Phase 1 clinical trials. Outer-membrane protein complex (OMPC) of *Neisseria meningitidis* serogroup B was used as a carrier protein for the bacterial capsular polysaccharide polyribosylribitol phosphate in a commercial conjugate vaccine (PedvaxHiB) against *Haemophilus influenzae* type b [170, 171]. Additionally, conjugation to OMPC was also shown to increase the immunogenicity of influenza virus M2 peptide [172]. Pfs25 was conjugated to OMPC (termed Pfs25-OMPC) [173] and this study revealed Pfs25-OMPC to be highly immunogenic and induced high and sustained (over 18 months) antibodies in selected animal models.

1.5.3.6.3 Viral vectored vaccine

In addition to the development of traditional protein-in-adjuvant vaccines, recombinant viral vectors have also received a lot of attention in recent years. The first viral vector vaccine used in humans for malaria vaccination was NYVAC-Pf7 [174] followed soon after by MVA [175], both of these are attenuated versions of the vaccinia virus. Due to the conserved nature of viruses within the Orthopoxvirus genus, MVA has been used as a successful smallpox vaccine. A good safety profile and its ability to accommodate large amount of foreign DNA have made MVA a very attractive antigen delivery vector [176]. Clinical studies using MVA as a vaccine vector targeting cancer [5], tuberculosis (TB) [177], malaria [178] and HIV [179] have been reported with more recent trials in influenza, hepatitis C and respiratory syncytial virus (RSV). MVA as a vaccine vector can induce both $CD4^+$ and $CD8^+$ T cells as well as antibody responses against the antigen expressed by the interested transgene.

Adenovirus has also been safely engineered to deliver antigens of interest [180]. Replication–deficient adenoviruses have been developed by deleting the E1 region which is essential for viral replication [181]. Most of the adenovirus vectors were originally based on human adenovirus serotype 5 (AdHu5), which is the serotype that commonly infects humans. AdHu5 viral vectored vaccines encoding different antigens have been shown to induce strong antigen specific B and T cell responses in several animal studies [182] [183] [184] [185]. However exposure of humans to AdHu5 due to natural infections results in sustained virus neutralizing antibodies [186], and these antibodies can decrease the immunogenicity of AdHu5 based vaccines in humans [187]. As a result, AdHu5 may have limited application in human populations where high titre antibodies are prevalent, such as in most developing countries. To overcome this, several alternative adenoviruses isolated

mainly from chimpanzee were studied, including chimpanzee adenovirus serotype 63 (ChAd63) against which there are much lower circulating neutralizing antibodies in humans [188]. Similar to AdHu5, ChAd63 have been shown to induce strong B and T cell responses in animal studies [189] [190]. A recent clinical trial using ChAd63 carrying *P. falciparum* pre-erythrocytic antigen ME-TRAP followed by recombinant MVA carrying the same insert demonstrated ChAd63 to be a safe and immunogenic viral vectored vaccine in humans [75].

To avoid the impairment of immunogenicity of booster doses of viral vectors caused by development of anti-vector immunity, a heterologous prime-boost regime for viral vectored vaccines has been developed. ChAd63 prime followed by MVA boost was demonstrated to be the most potent regime tested which resulted in long-lasting, antigen-specific B and T cell responses [73] [189]. Studies revealed that an extended 8 weeks interval between prime and boost played a role in developing strong antibody responses in mice [191]. Currently, the ChAd63 prime MVA boost immunisation regime is being studied in human clinical trials against malaria in the UK and several African countries [75] [89]. Recombinant ChAd63 and MVA expressing Pfs25 have been produced and tested in mice [147]. In this study, high anti-Pfs25 antibody titre was achieved and subsequent SMFA demonstrated that the IgGs exhibited strong TRA and TBA.These vectors are currently being manufactured to GMP clinical grade for a Phase 1 trial in 2015.

1.5.3.6.4 Multivalent vaccine

Multivalent vaccines consist of 2 or more separate immunogens combined in one single product. Multivalent vaccines may contain multiple antigens from different pathogens; therefore immunity against multiple diseases could be induced with one vaccination. Successful examples include measles-mumps-rubella (MMR) vaccine [192] and Diphtheria-

Tetanus-acellular Pertussis Vaccine (DTaP) [193]. Multivalent vaccines may also contain antigens from different variant strains of the same pathogen; therefore the vaccinee could be protectcted against different strains of the pathogen with one vaccine; pneumococcal conjugate vaccine is one of the successful examples [194].

Multivalent vaccines may also contain different antigens that are expressed on one specific stage of a pathogen or different stages of a pathogen. In principle, if the antigens induce a synergistic or even an additive immune response against that particular pathogen, the overall protection conferred should be better than monovalent vaccine [195] [196]. By mixing antiserum against Pfs25 and antiserum against Pfs28 together in SMFA, it was found that sera against Pfs28 acted synergistically with sera against Pfs25 [158]. Recombinant Pfs25-Pfs28 fusion protein vaccine has been developed and the results in a preclinical study have confirmed the synergistic effect in mice [160]. Studies to identify other effective antigens and vaccine formulations that may provide enhanced transmission blocking immunity when co-immunized with Pfs25 is another way to develop a Pfs25-based TBV.

1.5.3.6.5 Virus-like particle and nanoparticle vaccines

The structural proteins of many viruses have the ability to spontaneously form virus-like particles. After expression in various protein expression systems, these proteins retain the ability to form a particle without incorporating infectious genetic material. These non-infectious particles, with size range of viruses (22-150nm), are termed virus-like particle (VLP). Reviewed by Bachmann *et al* [197], VLPs typically have an icosahedral or rod-like structure. The VLPs' symmetry usually reflects the symmetry of the original virus. The VLPs have highly repetitive and dense surfaces epitopes which often lead to strong immune responses (discussed further in Chapter 5).

Several VLP based vaccines have been developed. Hepatitis B surface antigen (HBsAg) is the surface antigen of the hepatitis B virus (HBV). HBsAg self-assembles into VLPs and can be found in blood of hepatitis B virus infected patients [198]. Recombinant HBsAg have been produced from yeast and self-assembles into VLPs. These HBsAg VLPs are used as HBV vaccine in humans [199]. Similarly, recombinantly expressed major capside protein L1 from papillomaviruses can form VLP and was introduced as a papillomavirus vaccine for humans [200]. In addition to HBV VLP and papillomavirus VLP vaccines, in which VLPs are assembled from target pathogen components, chimeric VLPs (in which target antigens are genetically fused or chemically conjugated to a VLP carrier) have been developed and tested as candidate vaccines. The response to foreign antigens displayed on the VLP should be significantly improved when expressed from a VLP.

RTS,S is the most advanced malaria pre-erythrocytic vaccine which is a VLP. In this vaccine, the central repeats and the entire C-terminal region of the *P. falciparum* CSP are fused to the N terminus of the HBsAg. When co-expressed with HBsAg in *Saccharomyces cerevisiae* (insert copy ratio, CSP-HBsAg:HBsAg=1:4), CSP-HBsAg and HBsAg together form chimeric VLPs expressing CSP on the VLP surface [61]. The vaccine induces high antibody titres to CSP [59]. As described earlier, RTS,S has demonstrated safety as well as strong immunogenicity in clinical trials. Partial protection that lasted for 18 months in children aged 1 to 4 years was reported [67], and an early Phase 3 trial result showed a 50% reduction of clinical disease in younger children aged 5 to 17 months [201]. A recent study has genetically fused Pfs25 sequence with Alfalfa mosaic virus coat protein. After expression in *N. benthamiana*, this fusion protein self-assembles into a chimeric VLP carrying Pfs25 on the surface. Pfs25-

CP VLPs were demonstrated to be immunogenic in mice [157] and are currently being tested in a Phase 1 clinical trial.

In addition to using chimeric VLP vaccines as an antigen delivery system, antigens have been conjugated to nanoparticles such as synthetic polymer beads including carboxylated polystyrene microspheres in animal studies [202] [203]. High level B and T cell responses were observed.

1.6 Thesis aims and outline

As mentioned above, Pfs25 is the leading TBV candidate antigen. To achieve good transmission blocking immunity, a Pfs25-based vaccine needs to induce high antibody titres in humans. The only TBV *P. falciparum* candidate vaccine that has been tested in a human clinical trial, Pfs25 formulated in ISA51, showed inadequate safety and was not very potent. Therefore a more immunogenic Pfs25 vaccine formulation is needed. The first objective of my DPhil project was to improve Pfs25 protein immunogenicity by 1) heptamerisation using a nanoparticle platform called IMX313; 2) displaying Pfs25 on VLP platforms including HBsAg-VLP and the bacteriophage-based Qβ-VLP; 3) fusing it with Pfs28 and expressing as a multivalent protein vaccine to try and obtain higher efficacy. The second objective was to compare the immunogenicity of each of the above TBV candidates and find the best vaccination formulation to induce high levels of protective anti-Pfs25 antibody responses as measured by antibody titres and the functional membrane feeding assay.

1.6.1 Outline

Chapter 2 describes the material and methods used in this study

Chapter 3 describes the production, purification and immunogenicity of recombinant Pfs25 in *P. pastoris*.

Chapter 4 describes the production, purification and immunogenicity of recombinant Pfs25-IMX313 nanoparticle in *P. pastoris*.

Chapter 5 investigates the mechanisms of immunogenicity of Pfs25-IMX313 nanoparticle

Chapter 6 describes the production, purification and immunogenicity of recombinant Pfs25-HBsAg VLP, Pfs25-Qβ VLP and Pfs25-Pfs28 multivalent vaccine in *P. pastoris.*

Chapter 7 summarises the results of this thesis and discusses the possible future directions.

Chapter 2

Materials and Methods

2. Materials and Methods

2.1 Materials

2.1.1 Reagents

Material	Supplier	Catalogue Number
Phusion® High-Fidelity PCR Master Mix with HF Buffer	New England BioLabs, UK	M0531S
Agarose	Sigma-Aldrich, UK	A9539
Smartladder	Eurogentec	MW-1700-10
SYBR® Safe DNA Gel Stain	Life Technologies, UK	S33102
Tris-acetate-EDTA	Fisher, UK	S1804
EcoRI restriction enzyme	New England BioLabs, UK	R0101M
KpnI restriction enzyme	New England BioLabs, UK	R0142M
StuI restriction enzyme	New England BioLabs, UK	R0187M
T4 DNA Ligase	New England BioLabs, UK	M0202M
In-Fusion® HD Cloning Plus	Clontech, UK	638909
NEB 5-alpha Competent E. coli (High Efficiency)	New England BioLabs, UK	C2987H
Ampicilin	Sigma-Aldrich, UK	A9539
QIAprep Spin Miniprep Kit	Qiagen, UK	27104
QIAGEN Plasmid Midi Kit	Qiagen, UK	12143
QIAquick PCR Purification Kit	Qiagen, UK	28104
PichiaPink™ Expression Strain Set	Life Technologies, UK	A11154
PichiaPink™ Media Kit	Life Technologies, UK	A11156
Falcon® Round-Bottom Tubes	Fisher, UK	60819-524
Yeast Extract	Sigma-Aldrich, UK	Y1625-1KG
Peoptone	Sigma-Aldrich, UK	P0431-1KG
Casamino Acids	BD, UK	223120
Yeast Nitrogen Base	Sigma-Aldrich, UK	Y1251-1KG
Biotin	Sigma-Aldrich, UK	B4501-500MG
Corning® Erlenmeyer baffled cell culture flasks (2L)	Sigma-Aldrich, UK	CLS431256-6EA
Corning® Erlenmeyer cell culture flasks (125mL)	Sigma-Aldrich, UK	CLS431143-50EA
PureLink® Air Porous Tape	Life Technologies, UK	12262-010
HisTrap excel Column	GE Healthcare, UK	17-3712-06
HiTrap Heparin HP	GE Healthcare, UK	17-0407-03
HiLoad Superdex 200 PG	GE Healthcare, UK	28-9893-35
Disposable PD-10 Desalting Columns	GE Healthcare, UK	17-0851-01
Amicon Ultra-15 Centrifugal Filter Units (10kDa cut-off)	Merck Millipore, UK	UFC901024
Imidazole	Sigma-Aldrich, UK	I5513-100G

Phosphate Buffered Saline (PBS)	Sigma-Aldrich, UK	D8537
Trizma® HCL buffer solution (pH7.8, 1M)	Sigma-Aldrich, UK	T2569
Glass beads, acid-washed	Sigma-Aldrich, UK	G8772-500G
Benzonase® Nuclease	Sigma-Aldrich, UK	E1014-25KU
Cesium chloride	Sigma-Aldrich, UK	289329-100G
Caesium Chloride	Sigma-Aldrich, UK	203025
$MgCl_2$ (1M)	Sigma-Aldrich, UK	63069-100ML
Y-PER Yeast Protein Extraction Reagent	Thermo Scientific, UK	78991
Potassium phosphate monobasic	Sigma-Aldrich, UK	P5655-1KG
Potassium phosphate dibasic	Sigma-Aldrich, UK	P3786-1KG
Sodium phosphate monobasic	Sigma-Aldrich, UK	S8282-500G
Sodium phosphate dibasic	Sigma-Aldrich, UK	S7907-500G
Sodium chloride	Sigma-Aldrich, UK	S7653-1KG
Magnesium chloride	Sigma-Aldrich, UK	208337-1KG
CaptureSelect™ C-tag Affinity Matrix	Life Technologies, UK	191307005
XK 16/20 Column	GE Healthcare, UK	28-9889-37
Precise Tris-HEPES Gels	Thermo Scientific, UK	25220 (8%) 25221 (10%) 25222 (12%)
20X Tris-HEPES-SDS Buffer	Thermo Scientific, UK	28368
Pierce Silver Stain Kit	Thermo Scientific, UK	24612
NuPAGE® LDS Sample Buffer	Life Technologies, UK	NP0007
DTT	Life Technologies, UK	P2325
Trans-Blot® Turbo™ Mini Nitrocellulose Transfer Pack	Bio-Rad, UK	170-4158 (mini) 170-4159 (midi)
Bovine serum albumin	Sigma-Aldrich, UK	05470-1G
Sodium Azide	Sigma-Aldrich, UK	S2002
Alkaline phosphatise-conjugated Donkey Anti-Mouse IgG	Jackson ImmunoResearch	715-055-150
BCIP®/NBT	Sigma-Aldrich, UK	B5655-25TAB
NUNC Maxisorp 96-well plates	Fisher, UK	DIS-971-030J
Diethanolamine buffer	Thermo Scientific, UK	34064
p-Nitrophenyl phosphate Tablets	Sigma-Aldrich, UK	N1891-50SET
Alkaline Phosphatase-conjugated Goat Anti-mouse IgG	Sigma-Aldrich, UK	A3562-1ML
TWEEN® 20	Sigma-Aldrich, UK	P2287-500ML
Biotinylated anti-mouse IgG1	BD Bioscience, UK	553441
Biotinylated anti-mouse IgG2a	BD Bioscience, UK	553388
ExtrAvidin (Alkaline Phosphatase)	Sigma-Aldrich, UK	E2636-.5ML
Sodium thiocyanate	Sigma-Aldrich, UK	251410-500G
Anti-mouse GL7 APC	eBioscience, UK	51-5902
Anti-mouse CD95 PE	eBioscience, UK	12-0951
Anti-mouse B220 PeCy7	eBioscience, UK	25-0452
Anti-mouse B220 PE	eBioscience, UK	12-0452
Anti-mouse GL7 Alexa Fluor® 488	eBioscience, UK	53-5902
FC blocker	eBioscience, UK	14-0161

RPMI-1640	Sigma-Aldrich, UK	R0883
THP-1 cells	ATCC, UK	30-2001
Alexa Fluor® 488 Protein Labelling Kit	Life Technologies, UK	A-10235
Phorbol Myristate Acetate (PMA)	Sigma-Aldrich, UK	P8139-1MG
Optimal Cutting Temperature compound	Fisher, UK	12678646
Superfrost Ultra Plus Slides	Fisher, UK	10417002
Fluoromount G mounting medium	eBioscience, UK	00-4958-02
Formaldehyde 16%	Thermo Scientific, UK	28906

Table 2.1 details of all commercially available reagents used in this study.

2.1.2 Solutions

ACK Lysis Buffer: 8.29g NH_4Cl (0.15M), 1g $KHCO_3$ (1mM), 37.2mg Na_2EDTA in 1L dH_2O. The pH was adjusted to 7.2-7.4 with HCL (1M).

ELISA coating buffer: 15mM sodium carbonate and 35mM sodium bicarbonate capsules were dissolved in dH_20 and autoclaved.

Complete Medium: RPMI-1640 medium was supplemented with 5mL L-glutamine (2mM), 5mL pen/strep (100U penicillin, 100ug strep), 500µL 2-Mercaptoethanol (50µm) and 50mL of heat inactivated foetal calf serum (FCS) (10%).

FACS buffer: 5g (1%) Bovine Serum Albumin (BSA) was added to 500mL PBS.

PBS paraformaldehyde 4%: 10mL of 16% paraformaldehyde was added to 30mL PBS.

SDS-PAGE running buffer: 50mL of 20X Tris-HEPES-SDS buffer was added to 950mL dH_20.

Phosphate buffered saline (PBS) 0.01M: NaCl 0.138M, KCl 0.0027M, pH 7.4 in dH_2O.

PBS/Tween (PBS/T) 0.01M: NaCl 0.138M, KCl 0.0027M, Tween-20 0.05%, pH 7.4 in dH_2O.

Diethanolamine Buffer: A 5x stock was purchased and diluted to 1x with dH_20.

Tris buffer: A 1M stock was purchased and diluted to 10mM working concentration. pH was adjusted to 7.8.

Tris-acetate-EDTA (TAE) buffer: Made up from 50x concentrate stock with dH_2O.

Yeast lysis buffer: 1mL Triton (0.1%), 2mL 0.5M EDTA (1mM), 1mL 1M $MgCl_2$ (1mM), 10mL 1M Tris pH7.8 (10mM) in dH_2O.

YPD media: 10g yeast extract (1%), 20g peptone (2%) and 20mL 1M dextrose (2%) in 1L dH_2O.

1M potassium phosphate buffer: 132mL of 1M K_2HPO_4 and 868mL 1M KH_2PO_4, pH was adjusted to 6.0.

BMGY: 10g yeast extract (1%), 20g peptone (2%), 13.4g yeast nitrogen base with ammonium sulphate (1.34%), 0.004g biotin (0.0004%), 10mL glycerol (1%), 100mM potassium phosphate (pH 6.0), made up to 1L in dH_2O.

BMMY: 10g yeast extract (1%), 20g peptone (2%), 13.4g yeast nitrogen base with ammonium sulphate (1.34%), 0.004g biotin (0.0004%), 20mL methanol (2%), 100mM potassium phosphate (pH 6.0), made up to 1L in dH_2O.

BMMY +1% casamino acid: BMMY plus 10g casamino acid (1%), made up to 1L in dH_2O.

CsCl (1.1g/mL): 26.7g CsCl (0.79M), 2mL 1M Tris pH7.8 (10mM), made up to 200mL in dH_2O.

CsCl (1.2g/mL): 53.4g CsCl (1.58M), 2mL 1M Tris pH7.8 (10mM), made up to 200mL in dH_2O.

CsCl (1.3g/mL): 80.1g CsCl (2.38M), 2mL 1M Tris pH7.8 (10mM), made up to 200mL in dH_2O.

His-tag purification washing buffer: 0.68g imidazole (10mM) in 1L PBS.

His-tag purification elution buffer: 34g imidazole (500mM) in 1L PBS

10mM sodium phosphate buffer: 5.75mL 1M Na_2HPO_4, 4.24mL 1M NaH_2PO_4 in 1L dH_2O, pH was adjusted to 7.5.

Heparin column washing buffer: 11.7g NaCl (200mM) was added to 1L 10mM sodium phosphate buffer. pH was adjusted according to experiment.

Heparin column elution buffer: 116.9g NaCl (2M) was added to 1L 10mM sodium phosphate buffer, pH was adjusted according to experiment.

C-tag column elution buffer: 190.4g $MgCl_2$ (2M) was added to 1L PBS.

2.1.3 Adjuvants

All the adjuvants used in this study were obtained from the Jenner Institute Adjuvant Bank. Catalogue numbers of commercially available adjuvants are listed below. Adjuvants that were not commercially available were obtained through Material Transfer Agreements (MTA) with relevant companies.

- **Alhydrogel** (Brenntag Biosector, Denmark). Clinical grade. Lot no. 4565. Content: 3% Aluminium hydroxide (Al(OH)3).

- **Addavax** (InvivoGen, distributed by Source Bioscience). Preclinical grade. Lot no. vac-ad59-32-12-1. Content: Nano-emulsion (160nm) of 2 components, Sorbitan trioleate (0.5w/v) in squalene oil (5% v/v) and Tween 80 (0.5% w/v) in sodium citrate buffer (10mM, pH 6.5).

- **Matrix M** (Isconova, Sweden). Preclinical grade. Content: suspension of nano-sized (40nm) cage-like particles consisting of Purified saponins obtained from a crude extract of the plant Quillaja saponaria Molina; Cholesterol from Lanolin and phosphatidyl choline (phospholipid) from fresh egg yolk.

- **MF59** (Novartis). Clinical grade. Content: suspension of sub-micron (167 ± 20nm) oil-in-water emulsion containing 5% squalene, 1% Tween 80 and 1% Span 85 in 10mM citrate buffer.

- **LMQ** (Vaccine Formulation Laboratory, University of Lausanne, Switzerland). Preclinical grade. Content: liposomes, MPL and QS21 (saponin derived from Quillaja saponaria Molina)

2.2 Methods – Molecular Biology

2.2.1 Antigen insert

The antigen inserts involved in this study include Pfs25, Pfs25-IMX313H, Pfs25-IMX313HT, Pfs25-IMX313T, Pfs25-HBsAg, Pfs25-HBsAgC, Pfs25-GP-Pfs28 and Pfs25-GP-Pfs28-IMX313.

2.2.1.1 Pfs25

Pfs25 sequence (GeneBank locus AAN35500, from Alanine (Ala)-22 to Threonine (Thr)-193) with four potential N-linked glycosylation sites (112, 165, 187 and 202) mutated (described in [204]), was codon optimised for expression in humans and was previously cloned by Dr Anna Goodman [147] into plasmid p1957. In this study, Pfs25 sequence (from p1957) was cloned with a C-terminus His-tag (from p3058) using in-fusion technique. The recombinant sequence was then restriction digested followed by ligation into the PichiaPink (Invitrogen) secreted protein expression plasmid (pPinkα-HC) containing the *Saccharomyces cerevisae* α-mating factor pre-sequence for secretion of recombinant protein. The detailed cloning scheme is summarised in figure 2.1. The details of primer used are in section 2.2.2.

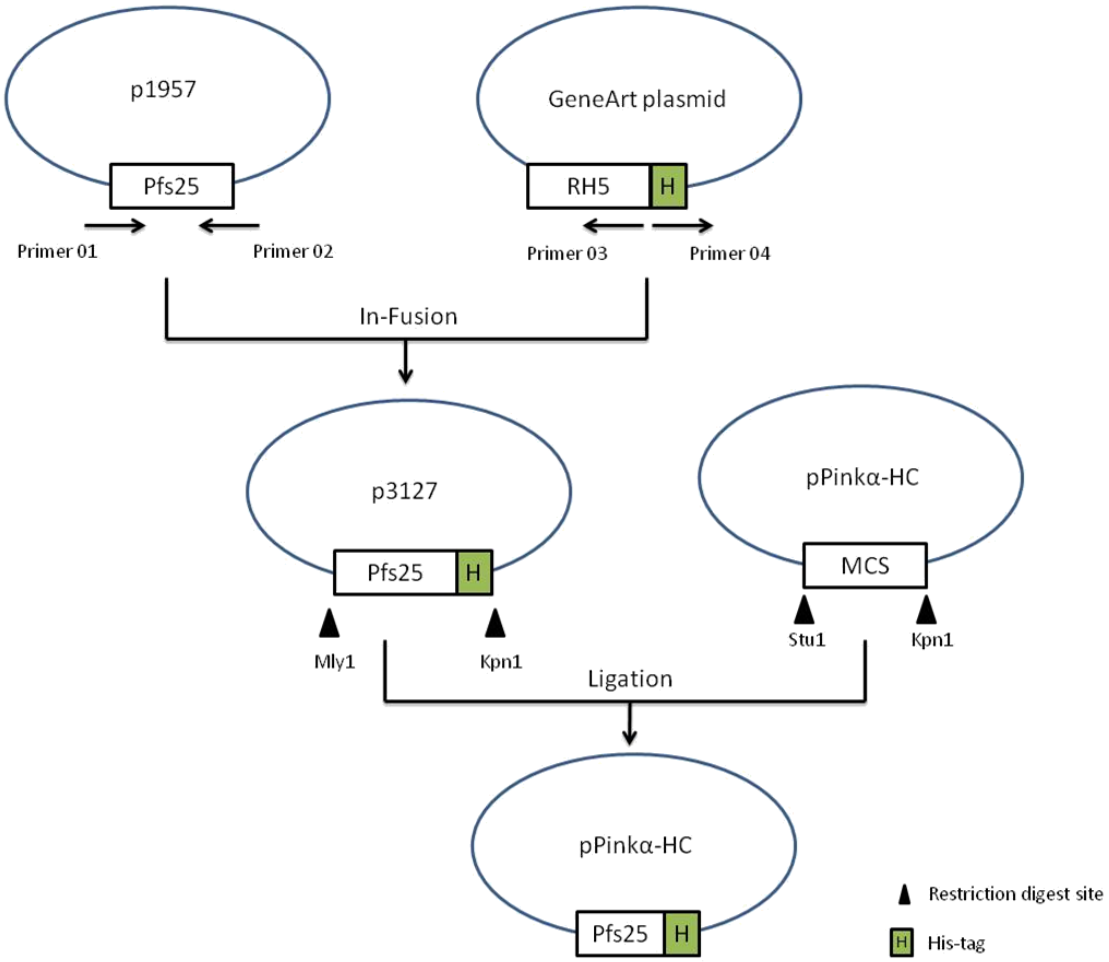

Figure 2.1 Cloning scheme for Pfs25 antigen into pPinkα-HC.

2.2.1.2 Pfs25-IMX313 (H/HT/T)

Pfs25 sequence (from p1957) was constructed with IMX313 sequence (codon optimised for expression in humans) and was previously cloned into plasmid p2797 by Dr Sumi Biswas. In this study, Pfs25-IMX313 was cloned with an N-terminus His-tag using polymerase chain reaction (PCR) into pPinkα-HC plasmid (Figure 2.2). This construct is termed Pfs25-IMX313H.

A modified version of Pfs25-IMX313 was constructed by Dr Fergal Hill (IMAXIO, France) into pPinkα-HC. This modified construct (modification in the C-terminus of IMX313 sequence) is termed Pfs25-IMX313T (fully codon optimised for expression in *P. pastoris*). I have also cloned Pfs25-IMX313T with an N-terminus His-tag into pPinkα-HC using PCR (Figure 2.3), termed Pfs25-IMX313HT.

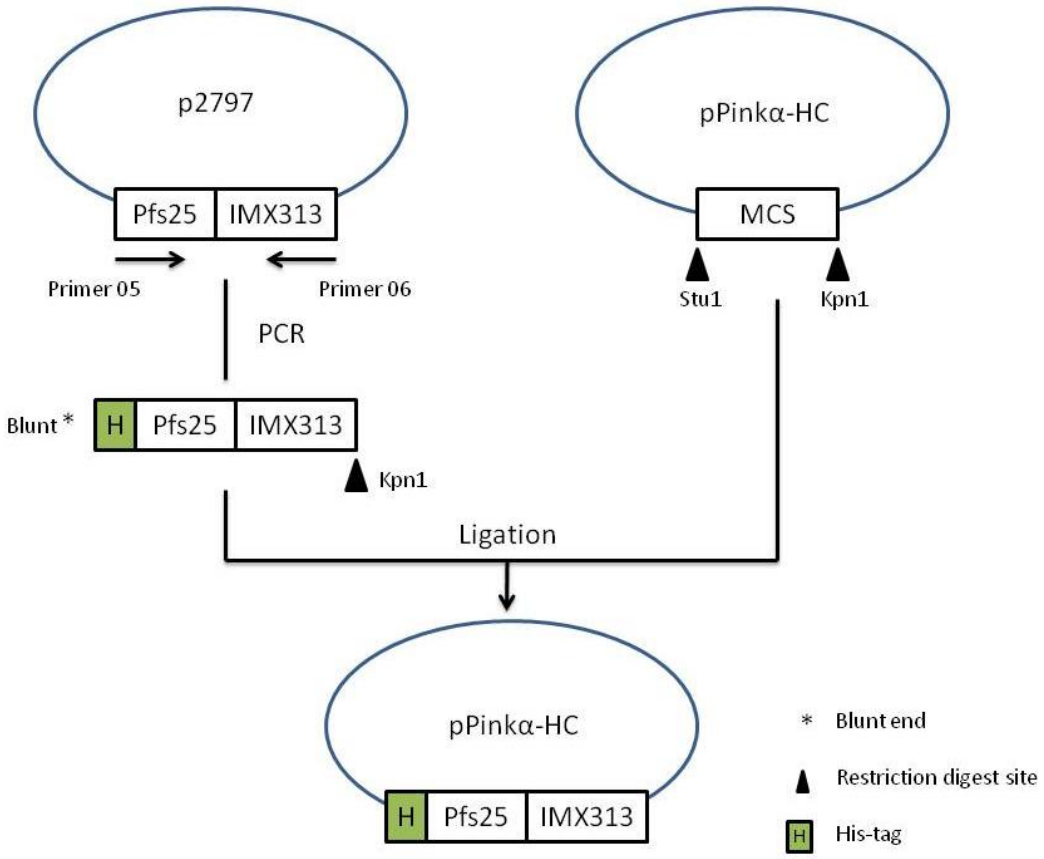

Figure 2.2 Cloning scheme for Pfs25-IMX313H antigen into pPinkα-HC.

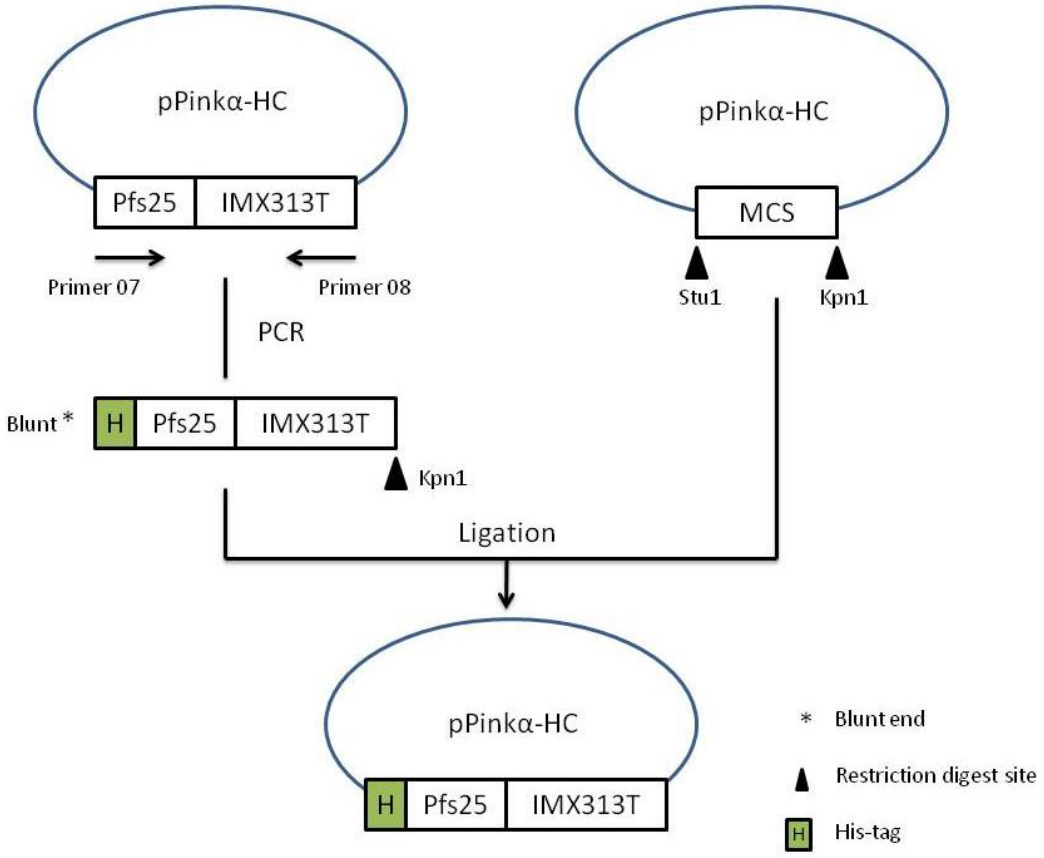

Figure 2.3 Cloning scheme for Pfs25-IMX313HT antigen into pPinkα-HC.

2.2.1.3 Pfs25-HBsAg and Pfs25-HBsAgC

Pfs25 sequence (from p1957) and four amino acids linker sequence (VPTN) plus full length HBsAg sequence (from p2483, plasmid containing sequence of R21, codon optimised for expression in *P. pastoris*) was cloned using PCR followed by infusion cloning into PichiaPink (Invitrogen) intracellular protein expression plasmids pPink-HC and pPink-LC (figure 2.4). This construct is termed Pfs25-HBsAg.

A modified version of Pfs25-HBsAg was cloned with a C-terminus C-tag using PCR into pPink-HC (figure 2.5). This modified construct is termed Pfs25-HBsAgC.

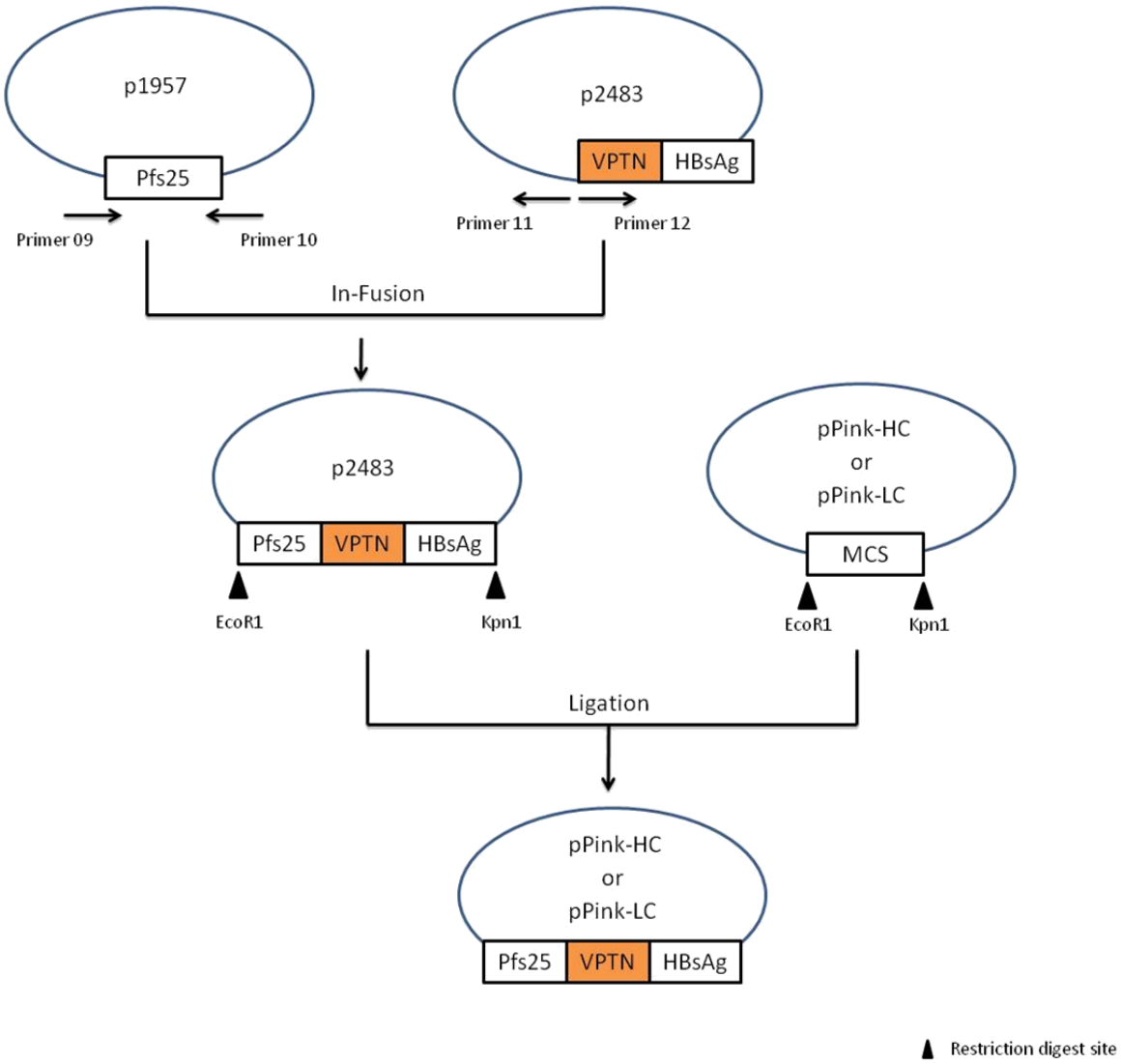

Figure 2.4 Cloning scheme for Pfs25-HBsAg antigen into pPink-HC and pPink-LC.

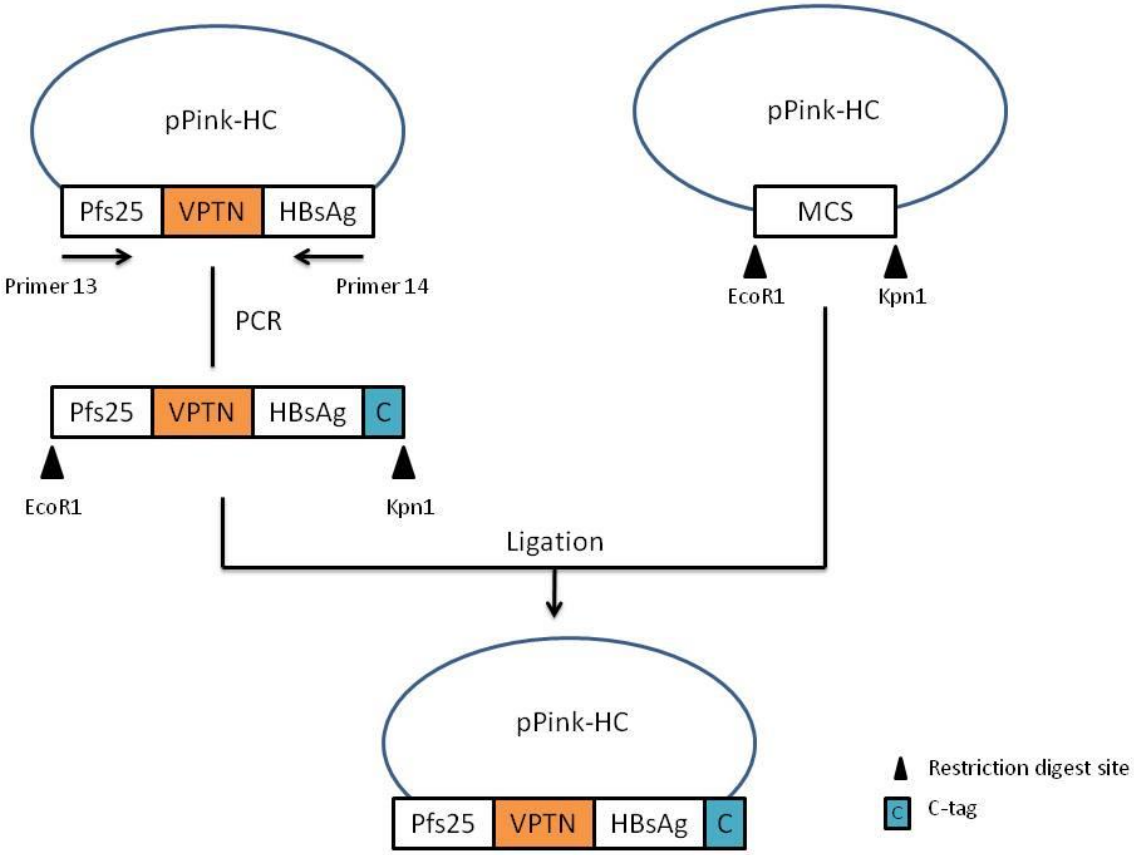

Figure 2.5 Cloning scheme for Pfs25-HBsAgC antigen into pPink-HC.

2.2.1.4 Pfs25-GP-Pfs28 and Pfs25-GP-Pfs28-IMX313

A gene construct (fully codon optimised for expression in human) with Pfs25 (same sequence as before) fused to Pfs28 (GeneBank locus AAT00624, from Valine-23 to Serine-196) with a GGGPGGG (termed GP) linker and a C-terminal IMX313 was ordered from GeneArt® Gene Synthesis (Life Technologies). This construct was codon optimised for expression in humans. Using PCR, Pfs25-GP-Pfs28 (figure 2.6) as well as Pfs25-GP-Pfs28-IMX313 (figure 2.7) was cloned with an N-terminus His-tag into pPinkα-HC plasmid.

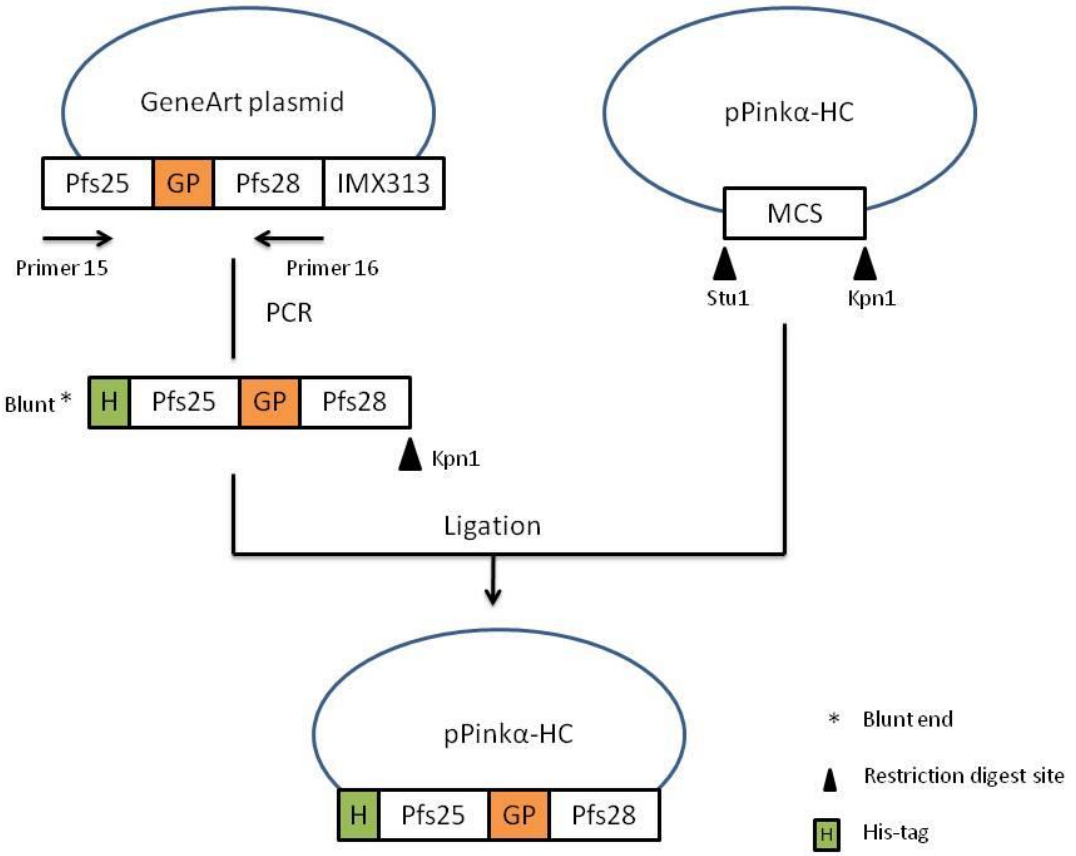

Figure 2.6 Cloning scheme of Pfs25-GP-Pfs28 antigen into pPinkα-HC.

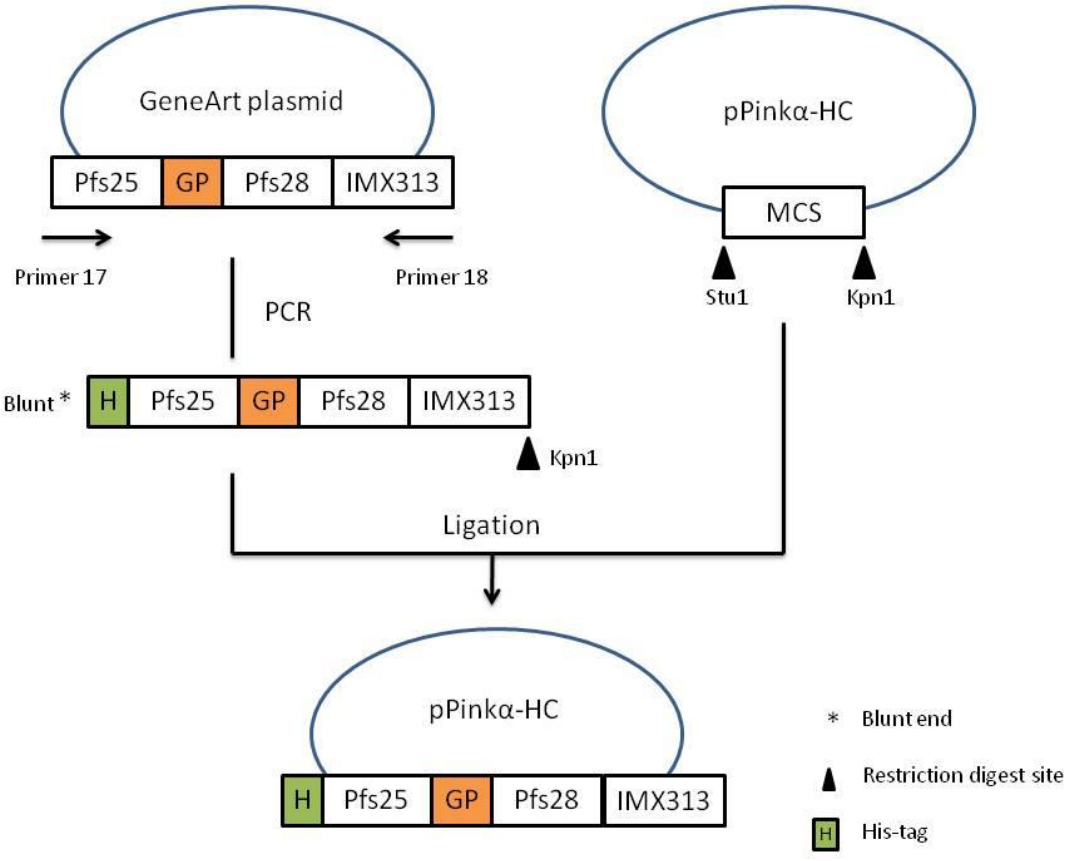

Figure 2.7 Cloning scheme of Pfs25-GP-Pfs28 antigen into pPinkα-HC.

2.2.2 Polymerase chain reaction (PCR)

PCR reaction in this study was carried out using the primer sets indicated in table 2.2. Phusion® High-Fidelity PCR Master Mix (NEB, UK) was used to carry out PCR reaction. The reason for using the Phusion® High-Fidelity DNA Polymerase was that this polymerase can create blunt end PCR product which was required for the DNA ligation reactions in this study. The standard PCR reaction mixture is summarised in table 2.3 and the PCR reaction temperature/time settings is summarised in table 2.4.

Primer name	Sequence 5'---3'
01	CATCACCATCACCACCACTAATAGG
02	ACGTCGACTCATGCGGCC
03	CGCATGAGTCGACGTGCCAAAGTGACCGTGGACACCG
04	GTGGTGATGGTGATGGGTGCAGATGCTGCTTTCCTGGTC
05	CATCACCATCACCACCACGCCAAAGTGACCGTGGACACCG
06	GGTACCTTATTACTCCTTGCTCAGTCCTTGCAA
07	CATCACCATCACCACCACGCCAAAGTGACCGTGGACACCG
08	GCCGGCCGGTACCTTATTAAGAAC
09	TCGAATTCAAAAATGGCCAAAGTGACCGTGGAC
10	CATATTGGTAACTGGGGTGCAGATGCTGCTTTCC
11	CATTTTTGAATTCGAGCTCATG
12	CCAGTTACCAATATGGAAAACAT
13	CGACAACTTGAGAAGATCAAAAAACA
14	AAGGTACCTTATTAAGCCTCTGGCTCAATGTAAACCCACAAGCAAAAGAA
15	CATCACCATCACCACCACGCCAAAGTGACCGTGGACACCG
16	CGGTACCTCATCACTCTTTGCTCAGGCCCTG
17	CATCACCATCACCACCACGCCAAAGTGACCGTGGACACCG
18	CGGTACCTCATCAGCTGTAGCTTGTGTCGGCCTGATCC

Table 2.2 Primers used in this study.

Components	25 µL Reaction	Final Concentration
10 µM Forward Primer	1.25 µL	0.5 µM
10 µM Reverse Primer	1.25 µL	0.5 µM
2X Phusion Master Mix	12.5 µL	1X
Template DNA	variable	<250 ng
Nuclease-Free Water	to 25 µL	

Table 2.3 Components of each PCR reaction.

Step	Temperature	Time
Initial Denaturation	98°C	30 seconds
30 Cycles	98°C	10 seconds
	variable (55°C-72°C)	30 seconds
	72°C	30 seconds/kb
Final Extension	72°C	10 minutes
Hold	4°C	

Table 2.4 General PCR reaction settings.

2.2.3 In-Fusion cloning

In-fusion cloning technique allows fusing DNA fragments into vectors without using traditional restriction digestion and ligation reactions. Instead, the in-fusion enzyme utilizes a 15bp overlap at the insertion site, which can be easily engineered by designing primers for amplification of the desired sequences. This technique is particularly helpful if the insert/vector lacks available restriction enzyme digestion sites. In-Fusion cloning was carried out using the In-FutionⓇ HD Cloning Kit (Clontech, UK) and the components of the reaction are summarised in Table 2.5.

Components	10 µL reaction
Purified PCR Fragment	100-200 ng
Linearized Vector	50-100 ng
5X In-Fusion HD Enzyme Premix	2 µL
Nuclease-Free Water	to 10 µL

Table 2.5 In-Fusion reaction components.

2.2.4 Restriction Digest

Restriction digest were carried out at 37°C and incubated for 2 hours. I used restriction endonucleases from New England Biolabs (NEB, UK) and the reaction components are outlined below in Table 2.6.

Components	20 µL reaction
NEB Restriction Enzymes (10,000U/mL)*	1 µL
NEB Restriction Buffer (10X)	2 µL
BSA (10X) (if required)	2 µL
DNA	0.5-1 µg
Nuclease-Free Water	To 20 µL

* double-digests using 1 µL of each enzyme

Table 2.6 Restriction digest reaction components.

2.2.5 Agarose Gel electrophoresis

PCR reaction products as well as other DNA reaction products including restriction enzyme digest were analyzed using 1% agarose gel electrophoresis (100V, 60min) in 1X Tris-acetate-EDTA (TAE) buffer. DNA was stained with SYBR Safe (Life Technology, UK) and the gel was

visualised on a transilluminator. The size of the bands was estimated by comparing it to the molecular weight marker: SmartLadder (Eurogentec, UK).

2.2.6 Ligation

Digested DNA fragments were cut and isolated from agarose gels. The DNA was purified from the gel using QIAquick PCR Purification Kit (QIAGEN, UK). T4 DNA ligase (NEB, UK) was used for overnight ligation reactions at 16°C (reaction components outlined in Table 2.7). Once the reaction was completed, the sample was stored at -20°C.

Components	**20 µL reaction**
10X T4 DNA Ligase Buffer	2 µL
Vector DNA	20-50 ng
Insert DNA	50-100 ng
T4 NDA Ligase	1 µL
Nuclease-Free Water	to 20 µL

Table 2.7 Ligation reaction components.

2.2.7 Bacterial transformation

Ligation or in-fusion reaction products were transformed into chemically competent *Escherichia coli*. Briefly, 50 µL High efficiency DH5α competent cells (NEB, UK) were thawed on ice for 10 min. 1-5 µL containing 100 ng or less plasmid DNA we added to the cell. After incubation on ice for 30 min, the cell and plasmid mixture was heat-shocked at 42°C for 30 seconds followed by further incubation on ice for 5 min. 950 µL S.O.C. medium (NEB, UK) (used in the final step of bacterial cell transformation to obtain maximal transformation efficiency of *E. coli.*) were added to the mixture and bacteria were allowed to grow at 37°C

for 1 hour. Bacteria were then plated onto LB agar containing selection antibiotics as required. The plates were incubated at 37°C overnight before storage at 4°C.

2.2.8 Plasmid DNA preparation

After bacteria transformation and incubation of plates, individual colonies were selected and cultured overnight at 37°C in 2mL LB medium under antibiotics selection. Next day, plasmids from the bacteria were purified using QIAprep spin miniprep kit (Qiagen, UK). PCR and/or restriction digest were performed to indentify if plasmids were correct. Colonies carrying the plasmids with the right DNA construct were amplified by incubation at 37°C overnight in 120mL LB medium with selection antibiotics. The plasmids were purified using QIAGEN plasmid midi kit. At this stage, the plasmids DNA construct were further confirmed by sequencing (Sanger sequencing services; Oxford, UK) and stored at -20°C.

2.2.9 *Pichia pastoris* transformation

Before transformation, 5µg to 10µg of PichiaPink expression plasmids containing insert were linearized by restriction enzyme EcoNI (NEB, UK) digest at 37°C for 2 hours. The linearized plasmid was purified by QIAquick® PCR Purification Kit (Qiagen, UK).

Each strain (strain 1, 2, 3 and 4) of *Pichia pastoris* were streaked from the PichiaPink Kit glycerol stock on YPD agar plates (1% yeast extract, 2% peptone, 2% dextrose and 2% agar). The plates were incubated at 25°C for 5 days until colonies were visible. One colony from each strain was selected and inoculated into a sterile 125mL flask (Corning) containing 10mL YPD media. The flasks were incubated in at 30°C (300 rpm). After 2 days, the whole 10mL starter culture was added to a sterile 1 litre flask (Corning) containing 100mL of YPD media (1% yeast extract, 2% peptone and 2% dextrose). The 1 litre flask was left in the same

incubator growing at the same conditions overnight. After the cell had reached the optimum OD_{600} density of 1.3-1.5 (log phase growth), the cultures were transferred into 250mL centrifuge tubes (Corning). Cells were pelleted at 1,500g at 4°C for 5 minutes. Cells were then washed with 250mL ice-cold sterile water, followed by 50mL ice-cold sterile water wash, and then 10mL of ice-cold 1M sorbitol. In the end, the cells were re-suspended in 500uL of ice-cold 1M sorbitol.

80uL of the electrocompetent cells from previous step were mixed with 5µg to 10µg of linearized plasmid DNA and transferred to an ice-cold 0.2 cm electroporation cuvette (Bio-Rad). The cuvette was incubated on ice for 5 minutes followed by electroporation in Bio-Rad GenePulser Xcell using pre-set manufacturer's protocol. Immediately after pulsing the cells, 1mL of ice-cold YPDS media were added into the cuvette which was then incubated at 25°C for another two hours. After the incubation, 200 uL of the cell mixtures were spread on PAD selection plates (adenine deficient). All strains of PichiaPink *P. pastoris* are adenine auxotrophs that are unable to grow in the absence of adenine due to the full deletion of the *ADE2* gene (encoding phosphoribosylaminoimidazole carboxylase) and part of its promoter. The expression plasmids contain the ADE2 genes (under its own promoter) which will restore the adenine metabolism once transformed into PichiaPink *P. pastoris.* The PAD plates were incubated at 25°C for 5 days until distinct white colonies were formed.

2.2.10 *Pichia pastoris* pilot (small scale) protein expression

4-5 colonies from each transformation have been selected, and inoculated into 5mL of BMGY medium (1% yeast extract, 2% peptone, 1.34% yeast nitrogen base without amino acid, 0.0004% biotin, 1% glycerol, 100mM potassium phosphate pH 6.0) in a 14mL round-bottom tube (BD Falcon). Cells were grown for 2 days at 25-30°C (depending on the protein

expressed) and 300rpm in a shaking incubator followed by centrifugation at 1500g for 5 minutes at room temperature. BMGY medium were then decanted and 1mL of BMMY medium (1% yeast extract, 2% peptone, 1.34% yeast nitrogen base without amino acid, 0.0004% biotin, 0.5% glycerol, 100mM potassium phosphate pH 6.0) was added to the culture. The cells in BMMY were returned to 25-30°C shaking incubator for further growth overnight. 4% methanol (v/v) was added to the culture every 24 hours. After 72 hours of induction, cells were separated from the supernatant by centrifugation for 10 minutes at 1500g. Both cells and supernatants were stored at -80°C for further analysis. The expression of different recombinant proteins were tested by running the supernatant (extracellular expression) or cell lysate (intracellular expression) on an SDS-PAGE followed by western blot and/or Coomassie blue staining. The yeast cell pellets were lysed using Y-PER yeast lysis reagent (Thermo Scientific, UK).

2.2.11 *Pichia pastoris* large scale protein expression

After the pilot expression, the clone with the highest protein expression (determined by western blot in 2.2.10) was selected for large scale protein expression. A single colony was inoculated with 25mL of BMGY in a 250mL flask (Corning).This starter culture was grown at 25-30°C in the shaking incubator (300rpm) for two days. Then this 25mL start culture was inoculated in a total of 2L BMGY in four 2L flask (Corning). The cells were grown under the same condition for a further 2 days after which BMGY were decanted and cells were re-suspended in a total of 800mL (intracellular expression) or 400mL (extracellular expression) BMMY and split in two 2L flasks (Corning). The cells were then grown at 25-30°C with continuous shaking. PureLink Air Porous Tape (Invitrogen) was used to cover the flask to ensure sufficient aeration. 2%-4% Methanol (v/v, depending on the protein expressed) was

added to every 24 hours until the optimal time of induction was reached. After the fermentation, cell pellets (intracellular expression) were stored at -80°C and the supernatant (extracellular expression) were subjected to purification straight away.

2.2.12 Purification of Pfs25, Pfs25-IMX313H/HT, Pfs25-GP-Pfs28

The culture supernatants from 2.2.11 were filtered through a 0.22 µm polyethersulfone (PES) membrane filter (Thermo Scientific, UK). The sample was then immediately loaded onto HisTrap excel column (GE healthcare, UK) using a Peristaltic pump (Gilson, UK). The column was washed with 5 column volumes (CV) of PBS containing 10mM imidazole (pH 7.4) and the protein sample was eluted into fractions using 500mM imidazole, PBS (pH 7.4). SDS-PAGE followed by Coomassie blue staining and/or western blot was performed to identify protein containing fractions. Fractions with protein were pooled and concentrated using a 10,000MW cut-off ultrafiltration unit (Amicon, UK). Depending on the study, some of the proteins were then buffer exchanged using PD-10 column (GE healthcare, UK); others were purified further by size exclusion chromatography using Superdex 200pg gel filtration column (GE healthcare, UK) connected to AKTA purifier (GE healthcare, UK). Purified protein was concentrated and the protein concentration was determined by nanodrop (Thermo Scienctific).

2.2.13 Purification of Pfs25-IMX313T

The culture supernatant from 2.2.11 was first filtered through a 0.22 µm PES membrane. The sample was then subjected to tangential flow filtration (TFF) using 10kDa cut off membrane (Millipore, UK). The supernatant was then loaded onto HiTrap Heparin HP column (GE healthcare, UK) using AKTA purifier and washed with 10mM phosphate buffer containing 200mM NaCl. The protein was eluted with 10mM phosphate buffer containing

2M NaCl. Positive elution fractions containing the protein were pooled and size exclusion chromatography purification was performed using Superdex 200pg column. Purified protein was canalysed by Coomassie blue staining and/or western blot, followed by protein concentration measurement using nanodrop.

2.2.14 Purification of Pfs25-HBsAg

Pfs25-HBsAg expressing *Pichia pastoris* cell pellet (20mL) was resuspended in 6mL of lysis buffer together with 3 grams of 425-600µm acid washed glass beads (Sigma Aldrich, UK) and 1500 units of benzonase (Sigma-Aldrich, UK). The mixture was vortexed for 1 minute and then incubated on ice for another 1 minute. This procedure was repeated for 10 times after which the sample was incubated at room temperature for another 15 minutes. Samples were then centrifuged at 1500xg for 5 minutes at 4°C. The supernatant was transferred to a fresh tube followed by clarification (by centrifugation at 13,000xg for 20 minutes using benchtop ultra centrifuge (Beckman Coulter)). Clarified supernatant was then subjected to a two-step purification using cesium chloride (CsCl) density gradient centrifugation. First, 3.5mL of 1.1g/mL CsCl followed by 4mL of 1.3g/mL CsCl were carefully placed into one 13.2mL ultraclear centrifuge tubes (Beckman Coulter, UK). 4.5mL of clarified yeast extract were added into each tube followed by 2 hours centrifugation at 41,000 rpm in Optima L-100 XP Ultracentrifuge (Beckman Coulter, UK). After the first step centrifugation, the sample band was extracted by a needle and syringe followed by buffer exchange in 10mM Tris pH7.8 using PD-10 column. After this the buffer exchanged samples were subjected to a "continuous" CsCl purification, this time only 1.3g/mL CsCl were used to mix with the sample. The centrifugation was done at 41,000 rpm for 20 hours, after which the sample band was collected again by needle and syringe. Collected samples were buffer exchanged

again by PD-10 and confirmed by Coomassie blue staining and western blot before transmission electron microscope (TEM) analysis.

2.2.15 Purification of Pfs25-HBsAgC

Pfs25-HBsAgC expressing *Pichia pastoris* cell pellets (20mL) were lysed and clarified using the same methods as described in 2.2.14. Cell lysate were then loaded onto XK 16/20 column (GE healthcare, UK) packed with C-tag resin (Life technology, UK) using AKTA start (GE healthcare, UK). The column was washed with 10 column volumes (CVs) of PBS and the protein was eluted with PBS containing 2M MgCl. PD-10 columns were used to buffer exchange the protein into 10mM Tris pH7.8. Coomassie blue staining and western blot were performed to identify the purified protein and sent for TEM analysis.

2.2.16 SDS-page and western blot analysis

All protein samples were prepared in 4X Lithium dodecyl sulfate (LDS) sample buffer (Life Technology, UK); if protein samples needed to be reduced, 250mM of DTT (Life Technology, UK) was added. The samples were heated to 70°C for 10 minutes then resolved on precast Precise SDS Tris-HEPES gels (Thermo Scientific, UK). SDS-PAGE was analyzed by Imperial Protein Stain (Thermo Scientific, UK) or Pierce Silver Stain (Thermo Scientific, UK) according to the manufacturer's protocols.

Western blots were performed using Trans-Blot® Turbo™ transfer system and related nitrocellulose membrane (Bio-Rad, UK). Blots were probed with various primary antibodies in this study including: anti-HBsAg mAb (AbD Serotec, UK), anti-Pfs25 4B7 mAb (MR4, USA), Pfs25 antiserum (from mice vaccinated with viral-vectors expressing Pfs25 or recombinant Pfs25 protein), and anti-Histag mAb (Invitrogen, UK); the secondary antibody was alkaline

phosphatise conjugated donkey anti-mouse secondary antibody (Jackson ImmunoResearch Laboratories, UK). The blot was visualised using BCIP/NBT (Sigma-Aldrich, UK) and digital images were taken using CANOSCAN LIDE 200 scanner.

2.2.17 Transmission electron microscopy

Transmission electron microscopy (TEM) was performed either at the Dunn school bio imaging facility (Sir William Dunn School of Pathology, University of Oxford) by Dr Errin Johnson or in collaboration with Dr Juha T Huiskonen at the Oxford Particle Imaging Centre (Wellcome Trust Centre for Human Genetics, University of Oxford). Samples were negative stained with uranyl acetate on TEM grid for 30 seconds followed by PBS washes before visualisation on TEM.

2.3 Methods-Immunology

2.3.1 Animals

All animal work was performed in accordance with the terms of the UK Animals (scientific Procedures) Act Project Licence (PPL 30/2889) and was approved by the University of Oxford Animal Care and Ethical Review Committee. All mice involved in this study were housed in the Wellcome Trust Centre for Human Genetics animal facility under Specific Pathogen Free (SPF) conditions. Female BALB/c mice were ordered from Harlan (UK) and were at 6-10 weeks old at the start of experiments.

2.3.2 Protein-in-adjuvant formulation

For protein-in-adjuvant vaccines the proteins were stored in either PBS or Tris (20mM) and formulated with adjuvant as summarised in table 2.8.

Adjuvant	Formulation
Alhydrogel	Mixed with antigen in 10mM Tris buffer. 85µg (8.5µL) Alhydrogel per dose in mice
Addvax	Mixed with antigen in PBS at a 1:1 volume ratio. 25µL of Addavax per dose in mice
Matrix M	Mixed with antigen in PBS. 12µg (5µL) of Matrix M per dose in mice
MF59	Mixed with antigen in PBS at a 1:1 volume ratio. 25µL of MF59 per dose in mice
LMQ	Mixed with antigen in PBS. 30µg of LMQ per dose in mice

Table 2.8 Formulation of adjuvants used in this study.

2.3.3 Viral vectored vaccine formulatiuon

Viral vectored vaccine (ChAd63 and MVA) in this study was already available. Vaccines were stored in sterile, endotoxin tested PBS in -80. For ChAd63, 1×10^8 infectious unit (IU) and for MVA 1×10^7 plaque formation unit (PFU) were used per dose in mice.

2.3.4 Immunisation

Mice were anaesthetised before each immunisation by using inhalational anaesthetic (isofluorane (3.5%) and oxygen (2L/min)). All immunisations in this study were performed by the intramuscular (I.m.) route. Vaccines were administrated in 50 µL volume per mice (25 µL in each *musculus tibialis*) using 26G needles. The dose and the prime-boost intervals varied between experiments and are summarized in the relevant corresponding sections.

2.3.5 Pfs25 standardised ELISA

Blood from mice was collected from tail vein using microvette tubes or by cardiac puncture into eppendorf tubes. The blood was allowed to clot at 4°C overnight. Serum was then collected by centrifugation at 13,000G for 5 minutes and stored in clean eppendorf tubes at -20°C until use.

ELISA against Pfs25 was performed according to a standardized protocol using a reference standard serum. This protocol has been described previously [205]. Basically, Nunc-Immuno maxisorp plates (Thermo Scientific, UK) were coated with Pfs25 protein at 1 µg/mL concentration overnight at room temperature (RT). Plates were washed with PBS and blocked for an hour with 5% skimmed milk powder in PBS. Test serum samples were diluted and added to the plate so that their O.D. $_{405}$ lies in the linear part of the curve of the reference serum. Plates were incubated for 2 hours at room temperature and then washed with PBS as before. Donkey anti-mouse total IgG conjugated to alkaline phosphatease (Jackson ImmunoResearch Laboratories, UK)) was added to the plate (1:5000 dilution in PBS) for 1 hour at RT. After a final wash in PBS/T, p-nitrophenylphosphate (Sigma, UK) at 1mg/mL diluted in diethanolamine buffer (Thermal Scientific, UK) was used as a developing substrate. Optical density (OD) was read at 405 nm using ELx800 absorbance microplate reader (Biotek, UK).

All samples were tested against a set of serially diluted standard reference serum (supplied by NIH and was previously reported [173]) with known antibody titre. The absorbance of individual test samples was converted into arbitrary antibody units (AU) using a standard curve generated by this standard reference serum. The antibody unit value of a standard was assigned as the reciprocal of the dilution giving an O.D. $_{405}$ = 1. An internal control (IC) with known Pfs25 antibody unit was included in each plate. The plate was allowed to develop until the AU readout of IC reaches the actual AU. And as described previously [205], the result of a plate was only accepted when: 1. Standard curve R^2 value was more than 0.994; 2. Sample O.D. value was between 0.2 and 1.6 (which mostly represented the linear part of the standard curve).

2.3.6 Whole IgG ELISA

Similar to Pfs25 standardised ELISA, Nunc-Immuno maxisorp plates (Thermo Scientific, UK) were coated with the protein of interests at 1µg/mL concentration and left overnight at RT. The next day the plates were washed in PBS and blocked with 5% skimmed milk powder in PBS. Test serum samples were diluted down the plate as required and each sample was run in duplicate.The plate was then incubated at room temperature for 2 hours followed by washing in PBS/T. Donkey anti-mouse total IgG conjugated to alkaline phosphatase was added (1:5000). The plates were developed using the same reagent as for Pfs25 standardised ELISA. The OD was read at 405 nm using the same ELISA reader. The readout for whole IgG ELISA is endpoint titer which is defined as the X-axis intercept of the dilution curve at an absorbance value ($\pm$ three standard deviations) greater than the OD for serum sample from naïve mouse. Both positive serum sample and naïve serum sample were included in each assay to serve as controls.

2.3.7 Isotype ELISA

To detect antigen-specific IgG1 and IgG2a responses, Nunc-Immuno maxisorp plates were coated at a concentration of 1µg/mL with Pfs25 as before. The plates were washed, blocked and serum samples were added as described in section 2.3.6. For the secondary antibody, biotinylated anti-mouse IgG1 or IgG2a (BD bioscience, UK) was diluted at 1:500 dilution in PBS, added to the wells and the plates were incubated at room temperature for 1 hour. Following the wash in PBS/T, alkaline phosphatase conjugated ExtrAvidin (Sigma-Aldrich, UK) was added at 1:5000 in PBS and incubated for 30 minutes at room temperature. The development and measurement of OD was the same as described in 2.3.6.

2.3.8 Avidity ELISA

Antibody avidity was assessed using a sodium thiocynate (NaSCN)-dissociation ELISA. Basically, Nunc-Immuno maxisorp plates were coated with Pfs25 and blocked, washed as whole IgG ELISA. All individual serum samples with known Pfs25 antibody unit were diluted to give a Pfs25 antibody unit of 1. Samples were added in duplicates, following incubation and washing, an ascending concentration of the NaSCN (0-7M) was added to the well. The plates were incubated at room temperature for 15 minutes followed by washing and further development similar to the whole IgG ELISA. Two readouts were used to analyze the result: the first readout was plotted as the percentage of binding against the molar concentration of NaSCN (assuming at 0M NaSCN, the percentage of binding was 100%); the second readout was the intercept of the curve (molar concentration of NaSCN/OD) where OD reached a 50% reduction of the OD in NaSCN-free samples.

2.3.9 Splenocyte preparation

Mice were sacrificed at day 9 and day 14 after intramuscular (i.m.) immunisation. Spleens were excised and collected into 5mL complete medium. The spleen was mashed in a 6-well plate and cells were recovered by passing through a 70µm strainer (Corning) followed by centrifugation at 1350 rpm for 5 minutes. Supernatant were discarded and pellets resuspended in ACK lysis buffer for 5 minutes before addition of 25mL PBS. The mixture was immediately centrifuged again and resuspended in 5mL complete medium. Cells were counted using a CASY counter (Scharfe System, Germany).

2.3.10 Draining lymph node preparation for FACS staining

Mice were sacrificed at day 9 and day 14 after intramuscular (i.m.) immunisation. The inguinal and popliteal lymph nodes (LNs) were excised. Lymph nodes were collected into

5mL complete medium. LNs were then crushed in a 6-well plate and cells were recovered by passage through a 70µm strainer (Corning) followed by centrifugation at 1350 rpm for 5 minutes. Supernatant were discarded and cells were resuspended in FACS buffer before staining.

2.3.11 Germinal centre staining

Draining inguinal and popliteal LNs and spleens were prepared as described in 2.3.9 and 2.3.10. Cells were transferred to 96 well V-bottom plates and centrifuged (300g, 5 min). Supernatants were then discarded and cells were resuspended in FC block (1:50) for 15 minutes. Following a wash in FACS buffer, cells were stained with anti-GL-7 AlexaFluor 647 (eBioscience, UK) at 1:100 dilution, anti-CD95 PE (eBioscience, UK) at 1:100 dilution and anti-B220 PeCy7 (eBioscience, UK) at 1:200 for 30 minutes at room temperature in the dark. After this incubation, cells were washed twice and resuspended in FACS buffer and data were acquired on a LSR2 and analysed by FlowJo (TreeStar Inc).

2.3.12 Follicular helper T cell staining

Draining inguinal and popliteal LN was prepared as described in 2.3.9. Cells were transferred to 96 well V-bottom plates and centrifuged (300g, 5 min). Supernatants were discarded and the cells were resuspended in FC block (1:50) for 15 minutes. Following a wash in FACS buffer, cells were stained with APC conjugated anti-mouse CD4 (eBioscience, UK) at 1:100, PE-Cy7 conjugated anti-mouse CXCR5 (eBioscience, UK) at 1:50 and PE conjugated anti-mouse PD1 (eBioscience, UK) at 1:100 for 30 minutes at room temperature in the dark. After this incubation, cells were washed twice and resuspended in FACS buffer and data were acquired on a LSR2 (BD Biosciences, UK) and analysed by FloJo (TreeStar Inc). The

CXCR5+ and PD1+ gates were set using a Fluorescence Minus One (FMO) control, which contained only anti-CD4 and anti-PD1 or anti-CXCR5 antibodies respectively.

2.3.13 Draining lymph node sectioning and immunostaining

Mice were sacrificed at day 14 after intramuscular (i.m.) immunisation. The inguinal and popliteal lymph nodes (LNs) were excised. LNs were then immediately frozen in Optimal Cutting Temperature (OCT) compound (Thermo Scientific, UK) on dry ice. The sectioning was performed using Cryostat Leica CM3050S (Leica Biosystems, UK). 10 µm sections were taken and fixed on glass slides. Slides were stored in -80 before immunostaining.

Glass slides containing sectioned LN sample were fixed with 100% acetone for 10 minutes at -20°C and then air dried for 30 minutes. Slides were rehydrated in PBS for 10 minutes and then blocked with 5% PBS/BSA for 45 minutes. After a wash with PBS, the slides were incubated with primary antibodies: Alexa Fluor 488 conjugated anti-mouse GL-7 (1:100) and PE conjugated anti-mouse B220 (1:100) at room temperature for 1 hour. The slides were then washed 3 times for 10 minutes each with PBS. After this, FLuoromount G mounting medium (eBioscience, UK) was applied to the slides and coverslips were placed. Slides were then visualised using DMI3000B (Leica Microsystems, UK). Digital picture of the slides were taken and analysed by ImageJ.

2.3.14 Protein fluorescence labelling

Alexa Fluor 488 protein labelling kit (Invitrogen, UK) was used to label both Pfs25 monomeric and multimeric proteins. The method used was according to the commercial kit protocol. Basically, 0.5mL of protein at 2mg/mL concentration was incubated with AF488 and 100mM bicarbonate (provided by kit) at room temperature for 1 hour. After incubation,

unconjugated fluorescence dye was removed by size exclusion column (provided in the kit). Protein concentration after conjugation was measured by the absorbance at 280 nm and 494 nm (A280 and A494) with 1 cm pathlength and calculated using the following equation:

$$Protein\ concentration\ (M) = \frac{[A280 - (A494 \times 0.11)] \times dilution\ factor}{molar\ extinction\ coefficient\ of\ protein}$$

The degree of labelling was calculated using the flowing equation:

$$Moles\ dye\ per\ mole\ protein = \frac{A494 \times dilution\ factor}{71{,}000 \times protein\ concentration\ (M)}$$

2.3.15 In vitro macrophage culturing and antigen uptake analysis

In this study, the THP-1 leukemic monocyte cell line (ATCC, UK) was kindly provided by Dr Paulo Bettencourt. The THP-1 cells were passaged and cultured in T75 tissue culture flask (Sigma-Aldrich, UK) with complete medium at 37°C and 5% CO_2. After the cell density reached the required level (less than $1x10^6$ cells/mL), cells were spun down, resuspended in complete medium and counted. 1 million cells were seeded with 2 mL complete medium plus 20 nM PMA (Sigma-Aldrich, UK) into each well of 12 well plates (Sigma-Aldrich, UK). Cells were incubated overnight followed by replacement of 2mL fresh complete medium the next day. After overnight incubation and replacement of medium, 10 µg of AF488 conjugated protein (Pfs25 and Pfs25-IMX313H) as well as PBS (negative control) were added to the wells. Cells were collected by treatment of Trypsin/EDTA (Life technology, UK) after 1, 3, 6 and 24 hour of incubation. Cells were immediately fixed after collection with 4% paraformaldehyde for 15 minutes and washed with PBS twice. Data on AF-488 positive cells was acquired using LSR 2 and analyzed using flowjo software.

2.3.16 Standard membrane feeding assay (SMFA)

Individual serum samples from each test group were pooled and sent to Dr Kazutoyo (NIH) and the rest of the SMFA was performed at the MVI SMFA reference laboratory at the NIH led by Dr Carole Long. Total IgG were purified using protein G columns. The ability of these vaccine induced IgGs to block the development of *P. falciparum* was measured using SMFA as described before [206]. The purified IgGs were diluted in heat-inactivated human AB+ sera and mixed with *in vitro* cultured mature Stage V *P. falciparum* NF54 gametocytes (the % of mature Stage V gametocytes was adjusted to 0.15% ± 0.05% and the male-female ratio is stable (almost always 1 male: 2-3 female)) at total IgG concentrations of 375 µg/mL, 188 µg/mL, 94 µg/mL or 47 µg/mL. Purified IgGs from ovalbumin (OVA) vaccinated mice served as a negative control and was mixed with NF54 gametocytes at a total IgG concentration of 375 µg/mL. These mixtures were fed to 4-6 day old starved female *A. stephensi* via a parafilm® membrane. The mosquito mid-gut was dissected after 7 days of the feed and the oocysts count were recorded for further analysis. Both transmission reducing activity (TRA) and transmission blocking activity (TBA) was measured for the test samples in relation to the control as follows: TBA=100*(1-prevalence of infection for mosquitoes fed with immune plasma/ prevalence of infection forcontrol group). TRA=100* (1 - mean oocyst number with immune plasma/ mean oocyst number in control group).

2.4 Statistical Analysis

For ELISA and GC FACS staining data, statistical analysis was performed using Prism 5 (Graphpad Software Inc., La Jolla, CA, USA). Mann-Whitney test or Kruskal-Wallis test with Dunn's multiple comparison post-test was performed depending on the number of groups in a test. For GC and Tfh correlation analysis, Spearman's rank correlation coefficient was

calculated. The ability of vaccine-induced antibodies to inhibit oocyst intensity (TRA) of *P. falciparum* in SMFA was assessed in Malaria Vaccine Initiative (MVI) SMFA reference centre using a negative binomial with zero inflated model as previously described in [120]. Significance was taken as $p<0.05$.

Chapter 3

Expression, purification and immunogenicity of recombinant soluble Pfs25

3 Expression, purification and immunogenicity of recombinant soluble Pfs25

3.1 Introduction

Pfs25 has been successfully expressed as recombinant protein from various expression systems including *E.coli* [207], *Saccharomyces cerevisiae* [208], *Pichia pastoris* [209], *C. reinhardtii* [151] and using a Wheat Germ Cell-Free (WGCF) expression system [210]. These Pfs25 recombinant proteins all showed the ability to induce functional anti-Pfs25 antibodies that exhibited transmission blocking activity.

The recombinant Pfs25 protein (produced by the National Institutes of Health (NIH)) used in the Phase 1 clinical trial was produced from *Pichia pastoris* [209]. Pfs25 sequence (GeneBank locus AAN35500, from Alanine (Ala)-22 to Threonine (Thr)-193) with four potential N-linked glycosylation sites (112, 165, 187 and 202) mutated was cloned into *P. pastoris* expression plasmid pPIC9K which was subsequently transformed into *P. pastoris* (GS115 strain). Due to the cloning strategy and the restriction enzyme digest sites available at the time, the recombinant Pfs25 (NIH) protein secreted from *P. pastoris* contained 8 (excluding the 6 histidine (His)-tag) non-Pfs25 coding amino acids in the protein sequence, 6 at the N-terminus and 2 between the C-terminal Pfs25 amino acid and the His-tag: EAEAYV**KVTVDT…SSICT**DPHHHHHH (underlining and bold face depicts the Pfs25 coding sequence).

For my DPhil study I have expressed Pfs25 in *P. pastoris* and removed the non-Pfs25 coding amino acids. Pfs25 (Ala-22 to Thr-193) with the same N-glycosylation mutations as the Pfs25 (NIH), was cloned into *P. pastoris* expression plasmid pPinkα-HC (Life Technologies, UK). pPinkα-HC plasmid encodes a α-factor secretion signal sequence (derived from α-mating

factor pre-sequence from *Saccharomyces cerevisiae*) and was designed to carry a StuI restriction enzyme digest site right at the end of the α-factor sequence. With the help of this restriction enzyme digest, the Pfs25 sequence was inserted in-frame just after the α-factor sequence without introducing any unwanted "cloning artefacts" (details of this cloning are described in materials and methods section 2.2.1.1). As with the Pfs25 (NIH) sequence, a C-terminus His-tag was included. After insertion of the Pfs25 sequence into pPinkα-HC, the plasmid was transformed into PichiaPink™ *P. pastoris* (Life Technologies, UK). The recombinant Pfs25: **AKVTVDT…SSICT**HHHHHH (underlining and bold face depicts the Pfs25 coding sequence) was secreted and purified from culture supernatant and tested for its immunogenicity in mice.

3.2 Results

3.2.1 Expression and purification of recombinant Pfs25

The PichiaPink™ expression system comes with 4 different strains of *P. pastoris*. Strain 1 is the protease wild-type, strain 2 is a pep4 knockout, and strain 3 is a prb1 knockout, strain 4 is a double knockout for both pep4 and prb1. Pep4 gene encodes the Proteinase A which is a vacuolar aspartyl protease and involves in the subsequent activation of additional vacuolar proteases: proteinase B and carboxypeptidase Y [211]. Prb1 gene encodes Proteinase B, a vacuolar serine protease, which is involved in protein degradation in the vacuole [212]. In wild-type *P. pastoris*, proteinase A, proteinase B and carboxypeptidase Y have all been found in both cytoplasm and culture medium after 48 hours of induction and peaked at 72 hours when the supernatant was harvested [213]. This increase of protease was found to correlate with the level of degradation of secreted recombinant bovine IFNγ, suggesting that protease activity could have a negative effect on target protein expression [213]. This is

probably because the secreted protein is exposed to yeast proteases as a result of cell lysis that occurs during fermentation. This finding was in agreement with another study which demonstrated that the disruption of proteinase in *P. pastoris* can improve target protein expression [214]. In light of the above results, Pfs25 was transformed into 4 different strains of *P. pastoris* provided in the PichiaPink™ expression kit in order to select the best strain for this particular expression. After transformation, 4 positive colonies (auxotrophic selection) from each strain were selected for a small scale protein expression (materials and methods section 2.2.10). After 72 hours of methanol induction, culture supernatant was collected and run on SDS-PAGE. Western blot was performed using Pfs25 antiserum (from mice vaccinated with viral-vectors expressing Pfs25). As figure 3.1 shows, half of the positive colonies secreted protein that was recognized by the Pfs25 antiserum and at the predicted size of 19 kDa.

Based on the western blot band intensity, strain 1 of *P. pastoris* seemed to yield the most recombinant Pfs25. Therefore colony 03 from strain 1 was picked as the working colony. Large scale protein expression (materials and methods section 2.2.11) was performed according to the manufacturer's protocol (Life Technologies, UK). The fermentation was performed at 29°C with 4% methanol added Volume/Volume (v/v) every 24 hours and the supernatant was harvested 72 hours after the induction. Culture supernatant was collected and His-tag purification using a HisTrap excel column (GE Healthcare, UK) was performed, The elution fractions F3 to F7 that contained Pfs25 protein (figure 3.2A) were pooled and concentrated using Amicon® ultracentrifugation tubes (EMD Millipore, UK). Pooled protein was then purified by size-exclusion chromatography (SEC) using Superdex 200pg column (GE Healthcare, UK). The SEC elution chromatography graph (figure 3.2B) revealed the presence

of monomeric and multimeric Pfs25 in the elution fractions. SEC fractions B9 to C10 were then analysed on western blot under both reducing and non-reducing conditions using Pfs25 antiserum (figure 3.2C). Multimeric forms of Pfs25 (B9 to C1) were observed when the samples were prepared at non-reducing condition (figure 3.2C left panel). Under reducing conditions, all multimeric Pfs25 were reduced into monomers (figure 3.2C right panel) suggesting Pfs25 multimer formation was disulfide bond dependent. Similarly, Pfs25 dimer and higher order multimers were observed previously when Pfs25 was produced from *P. pichia* (GS115 strain) [209] and *C. reinhardtii* expression systems [151]. The SEC fractions (C2 to C5) that contained monomeric Pfs25 were pooled. Purified Pfs25 (Jenner) together with Pfs25 (NIH) (provided by Dr Yimin Wu) were run head-to-head on reducing SDS-PAGE and analysed with Coomassie blue staining. Both proteins were pure on the gel and slight difference in the molecular weight was observed as expected (due to 7 amino acids difference in the length) (figure 3.3 left panel). To check for the presence of epitopes found in native Pfs25, Pfs25 (Jenner) was analysed on a western blot under both reducing and non-reducing conditions using the transmission blocking monoclonal antibody (mAb) 4B7. Although 4B7 mAb recognizes a linear epitope in Pfs25 [146], its recognition is to some degree conformation dependent, strongly recognizing non-reduced native Pfs25 and only reacting weakly to reduced native Pfs25 protein [215]. Figure 3.3 (right panel) shows that non-reduced Pfs25 reacts strongly with 4B7 mAb whereas reduced Pfs25 reacts very poorly to this antibody. Purified Pfs25 (Jenner) was stored at -20°C for further immunogenicity studies.

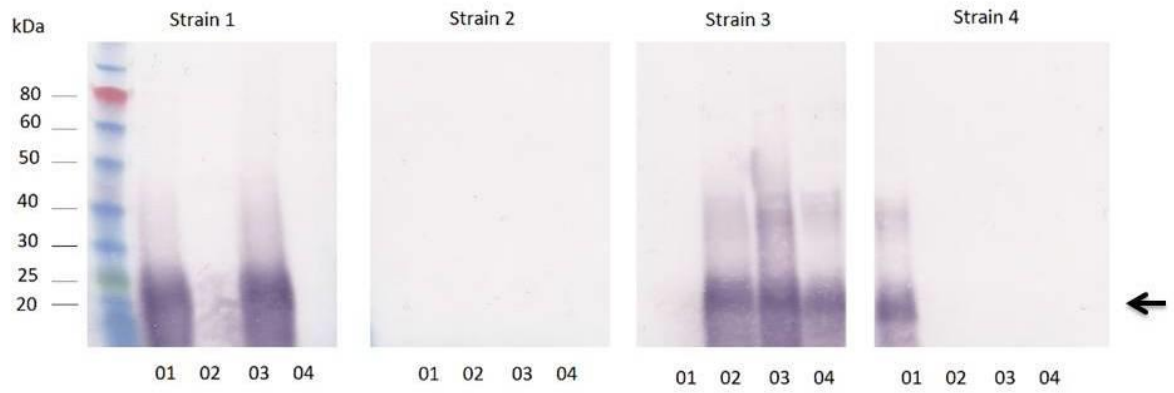

Figure 3.1 Strain selections for expression of Pfs25.

Four different *Pichia pastoris* strains from PichiaPink expression kit were transformed with pPinkα-HC plasmids containing Pfs25 (Ala-22 to Thr-193) sequence with a C-terminus His-tag. 4 colonies from each stain were picked for small scale protein expression test. Cell culture supernatant was harvested 72 hours after the fermentation (29°C, 4% methanol added v/v every 24 hours). Crude culture supernatant from each sample was loaded on reducing SDS-PAGE and analysed by western blot using Pfs25 antiserum. The figure shows the level of Pfs25 expression from each individual transformed *P. pastoris* colony. Arrow indicates the expected size of the Pfs25 monomer (19kDa).

A

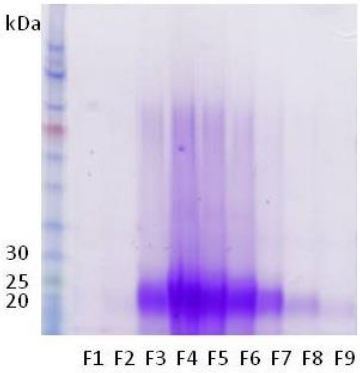
kDa
30
25
20
F1 F2 F3 F4 F5 F6 F7 F8 F9

B

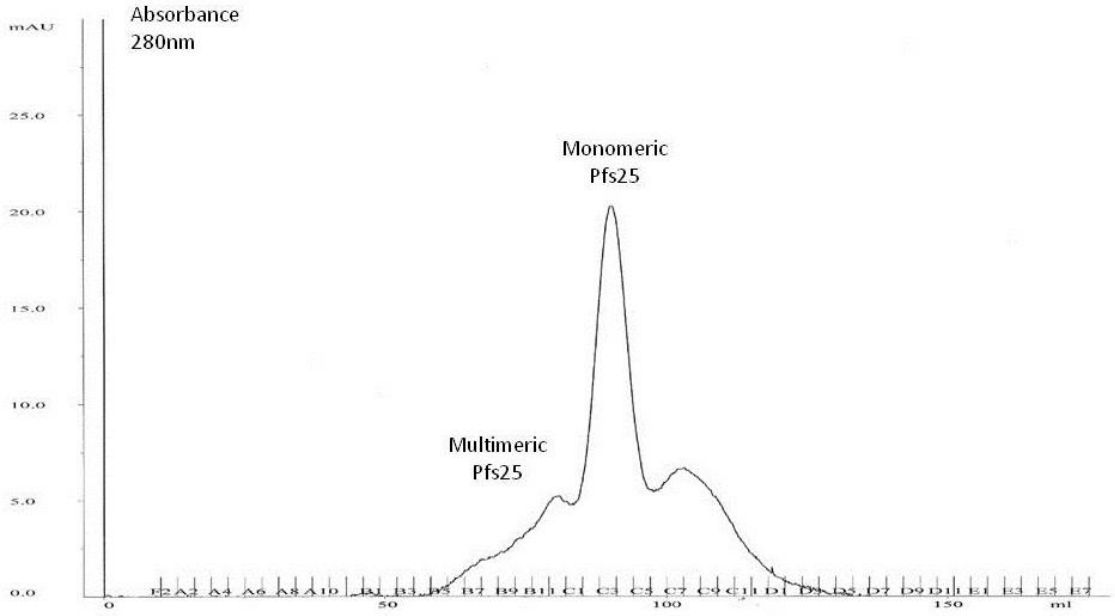
Absorbance
280nm
mAU
25.0
20.0
15.0
10.0
5.0
0.0
Monomeric
Pfs25
Multimeric
Pfs25
0
50
100
150
ml

C

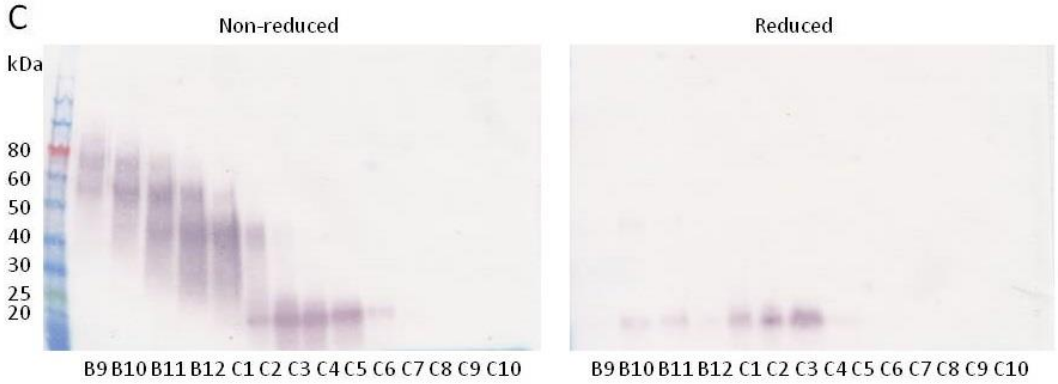
Non-reduced
Reduced
kDa
80
60
50
40
30
25
20
B9 B10 B11 B12 C1 C2 C3 C4 C5 C6 C7 C8 C9 C10
B9 B10 B11 B12 C1 C2 C3 C4 C5 C6 C7 C8 C9 C10

Figure 3.2 Purification of Pfs25 from culture supernatant.

Supernatant from Pfs25 transformed *P. pastoris* culture was collected after large scale protein expression. The supernatant was purified using a HisTrap excel column. His-tag elution fractions were collected and run on SDS-PAGE at reducing condition. Coomassie blue staining was performed to reveal protein containing fractions F3 to F7 (A). These fractions were pooled and purified further through a Superdex 200pg SEC column. SEC chromatography graph shows multimeric and monomeric Pfs25 peaks (B). SEC fractions B9 to C10 were analysed by western blot under both reducing and non-reducing conditions using Pfs25 antiserum (C).

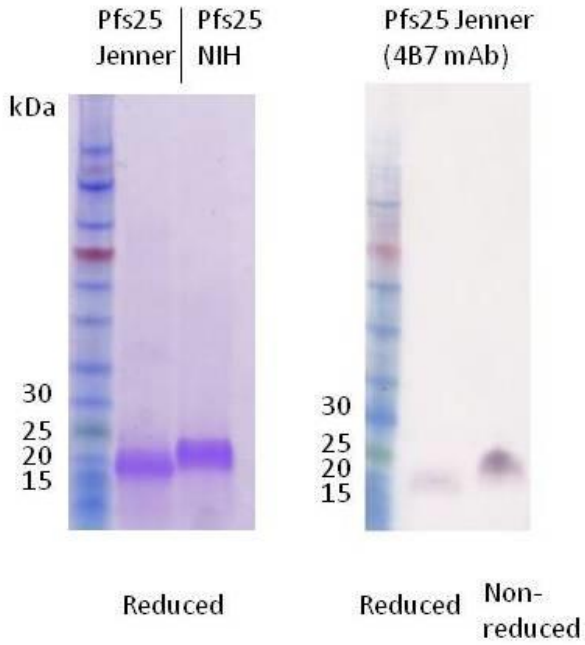

Figure 3.3 Pfs25 is recognised by anti-Pfs25 monoclonal antibodies 4B7.

SEC fractions C2 to C5 that contained monomeric Pfs25 were pooled and run on SDS-PAGE together with Pfs25 (NIH). Both proteins were analysed using Coomassie blue staining with reducing conditions (left panel). Monomeric Pfs25 (Jenner) was also analysed on western blot using 4B7 mAb, under both reducing and non-reducing conditions (right panel).

3.2.2 Humoral immunity of recombinant Pfs25

To assess the immunogenicity of the recombinant Pfs25 (Jenner), 2.5 µg of the protein was formulated in addavax (a squalene-based oil-in-water nano-emulsion adjuvant) and 6-8 week old BALB/c mice were immunized intramuscularly (IM). Mice were primed on day 0 and boosted on day 21; serum was collected on day 14, 20, 35 and 42 for ELISA. Recombinant Pfs25 (NIH) was also included in this study as a comparison. Details of the vaccination regimes are summarised in table 3.1.

Pfs25 standardised ELISA was performed to evaluate the total Pfs25-specific IgG levels in the serum sample collected. The ELISA plate was coated with recombinant Pfs25 from NIH. The Pfs25 standardised ELISA was performed as described in materials and methods (section 2.3.5) and the ELISA readout is summarised in figure 3.4. There was no statistically significant difference (Mann-Whitney test) between the Pfs25-specific IgGs induced after Pfs25 (Jenner) and Pfs25 (NIH) vaccinations. However after the boost, at both day 35 and day 42, there was a trend towards higher Pfs25-specific IgGs in the Pfs25 (Jenner) vaccinated group.

3.2.3 Investigation of a possible adjuvant effect of Pfs25 (Jenner)

The result from 3.2.2 was very interesting, roughly a log difference in Pfs25-specific IgG titres induced by Pfs25 (Jenner) and Pfs25 (NIH) was observed. Although Coomassie blue staining revealed Pfs25 (Jenner) was clean (figure 3.3 left panel), it is still possible that some impurities in the lab-scale production were acting as adjuvants. In order to investigate if this was the case, mice were immunised using the regimes described in table 3.2. Basically 10 µg ovalbumin (OVA) was used as a reference antigen. BALB/c mice were immunised IM with OVA in PBS (negative control), OVA formulated with Alhydrogel (positive control) or OVA

formulated with 2.5 μg of Pfs25 (Jenner) in PBS (test group). 3 weeks after the vaccination, serum was collected and whole IgG ELISA was performed against recombinant OVA. If Pfs25 (Jenner) contains an impurity which acts as adjuvant, the test group should show higher anti-OVA antibody response than the negative control group. As figure 3.5 shows, both the test group and the negative control group showed a statistically lower anti-OVA antibody response than that was measured in the positive control group. The result indicated that the Pfs25 (Jenner) preparation did not contain substances that acted as adjuvants.

Group	Day 0	Day14	Day 20	Day 21	Day35	Day 42
Pfs25 (Jenner)	2.5 µg + Addavax	Bleed	Bleed	2.5 µg + Addavax	Bleed	Bleed
Pfs25 (NIH)	2.5 µg + Addavax	Bleed	Bleed	2.5 µg + Addavax	Bleed	Bleed

Table 3.1 Vaccination regimes for recombinant Pfs25 immunogenicity study.

BALB/c mice (n=5/group) received 2.5 µg of Pfs25 (Jenner) or Pfs25 (NIH) protein formulated in Addavax. Mice were primed on day 0 and boosted on day 21. The serum was collected on day 14, day 20, day 41 and day 62 for ELISA analysis.

Group	Day 0	Day 21
Negative control	10 µg OVA + PBS	Bleed
Test group	10 µg OVA + 2.5 µg Pfs25 (Jenner)	Bleed
Positive control	10 µg OVA + Alhydrogel	Bleed

Table 3.2 Vaccination regimes for recombinant Pfs25 (Jenner) adjuvant effect study.

BALB/c mice (n=5/group) were immunised IM with 10 µg of OVA formulated in PBS (negative control), OVA formulated with 2.5 µg of Pfs25 (Jenner) in PBS (Test group) or OVA formulated with Alhydrogel (positive control). Mice were primed on day 0 and the serum was collected on day 21 for ELISA.

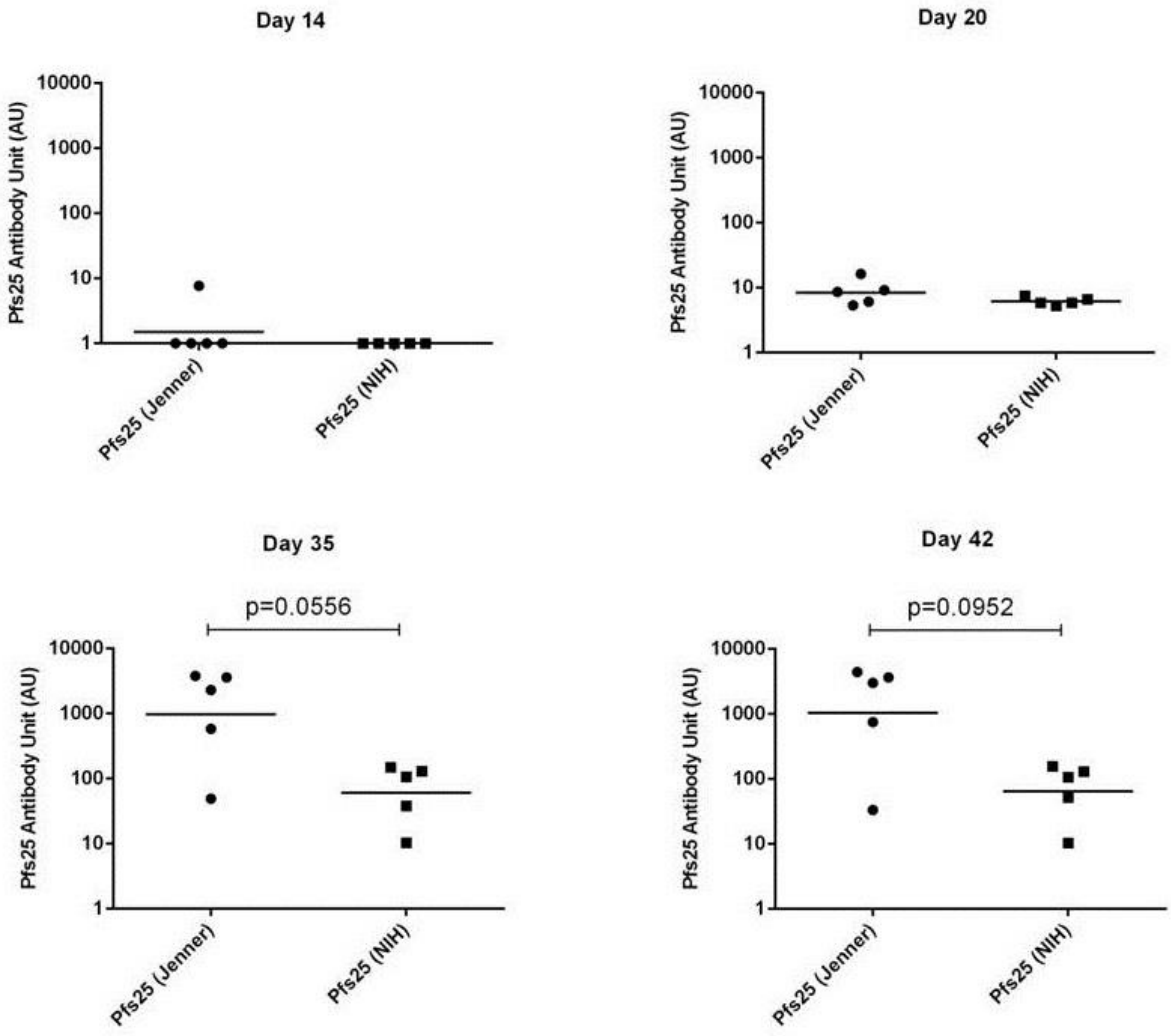

Figure 3.4 Immunogenicity study comparing recombinant Pfs25 (Jenner) and recombinant Pfs25 (NIH).

BALB/c mice (n=5/group) were immunised using protein-in-adjuvant (Addavax) prime boost regime as outlined in table 3.1. Mice were primed at day 0 and boosted at day 21. Total Pfs25-specific IgG levels were measured in serum samples taken at day 14, 20, 35 and 42 using a Pfs25 standardised ELISA. Median and individual data points are shown. There was no significant difference between two vaccinated groups as measured by Mann-Whitney test.

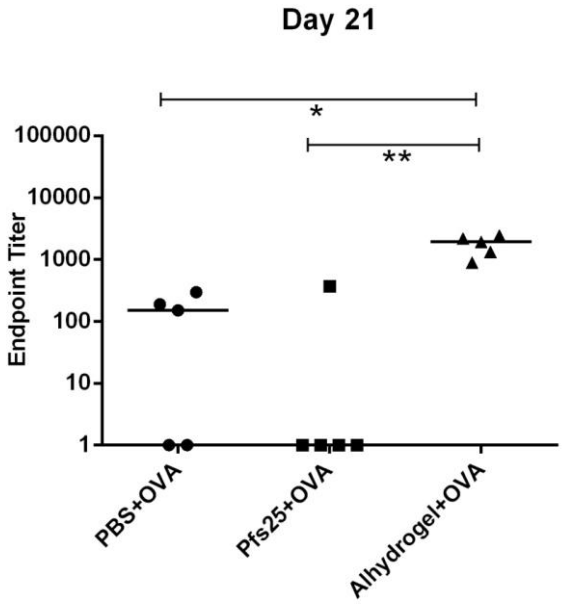

Figure 3.5 Recombinant Pfs25 (Jenner) did not act as an adjuvant.

BALB/c mice (n=5/group) were immunised with 10 µg OVA formulated in PBS, Pfs25 (Jenner) or Alhydrogel as outlined in table 3.2. Mice were vaccinated at day 0 and serum was collected at day 21. OVA specific total IgG levels were measured using whole IgG ELISA. Median and individual data points are shown. * $p<0.05$, ** $p<0.01$ by Kruskal-Wallis test with Dunn's multiple comparison post-test.

3.2.4 Discussion

In this chapter, I have described the production and purification of recombinant Pfs25 (Jenner) in *P. pastoris.* The NIH version of recombinant Pfs25 protein contained 8 (excluding the 6 histidine tag) non-Pfs25 coding amino acids out of which 6 were continuous at the N-terminus. The recombinant Pfs25 that I generated contained no foreign amino acids sequence except for the His-tag, which was needed for protein purification.

Recombinant protein vaccine with less or no non-antigen coding amino acids is essential. One reason is that regulatory authorities are reluctant to allow additional amino acids in subunit vaccine constructs for safety reasons. Another reason is that an antigen without any foreign amino acids will direct the immune response fully against the antigen bearing epitopes. Antigen with foreign amino acids can lead to two unwanted outcomes: 1) the foreign peptide sequence may affect the folding of the native antigen protein resulting in a conformational change. Indeed such conformational change has been observed by addition of small peptide sequence such as His-tag [216]. One type of B cell epitope is the conformational epitope, which is composed of amino acids that are not contiguous in primary sequence but are brought into close proximity within the folded protein structure [217, 218]. If the foreign sequence alters the conformation of target protein, this may block the generation of critical conformational epitopes. 2) B cells can also recognize linear epitopes and most of these epitopes are between 4 and 20 amino acids in length [219]. Watson *et al* [220] investigated the anti-His-tag IgG response after immunization with polyhistidine-modified antigens in mice. Anti-His-tag IgGs were detected after mice were immunised with antigens containing 10 histidines but not with 6 histidines, suggesting that a small peptide sequence of 10 amino acids in length (or even less) could be immunogenic in a

protein vaccine. Therefore, if a recombinant protein contains small foreign peptide sequences, it is likely that a host could develop an antibody response against it. And this unwanted immune response may also compete with the target immune response resulting in reduced antibody titres against essential target epitopes.

By comparing Pfs25 (Jenner) and Pfs25 (NIH) in the same vaccination regime, Pfs25 (Jenner) induced a noticeably higher Pfs25-specific IgG response after the boost. And this difference did not appear to be due to any adjuvant-like molecules present in the sample prep. Considering the ELISA plate was coated with Pfs25 (NIH) protein, which in theory should favour the Pfs25 (NIH) vaccinated group's ELISA readout, the actual difference of immunogenicity between Pfs25 (Jenner) and Pfs25 (NIH) could be larger. When Pfs25 (NIH) was initially expressed by *S. cerevisiae*, two conformational different isomers (ScPfs25H-A and ScPfs25H-B) were observed; similarly, two isoforms (PpPfs25H-A and PpPfs25H-B) were produced from *P. pastoris* [209]. Both the A forms reacted strongly to the anti-Pfs25 conformational-dependent mAb 1D2 as well as 4B7. In contrast, both the B forms reacted weakly. According to the N-terminal sequencing result, the PpPfs25H-A was the full length product whereas PpPfs25H-B had the first 4 amino acids (non-Pfs25 coding sequence) deleted at the N-terminus. After further purification and separation of the two isoforms, it was demonstrated that the isoform-A exhibited higher TRA in SMFA and the PpPfs25H-A was chosen as the recombinant protein used in the clinical trial [209]. Interestingly, based on the SDS-PAGE analysis (figure 3.3 left panel), there were no isoforms observed during Pfs25 (Jenner) purification. This is beneficial because the purification process for Pfs25 (Jenner) will be one step less than that for Pfs25 (NIH) as the latter requires hydrophobic interaction chromatography to separate PpPfs25H-A and PpPfs25H-B. Note that future

protein sequencing by mass spectrometry is required to further characterise the recombinant Pfs25 (Jenner) protein.

All in all, an improved version of recombinant Pfs25, with no foreign peptide sequence (except for the His-tag), was expressed successfully in *P. pastoris* and this protein is highly immunogenic. Pfs25 (Jenner) is used in the following vaccination studies in Chapter 4, 5 and 6.

Chapter 4

Production, purification and immunogenicity study of a Pfs25-IMX313 nanoparticle

4. Production, purification and immunogenicity study of a Pfs25-IMX313 nanoparticle

4.1 Introduction

In the previous Pfs25 Phase 1 clinical trial [154], recombinant Pfs25 formulated with adjuvant ISA51 was able to generate functional antibodies in human. However, the overall immunogenicity was poor and as a result, only 1 out of 5 volunteers who received the full dose (2 immunisations) of vaccination developed levels of antibody response that gave high TRA in SMFA. The antiserum derived from this particular volunteer was also tested in DMFA against *P. falciparum* isolates from patients in Thailand and Burkina Faso. The anti-Pfs25 antiserum showed significantly higher TRA and TBA (compared to the non-immune controls) in the DMFA against parasites from both regions [153]. TBVs aim to exclusively generate high titre antibodies that can target the parasite's development within the mosquito. In order to achieve this, it is important to induce the highest possible antibody titres in pre-clinical and clinical studies by improving vaccine platforms. Currently, there have been several successful pre-clinical studies using different platforms which significantly increased the Pfs25 antibody response. Such platforms include conjugation of Pfs25 to OMPC of *Neisseria meningitidis* serogroup B [173], and to recombinant EPA from *pseudomonas aeruginosa* [156, 168, 169]; recombinant viral vectored vaccine expressing Pfs25 [147] as well as chimeric VLP carrying Pfs25 on the surface [157] have been produced and tested in pre-clinical studies. However, all of these approaches have limitations such as manufacturing challenges and potential safety issues.

C4b-binding protein (C4BP) is an abundant plasma protein that is involved in the complement system where it acts as an inhibitor of C3 convertase. C4BP has a complex

structure; in humans, 75-80% of C4BP is composed of 7 identical α-chains and 1 β-chain. Other less abundant forms include 6 α-chains with 1 β-chain or 7 exclusively α-chains [221]. Both α and β chains are linked by the C-terminal oligomerization domain (57 amino acids) containing two cysteine residues and an amphiphatic α-helix both of which are required for this oligomerization (figure 4.1A). It was demonstrated that the whole α-helix region forms stable polymer, and disulfide bonds between the cysteine residues further stabilise this structure [222]. Studies revealed this polymerisation happens in the endoplasmic reticulum (ER) and under the electron microscope C4BP showed a spider-like shape with the chains forming extended tentacles (figure 4.1B) [223].

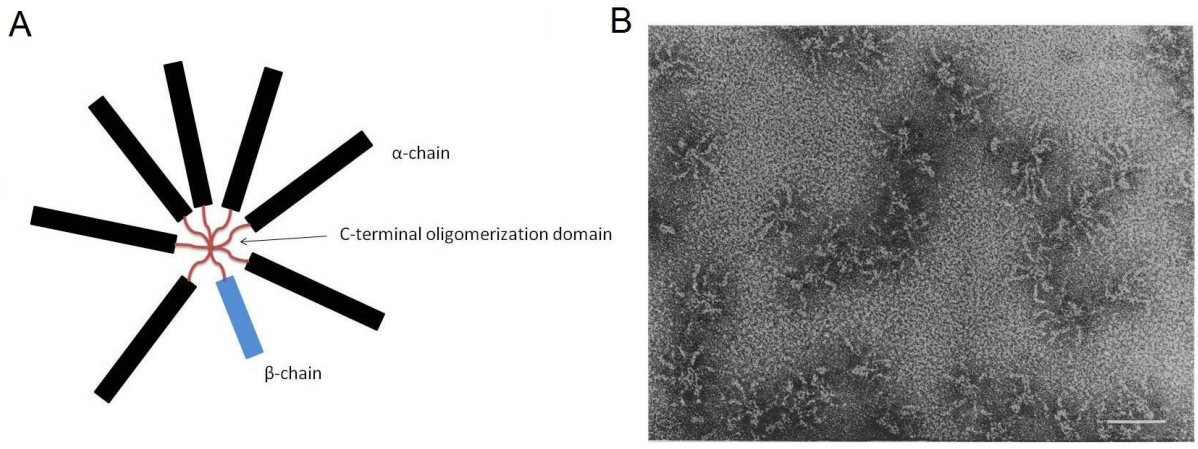

Figure 4.1 Structure of human C4BP protein.

Schematic representation of human C4BP with indicated α, β chains and their C-terminal oligomerization domain (A). Adapted from [223], electron micrographs of human C4BP , the scale bar represents 30 nanometre (B).

IMX313 is a nanoparticle platform developed by our collaborators at Imaxio (Lyon, France). IMX313 is a hybrid avian C4bp oligomerization domain. When an antigen is fused to the N-terminus of the IMX313 sequence and expressed, the IMX313 spontaneously self-assembles into a heptamer and exposes the antigen. Antigens fused to IMX313 (or its equivalent) have been demonstrated to increase both B cell and T cell responses in various studies using DNA vaccines [224], viral-vectored vaccines [224] [225] [191], as well as recombinant protein vaccine [226]. The mechanism as to why a heptamer is more immunogenic than monomeric antigen has not been investigated.

Pfs25 fused to IMX313 was successfully expressed from chimpanzee adenovirus and MVA vaccine vectors. When used in a ChAd63 MVA prime-boost vaccination regime, Pfs25-IMX313 induced a significant higher antibody response than ChAd63 MVA expressing Pfs25 alone (study was performed by Dr Sumi Biswas). IMX313 has only been expressed as nanoparticles from *E.coli* [226], and my hypothesis was that Pfs25-IMX313 recombinant protein could be expressed by *P. pastoris* and would self-assemble into a heptamer. In this chapter I will describe the production as well as the immunogenicity studies of Pfs25-IMX313 nanoparticle expressed from *P. pastoris*.

4.2 Results

4.2.1 Expression and purification of Pfs25-IMX313H

The DNA construct of Pfs25 fused to the N-terminal end of IMX313 was already designed for the generation of viral vectored vaccines in the lab. To expresses it as a recombinant protein, a His-tag was introduced at the N-terminus of Pfs25-IMX313 by PCR. The construct is referred to as Pfs25-IMX313H (H refers to the N-terminus His-tag) and the sequence was

cloned into a pPinkα-HC expression plasmid and transformed into 4 different strains of *P. pastoris* (cloning details are described in materials and methods section 2.2.1.2). 5 positive colonies (after auxotrophic selection) from each strain were selected for a small scale protein expression test. After 72 hours induction, culture supernatant was collected and run on reducing SDS-PAGE. Western blot (figure 4.2) was performed using Pfs25 antiserum derived from Pfs25 (Jenner) vaccinated mice (Chapter 3, section 3.2.2). The blot shows that all the selected positive colonies secreted protein that was recognized by Pfs25 antiserum and at the right predicted size of 26 kDa under reducing condition. Estimating from the western blot signal band intensity, strain 1 of *P. pastoris* seemed to show the best yield of this fusion construct. For this reason, stain 1 colony 05 was chosen as the working colony.

The fermentation time, temperature as well as the amount of methanol added to the culture may all have an influence on the protein yield [227]. Pfs25-IMX313H expression was tested under all different conditions in order to find the optimum condition for protein expression. The influence from the fermentation time and methanol concentration was investigated first. Yeast cells were grown in 50mL of BMGY media till the OD_{600} reached around 2.0 and then re-suspended in 10mL BMMY in shaking flasks. Fermentation was carried out at 25°C and different methanol concentrations (0.5%, 1%, 2% and 4%) were added v/v to the culture medium every 24 hours. The fermentation was monitored for 72 hours and the supernatant samples were taken every 24 hours for analysis. Supernatant samples were run on reducing SDS-PAGE and analysed by western blot using Pfs25 antiserum (figure 4.3A) and Coomassie blue staining (figure 4.3B). The results showed that the methanol concentration as well as the time of fermentation made a noticeable difference in the level of protein expressed. Using the ImageJ software (National Institutes

of Health, USA), the western blot band signal was converted into arbitrary numbers based on total band pixel intensity and is summarised in a histogram (figure 4.3C). Using 2% methanol and 48 hours fermentation, the protein expression seemed to reach a peak; a similar expression level was reached when the cells were treated with 1% methanol and 72 hours fermentation used. The influence of temperature was investigated in a separate test, during which the fermentation was carried out using 2% methanol and at 25°C or 29°C. The fermentation was monitored for 48 hours and the supernatant samples were collected as before and run on reducing SDS-PAGE followed by Coomassie blue staining analysis. As the result demonstrated, the protein expression was higher when the fermentation was carried out at 25°C (figure 4.3D).

Based on the results above, large scale Pfs25-IMX313H expression was performed at 25°C with 2% methanol and the supernatant was harvested 48 hours after the fermentation. Similar to Pfs25 purification, His-tag purification using HisTrap excel column was performed. His-tag elution fractions were collected and run on reducing SDS-PAGE followed by Coomassie blue staining analysis. Fractions F1 to F8 that contained the protein (figure 4.4A) were pooled and further purified by using SEC using a superdex 200pg column. The chromatography graph (figure 4.4B) revealed the presence of a Pfs25-IMX313H heptamer peak (labelled in figure 4.4B). SEC fractions that contained Pfs25-IMX313H heptamer (B4-B7) were pooled and run on reducing and non-reducing SDS-PAGE followed by silver staining and western blot analysis. Under non-reducing conditions, silver staining revealed a uniform sharp protein band at the predicted Pfs25-IMX313H heptamer size (180kDa) (figure 4.4C left panel). Under reducing conditions, a monomeric Pfs25-IMX313H protein band (26kDa) was observed (figure 4.4C left panel). Only Pfs25-IMX313H heptamer was bound by 4B7 mAb

(figure 4.4C right panel) which is in agreement with the fact that 4B7 is a conformation dependent mAb and binds very weakly to reduced Pfs25 [215]. The pooled Pfs25-IMX313H protein was stored at -20°C for further immunogenicity studies.

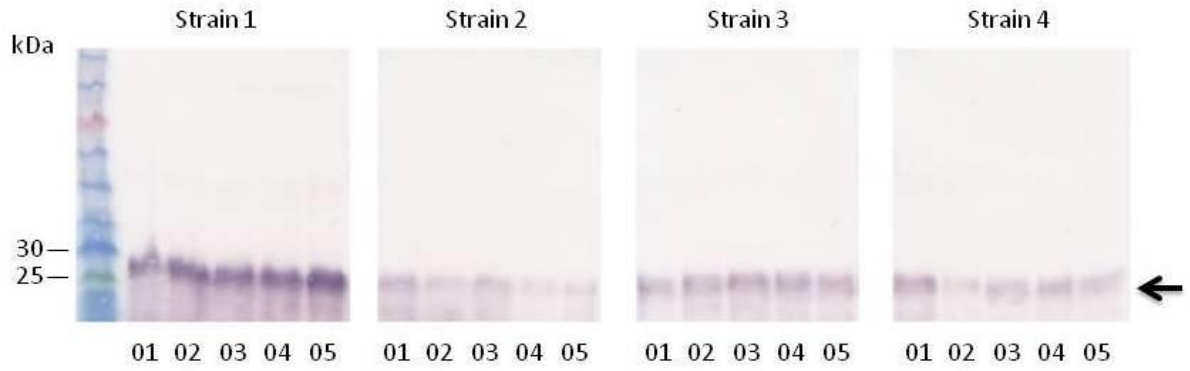

Figure 4.2 Strain selections for expression of Pfs25-IMX313H.

4 different *Pichia pastoris* strains from Pichiapink™ were transformed with Pfs25-IMX313H containing an N-terminus His-tag. 5 colonies from each stain were picked for small scale protein expression tests. Cell culture supernatant was harvested 72 hours after the fermentation (29°C, 4% methanol added v/v every 24 hours). After protein expression, crude culture supernatant was loaded on SDS-PAGE and tested by western blot under reducing condition using Pfs25 antiserum. Arrow indicates the expected size (26kDa) of Pfs25-IMX313H monomer.

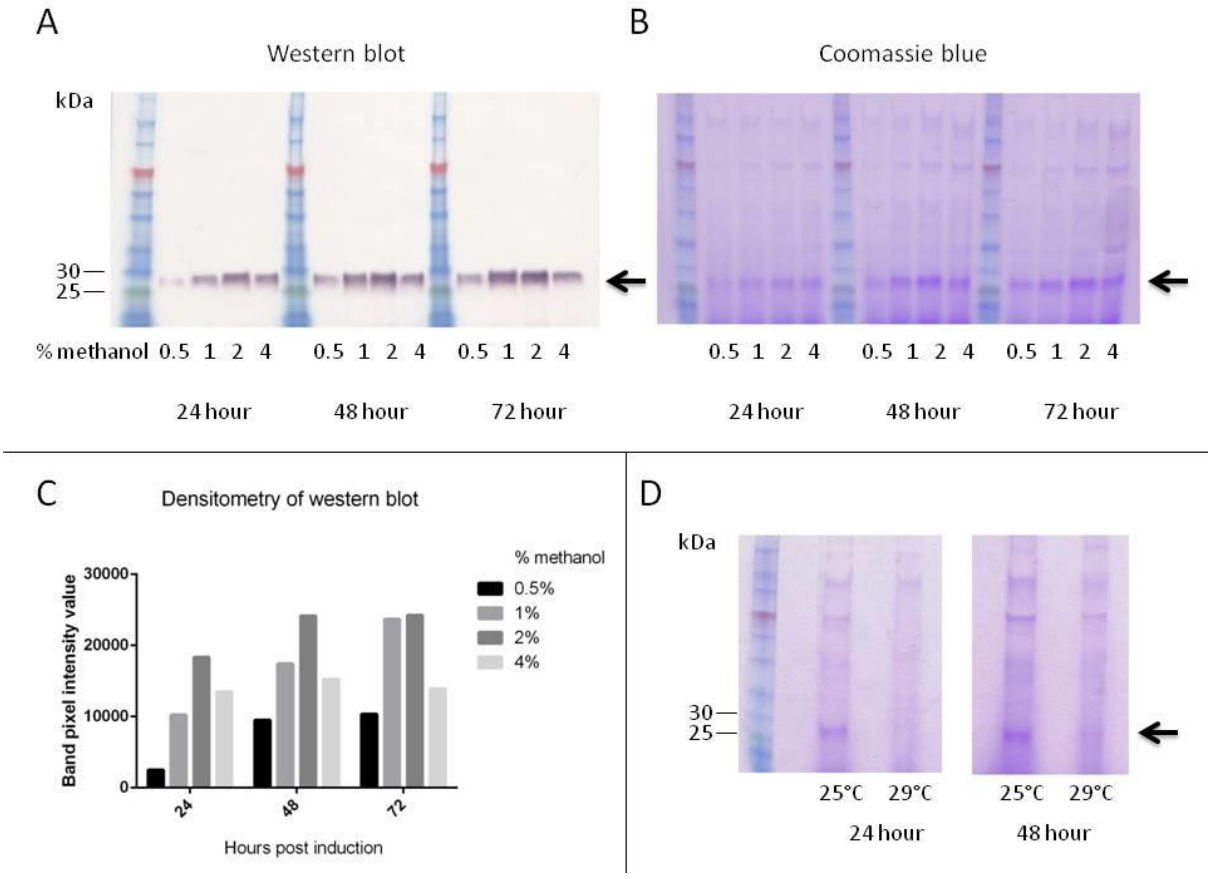

Figure 4.3 Pfs25-IMX313H expression is influenced by the fermentation time, methanol concentrations and temperature.

The Pfs25-IMX313H transformed *P.pastoris* was grown in 50mL of BMGY till the OD_{600} value was 2.0 followed by re-suspension in 10mL BMMY. The fermentation was carried out at 25°C with different methanol concentrations (0.5%, 1%, 2% and 4%) that was added v/v to the culture medium every 24 hours. The supernatant samples were collected every 24 hours and the fermentation was monitored for a total of 72 hours. All supernatant samples were run on reducing SDS-PAGE followed by western bolt (A) using Pfs25 antiserum and Coomassie blue staining (B) analysis. Using ImageJ software, western blot band signal was converted into arbitrary values based on the total band pixel intensity and displayed in a histogram (C). The protein expression was also tested at 25°C and 29°C with 2% methanol

added v/v every 24 hours. The supernatant samples were collected every 24 hours and the fermentation was monitored for a total of 48 hours. The supernatant was run on reducing SDS-PAGE followed by Coomassie blue staining analysis (D). Arrow indicates the expected size of Pfs25-IMX313H monomer.

A

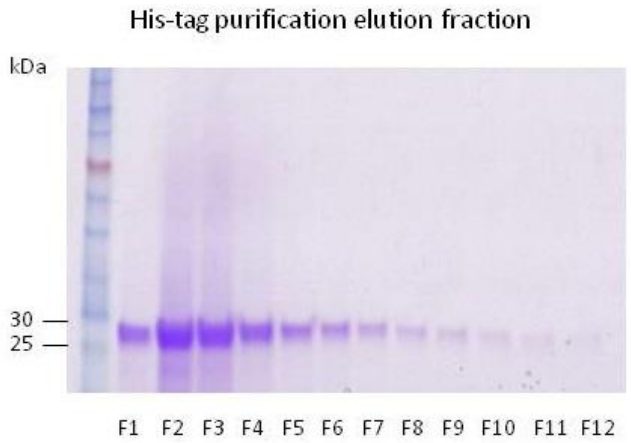
His-tag purification elution fraction
kDa
30
25
F1 F2 F3 F4 F5 F6 F7 F8 F9 F10 F11 F12

B

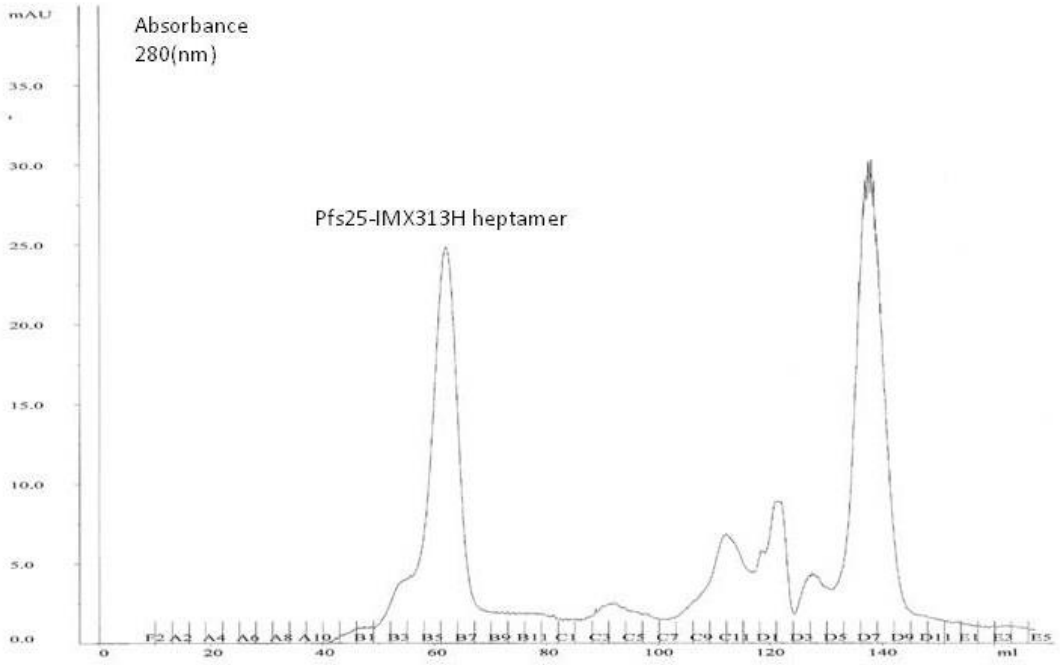
mAU
Absorbance
280(nm)
Pfs25-IMX313H heptamer
35.0
30.0
25.0
20.0
15.0
10.0
5.0
0.0
0
20
40
60
80
100
120
140
ml

C

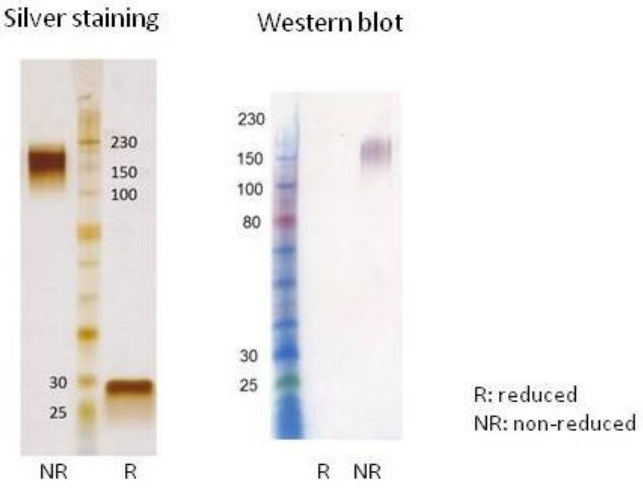
Silver staining
Western blot
230
150
100
30
25
NR
R
230
150
100
80
30
25
R
NR
R: reduced
NR: non-reduced

Figure 4.4 Purification of Pfs25-IMX313H from culture supernatant.

Supernatant from Pfs25-IMX313H transformed *P. pastoris* culture was collected after large scale protein expression. The supernatant was purified through the HisTrap excel column. His-tag elution fractions F1 to F12 were collected and run on SDS-PAGE under reducing conditions. Commassie blue staining was performed to reveal protein containing fractions F1 to F8 (A). These fractions were pooled and purified further using Superdex 200pg size-exclusion column. The chromatography graph shows the Pfs25-IMX313H heptamer peak (B) and SEC fractions B4 to B7 were pooled and analyzed under both reducing and non-reducing conditions by silver staining and western blot using 4B7 mAb (C).

4.2.2 Pfs25-IMX313H dose response study in mice

To assess the immunogenicity and the optimal dosage to be used in mice I carried out a dose response study of Pfs25-IMX313H nanoparticle. 2.5 μg, 5 μg and 10 μg of the nanoparticle and Pfs25 monomeric protein was formulated with Alhydrogel and injected IM to 6-8 weeks' old BALB/c mice. Mice were primed on day 0 and boosted on day 21 followed by another boost on day 42. The serum was collected on day 20, day 41 and day 62 for ELISA analysis. Details of the vaccination regime are summarised in table 4.1.

Pfs25 standardised ELISA was performed to evaluate the total Pfs25-specific IgG levels in the serum samples collected. The Pfs25 standardised ELISA was performed and the results are summarised in figure 4.5. There were two important observations:

1) Pfs25-IMX313H induced significantly higher anti-Pfs25 IgGs than monomeric Pfs25 at all the doses tested and at all time points, except in the 10 μg dose group on day 62 where Pfs25 and Pfs25-IMX313H induced similar levels of anti-Pfs25 IgGs (figure 4.5C). This may be because the antibody response reached a plateau after the third immunisation of 10 μg of the Pfs25-IMX313 nanoparticle vaccine. More importantly, 2 vaccinations of 2.5 μg Pfs25-IMX313H (figure 4.5A) was as immunogenic as 3 vaccinations of 10μg of Pfs25 (figure 4.5C). Together, this result demonstrated that Pfs25-IMX313H was significantly more immunogenic than monomeric Pfs25 produced in the same expression system.

2) By increasing the vaccination dosage, the Pfs25 vaccinated group responded by inducing more anti-Pfs25 IgGs, however this was not observed in the Pfs25-IMX313H vaccinated group. Pfs25-IMX313H induced similar level of anti-Pfs25 IgGs regardless of the vaccination dose, suggesting a strong "dose-sparing" effect. According to this trend, a lower dosage of

Pfs25-IMX313H could be administrated to achieve the same level of immunogenicity observed in this study.

Group (n=5)	Day 0	Day 20	Day 21	Day 41	Day 42	Day 62
1. Pfs25	2.5 µg	↑	2.5 µg	↑	2.5 µg	↑
2. Pfs25	5 µg		5 µg		5 µg	
3. Pfs25	10 µg	Bleed	10 µg	Bleed	10 µg	Bleed
4. Pfs25-IMX313H	2.5 µg		2.5 µg		2.5 µg	
5. Pfs25-IMX313H	5 µg		5 µg		5 µg	
6. Pfs25-IMX313H	10 µg	↓	10 µg	↓	10 µg	↓

Adjuvant: Alhydrogel

Table 4.1 Vaccination regimes for Pfs25 and Pfs25-IMX313H dose response study.

BALB/c mice (n=5/group) received 2.5 µg, 5 µg and 10 µg doses of Pfs25 monomeric protein or Pfs25-IMX313H nanoparticle formulated with Alhydrogel. Mice were primed on day 0 and boosted on day 21 followed by the third boost on day 42. The serum was collected on day 20, day 41 and day 62 for ELISA analysis.

A

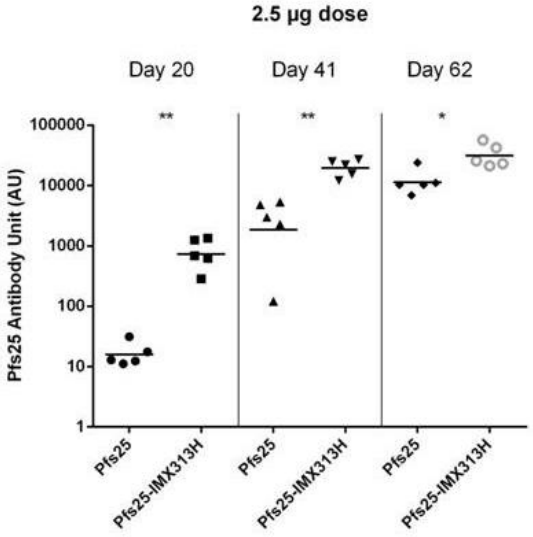
2.5 µg dose
Day 20
Day 41
Day 62
**
**
*
Pfs25 Antibody Unit (AU)
100000
10000
1000
100
10
1
Pfs25
Pfs25-IMX313H
Pfs25
Pfs25-IMX313H
Pfs25
Pfs25-IMX313H

B

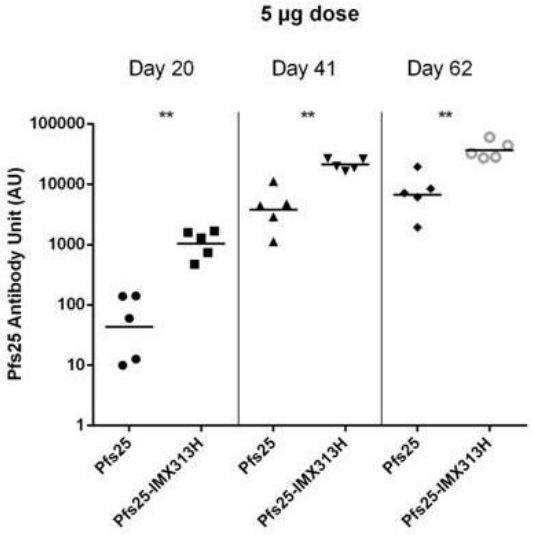
5 µg dose
Day 20
Day 41
Day 62
**
**
**
Pfs25 Antibody Unit (AU)
100000
10000
1000
100
10
1
Pfs25
Pfs25-IMX313H
Pfs25
Pfs25-IMX313H
Pfs25
Pfs25-IMX313H

C

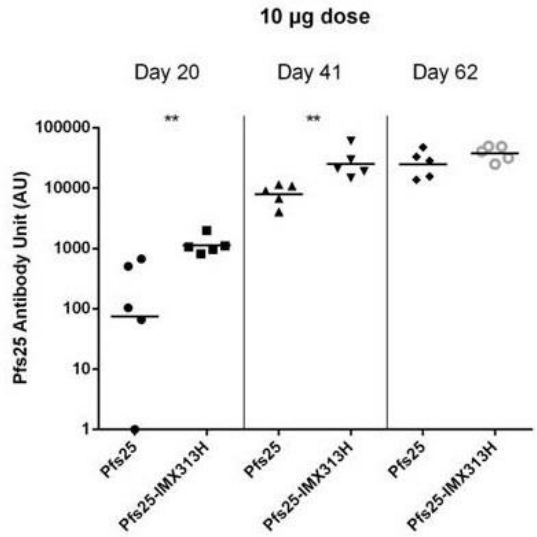
10 µg dose
Day 20
Day 41
Day 62
**
**
Pfs25 Antibody Unit (AU)
100000
10000
1000
100
10
1
Pfs25
Pfs25-IMX313H
Pfs25
Pfs25-IMX313H
Pfs25
Pfs25-IMX313H

Figure 4.5 Dose response study of Pfs25 and Pfs25-IMX313H.

BALB/c mice (n=5/group) were immunised using protein-in-adjuvant (Alhydrogel) prime boost regime as outlined in table 4.1. Mice were vaccinated at day 0 and boosted at day 21 and day 42 with either the Pfs25-IMX313 nanoparticle or monomeric Pfs25. Total Pfs25 specific IgG levels were measured in serum samples taken at day 20, 41 and 62, using a Pfs25 standardised ELISA. Median and individual data points are shown. * $p<0.05$, ** $p<0.01$, *** $p<0.001$ by Mann-Whitney test.

4.2.3 Functional activity of antibodies generated after vaccination with Pfs25-IMX313 nanoparticles

In the previous section, Pfs25-IMX313H nanoparticle was demonstrated to be more immunogenic than monomeric Pfs25 protein. Significantly more anti-Pfs25 IgGs was induced in mice that received Pfs25-IMX313H nanoparticle formulated with Alhydrogel. In order to assess the functional activity of the anti-Pfs25 IgGs induced by the vaccination, the IgG was tested using SMFA.

SFMA was done in collaboration with the Malaria Vaccine Initiative (MVI) SMFA reference laboratory at the National Institute of Health. Day 62 sera from groups of mice that received the 2.5 μg dose of Pfs25 or Pfs25-IMX313H vaccines were pooled. Sera from a group (n=5) of Balb/c mice immunized 3 times with ovalbumin (OVA) formulated with Alhydrogel was pooled as the negative control. IgGs were purified from these serum pools using protein G columns and tested in SMFA against *P. falciparum* NF54 using *Anopheles stephensi* mosquitoes.

At the NIH reference centre, by the standard protocol, the purified IgGs are normally tested first at 750 μg/mL total IgG concentration and then diluted down if required. A previous study performed by Dr Melissa Kapulu (submitted) showed IgGs purified from mice receiving viral vectored vaccines expressing Pfs25 exhibited 100% TRA and TBA at 250 μg/mL total IgG concentration. Anti-Pfs25 IgGs can exhibit strong parasite inhibition at a low IgG concentration, and if the experiment uses the standard IgG concentrations (750 μg/mL) at NIH reference centre, it will be difficult to differentiate and compare the TRA or TBA from the two vaccinated groups. Therefore, the total IgGs were diluted and tested at 375 μg/mL, 188 μg/mL, 94 μg/mL and 47 μg/mL concentrations. SMFA was then performed according to

NIH's SMFA protocol (described in material and methods section 2.3.16). The results are summarised in figure 4.6 and data points represent the number of oocysts in individual mosquitoes and the lines show the arithmetic mean. Both TRA and TBA were calculated; however TRA was the main readout for this SMFA study and only TRA was analysed by MVI using a negative binomial with zero inflated model for its 95% confidence interveal (CI) and the p value. As mentioned in the chapter 1 (section 1.5.3.3), TBA is highly influenced by the degree of parasite exposure (as measured by the mean oocyst number in the control group) and is not considered a reliable measurement for vaccine efficacy in SMFA where we usually have much more oocysts on average (55.9 in this SMFA study) compared to the numbers observed in the field (<5). At 375 µg/mL total IgG concentration, Pfs25 vaccinated group showed 79.7% inhibition of oocyst intensity (TRA) (p value=0.006, relative to the control group) and 5.3% inhibition of prevalence (TBA) whereas Pfs25-IMX313H group showed 99.8% TRA (p=0.001) and 94.7% TBA. At 188 µg/mL IgG concentration, Pfs25 group did not give a statistically significant TRA and the TBA was at 0%, whereas Pfs25-IMX313H group showed 95.9% TRA (p=0.001) and 26.3% TBA. At 94 µg/mL IgG concentration, Pfs25-IMX313 group still gave a statistically significant TRA by 70% (p=0.038). Overall, this experiment clearly demonstrated serum from Pfs25-IMX313H vaccinated mice was more potent at inhibiting parasite development in the mosquito.

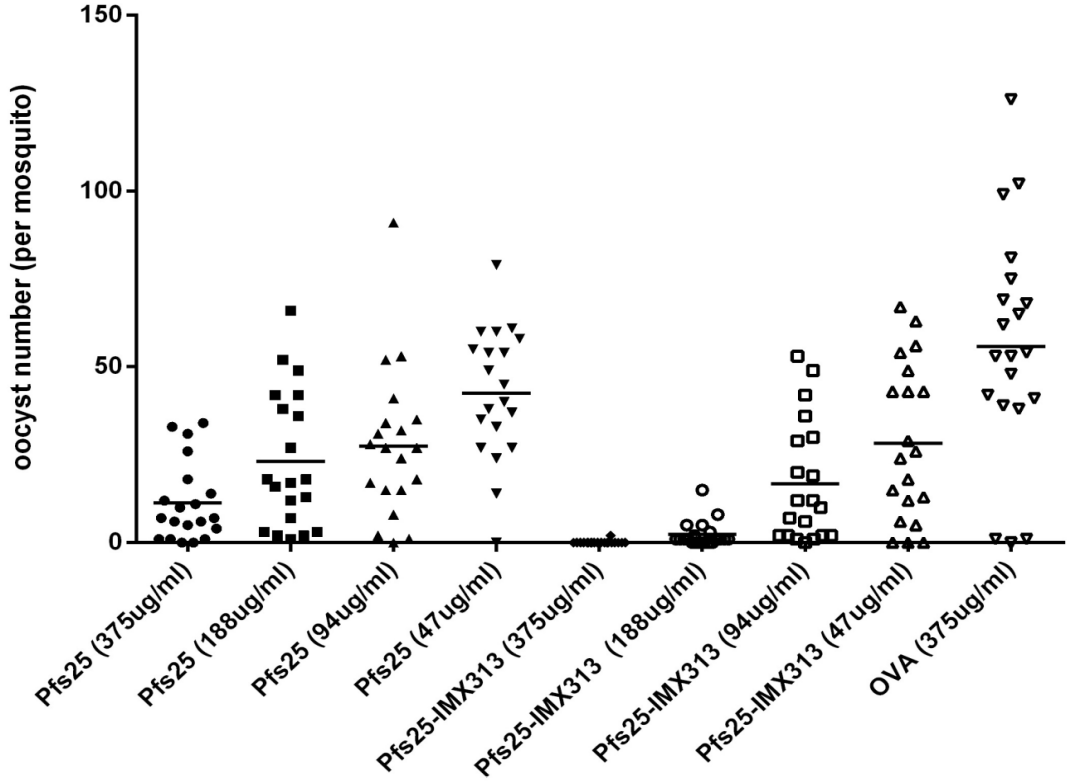

Group (N=20)	Mean oocyst	Inhibition of Intensity/TRA (%) (95% CI)	P value	No. of mosquitoes infected/No. dissected	Inhibition of prevalence/TBA (%)
Pfs25 (375 µg/mL)	11.4	79.7 (39.7, 93.4)	0.006	18/20	5.3
Pfs25 (188 µg/mL)	23.2	58.5 (-14.6, 85.6)	0.100	20/20	0
Pfs25 (94 µg/mL)	27.6	50.7 (-40.0, 83.1)	0.187	19/20	0
Pfs25 (47 µg/mL)	42.5	23.9 (-117.8, 74.5)	0.599	19/20	0
Pfs25-IMX313H (375 µg/mL)	0.1	99.8 (99.4, 100.0)	0.001	1/20	94.7
Pfs25-IMX313H (188 µg/mL)	2.3	95.9 (87.3, 98.7)	0.001	4/20	26.3
Pfs25-IMX313H (94 µg/mL)	16.8	70.0 (5.0, 89.4)	0.038	19/20	0
Pfs25-IMX313H (47 µg/mL)	28.3	49.3 (-46.8, 81.9)	0.222	17/20	10
OVA (375 µg/mL)	55.9	N/A	N/A	19/20	N/A

Figure 4.6: Effect of mouse IgG induced by Pfs25 and Pfgs25-IMX313H immunizations on *P. falciparum* NF54 parasite infectivity in *A. stephensi* mosquitoes.

(A) Day 62 serum pool from mice (n=5) vaccinated with 2.5 µg Pfs25 or Pfs25-IMX313H was used to purify total IgG. Serum pool from OVA vaccinated mice was included as a negative control. Purified IgGs were mixed at different concentrations (as indicated on the x-axis)

with *P.falciparum* NF54 parasites and tested in SMFA. After 7 days, the mosquito midguts were dissected and the numbers of oocysts were counted. Data points represent the number of oocysts in individual mosquitoes and the lines show the arithmetic mean.

(B) The table shows the number of mosquitoes dissected (N) per antigen, mean number of oocysts, % inhibition of infection intensity (TRA) with 95% CI and % inhibition of prevalence (TBA) calculated relative to the IgG from OVA immunized mice (control group). The % inhibition of intensity (TRA) was calculated by: TRA=100* (1 - mean oocyst number in immune plasma/ mean oocyst numberin control group). A negative binomial with zero inflated model was used to calculate the 95% CI and the p value for TRA. The % inhibition of prevalence was calculated by: TBA=100*(1-prevalence of infection for mosquitoes fed with immune plasma/ prevalence of infection for control group).

4.2.4 Avidity and isotype analysis of Pfs25 and Pfs25-IMX313H induced IgGs

I investigated the avidity and isotypes of the anti-Pfs25 IgGs to test if there was a difference in the quality of the antibody response after vaccination with Pfs25-IMX313H nanoparticle and monomeric Pfs25. An avidity ELISA was performed on day 62 serum, collected from mice that received 2.5 μg of Pfs25 or Pfs25-IMX313H vaccine. All individual serum samples with known Pfs25 antibody unit were diluted to give a Pfs25 antibody unit of 1. When mean % of total binding (assuming the binding without the NaSCN was 100%) was plotted against molarity of NaSCN applied, a trend towards higher avidity in groups received Pfs25-IMX313H vaccine was observed (figure 4.7A). There was a difference in the shape of the curves but this was statistically not significant (figure 4.7B).

Isotype ELISA was performed using the same samples as for the avidity ELISA. As the results indicated, the predominant IgG isotypes was IgG1, and similar levels of IgG1 response were observed in Pfs25 and Pfs25-IMX313H vaccinated mice (figure 4.8A). In general, a lower level of IgG2a response was detected in both groups but the IgG2a response in the Pfs25-IMX313H vaccinated group was significantly higher (figure 4.8B).

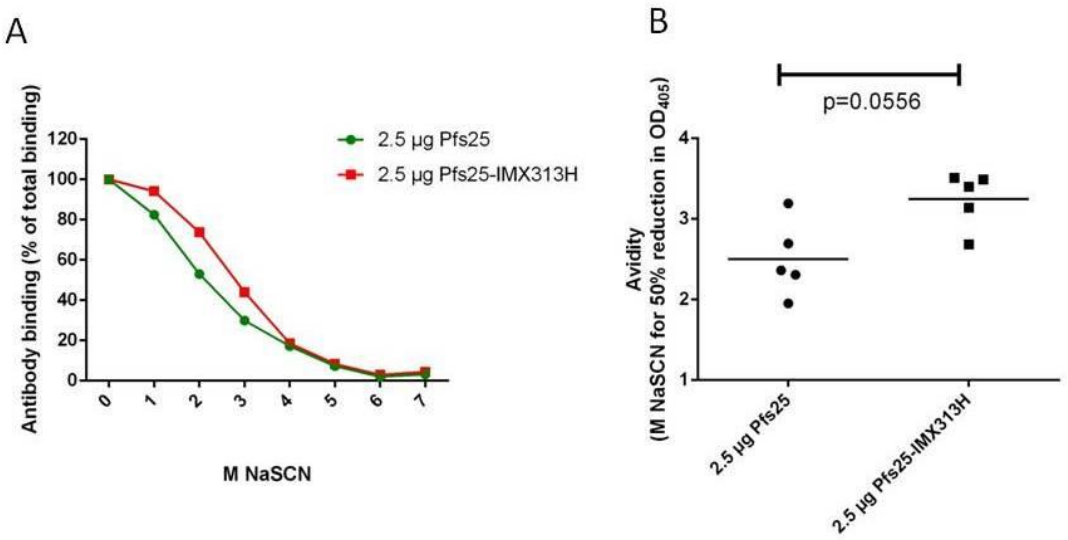

Figure 4.7 Antibodies induced by Pfs25-IMX313H exhibited a higher avidity.

BALB/c mice were immunised with 2.5 µg Pfs25 or Pfs25-IMX313H using the regimes outlined in table 4.1. Day 62 serum was tested for anti-Pfs25 IgG avidity and the data was plotted in two readouts: mean % of total binding (assuming the binding without the NaSCN was 100%) against molar of NaSCN (A) and molar of NaSCN giving 50% reduction of OD_{405} (B). Mann-Whitney test was performed for statistical analysis on B and showed no significant difference in the antibody avidity but the P value was close to significance (p=0.0556).

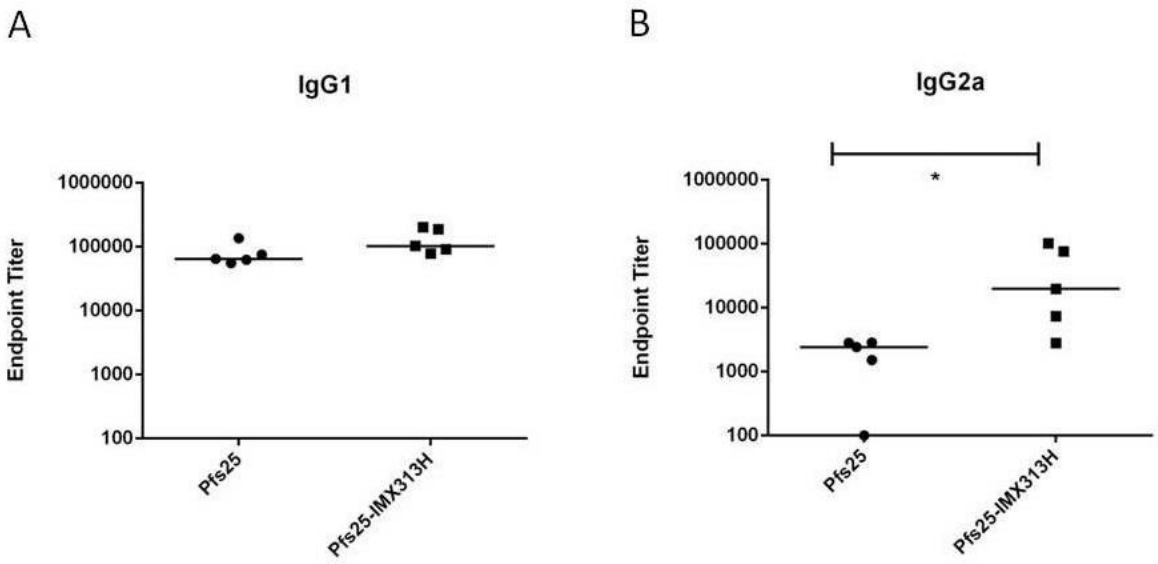

Figure 4.8 Pfs25-IMX313H induced higher IgG2a response.

BALB/c mice (n=5/group) were immunised with 2.5 µg Pfs25 or Pfs25-IMX313H using the regimes outlined in table 4.1. Day 62 serum was tested in whole IgG ELISA and individual isotype IgG responses against recombinant Pfs25 protein were measured: IgG1 (A) and IgG2a (B). * $p<0.05$ by Mann-Whitney test.

4.2.5 Antibody immunogenicity of Pfs25-IMX313H formulated with different adjuvants

In the previous studies I had only tested Pfs25-IMX313H formulated with Alhydrogel. Alhydrogel is alum based adjuvant which is safe but often not very potent. To investigate if the antibody response could be boosted further by formulation with more potent adjuvants, a head-to-head adjuvant comparison using Alhydrogel, MF59 and LMQ was performed. Both Alhydrogel (alum-based adjuvant) and MF59 (oil-in-water emulsion) are adjuvants that have already been used in commercial vaccines, on the other hand, LMQ composed of liposomes, MPL and saponin (similar in composition to AS01 which is used as the adjuvant with RTS,S malaria vaccine) is a preclinical adjuvant. The vaccination regime is summarised in table 4.2. BALB/c mice (n=6/group) were vaccinated with Pfs25-IMX313H nanoparticle formulated with Alhydrogel, MF59 or LMQ. Mice were primed on day 0 and boosted on day 21. Serum was collected on day 20 and day 41 for ELISA. 3 weeks after prime (day 20), LMQ formulated vaccine induced significantly higher anti-Pfs25 IgGs than the other two groups (figure 4.9A). The same trend was observed after the boost. On Day 41, LMQ formulated vaccine out-performed the others. The antibody response after vaccination with MF59 formulated vaccine tended to be higher than the Alhydrogel group but this difference was not statistically significant (figure 4.9B).

Group	Day 0	Day 20	Day 21	Day 41
1. Pfs25-IMX313H **Alhydrogel**	2.5 µg	Bleed	2.5 µg	Bleed
2. Pfs25-IMX313H **LMQ**	2.5 µg	Bleed	2.5 µg	Bleed
3. Pfs25-IMX313H **MF59**	2.5 µg	Bleed	2.5 µg	Bleed

Table 4.2 Vaccination regimes for comparing immunogenicity of Pfs25-IMX313H formulated with different adjuvants.

BALB/c mice (n=6/group) received 2.5 µg of Pfs25-IMX313H nanoparticle vaccines formulated with Alhydrogel, LMQ or MF59. Mice were primed on day 0 and boosted on day 21. The serum was collected on day 20, day 41 for ELISA.

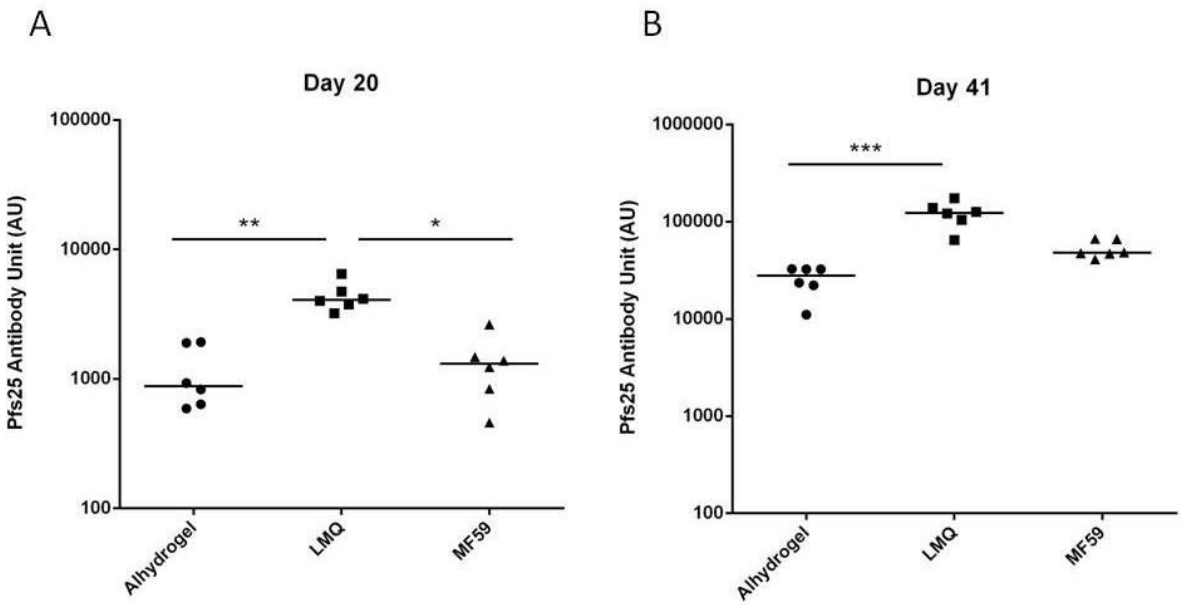

Figure 4.9 immunogenicity study of Pfs25-IMX313H formulated with different adjuvants.

BALB/c mice (n=6/group) were immunised with 2.5 µg Pfs25-IMX313H formulated with Alhydrogel, LMQ or MF59 using the regimes outlined in table 4.2. Serum from day 20 (A) and day 41 (B) was tested using Pfs25 standardised ELISA. Median and individual data points are shown. * $p<0.05$, ** $p<0.01$, *** $p<0.001$ by Kruskal-Wallis test with Dunn's multiple comparison post-test.

4.2.6 Antibody immunogenicity of Pfs25-IMX313H using different vaccination regimes

To compare and find the best vaccination regime to induce the highest anti-Pfs25 antibody response, mice were vaccinated according to the following regimes 1) ChAd63 prime followed by MVA boost (termed A-M), 2) ChAd63 prime followed by protein-in-adjuvant boost (termed A-P) and 3) protein-in-adjuvant prime boost (termed P-P). Matrix M was used as adjuvant to formulate with protein vaccines and the vaccination regime is summarised in table 4.3. BALB/c mice (n=5/group) were vaccinated with Pfs25 A-M, Pfs25-IMX313 A-M, A-P and P-P. $1x10^8$ infectious unit (i.u) of ChAd63, $1x10^7$ plaque-forming unit (pfu) of MVA and 2.5 µg of protein vaccine was used per immunisation. Mice were primed on day 0 and boosted on day 56 (A-M and A-P) or day 28 (P-P), 2 weeks after the boost vaccination (day 70 for A-M and A-P and day 42 for P-P), serum was collected and analyzed using Pfs25 standardised ELISA (figure 4.10). Pfs25-IMX313 P-P regime induced the highest Pfs25-specific antibody response followed by A-P regime. There was no statistically significant difference between the two groups. ChAd63 MVA Pfs25-IMX313 induced a significantly higher response than ChAd63 MVA Pfs25 but this was lower than the other two groups.

Group	Day 0	Day 28	Day 42	Day 56	Day 70
A-M Pfs25	$1X10^8$ i.u			$1x10^7$ pfu	Bleed
A-M Pfs25-IMX313	$1X10^8$ i.u			$1x10^7$ pfu	Bleed
A-P Pfs25-IMX313(H)	$1X10^8$ i.u			2.5 µg + Matrix M	Bleed
Pfs25-IMX313(H) x2	2.5 µg + Matrix M	2.5 µg + Matrix M	Bleed		

Table 4.3 Vaccination regimes for comparing antibody immunogenicity after different prime boost immunisations.

BALB/c mice (n=5/group) were vaccinated with Pfs25 A-M, Pfs25-IMX313 A-M, A-P and P-P. The dosages and prime-boost intervals of each vaccination are shown in the table (i.u: infectious unit; pfu: plaque-forming unit). 2 weeks after the boost vaccination (day70 for A-M and A-P and day 42 for P-P), serum was collected for ELISA.

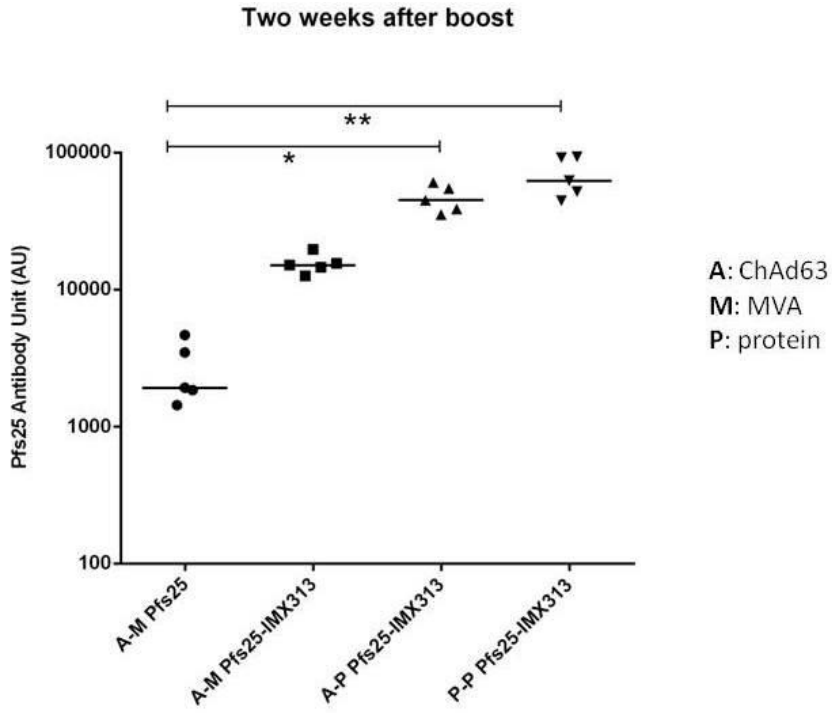

Figure 4.10 Antibody responses after different prime boost immunisations.

BALB/c mice (n=5/group) were immunised according to regimes outlined in table 4.3. 2 weeks after the boost vaccination (day 70 for A-M and A-P, day 42 for P-P), serum was collected and tested using Pfs25 standardised ELISA. Median and individual data points are shown. * $p<0.05$, ** $p<0.01$ by Kruskal-Wallis test with Dunn's multiple comparison post-test.

4.2.7 Expression and production of Pfs25-IMX313T/HT

It is preferable to have a clinical vaccine without a His-tag for the following 2 reasons. 1) Tag-less protein will fully consist of antigen coding sequence and the resulting immune response will be 100% towards the target and 2) because these proteins are purified through nickel coated affinity columns, there are concerns with using such vaccines on nickel sensitive individuals for large scale trials and development.

In order to create a tag-less IMX313 platform, IMAXIO has modified the C-terminus of the IMX313 sequence to contain an arginine repeat (termed IMX313T). The stretch of arginine repeats shifts the overall protein charge and allows an easier separation using ion-exchange chromatography. Heparin is a highly negatively charged glycosaminoglycan, which has a high affinity for arginine via hydrogen bonding as well as electrostatic interaction [228]. As a result, HiTrap Heparin HP column (GE Healthcare, UK) was selected to purify IMX313T. In IMAXIO's lab in Lyon, a heparin column was able to separate IMX313T from *E. coli* lysate with very high purity (unpublished results). In addition, DNA vaccination at IMAXIO showed higher immunogenicity of IMX313T compared to IMX313 (unpublished); the mechanism of this observation was however not studied.

Pfs25-IMX313T cloned in a *P. pastoris* expression plasmid was received from IMAXIO and a His-tagged version of Pfs25-IMX313T (termed Pfs25-IMX313HT, H refers to N-terminus His-tag) was also included for the purpose of 1) improving the protein purity by providing additional an purification option and 2) providing a head-to-head comparison between Pfs25-IMX313H, Pfs25-IMX313HT and Pfs25-IMX313T nanoparticle vaccines to detect if the antibody response is influenced by addition of His-tag and arginine repeats. Both proteins sequences were cloned into pPinkα-HC plasmid and transformed into strain 1 *P. pastoris*.

Small scale protein expression tests showed that both proteins were successfully secreted (figure 4.11). Colony number 02 from both transformed *P. pastoris* preparations were chosen as the working colonies. Large scale production for both proteins was performed under the same condition as Pfs25-IMX313H (48 hours fermentation at 25°C with 2% methanol added v/v every 24 hours). To purify Pfs25-IMX313T, supernatant was desalted using tangential flow filtration (TFF) against 10mM phosphate buffer. Desalted supernatant was then loaded onto the heparin column and eluted with 2M NaCl in 10mM phosphate buffer. To find the best pH to separate target protein from yeast contaminants using heparin column, a gradient elution was set up under 3 different pH conditions (6.5, 7.0 and 7.5). It was found by using elution buffer at pH7.5, that Pfs25-IMX313T protein can be separated with the highest purity (figure 4.12). After the heparin column purification, Pfs25-IMX313T was further purified by SEC and the final pooled protein was analysed on SDS-PAGE with silver staining (figure 4.13A). Pfs25-IMX313HT was purified using the same methods as for Pfs25-IMX313H (via His-tag purification followed by SEC), purified protein was also analysed on SDS-PAGE with silver staining (figure 4.13B). Silver staining revealed that both proteins were very pure and appeared to form heptamers (~180kDa) in non-reducing conditions.

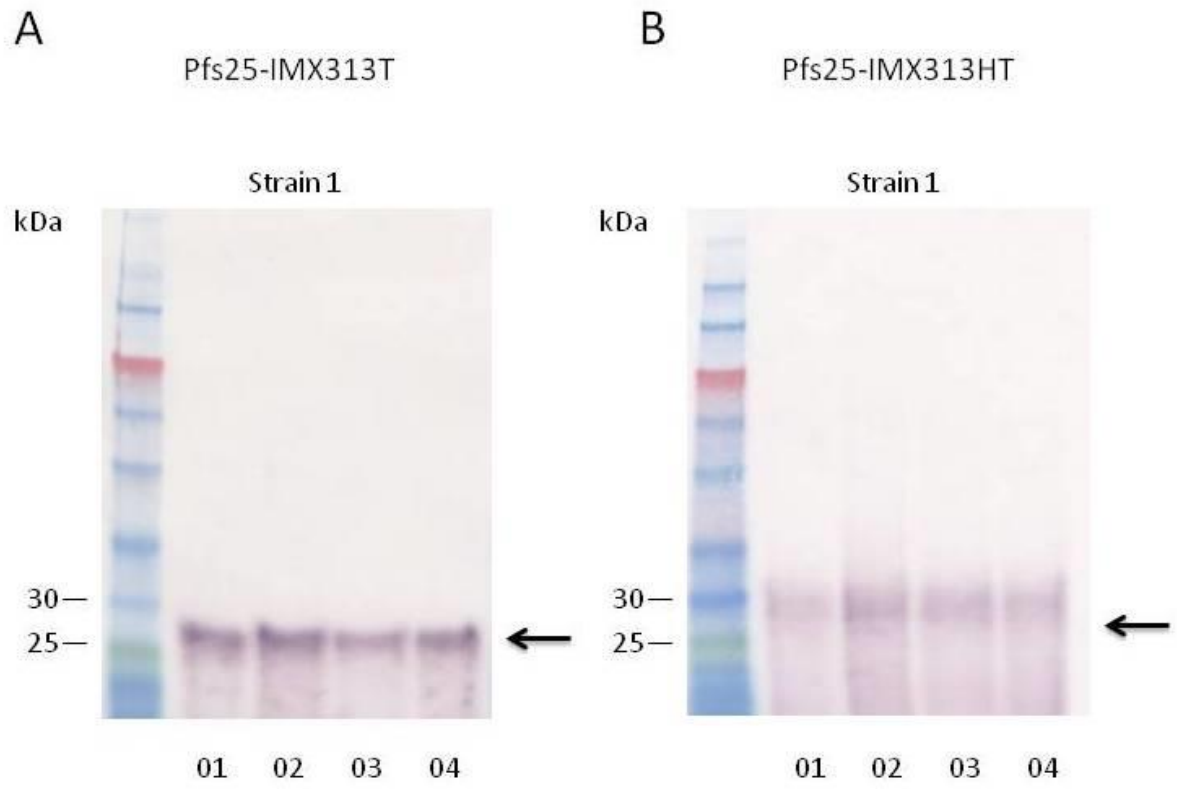

Figure 4.11 Selection of *P. pastoris* for expression of recombinant Pfs25-IMX313T and Pfs25-IMX313HT.

Strain 1 *Pichia pastoris* from Pichiapink™ was transformed with pPinkα-HC expression plasmid containing Pfs25-IMX313T (A) and Pfs25-IMX313HT (B) sequence. 4 positive colonies were picked for small scale protein expression test. Cell culture supernatant was harvested 72 hours after the fermentation (29°C, 4% methanol added v/v every 24 hours). After protein expression, crude culture supernatant was loaded on SDS-PAGE under reducing condition and analysed by western blot using Pfs25 antiserum. Arrow indicates the expected size (26kDa) of Pfs25-IMX313T and Pfs25-IMX313HT monomer.

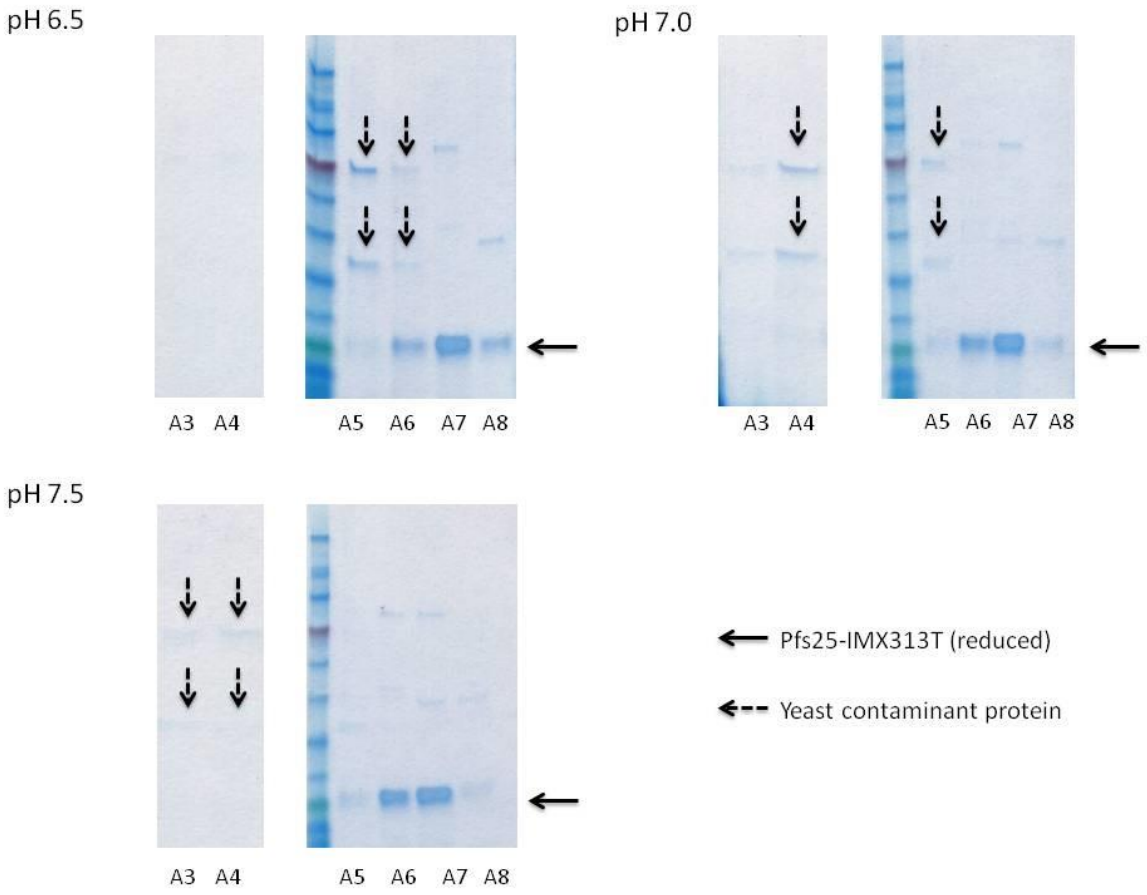

Figure 4.12 Investigation of optimum pH to elute Pfs25-IMX313T from Heparin column.

Pfs25-IMX313T transformed yeast culture from a large scale (2L) expression was fermented for 48 hours at 25°C with 2% methanol added v/v every 24 hours in shaking flasks. The supernatant was desalted using TFF against 10mM phosphate buffer and loaded onto heparin column. Gradient elution using the 2M NaCl in 10mM phosphate buffer at different pHs was set up and the elution fractions were collected and run on reducing SDS-PAGE. Coomassie blue staining analysis revealed both Pfs25-IMX313T monomeric protein (solid arrows) and yeast contaminant proteins (dotted arrows). The result shows that elution using 2M NaCl in 10mM phosphate buffer at pH7.5 can separate Pfs25-IMX313T from the majority of the yeast contaminant proteins.

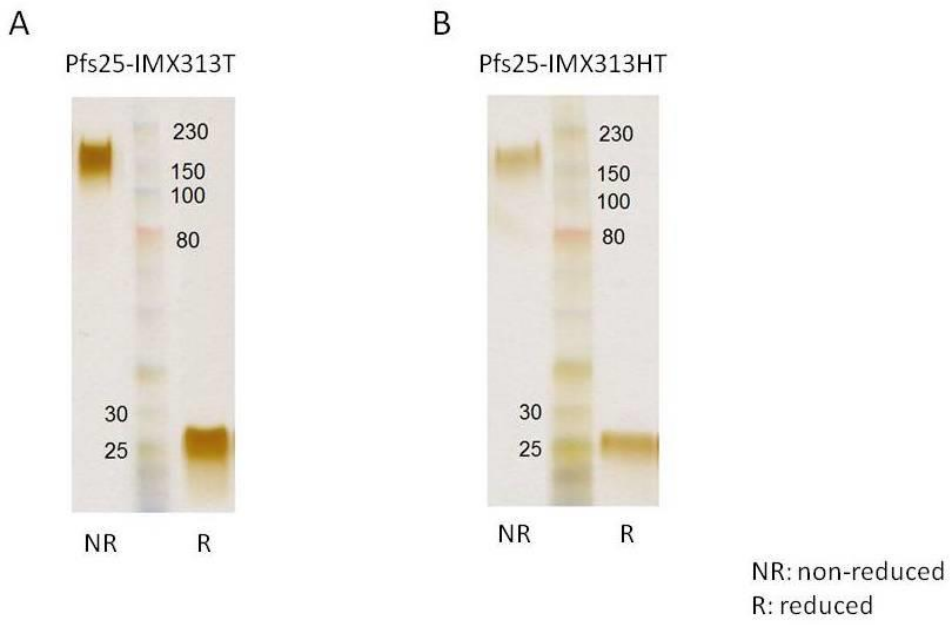

Figure 4.13 Silver staining analyses revealed both Pfs25-IMX313T and Pfs25-IMX313HT formed heptamers.

After SEC, Pfs25-IMX313T (A) and Pfs25-IMX313HT (B) from protein containing fractions were pooled and run on SDS-PAGE under both reducing and non-reducing conditions. Silver staining analysis revealed both the heptameric (~180KDa) and monomeric (~26kDa) forms of the nanoparticle protein.

4.2.8 Immunogenicity study comparing Pfs25-IMX313 nanoparticle fused with different tags

Pfs25-IMX313T was generated in order to have a tag-less and potentially more immunogenic substitute for Pfs25-IMX313H. To compare the antibody immunogenicity between Pfs25-IMX313H, Pfs25-IMX313HT and Pfs25-IMX313T, BALB/c mice were vaccinated with these 3 nanoparticles formulated with Alhydrogel; the detailed vaccination regime is summarised in table 4.4. No significant difference in the anti-Pfs25 IgG response was observed between these three protein vaccines either after prime (figure 4.14A) or after boost (figure 4.14B).

Group	Day 0	Day 20	Day 21	Day 41
Pfs25-IMX313H	2.5 μg	Bleed	2.5 μg	Bleed
Pfs25-IMX313HT	2.5 μg	Bleed	2.5 μg	Bleed
Pfs25-IMX313T	2.5 μg	Bleed	2.5 μg	Bleed

Adjuvant: Alhydrogel

Table 4.4 Vaccination regimes for comparing the immunogenicity of Pfs25-IMX313H, Pfs25-IMX313HT and Pfs25-IMX313T nanoparticles.

BALB/c mice (n=6/group) received 2.5 μg of Pfs25-IMX313H, Pfs25-IMX313HT and Pfs25-IMX313T nanoparticle vaccines formulated with Alhydrogel. Mice were primed on day 0 and boosted on day 21. The serum was collected on day 20, day 41 for ELISA.

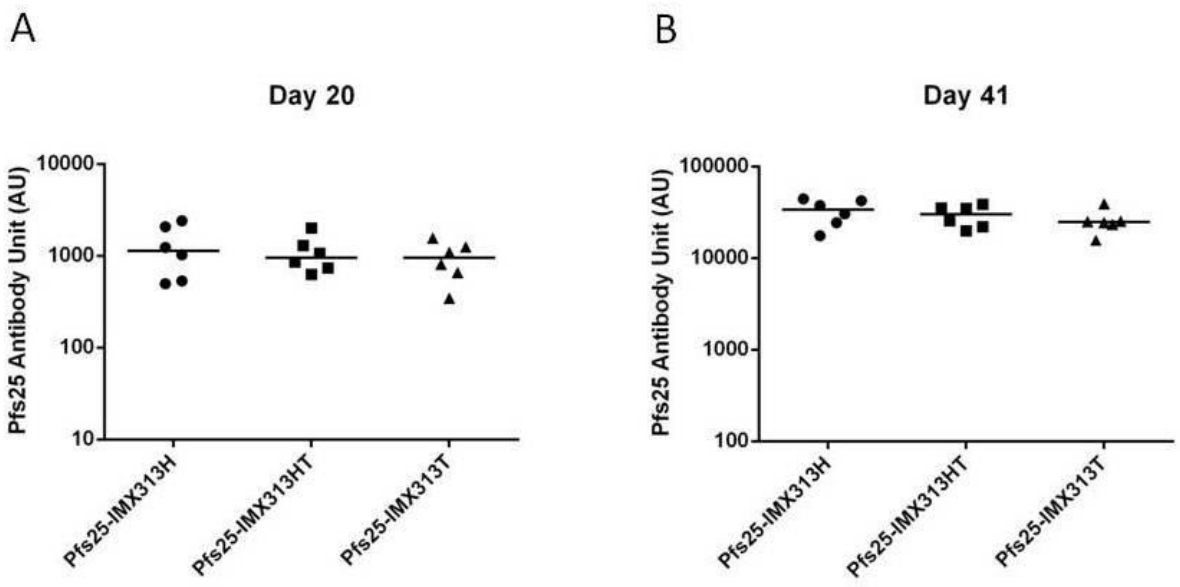

Figure 4.14 Pfs25-IMX313H, Pfs25-IMX313HT and Pfs25-IMX313T exhibited similar antibody response.

BALB/c mice (n=6/group) were immunised according to regimes outlined in table 4.4. Serum from day 20 (A) and day 41 (B) was collected and tested using Pfs25 standardised ELISA. Median and individual data points are shown. There was no significant difference seen between the groups (Kruskal-Wallis test with Dunn's multiple comparison post-test).

4.2.9 Safety study of Pfs25-IMX313H and Pfs25-IMX313T

IMX313 is a hybrid chicken equivalent of human C4bp oligomerization domain. The IMX313 sequence has less than 20% homology to human C4bp (Hc4bp). There might be a concern that vaccination with protein fused to IMX313 could generate immune responses against IMX313 itself and that these antibodies could cross-react with the Hc4bp oligomerization domain. To test this, day 41 serum from mice that received 2 immunisations of 2.5 µg Pfs25-IMX313H or Pfs25-IMX313T vaccines (from study in section 4.2.8) and day 62 serum from mice received 3 immunisations of 2.5 µg Pfs25 monomeric protein (from study in section 4.2.2, negative control) were first tested for the antibody response against IMX313. ELISA plate was coated with IMX313 protein (provided by Dr Fergal Hill, IMAXIO) and a whole IgG ELISA was performed. Anti-IMX313 IgGs, as expected, were detected and were significantly higher in Pfs25-IMX313H and Pfs25-IMX313T vaccinated mice than the Pfs25 negative control group (figure 4.15A). When these serum samples were tested against Hc4bp isolated from human plasma (provided by Dr Fergal Hill), none of them were positive (figure 4.15B). Hc4bp antiserum from mice vaccinated with Hc4bp (provided by Dr Fergal Hill) was included in the ELISA as positive control which showed significantly higher anti-Hc4bp IgG titres than the rest of the test groups (figure 4.15B). Together, these data demonstrated that Pfs25-IMX313H and Pfs25-IMX313T nanoparticles did not induce antibodies to Hc4bp supporting the potential safety of these constructs (in terms of antibody responses that can cross-react to Hc4bp) for use as vaccine candidates in humans.

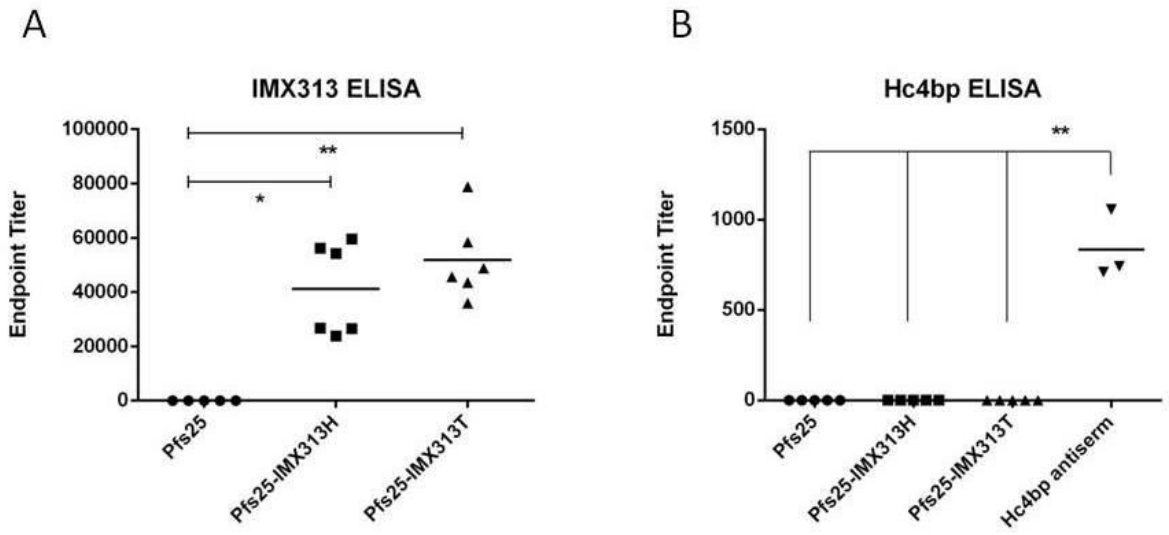

Figure 4.15 Both Pfs25-IMX313H and Pfs25-IMX313T nanoparticles induced antibody response against IMX313, but not to Hc4bp.

Serum from mice previously vaccinated with Pfs25, Pfs25-IMX313H and Pfs25-IMX313T were tested for their antibody response against IMX313 (A) and Hc4bp (B) using the whole IgG ELISA method. Median and individual data points of endpoint ELISA titre are shown. * $p<0.05$, ** $p<0.01$ by Kruskal-Wallis test with Dunn's multiple comparison post-test.

4.2.10 Discussion

In this chapter, I have described the production, purification, immunogenicity as well as functional studies of Pfs25-IMX313 based nanoparticle vaccines. This was the first time IMX313 fused constructs were expressed as a secreted heptameric protein in *P. pastoris*.

Comparing *P. pastoris* expressed Pfs25 and Pfs25-IMX313H, Pfs25-IMX313H nanoparticle induced significantly higher antibody response than monomeric Pfs25 protein (figure 4.5) when vaccinated based on total protein. Calculation based on the molecular weight revealed only 74% of the Pfs25-IMX313H is Pfs25 (i.e. 2.5 μg of Pfs25-IMX313H contains 1.85 μg of Pfs25 plus 0.65 μg of IMX313). As a result, when the dosage of immunisation was normalized based on the Pfs25 content, one would expect even higher antibody responses than what was seen in this study. In addition to a higher antibody response, a clear "dose-sparing" effect was demonstrated with Pfs25-IMX313H vaccine, suggesting a possibility of using a lower vaccination dose to achieve similar level of antibody response observed in this study. A vaccine with good immunogenicity profile together with a lower vaccination dosage requirement will be preferable over vaccines that require higher dosages because the former will be considered more cost-effective for future development.

SMFA was performed to test if vaccine induced antibodies are functional and inhibit parasite development in the mosquito. At 375 μg/mL total IgG concentration, IgGs purified from mice that received both vaccines exhibited statistically significant TRA compared to the OVA vaccinated group (negative control) (figure 4.6). At lower concentrations, IgGs from Pfs25 vaccinated mice failed to show significant TRA while IgGs from Pfs25-IMX313H vaccinated group exhibited significant TRA even at concentration of 94 μg/mL. A similar trend was observed for TBA. The result from SMFA demonstrated both Pfs25 and Pfs25-IMX313H can induce functional antibodies that exhibit TRA and TBA in mosquitoes and serum from Pfs25-IMX313H vaccinated mice was more potent at inhibiting parasite development. This difference in SMFA could be simply due to more Pfs25-specific IgGs present (within the total IgG tested) in Pfs25-IMX313H vaccinated mice serum as expected from the ELISA readout

(figure 4.5A). Another possible contributing factor is that Pfs25-313H probably induced a qualitatively (based on avidity and/or isotypes) different anti-Pfs25 IgG than monomeric Pfs25.

Compared to Pfs25, Pfs25-IMX313H induced Pfs25-specific IgGs with higher avidity, though this was not statistically significant (figure 4.7). Antibody avidity, measures the overall strength of antibody-antigen interactions [229] and could in theory contribute to a better TRA and TBA in SMFA since the only known mechanism of inhibition for Pfs25-specific IgGs is through antibody mediated parasite neutralisation. It is interesting to see a qualitative difference in the antibody because both protein vaccines contained exactly the same Pfs25 sequence. One possible explanation would be that the two Pfs25 proteins in these two vaccines had different conformations. The change of protein overall conformation could alter the B cell epitopes displayed by the vaccine antigen. As a consequence, the antibodies generated by both vaccines may have a different Pfs25 target epitope profile. Since different epitopes tend to have different interaction affinity to their corresponding antibodies, this could provide an explanation for the probable difference in antibody avidity observed in this study. Conformational dependant mAbs such as 1D2 [215] may help to detect conformational changes. However, we do not have access to these mAbs currently but it will be interesting to investigate in the future. Another possible explanation could be that Pfs25-IMX313H vaccinated mice developed higher germinal centre (GC) responses (where antigen specifc B cells undergo somatic hypermutation (SHM)). During SHM, the variable regions of immunoglobulin genes undergo programmed mutation from which the B cells with highest affinity for the antigen (in this case, Pfs25) are selected [230]. The difference in the level of GC response can result in a difference of B cell affinity maturation

and hence difference in the overall antibody avidity. Antibody avidity has been used as a marker of B cell maturation (to discriminate between primary and secondary responses) in many infections disease studies including of dengue virus [231], rubella virus [232], cytomegalovirus [233], herpesvirus [234] and Vibrio cholera infection [235]. In the next chapter, possible differences in the GC response between the two vaccines are investigated.

Comparing Pfs25 and Pfs25-IMX313H induced IgG subtypes; IgG1 seemed to be the predominant isotype induced by both vaccines and there was no significant difference in the IgG1 response (figure 4.8A) but significantly higher IgG2a response was induced by Pfs25-IMX313H nanoparticle (figure 4.8B). Regardless of isotypes, higher anti-Pfs25 antibody titres will evidently improve the transmission blocking activity; however it is still unclear whether induction of specific IgG isotypes is important to this activity. Coban *et al* [236] demonstrated recombinant Pfs25 (NIH) formulated with alum plus CpG Oligodeoxynucleotide induced both IgG1 and IgG2a responses in mice, and the Pfs25-specific IgG2a antibodies exhibited a lower avidity than the IgG1. If this is true, the anti-Pfs25 IgG1 is a qualitatively better isotype over IgG2a in terms of antibody avidity and the anti-Pfs25 IgG1 would be a preferred isotype if the mechanism of transmission-blocking in mosquitoes is only based on antibody mediated neutralisation. Anti-Pfs230 63F2A2 mAb isotype IgG2a and IgG2b exhibited significantly better TBA in SMFA than IgG1 only in the presence of active complement [237]. These complement dependent transmission-blocking effects of 63F2A2 mAb IgG2a and IgG2b was confirmed *in vitro* by the rapid lysis of newly formed macrogametes or zygotes [237]. Additionally, 8 other anti-Pfs230 mAbs of isotype IgG2a and 3 isotype IgG2b were reported effective in blocking transmission in a complement dependent manner, whereas 14 tested anti-Pfs230 IgG1 mAbs were not [237]. These results

suggest IgG2a and IgG2b isotypes may provide extra transmission blocking activity by interacting with complement proteins ingested by the mosquito during blood meal. However it is not clear if this mechanism could occur for anti-Pfs25 antibodies. Pfs25 is expressed at a later parasite stage (zygote and ookinete) than Pfs230 (gametocyte and gamete). According to Angrisano *et al* [238], the zygote is formed inside mosquito within the first hour after blood meal and develops over the next 24 hours into the ookinete. Though no evidence from the literature was found, it might be possible for the complement proteins to perform Pfs25-specific antibody mediated complement dependent parasite lysis if the proteins are still active in the midgut (i.e. not degraded by protease) at the zygote/ookinete stage. However, the SMFA performed in this study used heat inactivated serum and does not contain active complement proteins therefore the mechanism of parasite inhibition observed in this study should be purely based on the antibody mediated neutralisation. Furthermore, a recent study performed by Goodman *et al* [147] demonstrated no correlation between Pfs25 viral vectored vaccine induced IgG1, IgG2a or IgG2b, IgG1:IgG2a ratio and TRA or TBA in DFA in mice; suggesting the specific anti-Pfs25 isotypes may not play as an important role as the total anti-Pfs25 antibody titres or avidity in the membrane feeding assays. Perhaps SMFA directly comparing affinity purified anti-Pfs25 IgG1 and IgG2a could be performed in the future to assess their individual transmission-blocking functionality. IgG1 and IgG2a are classical markers of T-helper cell type 2 (Th2) response and T-helper cell type 1 (Th1) response respectively [239]. The study also demonstrated that the IMX313 nanoparticle platform is capable of inducing a more balanced Th1 and Th2 response than soluble protein alone which induces predominantly Th2 responses.

Because antibody is the sole immune component TBV rely on, different adjuvants as well as different vaccination regimes including AdCh63-MVA (A-M), AdCh63-protein (A-P) heterologous prime-boost immunizations and two-shot protein regimes have been looked at and evaluated by ELISA to find the best combination to induce the highest antibody response in mice. Both Alhydrogel and MF59 are adjuvants that have already been used in commercial vaccines; on the other hand, LMQ (which has a very similar composition to AS01 which is used as the adjuvant with the RTS,S malaria vaccine) is a preclinical adjuvant. The results (figure 4.9) clearly demonstrated a significantly higher antibody response was generated in mice when Pfs25-IMX313H was formulated with LMQ suggesting that formulation with a potent adjuvant is as important as the vaccine platform and Pfs25-IMX313H induced antibody response could be further elevated by a potent adjuvant.

Pfs25-IMX313 based vaccines were also tested in A-M, A-P and P-P heterologous and homogenous prime-boost regimes. Adenovirus vaccination primes a very good antibody response and A-M [73, 147], A-P [88, 240, 241] heterologous prime-boost regimes was reported to induce strong T and B cell responses. In addition, using AdHu5 expressing OVA and OVA protein formulated with adjuvants (Abisco®100, Adju-Phos®, Alhydrogel®, CoVaccineHT™, Freund's Adjuvant and Montanide® ISA720), it was demonstrated AdHu5-protein vaccination regime induced higher OVA-specific IgG response than three-shot protein regime except for when OVA was formulated with Freund's Adjuvant and Montanide® ISA720 [241]; suggesting A-P regime is highly immunogenic. The results (figure 4.10) from this study indicated that the P-P regime induced the highest Pfs25-specific IgG response followed by the A-P regime. There was no significant difference in the antibody responses between the two regimes and in view of cost of goods, the manufacturing of a

single component (P-P) is more attractive and hence this was chosen as the preferred regime.

Pfs25-IMX313T was produced as a tag-less version of Pfs25-IMX313H. There was no difference in the antibody response between the His-tagged and the tag-less version of Pfs25-IMX313 judged by Pfs25 standardized ELISA (figure 4.14). Based solely on the ELISA titre together with the knowledge that there was very little sequence change between the two proteins (Pfs25-IMX313H and Pfs25-IMX313T) and both proteins formed heptamers, it is probably safe to assume that both protein vaccines would have similar transmission blocking effect in the SMFA. Both proteins induced antibody responses against IMX313 (figure 4.15A) but not against Hc4bp (figure 4.15B) supporting their likely safety for testing in humans. Indeed, IMX313 has recently been safely used to try and adjuvant Antigen 85 from M. tuberculosis in an MVA vector in a Phase 1 trial at oxford [224].

To summarise, IMX313 is a very immunogenic vaccine platform; compared to monomeric Pfs25 protein expressed in the same system, Pfs25 fused to IMX313 were expressed as a heptamer and induced quantitatively as well as qualitatively better IgG response in mice. The vaccine is very promising for further studies in non human primates and human clinical trials as a transmission-blocking vaccine alone or in combination with pre-erythrocytic and blood-stage vaccines.

Chapter 5

Investigating mechanisms of immunogenicity of the Pfs25-IMX313 nanoparticle

5. Investigating mechanisms of immunogenicity of the Pfs25-IMX313 nanoparticle

5.1 Introduction

In chapter 4, I described the production, purification as well as immunogenicity of the Pfs25-IMX313 based nanoparticle vaccine. Using a protein-in-adjuvant prime boost regime, Pfs25-IMX313H demonstrated superior antibody immunogenicity. In this chapter, I investigate the mechanisms underlying the high immunogenicity of the Pfs25-IMX313 nanoparticle.

The fundamental differences between monomeric Pfs25 protein and Pfs25-IMX313H nanoparticle are the protein size and the number of antigen epitopes displayed by the vaccine. The Pfs25-IMX313H heptamer has a much higher molecular weight (180kDa) than monomeric Pfs25 (19 kDa). IMX313 heptamer (47 kDa) was determined by crystallography analysis to be a particle of 6 nm in size (personal communications with Dr Fergal Hill). Although not assessed, it is reasonable to assume that the Pfs25-IMX313H fusion will be of size similar or larger (due to the addition of Pfs25) than 6 nm and hence referred to as a nanoparticle. (defined as any particulate material with size 1–1000 nm [242]). As reviewed by Bachman, M.F. and Jennings, G.T. [197], the size of antigen is an important factor for antigen uptake by APCs. Particulate antigens such as nanoparticles and VLPs have large surface areas that could carry positive charged [243], hydrophobic [244] or receptor-interacting (PAMP) properties all of which could lead to a better interaction with APCs than soluble protein antigens. Particulate antigens also carry highly repetitive epitopes that can lead to a more efficient binding of low-affinity natural IgM [245], which in turn promotes antigen uptake (opsonisation) by APCs via the Fc-Fc receptor interactions as well as activation of complement cascade through the classical pathway resulting in recruitment of

more immune cells. In addition, natural IgM together with complement proteins were able to transport particulate antigen, but not soluble protein, to follicular dendritic cells (FDC, type of cells resident in GC and trap immune-complexed antigen thus providing sustained stimulation to B cells [246]) without prior immunity [245]. To date, several studies have already demonstrated that the size of the antigen plays an important role in the kinetics of antigen-uptake by APCs [202, 247], and the antigen with the optimal uptake kinetics induced the highest immune response [202]. In addition, nanoparticles with a size range of 20-200nm including VLPs (of 30nm) have been found to be able to diffuse through lymphatic endothelial cell junctions and reach the lymph nodes (LNs) in a dendritic cell (DC) independent manner; in comparison, large particles (500-2000nm) require DCs to transport them to the LN [248]. This study suggested small particles such as VLPs can efficiently transport to LN and activate immune cells. This difference in the antigen uptake could be one of the mechanisms behind Pfs25-IMX313H nanoparticle's high immunogenicity.

Apart from increased antigen uptake and antigen distribution, the highly repetitive epitopes found on nanoparticles or VLPs can promote cross-linking of BCRs which send a strong B cell activation signal and can activate B cells without the co-stimulatory signal from Th cells. Using hapten as a model antigen, it has been shown that roughly more than 15 molecules spaced 5-10 nm apart are enough to stimulate naïve B cells (T cell-independent activation) [249]. In addition, repetitive protein antigens are also targets of the complement system (via natural IgM). A complement tagged antigen can interact with the CD19/CD21 complex on B cell surface and facilitate B cell activation by lowering the activation signal threshold [250]. More efficient production of antigenic peptide/class II complexes through this engagement was also reported [251] which is crucial for the development of T cell-dependent B cell

responses. Jegerlehner *et al* [252] investigated the relationship between antigen epitope density and antibody response in mice, using hepatitis B core antigen (HBcAg) VLP as an antigen carrier. The study revealed that early B cell activation, such as T cell-independent IgM production, was not significantly influenced by antigen epitope densities. In contrast, the T cell-dependent IgG response was significantly affected and antigen with a high epitope density induced significantly higher antigen-specific IgG responses. This epitope density dependent IgG response was observed in another study where Pfs25 conjugated to OVA at high Pfs25/OVA molar ratios induced higher Pfs25-specific IgG response than constructs with a low Pfs25/OVA ratio [169]. This difference in the antigen epitope density could be another mechanism behind Pfs25-IMX313H nanoparticle's high immunogenicity.

During natural infection or after vaccination, activated follicular B cells undergo SHM in GCs with the help from Tfh cells and FDC and develop into plasma B cells capable of producing high levels of class-switched antibodies with matured antigen affinity. One recent study by Moon *et al* [253] compared the immunogenicity induced by soluble recombinant *Plasmodium vivax* CSP antigen and CSP foumulated in nanoparticle composed of multilamellar "stapled" lipid vesicles. The nanoparticle induced significantly higher anti-CSP antibodies with higher avidity than soluble CSP. Furthermore, the nanoparticle vaccinated mice developed significantly a higher GC B cell response in the draining lymph nodes (LNs) confirmed by flow cytometry analysis and LN section staining. A significantly higher Tfh cell was also observed by flow cytometry analysis. A separate study has demonstrated that the level of GC B cell response correlated with antigen-specific antibody titres [254]. Higher anti-Pfs25 antibody titre was induced by Pfs25-IMX313H and these antibodies had a higher avidity than antibodies induced by monomeric Pfs25. From the above results, it seems

possible that the Pfs25-IMX313H nanoparticle could have induced higher level of GC and/or Tfh response than Pfs25 monomeric protein. And this difference may be the direct mechanism behind the higher antibody titre and avidity measured in Pfs25-IMX313H vaccinated mice.

5.2 Results

5.2.1 Germinal centre response after Pfs25-IMX313H vaccination

BALB/c mice were immunised IM with 2.5 μg of Pfs25 or Pfs25-IMX313H formulated with Alhydrogel. The draining inguinal and popliteal lymph nodes (dLNs) as well as the spleens were harvested at days 9 and 14 post-vaccination. The cells were isolated and surface stained for germinal centre B cells and analysed using flow cytometry. Germinal centre B cells express the B and T cell activation marker (GL7) and Fas (CD95) which is responsible for their programmed cell death via Fas-Fas ligand interaction in the absence of survival signals from Tfh [255]. With another GC B cell marker B220 [256], germinal centre B cells in this study were defined as GL7+CD95+B220+ cells. The gating strategy in this study for GC B cells is shown in figure 5.1. Because the staining is not antigen-specific, tissues from naïve mice were also harvested as a control to measure the background GC response.

In the dLNs (figure 5.2A), there was a trend of increased GC B cells in Pfs25-IMX313H vaccinated mice on day 9 post-vaccination. On day 14, this difference in GC B cell response between Pfs25 and Pfs25-IMX313H was significantly different; Pfs25-IMX313H induced significantly more GC B cells while the level of GC B cells in the Pfs25 vaccinated group was similar to the background level in the naïve mice. In the spleen (figure 5.2B), there was no significant difference seen between the two vaccinated groups and naïve mice on both days

but an elevated level of GC B cell response were observed in both vaccinated groups on day 14.

To confirm the difference of GC response observed in the draining lymph node on day 14. DLNs were sectioned and the samples were stained with fluorescence labelled anti-GL7 and anti-B220 antibodies. Samples were visualised under a fluorescence microscope DMI3000B (Leica Microsystems, UK), and the fluorescent image is shown in figure 5.3. GCs (GL7+) were clearly visible and stained in sections derived from Pfs25-IMX313H vaccinated mice. On the other hand, no GCs were observed in sections from mice vaccinated with monomeric Pfs25.

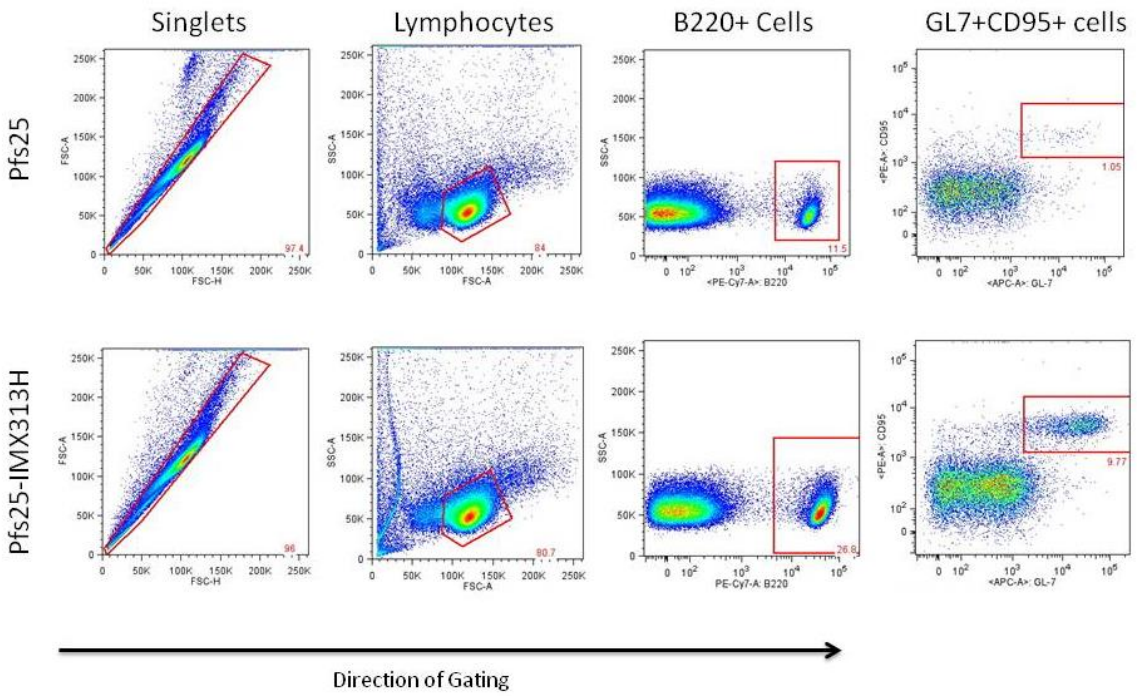

Figure 5.1 Gating strategy to identify Germinal centre B cells.

BALB/c mice were immunised IM with 2.5 µg of Pfs25 or Pfs25-IMX313H formulated with Alhydrogel. 9 or 14 days after the vaccination, the draining inguinal and popliteal lymph nodes as well as spleen were harvested and stained for GC B cells. The sequential gating strategy is shown and the gates show the percentage of parent.

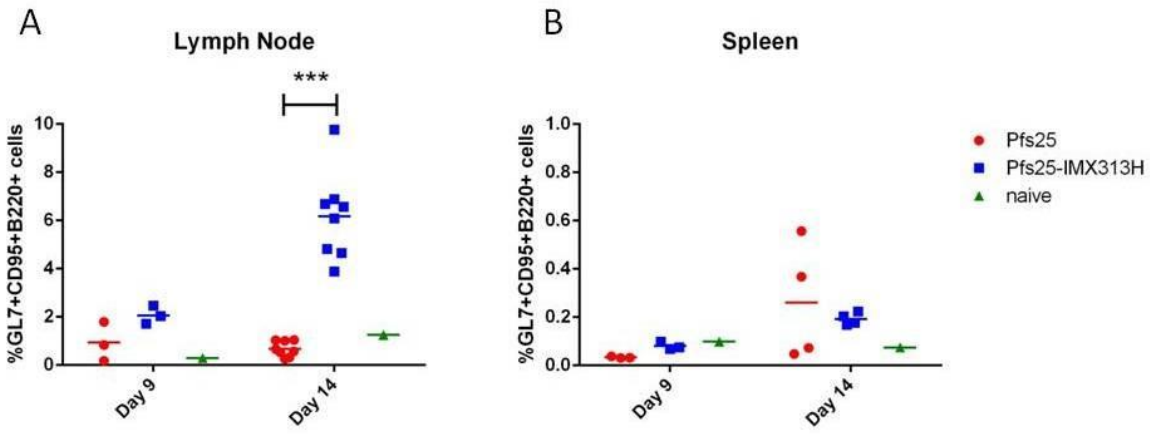

Figure 5.2 GC B cell responses at 9, 14 days after vaccination.

BALB/c mice were immunised IM with 2.5 µg of Pfs25 or Pfs25-IMX313H formulated with Alhydrogel. 9 or 14 days after the vaccination, the draining inguinal and popliteal lymph nodes (A) as well as the spleen (B) were harvested and stained for GC cells as outlined in 5.2.1. The median and individual % of GL7+CD95+B220+ cells is shown, *** $p<0.001$ by Mann-Whitney test.

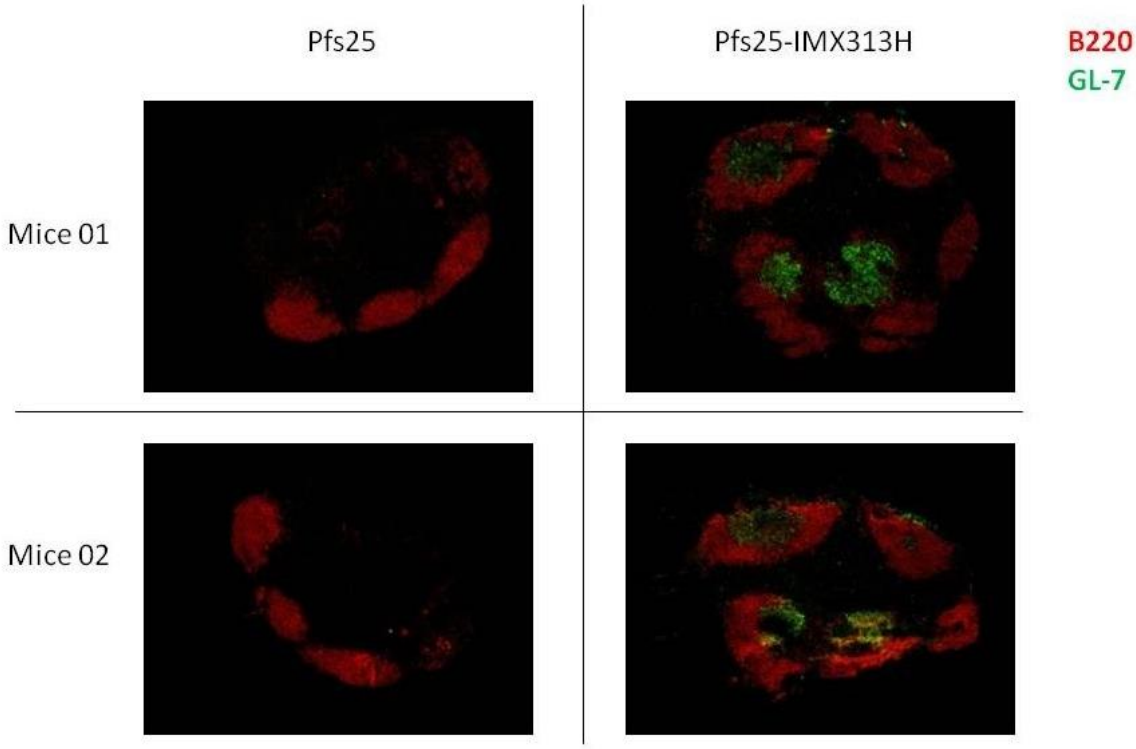

Figure 5.3 GCs were observed in dLN 14 days after Pfs25-IMX313H vaccination.

BALB/c mice (n=2/group) were immunised IM with 2.5 μg of Pfs25 or Pfs25-IMX313H formulated in Alhydrogel. 14 days after the vaccination, the draining inguinal and popliteal lymph nodes was harvested, sectioned and stained with fluorescence labelled anti-GL7 (green) and anti-B220 (red) antibodies. A representative LN section from each mouse is shown. Green signal indicates GCs.

5.2.2 Tfh response after vaccination

T follicular helper cells (Tfh) are a type of T cell localised to B cell follicles of GCs which promote antibody production by assisting in GC formation [20]. Cytokines produced by Tfh cells were shown to improve the antibody repertoire by promoting class-switching and SHM [257]. This type of cell was reported to have a special phenotype of CD4+PD1+CXCR5+ [255]. Because there was a difference in germinal centre formation in mice vaccinated with Pfs25 and Pfs25-IMX313H measured at day 14, the % of Tfh cells is investigated and correlation between the GC response and the Tfh cell response is analysed.

BALB/c mice were vaccinated IM with 2.5 μg of Pfs25 or Pfs25-IMX313H formulated with Alhydrogel. 14 days after vaccination, the draining inguinal and popliteal lymph nodes were harvested, cells were isolated and then surface stained for CD4+PD1+CXCR5+ Tfh cells and analysed using flow cytometry. The gating strategy in this study to identify Tfh cells is shown in figure 5.4. The CXCR5+ and PD1+ gates were set using a Fluorescence Minus One (FMO) control. Because the staining is not antigen-specific, tissues from naïve mice were also harvested as a control to measure the background Tfh response.

14 days post vaccination, the % of Tfh cells in the dLNs of mice that received Pfs25 vaccine was similar to the background level in naïve mice. In contrast, there was a noticeable, but not statistically significant, increase of the % of Tfh cells in mice that received the Pfs25-IMX313H vaccine (figure 5.5A). There was also a trend of positive correlation between the level of Tfh cells and GC cells ($r=0.57$, $p=0.13$ by Spearman Rank Correlation) (figure 5.5B) but this was not statistically significant either.

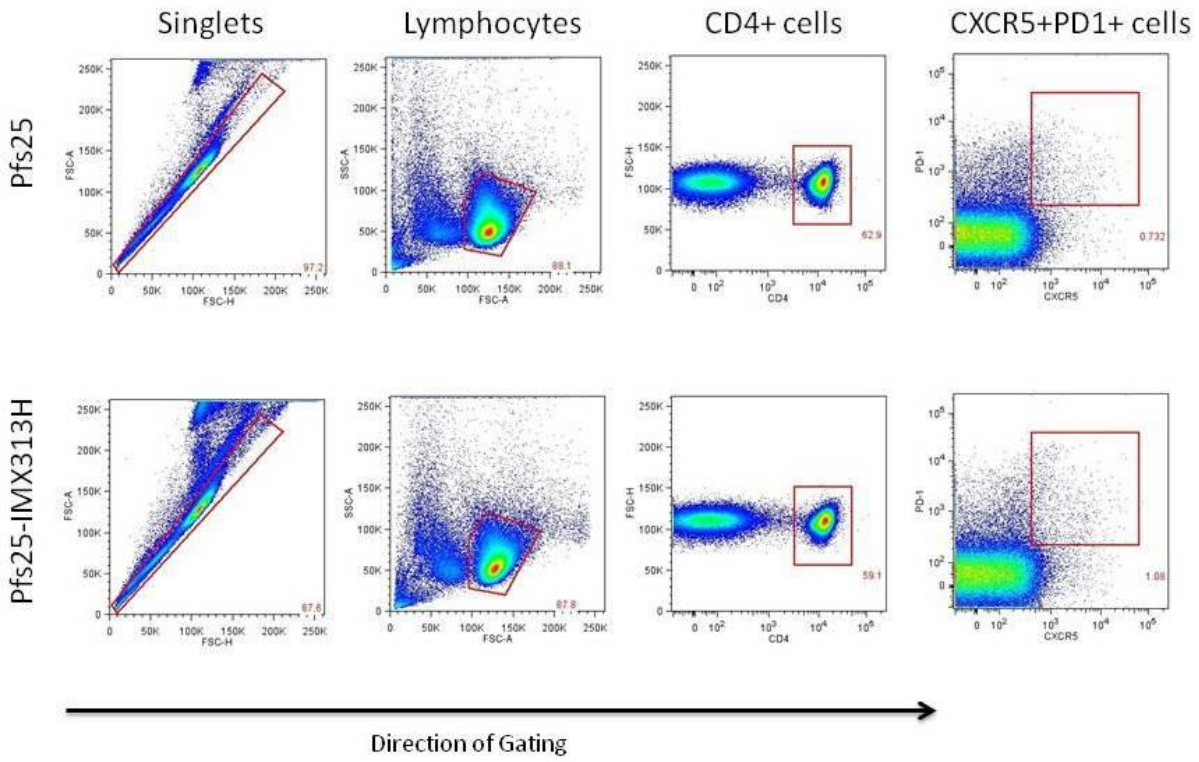

Figure 5.4 Gating strategies to identify Tfh cells.

BALB/c mice were immunised IM with 2.5 µg of Pfs25 or Pfs25-IMX313H formulated with Alhydrogel. 14 days after the vaccination, the draining inguinal and popliteal lymph nodes were harvested and stained for CD4+PD1+CXCR5+ Tfh cells. The sequential gating strategy is shown and the gates show the percentage of parent.

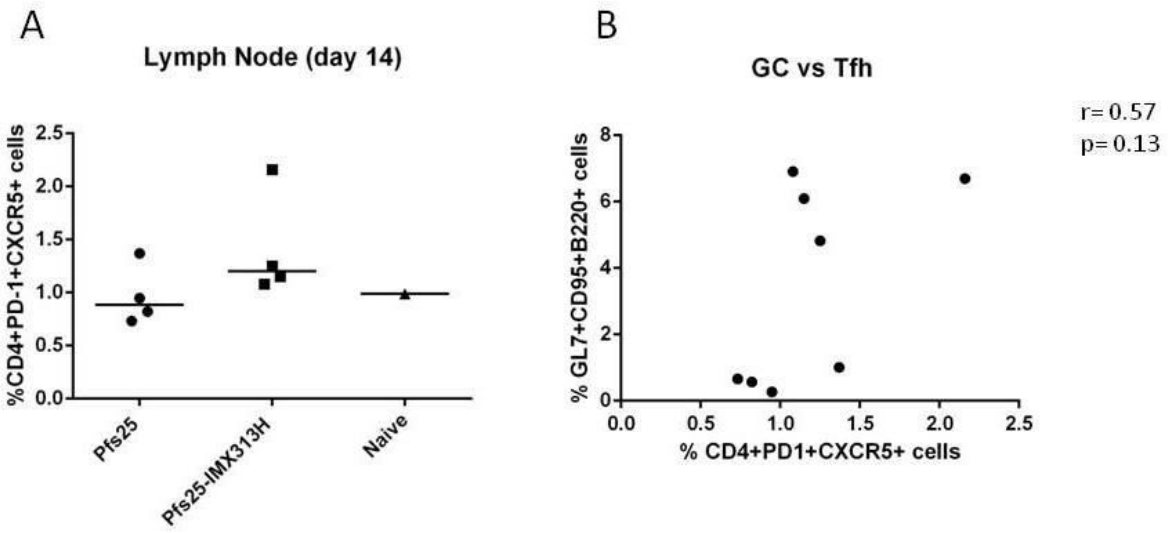

Figure 5.5 Pfs25-IMX313H and the Tfh cell response at 14 days after vaccinations.

BALB/c mice were immunised IM with 2.5 µg of Pfs25 or Pfs25-IMX313H formulated with Alhydrogel. 14 days after the vaccination, the draining inguinal and popliteal lymph nodes were harvested and stained for Tfh cells as outlined in figure 5.4. The median and individual % of CD4+PD1+CXCR5+ cells is shown (A). The % of Tfh cells (CD4+PD1+CXCR5+) were correlated with the % of GC B cells (GL7+CD95+B220+) and the Spearman rank coefficient with p-value is shown (B).

5.2.3 Antigen uptake kinetic analysis *in vitro*

To measure antigen uptake *in vitro*, APCs can be isolated directly from animals or humans, however this method is not very practical due to the requirement of a donor. THP-1 is a human monocytic leukemia cell line, which can differentiate into highly pure and monotypic macrophage-like cells by phorbol-12-myristate-13-acetate (PMA) treatment. THP-1 cells activated by PMA closely resemble the phenotype of human monocyte-derived macrophages with respect to cell morphology, surface marker expression, phagocytic activity as well as cytokine secretion profile [258] [259].

I used the THP-1 cells to assess the antigen uptake kinetics of Pfs25 and Pfs25-IMX313H *in vitro*. Pfs25 and Pfs25-IMX313H were labelled with Alexa Fluor 488 (AF488) as described in materials and methods section 2.3.14. The THP-1 monocyte cell line was cultured in T75 flask with complete medium, followed by stimulation with PMA. Immediately after PMA stimulation, cells were split and transported to 12 well plates (one million cells per well). After 24 hour incubation, one million cells in each well were incubated with 10 µg of AF488 labelled Pfs25, Pfs25-IMX313H or PBS (negative control) for 1, 3, 6 and 24 hours and at the end of each time point, cells were harvested and fixed before analysis using flow cytometry. The gating strategy in this study to identify AF488+ THP-1 cells is shown in figure 5.6. The % of AF488 positive THP-1 cells (cells that took up AF488 labelled protein antigen) was calculated and is shown in figure 5.7. Cells incubated with PBS were used as negative control to set Alexa Fluor 488 positive gate.

There was a very large difference in the % of AF488+ THP-1 cells 1 hour after incubation: 27% of Pfs25-IMX313H incubated macrophages were positive compared to 7.5% in Pfs25 group (figure 5.7). This difference decreased after 3 hours, and after 6 hours of incubation the % of

AF488+ cells were the same in both test groups. This experiment has not been repeated and one should note that only one data set was collected at each timepoint therefore statistical analysis was not performed.

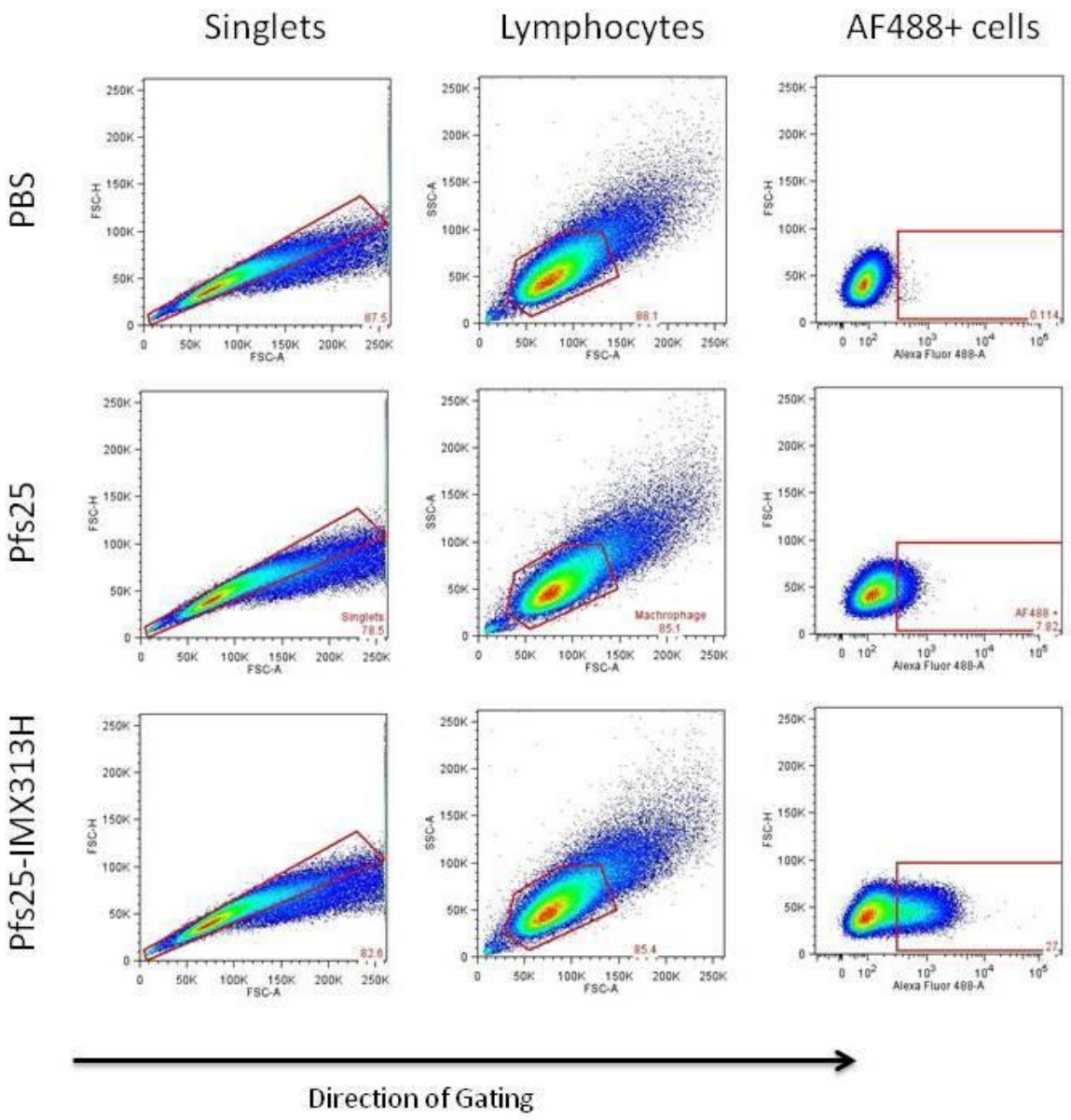

Figure 5.6 Gating strategy to identify % AF488+ THP-1 cells.

THP-1 monocyte cells was stimulated with PMA and transformed into macrophages-like cells. These cells were then incubated with 10 µg AF488 labelled Pfs25, Pfs25-IMX313H or PBS for 1, 3, 6 and 24 hours and at each time point, cells were harvested and analysed for their AF488 fluorescence level. The sequential gating strategy is shown and the gates show the percentage of parent.

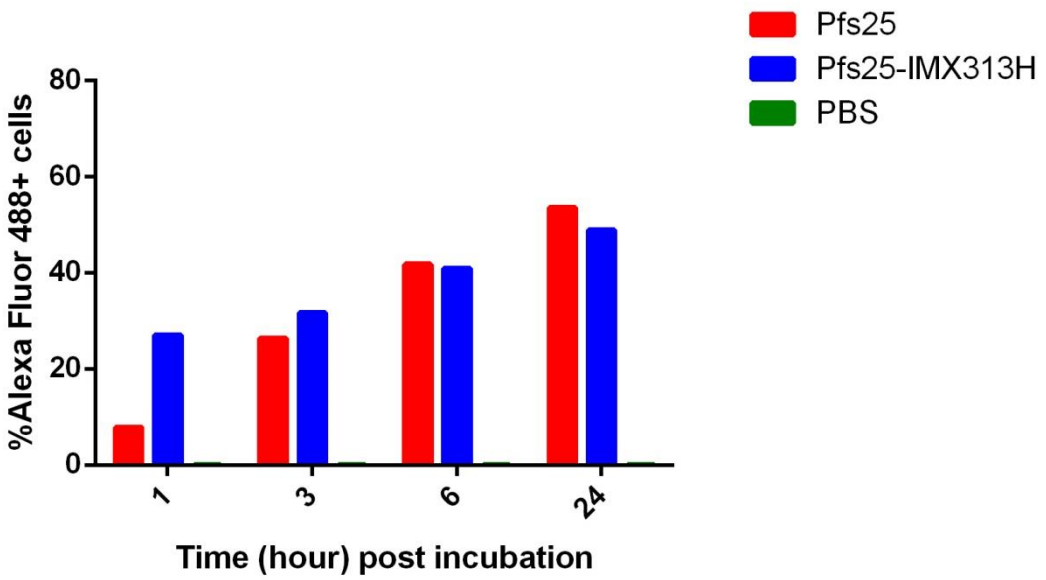

Figure 5.7 Pfs25-IMX313H exhibited a faster uptake by machrophages *in vitro*.

One million PMA stimulated THP-1 cells were incubated with 10 µg AF488 labelled monomeric Pfs25, Pfs25-IMX313H nanoparticle or PBS (negative control) for 1, 3, 6 and 24 hours. Cells were harvested after each time point and measured for the % of AF488+ THP-1 cells as outlined in figure 5.6. Each column represents a single set of data on the % of AF488+ THP-1 cells at each time point.

5.3 Discussion

In this chapter, I have compared the ability of monomeric Pfs25 protein and Pfs25-IMX313H nanoparticle to induce GC B cell and Tfh cell responses in the LN and spleen. I have also used an in vitro macrophage model to compare the kinetics of antigen uptake between the two proteins.

Compared to Pfs25 monomeric protein, Pfs25-IMX313H nanoparticle vaccinated mice induced higher GC B cell response in the dLNs 9 days after the vaccination and significantly more GC B cells were observed on day 14. Pfs25 vaccinated mice showed no increase in GC B cell response throughout the study and the level of GC B cells was similar to the background level in naïve mice (figure 5.2A). This observation was confirmed by the dLN section staining which showed no GC formation in Pfs25 vaccinated mice (figure 5.3). Interestingly, only a slight increase in the GC response was observed from both vaccinated groups in the spleen on day 14 and there was no significant difference in the level of GC response between the two groups (figure 5.2B). When mice received IM vaccination with $1x10^8$ i.u. of AdHu5 expressing OVA, Simone de Cassan demonstrated the total GC response (using the same gating strategy) peaked at day 9 in both LN and spleen (DPhil thesis). In contrast, The GC response in this study peaked in a later stage suggesting IM vaccination using protein in Alhydrogel formulation has a delayed systemic effect (i.e. at day 14), perhaps because the immune response was mainly localised at site of injection. This explanation can be supported by the depot theory of alum-based adjuvant. Although challenged by some studies, it was well established that alum-based adjuvant can form a depot at the injection site where protein antigens are slowly released resulting in a prolonged stimulation [260]. Perhaps if the GC response in this study was monitored for a

longer time, the same significant difference observed in the dLNs on day 14 between the 2 vaccination groups would occur in the spleen.

It is known that the level of GC response correlates with antigen-specific antibody titres [254]. Pfs25-IMX313H's ability to induce higher GC responses in the dLNs seemed to be the main mechanism behind the higher Pfs25-specific antibody titre induced by this nanoparticle as measured by ELISA. GCs are immunological sites where B cells undergo SHM and isotype switch, resulting in maturation of B cells with highest affinity to the corresponding antigens [254], thus antibody with a higher affinity would be expected from vaccines having a stronger GC response. This is able to explain the observation of antibodies with higher avidity generated by Pfs25-IMX313H nanoparticle vaccine. However, one should also note that the GC staining panel in this study does not identify antigen-specific B cells, so for Pfs25-IMX313H, it is possible that part of the GC B cell response induced could be due to response against IMX313 protein. Indeed, we have observed antibody response against IMX313 after Pfs25-IMX313H vaccination (figure 4.15A).

The induction of Tfh cells after vaccination was also investigated since these cells have been demonstrated to assist the maintenance and formation of GCs as well as promoting B cell maturation through the secretion of cytokines [257]. On day 14, the Tfh cells in LN of mice vaccinated with Pfs25-IMX313H were higher than the background level in naïve mice whereas Pfs25 vaccinated group were not (figure 5.5A). A weak but positive correlation between the level of Tfh cells and GC cells were observed though this wasn't statistically significant (figure 5.5B). This data suggested the Tfh cell response may have also contributed to the Pfs25-IMX313H induced immunity. It is important to note that in this study only 8 samples were acquired for the correlation analysis, and the result may be clearer if more

samples were tested. A significant correlation between % of GC B cells and % of Tfh cells in dLNs 9 days after mice received immunisation of AdHu5 expressing OVA, OVA in Abisco®100 or ISA720 and MVA expressing OVA was observed by Simone de Cassan (DPhil Thesis).

Antigen uptake was assessed by incubating fluorescence labelled proteins with macrophages derived from human monocyte cell line (THP-1) *in vitro*. There was a difference in the antigen uptake during the first hour of incubation. 27% of gated macrophages that were incubated with Pfs25-IMX313H were AF488 positive compared to only 7.5% in Pfs25 incubated group (figure 5.7). This difference disappeared after 6 hours post incubation and the level of % AF488+ cells stayed the same as expected since both groups were incubated with the same amount of fluorescence labelled proteins. Note that this experiment only obtained one data set per timepoint and as a result, no statistical analysis was performed. This assay needs to be repeated in the future to confirm the observation. This preliminary experiment suggests that the Pfs25-IMX313H nanoparticle is more efficiently taken up by macrophages *in vitro* and presumably the same for other APCs (i.e. DCs) *in vitro* and *in vivo*. A faster antigen uptake can in theory result in a faster antigen distribution to the secondary lymphoid organs (i.e. LNs and spleen) hence a quicker activation of adaptive immune response. This *in vitro* macrophage model was chosen because it was easy to set up and also provide a reliable analysis. However it will be interesting to perform an *in vivo* experiment to measure antigen uptake as well as antigen accumulation in the LN which could provide a better understanding on antigen uptake because an *in vivo* study takes into account the effects from other components of the immune system such as the natural IgM and the complement system both of which play important roles in antigen uptake and distribution as described in section 5.1.

Chapter 6

Evaluation of other Pfs25-based VLP vaccine platforms

6. Evaluation of other Pfs25-based VLP vaccine platforms

Similar to IMX313 nanoparticle vaccine platform, there are several well established particulate vaccine platforms including HBsAg and Qβ VLP both of which are able to stimulate a good antibody response in animals and/or humans. In this chapter, I describe the expression of recombinant Pfs25 with HBsAg and Qβ VLP systems. Recombinant Pfs25 fused to Pfs28 was also expressed as a multivalent TBV candidate.

6.1 HBsAg based VLP

6.1.1 Introduction

Hepatitis B virus (HBV) is a member of the hepadnaviradae family of viruses which cause a potentially life-threatening liver infection and more than 350 million people have been infected worldwide [261]. Hepatitis B surface antigen (HBsAg) is the envelope glycoprotein of the hepatitis B virus (HBV) which consists of 3 related proteins L, M and S: large (L-) HBsAg containing preS1, preS2 and S domains, middle (M-) HBsAg containing preS2 and S domains and small (S-) HBsAg containing only S domain [262]. The S domain is the main component of the viral envelope. It was found that S-HBsAg could self-assembles into a stable VLP (initially termed Australia antigen) anchoring M and L antigens in the lipid membrane and displaying the preS1 and preS2 domains. Since S-HBsAg is the major component of the VLP, it is also termed the major surface antigen or more commonly known as HBsAg. This VLP varies in sizes between 17-25 nm and was initially found in the plasma of hepatitis B virus infected patients [198]. This plasma derived Australia antigen was then demonstrated to be immunogenic and could induce immune protection against HBV infection [263-266]. Recombinant HBsAg was synthesized in the yeast *Saccharomyces cerevisiae* as a 25 kDa protein with 226 amino acids and demonstrated to self-assemble into

an immunogenic 22 nm VLP similar to the Australia antigen derived from patients' plasma [267] [268]. These particles contained yeast cell derived lipids and around 100 copies of recombinant HBsAg molecules. The HBsAg monomer contains a high number of cysteines (14 in total) and the formation of HBsAg VLP is dependent on the formation of disulphate bonds cross-linking HBsAg monomers [269]. Similar to Australia antigen, immunisation using recombinant HBsAg VLP induces antibody responses against HBsAg antigen and protects vaccinees against HBV infection [7]. As a result, recombinant HBsAg VLP successfully replaced plasma-derived HBsAg particle and is widely used in humans as a HBV vaccine.

Inspired by this self-assembly property of the HBsAg, it has been developed as a vaccine antigen carrier and has been successfully utilized by GSK for the development of *P. falciparum* CSP-HBsAg hybrid VLP vaccine (known as RTS,S) [270]. In the RTS,S vaccine, the central repeats and the entire C-terminal region of the CSP is fused to the N terminus of the HBsAg through a PVTN linker. When co-expressed with HBsAg (insert copy ratio, CS-HBsAg:HBsAg=1:4) in *Saccharomyces cerevisiae*, CS-HBsAg and HBsAg together form a 22 nm chimeric VLP expressing CS on the VLP surface [61]. RTS,S is very immunogenic. The VLPs were shown to induce significantly more antigen-specific antibodies response than soluble CSP [271]. RTS,S is the only malaria vaccine that has reached Phase 3 clinical trials and was demonstrated to be safe and highly immunogenic. At the Jenner institute, a version of RTS.S (known as R21) was developed; the same antigen CS-HBsAg was inserted without co-expression of HBsAg (co-expression with HBsAg was required for the particle formation for RTS,S) into *P. pastoris* resulting in a 22 nm hybrid VLP. This VLP was demonstrated to be equally, if not more, immunogenic than RTS,S (unpublished data). In addition to RTS,S and R21, HBsAg was also successfully expressed with dengue virus type 2 envelope protein

(Den2E) as a fusion protein in *P. pastoris* [272]. This Den2E-HBsAg hybrid proteins self-assembled into VLPs and elicited antibody response against Den2E [273]. With all this evidence, it was attractive to try and develop a Pfs25 fused HBsAg hybrid VLP in *P. pastoris*.

6.1.2 Results

6.1.2.1 Production and purification of Pfs25-HBsAg

A Pfs25 (Ala-22 to Thr-193) sequence with all the N-glycosylation sites removed as in previous constructs was fused to the N-terminal of HBsAg through the VPTN linker. The fusion gene was then cloned into the *P. pastoris* intracellular expression plasmid pPink-HC. Strain 1 of *P. pastoris* was chosen to express Pfs25-HBsAg recombinant fusion protein due to its higher protein yields for previous constructs. After transformation, 5 positive colonies were chosen for small scale protein expression. After 72 hours of induction (29°C, 4% methanol added v/v every 24 hours) cell pellets were collected and lysed, the lysate was collected and run on reducing SDS-PAGE followed by western blot analysis using anti-HBsAg mAb (Bio-Rad, UK). As the western blot (figure 6.1A) demonstrated, 4 out of 5 colonies expressed Pfs25-HBsAg (44kDa). Colony 05 was chosen as the working colony. The protein expression was then tested at 29°C with different methanol concentrations (0.5%, 1%, 2% and 4%) added v/v every 24 hours to the culture medium. The fermentation was monitored for 72 hours and the yeast cells were collected every 24 hours. The cell lysate was analyzed under reducing condition on western blot using an anti-HBsAg mAb. As figure 6.1B shows, the overall protein expression was low during the first 24 hours of fermentation and increased afterwards. The protein expression level (based on western blot signal intensity) was the highest when cells were fermented for 72 hours with 4% methanol at 29°C; hence these conditions were used for larger scale protein expression.

After large scale protein expression, the cell pellets were collected and lysed as described in material and methods section 2.2.14. In order to purify the Pfs25-HBsAg particles, CsCl gradient ultracentrifugation was performed. This method has been commonly used to separate viruses [274] and VLPs [270] [275] from other cellular material based on their specific buoyant density. According to Rutgers *et al* [270], the buoyant density of RTS,S was found to be slightly higher than 1.20 g/cm^3. Assuming Pfs25-HBsAg can form VLP and is roughly within a similar density range, a two-step CsCl gradient ultracentrifugation was performed. Firstly, crude lysate extracted from cell pellet was purified by a "discontinuous" CsCl gradient containing of 2 layers of CsCl solution (1.10 g/cm^3 CsCl layered on top of 1.30 g/cm^3 CsCl). This "discontinuous" gradient traps particles with a specific buoyant density between the high and low solution concentration. 3 product bands were observed after the ultracentrifugation and were termed F1, F2 and F3 (figure 6.2A). These fractions were extracted and run on reducing SDS-PAGE followed by western blot analysis using anti-HBsAg mAb. The result showed that only F3 contained Pfs25-HBsAg recombinant protein (figure 6.2B). F3 fraction was then buffer exchanged using a PD10 desalting column (GE Healthcare, UK) and subjected to a "continuous" gradient consisted of only 1.3 g/cm^3 CsCl. A "continuous" gradient will form and be maintained during an ultracentrifugation for over 16 hours. This gradient has a gradual transition from low to high density and allows a fine separation of material with close buoyant densities. After overnight ultracentrifugation (16-20 hours), only one band was visible (figure 6.2C) and the content was positive on western blot with both anti-HBsAg mAb and Pfs25 antiserum under reducing conditions (figure 6.2D). To examine whether purified Pfs25-HBsAg forms particles, western blot analysis was performed on purified Pfs25-HBsAg protein under both reducing and non-reducing conditions using anti-HBsAg mAb. Commercial HBsAg VLP (Engerix B vaccine made by GSK)

was also included for comparison. At non-reducing condition, HBsAg VLP and Pfs25-HBsAg both were positive showing a band (high oligomer) at very high molecular weight position. Both of the bands were disulfide bond dependent as they both could be reduced to monomers under reducing conditions (figure 6.3). This observation was consistent with the fact that disulfide bonds are required for the formation of HBsAg VLP [269]. Transmission electron microscopy (TEM) revealed small particles around 10 nm in purified Pfs25-HBsAg sample whereas homogeneous 22nm VLP was observed in HBsAg vaccine sample (figure 6.4). The observation of this small particle was surprising; one would only expect the particle to be larger, if not the same, as the recombinant HBsAg VLP. Evidently CsCl purification worked well for the purification of RTS,S [270] as well as R21 and in both cases, 22 nm VLPs were observed. This experiment was repeated and same outcome was observed.

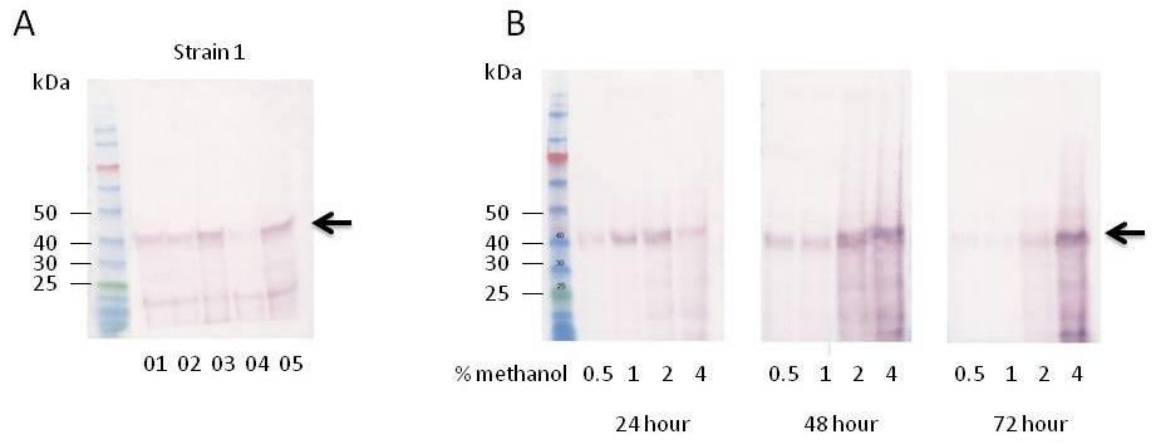

Figure 6.1 Expression of Pfs25-HBsAg in *P. pastoris*.

(A) Strain 1 of *Pichia pastoris* was transformed with the pPink-HC plasmid encoding Pfs25-HBsAg. 5 colonies from each strain were picked for small scale protein expression (72 hours of fermentation at 29°C and 4% methanol was added v/v every 24 hours). After the expression, cells were collected and the crude culture lysate was loaded on reducing SDS-PAGE and analysed by western blot using anti-HBsAg mAb. Arrow indicates the expected size of the Pfs25-HBsAg monomer (44 kDa).

(B) The protein expression was tested in a time course experiment (72 hours) at 29°C with different methanol concentrations (0.5%, 1%, 2% and 4%) added v/v every 24 hours. Cells were collected every 24 hours and the crude lysate was run on reducing SDS-PAGE and analyzed by western blot using anti-HBsAg mAb. Arrow indicates the expected size of the Pfs25-HBsAg monomer.

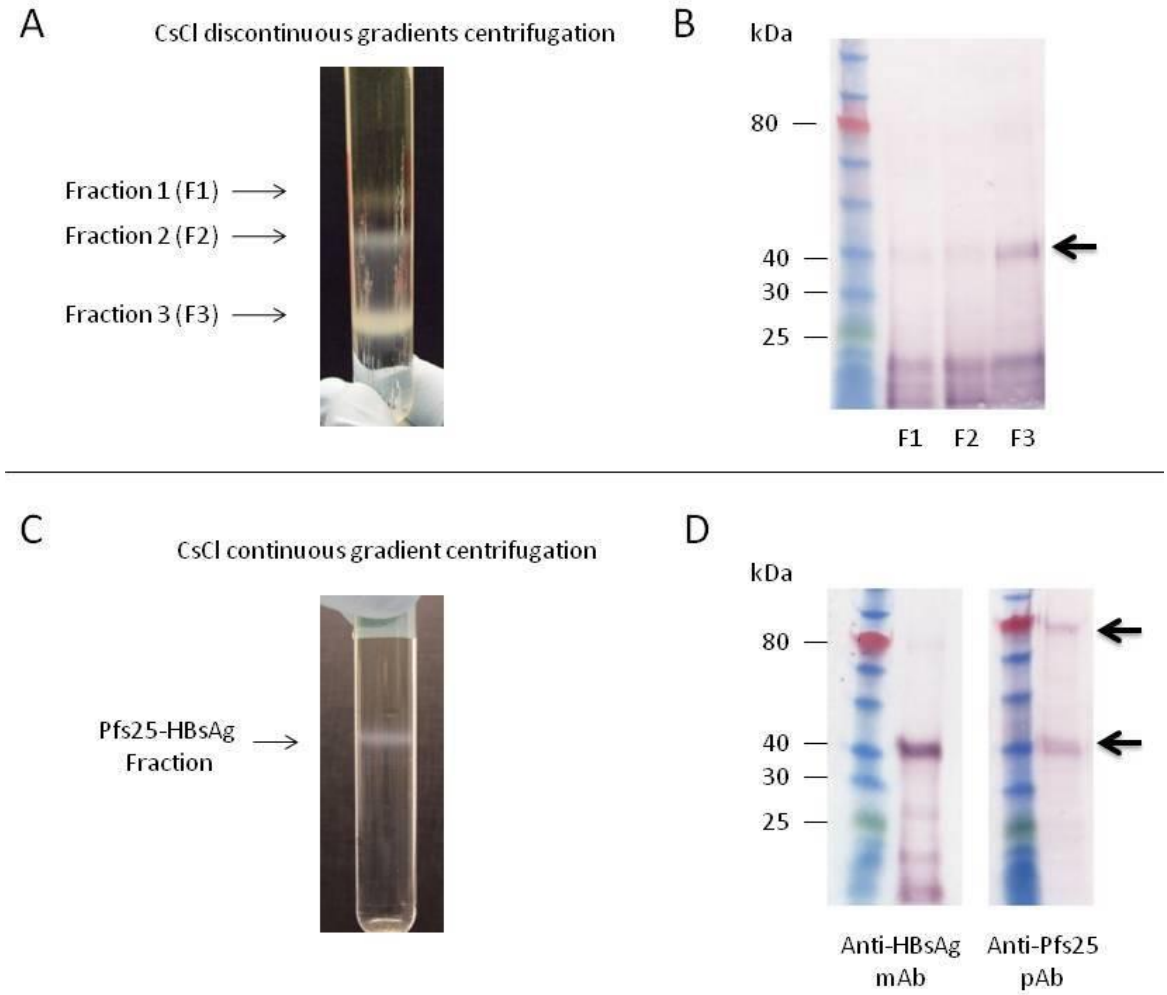

Figure 6.2 Pfs25-HBsAg particle purification using CsCl gradient centrifugation.

(A) After large scale protein expression, the crude cell lysate was purified using a "discontinuous" CsCl gradient containing 2 layers of CsCl solution (1.10 g/cm^3 CsCl layered on top of 1.30 g/cm^3 CsCl) and centrifuged at 41,000 rpm for 2 hours. (B) Fraction 1, 2 and 3 were run on reducing SDS-PAGE followed by western blot analysis using anti-HBsAg mAb. Arrow indicates expected size of the Pfs25-HBsAg monomer. (C) Fraction 3 was buffer exchanged and loaded on a "continuous" CsCl gradient containing 1.30 g/cm^3 CsCl and centrifuged at 41,000 rpm for 16-20 hours. (D) Pfs25-HBsAg fraction was extracted and run on reducing SDS-PAGE followed by western blot analysis using both anti-HBsAg mAb and anti-Pfs25 antiserum. Arrows indicate expected size of the Pfs25-HBsAg monomer (44kDa) or dimer (88kDa).

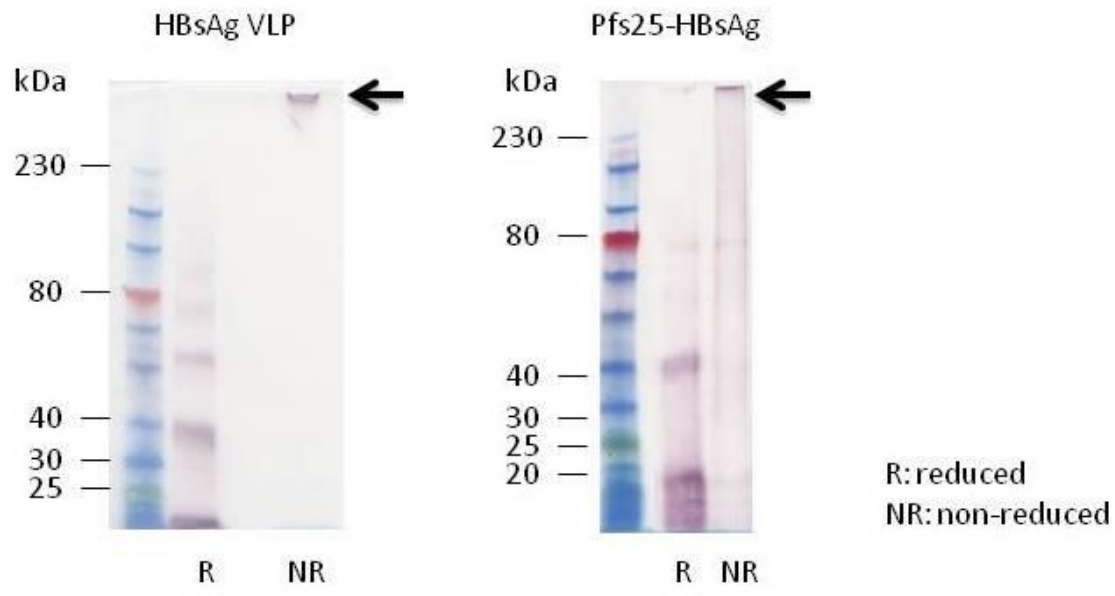

Figure 6.3 Pfs25-HBsAg formed disulfide bond-dependent high oligomer.

Commercial Engerix B vaccine (recombinant HBsAg VLP, left panel) and CsCl purified Pfs25-HBsAg (right panel) were run on both reducing and non-reducing SDS-PAGE and analysed by western blot using anti-HBsAg mAb. Arrows indicate high oligomer of both proteins.

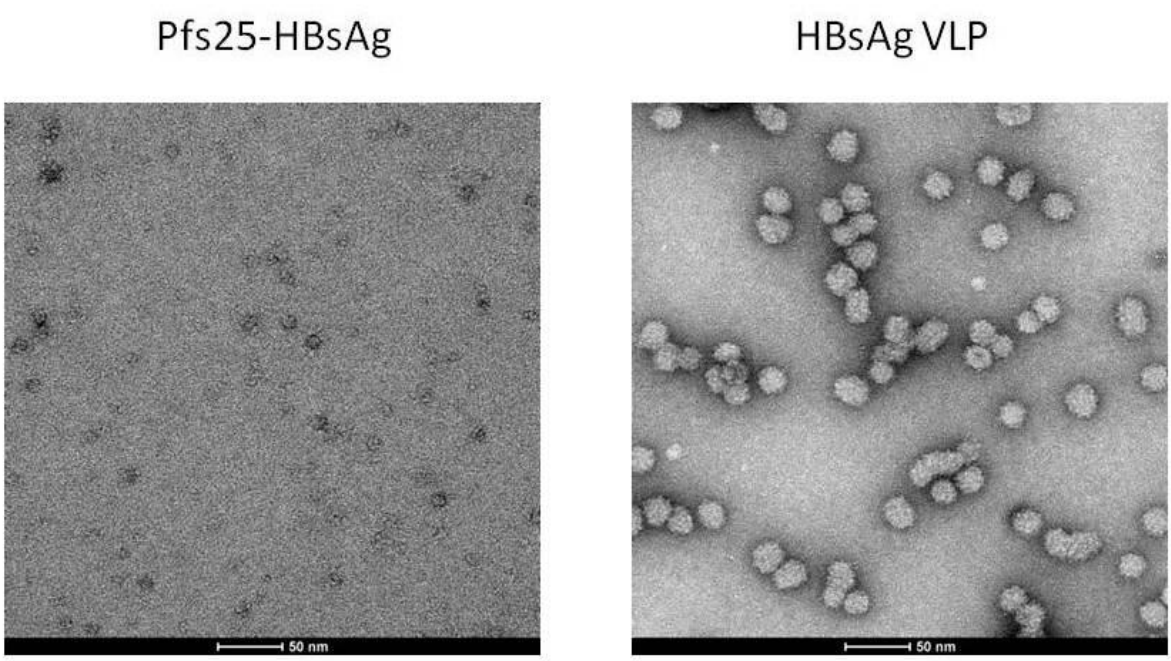

Figure 6.4 Particles of 10 nm were observed in purified Pfs25-HBsAg under TEM.

Purified Pfs25-HBsAg (left panel) as well as HBsAg VLP vaccine (Engerix B, right panel) were visualised under TEM by negative staining with uranyl acetate. The scale bar represents 50 nm.

6.1.2.2 Production and purification of Pfs25-HBsAgC

In the previous section, Pfs25-HBsAg particles were formed but these were smaller than the expected size. The CsCl purified Pfs25-HBsAg fusion protein contained moderate contamination as revealed by SDS-PAGE (data not show). SEC using Sephacryl S-500 HR column (GE) could be applied and was indeed successfully used in R21 purification, but the loss during the purification was huge (according to R21 study). In the case of Pfs25-HBsAg, the expression was much lower than R21; SEC was attempted and failed to provide satisfactory recoveries (data now shown).

Studies of interaction between a nanobody (a single domain antibody, which consists of only a single monomeric variable antibody domain) NbSyn2 and α-synuclein revealed the interaction was dependent and specific to only the four C-terminal residues (EPEA) of the α-synuclein [276]. This discovery has led to a development of new affinity purification strategy known as C-tag purification. The nanobody NbSyn2 is conjugated to beads and is available as a commercial resin. A protein of interest fused to EPEA peptide sequence at its C-terminus can be purified using this resin. The advantage of this C-tag purification is its high affinity, because the affinity is based on antibody-antigen interaction. The specificity of this interaction is very high [277] and it is also less likely to generate anti-tag immune response against a 4 amino acids tag in humans, so a C-tag purification seemed to be a better choice over other tag based purification methods (i.e. His-tag). C-tag has been successfully used at the Jenner institute for the purification of R21 and also the blood-stage antigen RH5 which has been difficult to produce in a lot of expression systems.

The EPEA sequence (C-tag) was cloned at the C-terminus of Pfs25-HBsAg sequence by PCR and cloned into pPink-HC. This construct is termed Pfs25-HBsAgC and was then transformed

into strain 1 of *P. pastoris*. As for selecting Pfs25-HBsAg, 5 positive colonies (auxotrophic selection) were tested for small scale protein expression. Colony 05 showed the best expression hence was selected as the working colony (figure 6.5A). Large scale protein expression was performed (under the same condition as for Pfs25-HBsAg) and the cell lysate was extracted and purified using C-tag affinity matrix (Life Technologies, UK) packed in empty column XK 16/20 (GE Healthcare, UK). During the elution, chromatography graph (figure 6.5B) revealed a single sharp elution peak. Samples from the peak fractions were collected and concentrated and were run on SDS-PAGE under reducing condition. Coomassie blue staining and western blot using both anti-HBsAg mAb and anti-Pfs25 antiserum revealed monomeric as well as multimeric Pfs25-HBsAgC with minor contamination (figure 6.5C). TEM analysis (figure 6.6) on the purified sample revealed particles. Though the particles were not homogenous, notably there were several particles with approximately 20 nm size (arrow indicated). This experiment was repeated and similar outcome was observed.

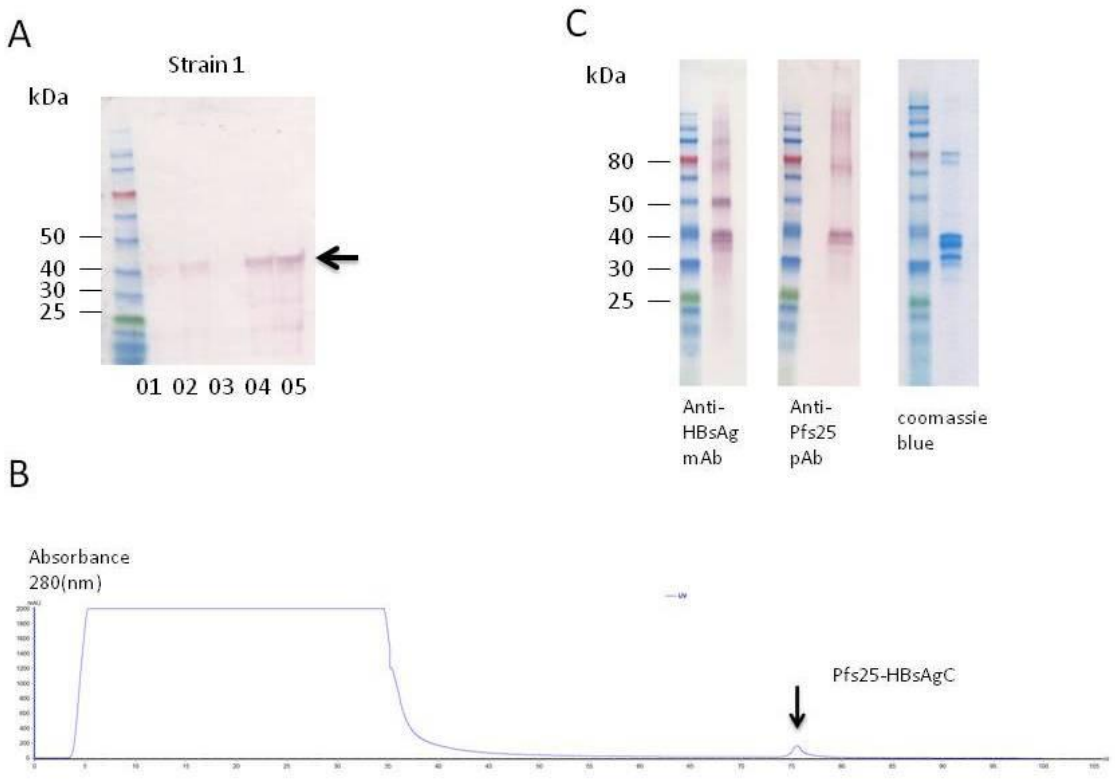

Figure 6.5 Pfs25-HBsAgC expression and purification.

(A) Strain 1 of *Pichia pastoris* was transformed with Pfs25-HBsAgC. 5 colonies were picked for small scale protein expression test. After small scale protein expression, crude cell lysate was loaded on SDS-PAGE and tested by western blot under reducing condition using anti-HBsAg mAb. Arrow indicates the expected size of the Pfs25-HBsAgC monomer (44kDa).

(B) Crude lysate extracted from cell pellet after large scale protein expression was purified using C-tag affinity matrix packed in empty column XK 16/20. Chromatography graph is shown and the arrow indicates the elution peak.

(C) Purified Pfs25-HBsAgC was run on reducing SDS-PAGE and analysed using Coomassie blue staining and western blot with both anti-HBsAg mAb and anti-Pfs25 antiserum.

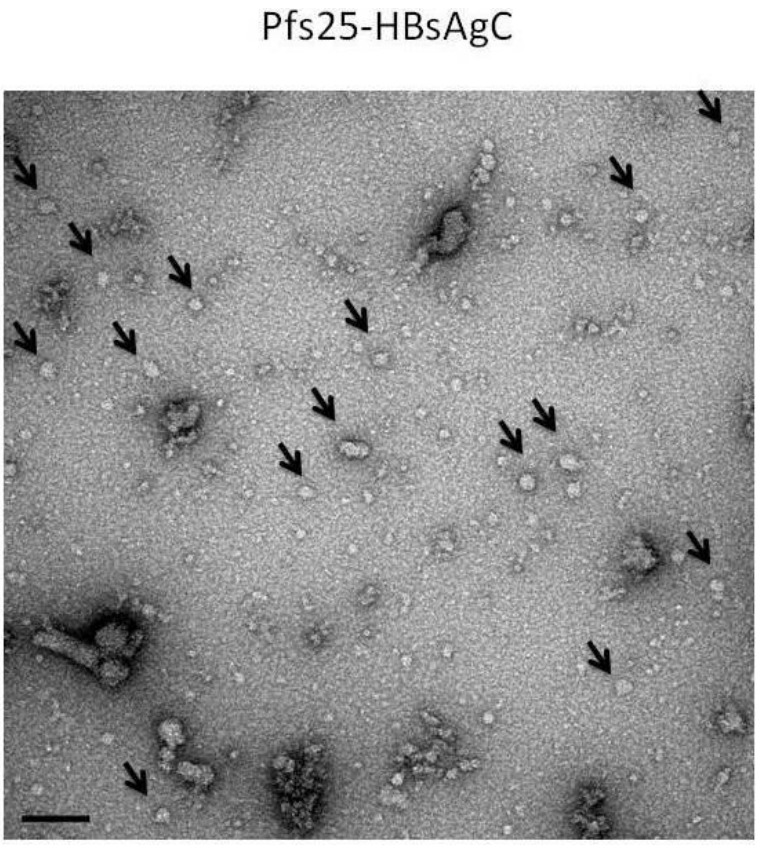

Figure 6.6 Larger particles approximately 20 nm in size were observed in purified Pfs25-HBsAgC under TEM.

C-tag purified Pfs25-HBsAgC was visualized under TEM by negative staining with uranyl acetate. Arrows indicate particles around expected size (20 nm). The scale bar (left bottom) represents 100 nm.

6.2 Bacteriophage Qβ VLP

6.2.1 Introduction

Bacteriophage Qβ is an icosahedral virus from the *Allolevivirus genus* of the *Leviviridae* family and its host is *E. coli* [278]. The viral coat protein (CP), when expressed as recombinant protein on its own in *E. coli*, was found to self-assemble into Qβ viral capsid consisting of 180 copies of CPs and was indistinguishable, both morphologically and immunologically from native Qβ phage particles [279]. This has led to the development of Qβ VLPs as a vaccine carrier and it has been used to display peptides/antigens on the surface either by chemical conjugation [280] or by genetic recombination [281]. *E. coli* is the preferred expression system for generating Qβ VLP, though successful expression and formation of VLP has been reported in other expression systems such as *Saccharomyces cerevisiae* and *Pichia pastoris* [282].

Qβ VLPs have been tested as a vaccine carrier matrix for several antigens of interest. In one study [280], Qβ VLP was chemically conjugated to the globular head domain of influenza haemagglutinin. This VLP was very potent in inducing a strong antibody response and complete protection against challenges using different strains of influenza in mice was achieved. Another study [283] demonstrated that conjugation of Tn antigen (tumor associated carbohydrate antigen), which was a poor immunogen on its own, to Qβ VLP drastically increased the antigen-specific antibody response in mice. In addition, Qβ VLP has been conjugated to nicotine to induce anti-nicotine antibody responses to prevent nicotine addiction and has subsequently reached Phase 2 clinical trials [284]. Although the nicotine-Qβ VLP did not significantly increase continuous abstinence rates in the intention-to-treat population, the data suggested that Qβ VLPs are not only safe, but also immunogenic in

humans. Furthermore, preclinical therapeutic vaccine candidates against autoimmune arthritis [285] and type 2 diabetes mellitus [286] utilising Qβ VLP as a carrier to induce antigen-specific antibodies are under development. As results suggested, Qβ VLP is a VLP platform capable of inducing strong antibody response and in this section I describe the production of Qβ VLPs displaying Pfs25.

6.2.2 Results

6.2.2.1 Pfs25-Qβ VLP production and purification

This part of the project was done in collaboration with Prof. Martin Bachman's group in Zurich, Switzerland. Purified monomeric Pfs25 (from study in Chapter 3) was sent to Switzerland and Dr Franziska Zabel conjugated it onto the surface of Qβ VLPs, which were produced and purified in Switzerland. In brief, sulfhydryl groups were introduced onto Pfs25 by incubating with N-succinimidyl S-acetylthioacetate (SATA) according to the manufacturer's instruction (Thermo Scientific, UK) followed by deacetylation using hydroxylamine-HCl. In the mean while, the purified Qβ VLP was conjugated to the SMPH (Thermo Scientific, UK) crosslinker. The coupling between Pfs25 and Qβ VLP was achieved based on the reaction between SMPH and deacetylated SATA. The conjugated Pfs25-Qβ VLP was buffer exchanged and sent back to the Jenner Institute for further purification and studies. The conjugated particle was purified further using SEC (Superdex 200pg) to remove any unconjugated Pfs25 (data not shown). The final product was run on reducing SDS-PAGE and analysed using Coomassie blue staining and western blot using Pfs25 antiserum. Both un-conjugated Qβ monomer and multimers (14 kDa Qβ monomer, 28 kDa Qβ dimer, 42 kDa Qβ trimer and 56 kDa Qβ tetramer) as well as Pfs25 conjugated Qβ monomer and multimers (arrow indicated, 33 kDa monomer, 47 kDa dimer and 61 kDa trimer) were observed (figure

6.7A). To estimate the coupling efficiency, both conjugated and un-conjugated protein bands in the SDS-PAGE were converted into arbitrary values based on the pixel intensity and expressed as % of total using ImageJ software. The result revealed around 2% of the total Qβ proteins were coupled with Pfs25. Giving there were 180 copies of Qβ monomers per VLP, only ~3 or 4 Pfs25 molecules were expected on each conjugated VLP. The coupling efficiency was defined as the molar ratio of Pfs25 conjugated Qβ proteins to total Qβ proteins [285] and was calculated to be 4.6% in this study. The VLP sample was also subjected to TEM revealing homogenous 30 nm VLPs (figure 6.7B).

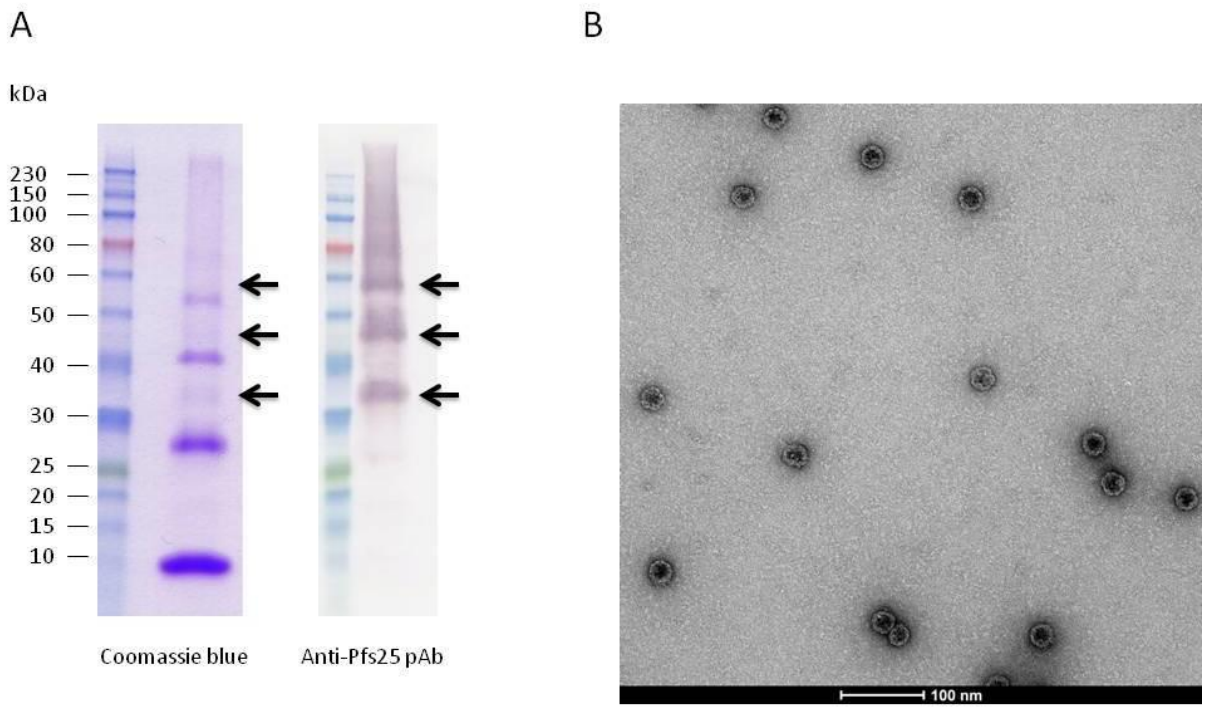

Figure 6.7 Pfs25 conjugated to Qβ VLP

(A) Pfs25 was chemically conjugated to Qβ VLP using the SATA and SMPH crosslinkers (described in 6.2.2.1). Purified VLP was run on reducing SDS-PAGE and analysed using Coomassie blue and western blot using Pfs25 antiserum. Arrow indicates the expected size of Pfs25 conjugated Qβ monomer and multimers.

(B) Purified Pfs25-Qβ VLP was visualized under TEM by negative staining with uranyl acetate. The scale bar represents 100 nm.

6.3 Pfs25-Pfs28 multivalent vaccine

6.3.1 Introduction

Pfs28 is a *P. falciparum* sexual stage outer membrane protein expressed on the surface of late stage ookinete [158]. Pfs28 has been expressed as recombinant protein in *S. cerevisiae* and in mice models this protein was immunogenic and elicited antibodies that blocked transmission of *P. falciparum* in SMFA [158]. A recent study demonstrated that conjugating Pfs28 to EPA (ExoProtein A of *Pseudomonas aeruginosa*) significantly increased the antibody response and presumably its transmission blocking activity (but this was not tested) [287]. Pfs25 and Pfs28 are both expressed on the same stage of the parasite life cycle in the mosquito. A study using *P. berghei* revealed that a single gene knockout of either Pbs25 (the orthologue of Pfs25) or Pbs21 (orthologue of Pfs28) caused partial inhibition of ookinete/oocyst development in the mosquito compared to a more than 90% inhibition when both genes were disrupted [159]. This study suggested the function of Pfs25 and Pfs28 was partially redundant and strengthened the case for development of Pfs25/Pfs28 multivalent vaccine. Furthermore, mixing serum against Pfs25 and Pfs28 has been shown to act synergistically in an SMFA [158]. This synergistic effect could be achieved by mixing *S. cerevisiae* produced recombinant Pfs25 and Pfs28 proteins together in one vaccination or by vaccination using Pfs25-Pfs28 recombinant fusion protein produced by *S. cerevisiae* [160]. These studies were published more than 15 years ago and there have been no published follow up studies. With the current *P. pastoris* system, I revisited this topic and generated recombinant Pfs25-Pfs28 fusion protein.

6.3.2 Results

6.3.2.1 Pfs25-GP-Pfs28 expression and production

A Pfs25 (Ala-22 to Thr-193) sequence with the same N-glycosylation sites removed as in previous constructs, was fused to Pfs28 (GeneBank locus AAT00624, Valine (Val)-23 to Serine (Ser)-196) using a GP linker (GGGPGGG). This Pfs25-GP-Pfs28 sequence was fused to the N-terminus of IMX313; the whole sequence was codon optimised for expression in humans and synthesised as DNA plasmid from GeneArt® Gene Synthesis (Life Technology, UK). Both of the Pfs25-GP-Pfs28 and Pfs25-GP-Pfs28-IMX313 sequences were cloned with an N-terminus His-tag using PCR followed by insertion using restriction digest and ligation into pPinkα-HC expression plasmid. Strain 1 of *P. pastoris* was then transformed with both inserts and 5 positive colonies (auxotrophic selection) from each transformant were subjected to small scale protein expression as before. The supernatants were collected and run on reducing SDS-PAGE followed by western blot analysis using Pfs25 antiserum. Surprisingly, with 2 separate attempts, Pfs25-GP-Pfs28-IMX313 failed to express. On the other hand, Pfs25-GP-Pfs28 was a success. The western blot revealed all 5 test colonies expressed the recombinant Pfs25-GP-Pfs28 fusion protein at the predicted size 42 kDa (figure 6.8A). Colony 01 was selected for large scale protein expression. Large scale expression was performed under the same condition as Pfs25 monomeric protein. After the fermentation (72 hours at 29°C and 4% methanol was added v/v every 24 hours), the supernatant was first purified using a HisTrap excel column (data not shown). His-tag elution fractions that contained recombinant protein were pooled and purified again using SEC (Superdex 200pg column). The SEC chromatography graph showed both monomeric and multimeric Pfs25-GP-Pfs28 peaks (figure 6.8B). SEC fraction B7 to C4 that contained both

peaks were run on non-reducing and reducing SDS-PAGE and stained by Coomassie blue. The results revealed the presence of monomeric as well as multimeric (dimer and trimer) Pfs25-GP-Pfs28 fusion proteins in the SEC fractions B7 to C4 (figure 6.8C left panel). The multimeric form of recombinant protein was disulfide bond dependent and can be reduced to monomers (figure 6.8C middle panel) which were also recognized by Pfs25 antiserum (figure 6.8C right panel). SEC fraction B12 to C2 that contained monomeric Pfs25-GP-Pfs28 protein were pooled and stored at -20°C for future studies.

A

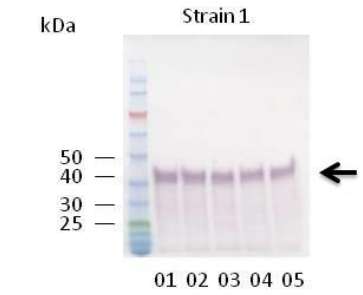
kDa
Strain 1
50
40
30
25
01 02 03 04 05

B

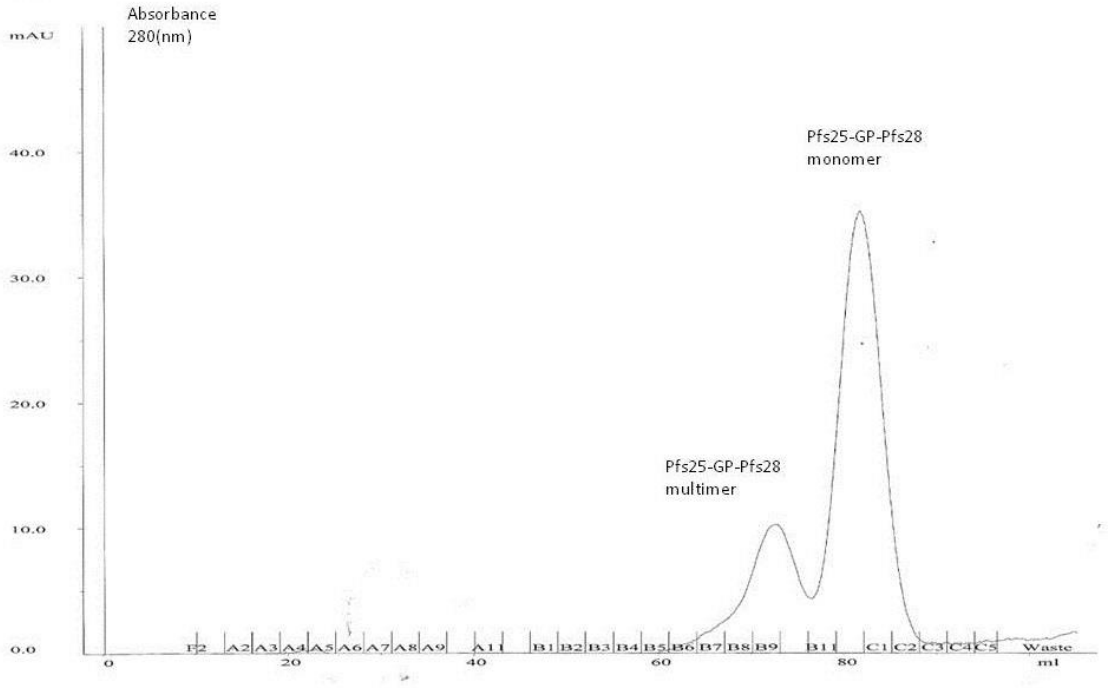
Absorbance
280(nm)
mAU
40.0
30.0
20.0
10.0
0.0
Pfs25-GP-Pfs28
monomer
Pfs25-GP-Pfs28
multimer
A2 A3 A4 A5 A6 A7 A8 A9 A11 B1 B2 B3 B4 B5 B6 B7 B8 B9 B11 C1 C2 C3 C4 C5 Waste
0
20
40
60
80
ml

C

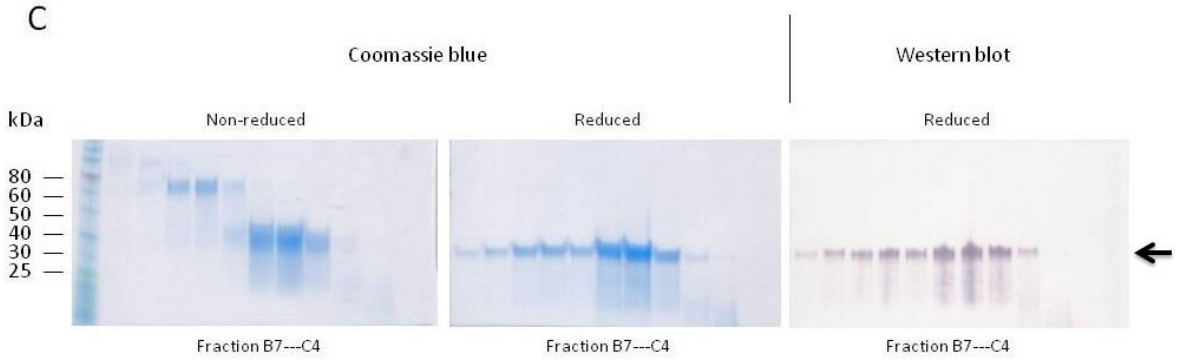
Coomassie blue
Western blot
kDa
Non-reduced
Reduced
Reduced
80
60
50
40
30
25
Fraction B7---C4
Fraction B7---C4
Fraction B7---C4

Figure 6.8 Pfs25-GP-Pfs28 expression and purification.

(A) Strain 1 of *P. pastoris* was transformed with Pfs25-GP-Pfs28. 5 colonies were picked for small scale protein expression test. After small scale protein expression (72 hours of fermentation at 29°C and 4% methanol was added v/v every 24 hours), crude supernatant was loaded on SDS-PAGE and analysed by western blot under reducing condition using Pfs25 antiserum. Arrow indicates expected size of Pfs25-GP-Pfs28 monomer (42kDa)

(B) Supernatant from large scale expression (72 hours of fermentation at 29°C and 4% methanol was added v/v every 24 hours) was first purified using His-tag purification using HisTrap excel column, followed by SEC using Superdex 200pg column. The SEC chromatography graph showed both monomeric and multimeric Pfs25-GP-Pfs28 peak.

(C) SEC fraction B7 to C4 were run on non-reducing (left panel) and reducing (middle panel) SDS-PAGE and stained by Coomassie blue. Western blot under reducing condition using Pfs25 antiserum was also performed (right panel).

6.4 Immunogenicity study comparing Pfs25 particulate vaccines

This section describes a head-to-head comparison study of the different protein and particulate vaccines that I generated including: monomeric Pfs25, Pfs25-IMX313T, Pfs25-HBsAgC, Pfs25-Qβ VLP and Pfs25-GP-Pfs28. The objective was to identify candidate vaccines that induce the highest level of anti-Pfs25 antibody response.

The dose of the different vaccine candidates tested was normalised on the Pfs25 content and contained 1 μg of Pfs25. The vaccination regime is summarised in table 6.1. BALB/c mice (n=5/group) received 2 doses of the vaccines formulated with Alhydrogel. The mice were bled at day 20 (post-prime) and day 42 (post-boost) for ELISA analysis. Because monomeric Pfs25, Pfs25-GP-Pfs28 and the Pfs25-Qβ VLP contained His-tag, and the recombinant Pfs25 used to coat the ELISA plate also contained His-tag, all serum samples were mixed and incubated with a short peptide containing His-tag sequence (kindly provided by Daria Nikolaeva) in 20 μg/mL concentration for 30 minutes before incubating on ELISA plate. This was done to deplete any antibodies to the His-tag present in the serum samples. The rest of the ELISA protocol was the same as before. The Pfs25 standardised ELISA was performed to evaluate the Pfs25-specific IgG responses. Pfs25-IMX313T was the only construct that elicited significantly higher antibody response than monomeric Pfs25 after both prime and boost (figure 6.9A and B). Pfs25-GP-Pfs28 construct was the second best in terms of antibody response followed by Pfs25-Qβ VLP. There was no detectable antibody response in Pfs25-HBsAgC vaccinated group which was surprising. Comparing day 42 serum samples with and without anti-His-tag antibody depletion (figure 6.10), there was no noticeable difference in the level of overall anti-Pfs25 antibody response suggesting very little or no anti-tag antibodies were induced by vaccination in this study.

To measure the Pfs28 antibody response induced by Pfs25-GP-Pfs28 vaccination, both day 21 and day 42 serum (anti-tag antibody depleted) were analysed using Pfs25 and Pfs28 whole IgG ELISA. Recombinant Pfs28 (His-tagged) ELISA coating protein was kindly provided by Daria Nikolaeva, which was produced in HEK 293 expression system. The ELISA result demonstrated that Pfs25-GP-Pfs28 elicited strong antibody response against both Pfs25 and Pfs28 (figure 6.11B). A low degree of homology between Pfs25 and Pfs28 was noted by Duffy, P.E. and Kaslow, D.C [158]. Basic Local Alignment Search Tool (BLAST) revealed 70 amino acids matches when Pfs25 sequence (GeneBank locus AAN35500, from Alanine-22 to Threonine-193) was aligned with Pfs28 sequence (GeneBank locus AAT00624, from Valine-23 to Serine-196) (figure 6.12). Day 62 serum from mice which had received 3 immunisations of 2.5 μg Pfs25 (chapter 4, section 4.2.2) (with anti-His-tag antibody depleted) was tested against Pfs28 in a whole IgG ELISA to examine if there were any cross-reactive antibodies between Pfs25 and Pfs28. Serum from mice vaccinated with recombinant viral-vectors expressing Pfs28 (performed by Kerry Jewell) was included as a positive control. The serum from mice vaccinated with Pfs25 did not show any reactivity to Pfs28 protein in the ELISA (figure 6.13) suggesting there was no cross-reactivity between antibody responses to Pfs25 and Pfs28. Therefore, the anti-Pfs25 IgG response induced by Pfs25-GP-Pfs28 protein in figure 6.9 was likely specifically induced by Pfs25.

Group	% Pfs25 (based on MW)	Day 0	Day 20	Day 21	Day 42
1. Pfs25	100	1 µg		1 µg	
2. Pfs25-GP-Pfs28	48	2.08 µg		2.08 µg	
3. Pfs25-IMX313T	74	1.35 µg	Bleed	1.35 µg	Bleed
4. Pfs25-HBsAgC	42	2.38 µg		2.38 µg	
5. Pfs25-Qβ-VLP	2.6	38.5 µg		38.5 µg	

Adjuvant: Alhydrogel

Table 6.1 Vaccination regimes for comparing the immunogenicity of Pfs25-based protein and particulate vaccines.

BALB/c mice (n=5/group) were immunised with Pfs25, Pfs25-GP-Pfs28, Pfs25-IMX313T, Pfs25-HBsAgC or Pfs25-Qβ VLP. The vaccines were formulated with Alhydrogel and the dosage was normalised based on the Pfs25 content and contained 1 µg of Pfs25. The mice were bled at day 20 (post-prime) and day 42 (post-boost) for ELISA analysis.

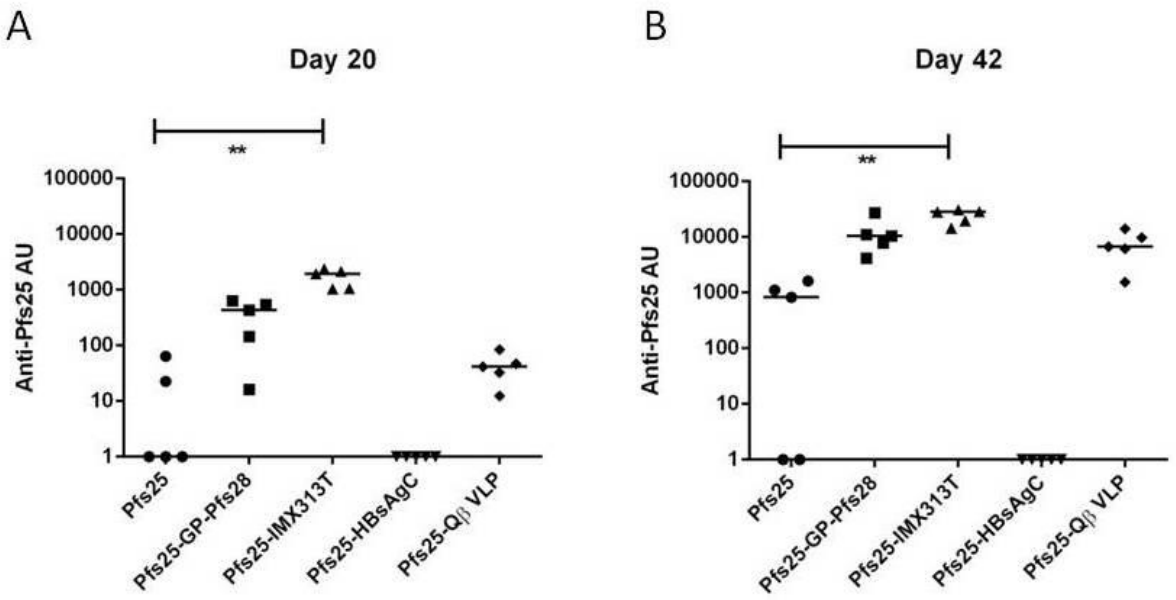

Figure 6.9 Immunogenicity of the different protein and particulate vaccine constructs targeting Pfs25.

BALB/c mice (n=5/group) were immunised using protein with Alhydrogel prime-boost regime as outlined in table 6.1. Mice were vaccinated at day 0 and boosted at day 21. Serum samples from Pfs25, Pfs25-GP-Pfs28 and Pfs25-Qβ VLP were pre-treated with a short peptide containing His-tag sequence at 20 µg/mL to deplete the anti-tag antibodies. Total Pfs25 specific IgG level was measured in the serum samples taken at day 20 (A) and day 42 (B), using Pfs25 standardised ELISA. Median and individual data points are shown. ** $p<0.01$ by Kruskal-Wallis test with Dunn's multiple comparison post-test.

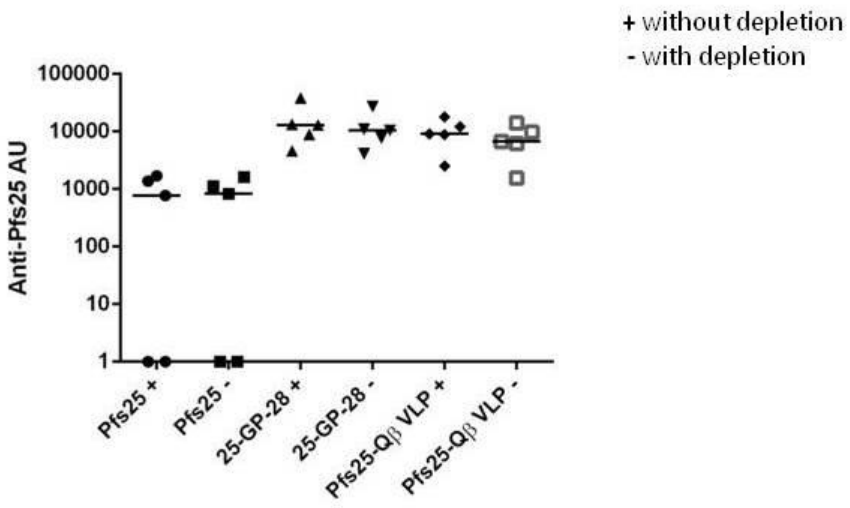

Figure 6.10 Anti-His-tag response was not detected.

Day 42 serum from Pfs25, Pfs25-GP-Pfs28 and Pfs25-Qβ VLP vaccination group outlined in table 6.1 was compared with and without treatment for anti-tag antibody depletion. To deplete the anti-tag antibody, serum samples were pre-treated with a short peptide containing His-tag sequence at 20 µg/mL for 30 minutes before loading onto an ELISA plate. The total Pfs25 specific IgG levels were then measured using Pfs25 standardised ELISA. Median and individual data points are shown. + indicates serum contains anti-tag antibody, – indicates serum has anti-tag antibody depleted.

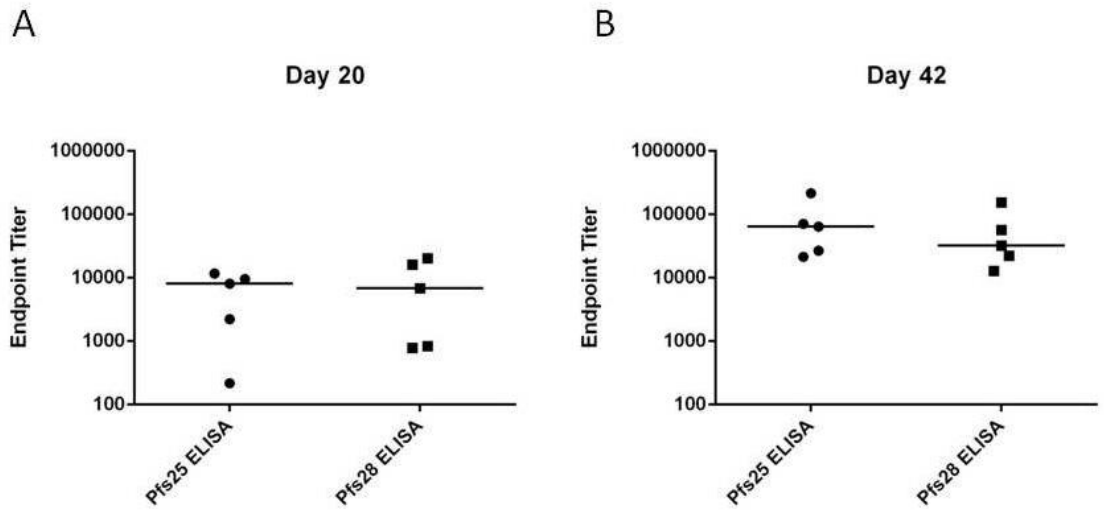

Figure 6.11 Pfs25-GP-Pfs28 induced antibody response against both Pfs25 and Pfs28.

Day 20 and day 42 serum (anti-tag antibody depleted) from Pfs25-GP-PFs28 vaccinated mice outlined in table 6.1 was tested for their antibody response against Pfs25 and Pfs28 protein antigens using whole IgG ELSIA. Median and individual data points are shown.

Score	Expect	Identities	Positives	Gaps
132 bits(333)	2e-43	70/158(44%)	91/158(57%)	10/158(6%)

```
Query  3    VTVDTVCKRGFLIQMSGHLECKCENDLVLVNEETCEEKVLKCDE-KTVNKPCGDFSKCIK  61
            VT +T+CK G+LIQMS H ECKC     VL+NE+TC +KV+ CD+ +    K C +++ C
Sbjct  1    VTENTICKYGYLIQMSNHYECKCIEGYVLINEDTCGKKVV-CDKVENSFKACDEYAYCFD  59

Query  62   I--DGNPVSYACKCNLGYDMVNNVCIPNECKQVTCGNGKCILDTSNPVKTGVCSCNIGKV  119
            +    N      C C   Y +   VC+PN C+   CG GKCI+D +N + T  CSCNIG +
Sbjct  60   LGNKNNEKQIKCMCRTEYTLTAGVCVPNVCRDKVCGKGKCIVDPANSL-THTCSCNIGTI  118

Query  120  PNVQDQNK-CSKDGETKCSLKCLKEQETCKAVDGIYKC  156
              N   QNK C   G+T CSLKC  E E C      Y C
Sbjct  119  LN---QNKLCDIQGDTPCSLKC-AENEVCTLEGNYYTC  152
```

Query: Pfs25 (GeneBank locus AAN35500, from Alanine-22 to Threonine-193)
Subject: Pfs28 (GeneBank locus AAT00624, from Valine-23 to Serine-196)

Figure 6.12 Homology between Pfs25 and Pfs28.

Pfs25 sequence (GeneBank locus AAN35500, from Alanine-22 to Threonine-193) and Pfs28 sequence (GeneBank locus AAT00624, from Valine-23 to Serine-196) was aligned using online BLAST (NCBI). The identical peptide sequence matches are marked by letter code, and conservative amino acid changes are shown by a "+" sign between the aligned residues. Places where gaps had to be introduced to achieve the alignment are signified by a "-" in the query or subject sequences.

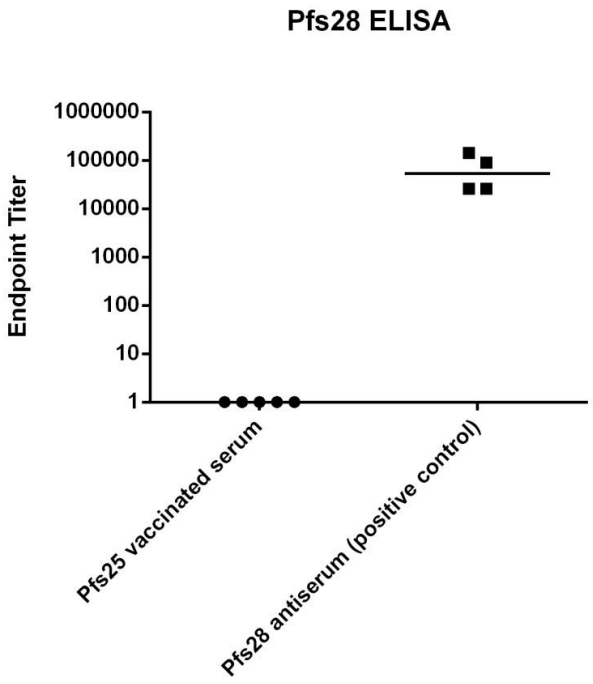

Figure 6.13 Pfs25 antiserum did not show cross-reactivity to Pfs28 protein.

Day 62 serum from mice (n=5) vaccinated with 3 immunisations of 2.5 μg Pfs25 (anti-tag antibody depleted) was tested against Pfs28 in a whole IgG ELISA. Serum from mice (n=4) that received viral vectored vaccine expressing Pfs28 was included as the positive control. Median and individual data points are shown.

6.5 Discussion

In this chapter, I have described the production of Pfs25-based particulate as well as multivalent (bivalent) vaccines. HBsAg and Qβ VLP are both VLP platforms and as an antigen carrier they were demonstrated to be very potent in inducing high titre antibody response in animal and human studies as discussed earlier. HBsAg and Qβ-VLP were selected as carrier matrix for Pfs25 in an attempt to produce TBV candidates to compare to Pfs25-IMX313T, which I had developed during my DPhil and was significantly better at inducing antibody response than monomeric Pfs25. Pfs25-GP-Pfs28 on the other hand, a soluble multivalent protein was designed to induce antibodies against both Pfs25 and Pfs28. Pfs25 and Pfs28 has been previously shown to act synergistically in SMFA.

The production of Pfs25-HBsAg was quite challenging. Firstly, the expression level of Pfs25-HBsAg in *P. pastoris* was lower than R21 both of which were designed as hybrid HBsAg proteins and generated in the same expression system. Comparing the pilot expression western blots, Pfs25-HBsAg expression level was much lower than R21 (data not shown). I tested the expression of a full *P. pastoris* codon optimised Pfs25-HBsAg but this did not improve the expression levels (data not shown). This difference in the expression level seemed to relate to the difference in the two malaria proteins. The second issue with Pfs25-HBsAg production was its VLP formation. For R21 as well as RTS,S, 22 nm VLP could be observed under TEM after CsCl gradient centrifugation. This was not the case for Pfs25-HBsAg; rather than 22 nm, 10 nm sized particles were observed. C-tag affinity purified Pfs25-HBsAgC showed improvement in VLP formation. Several particles of around 20 nm size were seen, however they did not appear to be homogenous (figure 6.6). However C-tag

purification significantly improved the protein purity as the SDS-PAGE and western blot analysis revealed only minor contaminations (figure 6.5C).

The formation of HBsAg VLP in yeast is disulfide bond dependent. The bond forms spontaneously between HBsAg monomers and they oligomerize in the pre-Golgi compartment [269] and eventually assemble into a particle resembling the naturally occurring Australia antigen when released upon cell lysis [288]. Because the disulfide bond is crucial for the VLP formation, if the antigen fused to HBsAg has free cysteine residues, this could disrupt this original HBsAg disulfide bonding, and in theory result in reduced particle integrity or a complete failure in particle formation. Pfs25 sequence used in this study contains 22 cysteines, this clearly is a very high number of cysteines compared to 14 cysteines found in HBsAg sequence and 4 in the CSP antigen. Although we do not know how many free cysteines are there in Pfs25, Pfs25 expressed by *P. pastors* clearly forms dimers and higher oligomers (figure 3.2C) under non-reducing condition suggesting the existence of free cysteines which might interfere with the HBsAg VLP formation. This was thought to be one of the reasons behind the Pfs25-HBsAg VLP's heterogeneity. In one study [289], Pfs25 has been expressed and tested as 4 protein domains (EGF1-EGF4). Serum generated against each individual domain was individually tested for the transmission blocking activity. Only sera from mice primed by EGF2 and boosted by full-length Pfs25 completely blocked the development of oocysts in the SMFA. In addition, depletion of antibodies to EGF2 from the sera of rabbits vaccinated with Pfs25 consistently reversed the ability of those sera to block oocyst development. This study suggested EGF2 domain of Pfs25 contains essential TBV epitopes. This EGF2 domain (Glu-59 to Glu-110) contains only 6 cysteine residues compared to 22 residues in the full length Pfs25 (Ala-22 to Thr-193). As an attempt to improve the

homogeneity of the Pfs25-HBsAg VLP, EGF2-HBsAg as well as the C-tag version (EGF2-HBsAgC) were cloned and transformed into strain 1 *P. pastoris*. The same downstream procedures were used for purification but neither EGF2-HBsAg nor EGF2-HBsAgC constructs showed any improvement in VLP formation (data not shown).

An early study [288] on yeast derived HBsAg VLP assembly revealed the initial HBsAg particle purified by sucrose gradient centrifugation (a similar method of purification as the CsCl gradient centrifugation used in this study) was weakly bonded and dissociation could occur in the presence of 2% sodium dodecyl sulfate (SDS) without reducing agent. Treatment with 3M thiocyanate, which could induce oxidative refolding, matured the particle into a fully disulfide-bonded VLP and the disassociation would only occur in the presence of reducing agent. Further studies [290] confirmed the treatment with thiocyanate together with heat would induce formation of additional intra- and inter-molecular disulfide bonds. Morphological changes including the uniformity and regularity were shown to improve by this maturation. In addition, conformational flexibility was also decreased. It could be that the heterogeneity observed in the Pfs25-HBsAgC VLP was partially due to the fact that the particle was not fully matured; follow on studies would be helpful to determine if this was the case. Furthermore, a novel membrane extraction procedure for purification of HBsAg from yeast was suggested [291]. The method resulted in the highest recovery of VLPs reported in the literature. This membrane extraction method could be of advantageous over mechanical extraction using glass beads and lysis buffer because the latter method often led to a poor protein yield.

As demonstrated in this study, there was no anti-Pfs25 IgGs induced in serum immunised with Pfs25-HBsAgC after prime and boost. There was also no anti-HBsAg IgG in the

immunised serum (data not shown) suggesting that the vaccine, at least at the current dose, was not immunogenic. As mentioned earlier, this version of Pfs25-HBsAgC was not homogeneous in terms of particle sizes and contains some contaminants. A few optimisation studies need to be carried to optimise the VLP formation.

The second VLP platform tested was Qβ VLP. Using a slightly different approach than Pfs25-HBsAg, the Pfs25 was chemically conjugated to Qβ VLP rather than genetically. The work was done in collaboration with Prof. Martin Bachman's group in Switzerland. This conjugation was only performed once and the resulting product was pure and homogenous 30 nm Pfs25-Qβ VLPs. The only drawback in this product was the poor antigen coupling efficiency (~4.6%). Pfs25 and Qβ VLP were first conjugated with SATA and SMPH (Thermo Scientific, UK) crosslinkers respectively. According to the suppliers' instructions, both SATA and SMPH contained N-hydroxysuccinimide (NHS) ester which reacts with the primary amines at pH7-9 to form amide bonds. The second reaction (coupling) happened between the maleimide groups in SMPH and sulfhydryl group in SATA resulting in the coupling of Pfs25-SATA to Qβ VLP-SMPH. The whole reaction in theory should work for every protein molecule and one would not expect a low coupling between Pfs25 and Qβ VLP. It is important to achieve a high coupling efficiency because In Qβ-VLP, local density of antigen, rather than the total amount of antigen was demonstrated to be crucial for high antibody response [283]. 20% and 28% estimated coupling efficiency were achieved when Qβ VLP was conjugated to IL-1α and IL-1β using SMPH crosslinker in previous report [285]. We are now repeating this at the Jenner institute to improve the coupling efficiency. The antibody response could be much higher if an optimum coupling was achieved.

Monomeric Pfs25, Pfs25-IMX313T, Pfs25-GP-Pfs28, Pfs25-HBsAgC and Pfs25-Qβ VLP were compared head-to-head for antibody immunogenicity. The dose was normalised on Pfs25 content. Pfs25-IMX313T out-performed the other constructs and induced significantly higher anti-Pfs25 IgGs than monomeric Pfs25. Surprisingly, Pfs25-GP-Pfs28 was the second most immunogenic construct which also induced high level anti-Pfs28 IgGs. A similar observation that Pfs25-Pfs28 fusion protein produced by *S. cerevisiae* induced higher anti-Pfs25 antibody response than monomeric Pfs25 was made by Kaslow *et al* [160]. The underlying mechanism is not known. Based on previous reports of the synergistic effect from anti-Pfs25 and anti-Pfs28 antibodies in SMFA, this Pfs25-GP-Pfs28 multivalent vaccine could actually confer similar or even better functional TBA and TRA as Pfs25-IMX313T. SMFA studies comparing IgGs induced by these two constructs are now important and need to be performed.

To sum up, based on the immunogenicity data acquired from ELISA, Pfs25-IMX313T, Pfs25-GP-Pfs28 and Pfs25-Qβ VLP are all promising future TBV candidates. Pfs25-HBsAgC on the other hand, though not immunogenic in this study, has room for improvements. A significant finding is that it was possible for the first time, judging by the literature, to show that HBsAg is compatible with Pfs25 and can form some particles.

Chapter 7

Conclusion and Future Directions

7. Conclusion and Future Directions

7.1 Summary

Malaria transmission-blocking vaccines (TBVs) are considered an essential tool to achieve elimination and eventually eradication of malaria. A TBV works by producing neutralising antibodies against antigens expressed during the sexual stages of parasite life cycle. The mosquito ingests these antibodies during a blood meal along with *Plasmodium* gametocytes. These antibodies function inside the mosquito gut by binding to corresponding parasite antigens of gametocytes, gametes, zygotes or ookinetes depending on the antigen of choice and prevent subsequent parasite development. TBV's do not directly protect the vaccinee from getting malaria or malaria related disease symptoms, but prevents the transmission from infected patient to the next human host and confers herd immunity.

Pfs25 is one of the leading TBV candidate antigens, which is expressed on the zygote and ookinete. Extensive studies have been done on this particular antigen in animal models and a limited number of human clinical trials. One issue for vaccines targeting Pfs25 in protein-in-adjuvant formulation is the poor immunogenicity in humans and the requirement for high antibody titres to achieve good transmission blocking activity [153, 154]. Vaccine efforts towards developing a Pfs25-based TBV are focused on increasing the humoral immunogenicity. Work in this thesis describes the production and assessment of different recombinant Pfs25 protein and particle vaccines produced in a *P. patoris* expression system. Nanoparticle/VLP platforms: IMX313, HBsAg, Qβ-VLP and multivalent (bivalent) Pfs25-Pfs28 constructs were generated and compared head-to-head. In general, compared to monomeric Pfs25, increased antibody response was observed when mice were vaccinated with the particulate constructs except for Pfs25-HBsAg which requires further optimisation

of the purification process. Pfs25-IMX313 based nanoparticle induced the highest antibody response with Alhydrogel and the immune response could be increased further by formulation with potent adjuvants. Different vaccination regimes using recombinant viral vectors and protein-in-adjuvant expressing Pfs25-IMX313 were compared and the results demonstrated that the protein-in-adjuvant formulations elicited the highest antibody response. Pfs25-IMX313 nanoparticle induced a strong GC and Tfh cell response post vaccination and was taken up faster *in vitro.* Pfs25-Qβ VLP induced higher anti-Pfs25 antibody responses than monomeric Pfs25, though not significant. Pfs25-Qβ VLP was poorly conjugated in this study with the coupling efficiency at around ~4.6%. A higher coupling efficiency is related to better antibody immunogenicity thus this construct needs some optimisation of the conjugation. Pfs25-GP-Pfs28 also elicited higher, but not significant, Pfs25-specific antibody response than monomeric Pfs25. In addition, this construct also induced anti-Pfs28 antibody response which is known to act synergistically to anti-Pfs25 antibodies in SMFA providing a better transmission blocking activity. Pfs25-IMX313, Pfs25-Qβ VLP as well as Pfs25-GP-Pfs28 are all considered promising TBV candidates worth for future study.

7.2 Conclusions

7.2.1 Pfs25 expressed in *P. pastoris* expression system is immunogenic.

The PichiaPink™ strain (Life Technology, UK) of *P. pastoris* allows direct insertion of Pfs25 DNA sequence just after the α secretory signal in the expression plasmid pPinkα-HC through restriction digestion followed by ligation. This Pfs25 protein was expressed and purified with high purity using a two-step procedure including His-tag purification and SEC. Unlike Pfs25 produced previously for human clinical trial expressed in GS115 (his4) strain of *P. pastoris*,

which produced two Pfs25 conformers each of which contained non-Pfs25 coding amino acids and required additional separation [209], Pfs25 expressed by PichiaPink™ strain 1 was homogenous. In addition, Pfs25 expressed in this study was more immunogenic than Pfs25 produced for human clinical trial and induced higher anti-Pfs25 antibodies. This higher immunogenicity appeared to be intrinsic to the protein itself and not related to the possibility of the presence of adjuvant-like molecules in the vaccine preparation.

7.2.2 Quality and functional activity of the antibodies produced after vaccination with Pfs25-IMX313 nanoparticle

Previous studies on the IMX313 platform were mainly focused on recombinant viral vectored vaccine constructs [224] [225] [191]. Only one study [226] expressed IMX313 as a recombinant protein in *E. coli*, however the protein was expressed intracellularly and required several steps of purification. This study demonstrated for the first time that IMX313 can be expressed as a secreted recombinant protein from *P. pastoris* and it forms a heptamer. Pfs25-IMX313H recombinant protein contained an N-terminus His-tag which can be purified using two-step purification and resulted in vaccine product with very high purity. Comparing to monomeric Pfs25, Pfs25-IMX313H induced significantly more Pfs25-specific IgGs after IM vaccination. IgG purified from mice that received 3 immunisations of Pfs25-IMX313H nanoparticle elicited significantly higher TRA in SMFA than the monomeric Pfs25 group. Higher overall anti-Pfs25 IgG titres and higher antibody avidity is the likely cause of the high TRA and TBA observed. While the IgG1 response was similar, Pfs25-IMX313H induced a significantly higher IgG2a response than monomeric Pfs25. However it is still not clear whether induction of a specific anti-Pfs25 IgG isotype is important for transmission blocking activity. Anti-Pfs25 IgG1 was shown to have a higher avidity than IgG2a in a

previous study using protein-in-adjuvant vaccination [236], suggesting IgG1 to be a preferred isotype in terms of antibody avidity. However Goodman *et al* [147] demonstrated no clear correlation between Pfs25 viral vectored vaccine induced IgG1, IgG2a and TRA or TBA in DFA in mice, suggesting the Pfs25-IgG isotypes might not play as an important role as the total IgG titres or avidity in the antibody mediated parasite inhibition in mosquitoes. Pfs25-IMX313H formulated with LMQ induced significantly higher anti-Pfs25 IgG than formulation with Alhydrogel or MF59. This suggested that more potent adjuvants could further increase the immunogenicity of such Pfs25 nanoparticle vaccines in human. LMQ and other potent adjuvant could be further tested and eventually selected for future TBV application. In addition, LMQ contains the same components (different source of raw materials) as AS01 which is an adjuvant used with RTS,S in human trials, suggesting a possibility of combining Pfs25-IMX313H with RTS,S and AS01 forming a multstage malaria vaccine. Pfs25-IMX313H nanoparticle was also tested using A-M, A-P and P-P vaccination regimes. Previous reports [88, 241] demonstrated A-M and A-P regimes not only induced high levels of T cell responses but also strong antigen-specific B cell responses. A-P was also demonstrated to be more immunogenic in terms of antibody response than P-P-P regime using OVA as a reference antigen [241]. In this study, using Pfs25-IMX313H formulated with Alhydrogel, the P-P vaccination regime was demonstrated to induce the highest antibody response that further encouraged the production of Pfs25 protein vaccine. His-tag less Pfs25-IMX313T was also produced in this study and purified by three-step purification with high purity. Pfs25-IMX313T was as immunogenic as Pfs25-IMX313H in terms of antibody response elicited. Both His-tagged and tag-less Pfs25-IMX313 nanoparticle induced antibody response against IMX313 protein but did not react with human C4BP protein in an ELISA.

7.2.3 Mechanism of higher immunogenicity of Pfs25-IMX313 nanoparticle

Compared to monomeric Pfs25, Pfs25-IMX313H not only induced higher titres of anti-Pfs25 antibodies, but the IgG induced after vaccination also had higher avidity as measured by ELISA. Investigation of the GC response revealed 14 days after vaccination with protein formulated with Alhydrogel, the GC B cell response in the dLNs in mice vaccinated with Pfs25-IMX313H was significantly higher than in mice that received monomeric Pfs25. This difference was confirmed by immunostaining of the sections of the dLNs at day 14. This revealed visible GC structures in Pfs25-IMX313 vaccinated mice but not in the soluble Pfs25 vaccinated mice. The levels of Tfh cells in the dLNs were also compared; Pfs25-IMX313H vaccinated mice showed increased Tfh cell responses whereas Pfs25 group did not induce noticeable Tfh cells. There was also a trend of positive correlation between GC B cells and Tfh cells. Because both GC and Tfh cells are important for B cell affinity maturation and antibody isotype switching [254] [257], Pfs25-IMX313H nanoparticle's ability to stimulate both responses upon vaccination was believed to be the cause of the improved immunogenicity. Interestingly, a faster antigen uptake was observed in Pfs25-IMX313H using an *in vitro* macrophage assay. Faster uptake by APCs could have an in vivo effect that leads to increased antibody titres.

7.2.4 Pfs25-GP-Pfs28 and Pfs25-Qβ VLP were immunogenic

Although not as immunogenic as Pfs25-IMX313T, Pfs25-GP-Pfs28 and Pfs25-Qβ VLPs were successfully produced and shown to induce higher anti-Pfs25 antibodies than monomeric Pfs25. Pfs25-GP-Pfs28 as a multivalent vaccine also induced similar levels of anti-Pfs28 antibodies which is promising as anti-Pfs25 and anti-Pfs28 antibodies were shown to act synergistically to block parasite development in the SMFA [158]. Pfs25-Qβ VLP on the other

hand induced good antibody response with only 4.6% coupling efficiency (~3 or 4 Pfs25 molecules displayed by each conjugated Qβ VLP). The local density of antigen on Qβ VLP, rather than the total amount of antigen, was crucial for high antibody response [283], so the immunogenicity of Pfs25-Qβ VLP could be further improved by optimising the chemical conjugation process.

7.2.5 Pfs25-HBsAg formed VLP but was not immunogenic

RTS,S has been successfully produced using HBsAg as a carrier matrix to display the CSP antigen expressed on the sporozoites. The work in this thesis describes the methods of producing a similar particle by fusion of Pfs25 to HBsAg to form a particulate vaccine. For the first time, Pfs25-HBsAgC was produced as recombinant fusion protein in *P. pastoris* and purified with good purity by a one-step purification using C-tag. Subsequent experiments demonstrated that the fusion protein retained the ability to form some particles. Unfortunately, vaccination with the Pfs25-HBsAgC VLP did not induce immune response against Pfs25 nor to HBsAg. One possible explanation could be that Pfs25 and HBsAg protein lost their native conformation when fused and expressed together. Both Pfs25 and HBsAg are rich in free cysteines with native disulfide bonds, which are important for native protein conformation and this could be disrupted in the fusion construct. In addition, the quality of the Pfs25-HBsAgC VLP in this study was not optimised, the VLP was not homogenous and some contaminants were present, which could also explain the poor immunogenicity.

7.3 Future Directions

7.3.1 Further assessment of the Pfs25-IMX313 nanoparticle

Pfs25-IMX313H was the most promising candidate vaccine in this study in terms of the anti-Pfs25 antibody response induced, which was measured using a standardised ELISA assay and supported by further SMFA test. A tag less version: Pfs25-IMX313T was shown to be as immunogenic as Pfs25-IMX313H by ELISA however functional assays were not conducted. SMFA needs to be conducted to show Pfs25-IMX313T induced IgGs are also functionally similar to the original His-tag version though there is no reason to believe that it will not be so. The SMFA result obtained from mice immunisation is difficult to translate to human application since the amount of antibody required to achieve the same level of inhibition in SMFA was shown to be significantly different across species. Cheru *et al* demonstrated that the IC_{50} of IgG in SMFA purified from mice, rabiits, monkeys and humans that received Pfs25 protein-in-adjuvant vaccines when converted to μg/mL was different (15.9, 4.2, 41.2 and 85.6 μg/mL for mouse, rabbit, monkey and human respectively). This difference among species was significant and was related to the difference in the antibody quality, since different avidity as well as competition patterns against 6 mouse anti-Pfs25 mAbs were observed in these purified IgGs [292]. Therefore, a 100% TRA observed in this study might not mean 100% TRA could be achieved by the same vaccination in other animal models. It will be interesting to test the same vaccine in different animal species and finally in human clinical trial to assess whether the vaccine performs as well in the different species and also if there is a difference in the IC_{50} of the anti-Pfs25 antibodies due to the quality of IgG induced.

TBV alone does not protect the vaccinee from being infected or developing symptoms. Strategies to combine pre-erythrocytic or blood stage vaccines with TBV in one vaccination are very attractive and would offer both protection to individuals and block parasite transmission via mosquitoes. A couple of *P.falciparum* multistage vaccines have been developed and tested in preclinical studies. Theisen *et al* constructed a recombinant protein containing blood stage antigen GLURP fused in frame to TBV antigen Pfs48/45 and expressed in *Lactococcus lactis* [293]. This multivalent vaccine induced antibody responses against both components, and vaccine induced antibodies exhibited both functional activity in the antibody dependent cellular inhibition assay and TBA in SMFA respectively. In a separate study, Kubler-Kielb *et al* cross-linked Pfs25 onto itself and used it as a carrier for NANP repeats (part of CSP antigen) [294]. This conjugated protein was immunogenic and induced antibody response against both antigens. Vaccine induced antibodies exhibited TRA in SMFA and also recognised native CSP antigen displayed on sporozoites. One possible issue with malaria multistage vaccines is antigen competition. Immunisation with the multivalent vaccine sometimes can elicits fewer antibodies than when the components are administered alone [295]. Or in some cases the response to one antigen remains the same while the responses to the others are suppressed [296] [297]. One of the plans for Pfs25-IMX313 vaccine is to test in combination with the leading malaria vaccine: RTS,S in AS01 (collaboration with GSK).

Long term antibody response need to be assessed for Pfs25-IMX313 nanoparticle vaccine and the vaccine induced memory responses also need to be evaluated. The antigen uptake experiment needs to be repeated both *in vitro* and *in vivo*. DCs as professional APCs are a better model than macrophages for analysing antigen uptakes. The THP-1 cell line can be

differentiated into DCs when cultured in serum-free medium containing GM-CSF, TNF-α, and ionomycin [298]. These THP-1 derived DCs can serve as an *in vitro* model for antigen uptake studies. The in vivo experiment could be performed as follows: after the vaccination of AF-488 conjugated antigens, dLNs and spleen can be collected at different time points and DCs can be extracted and analysed by flow cytometry. The *in vivo* antigen uptake experiment is important because it takes into account the effects of the other components of the immune system such as the natural antibodies and the complement system both of which may play a role in assisting the nanoparticle uptake as described in chapter 5 section 5.1.

7.3.2 Optimisation on Pfs25-Qβ and Pfs25-HBsAg VLP production

The Pfs25-Qβ VLP construct was immunogenic even at low antigen coupling efficiency. Future studies should focus on optimising the chemical conjugation between Pfs25 and Qβ VLP. In addition to the SATA-SMPH linker described in this study, other commercially available crosslinkers such as adipic acid dihydrazide (ADH) [169] could be used and compared. Hybrid Qβ VLP carrying genetically fused IgG-binding domain was produced [281] suggesting possibility to generate hybrid Qβ VLP using existing cloning technology other than chemical conjugation. If it works, the vaccine would be more cost-effective and easier to produce because the protein production steps will be reduced.

The Pfs25-HBsAgC purification process needs further optimisation. New membrane extraction methods (which could increase the total protein yield) and thiocyanate treatment (which could promote the maturation of particle) could improve the yield and formation of particles. The aim of such optimisation is to produce immunogenic Pfs25-HBsAgC VLP that is homogeneous and pure. It is also in theory possible to express CS-Pfs25-HBsAgC as a hybrid VLP since both CS and Pfs25 were individually shown to be compatible with HBsAg to form

particles. If CS-Pfs25-HBsAgC can be expressed as an immunogenic VLP, it in theory should offer protection to host as well as inhibition to malaria transmission and will be an ideal malaria multistage vaccine.

7.3.3 Further assessment of Pfs25-GP-Pfs28 vaccine

In this study, Pfs25-GP-Pfs28 was shown to induce both anti-Pfs25 and anti-Pfs28 antibodies. Additionally, the level of antibody responses against both antigens were shown to be at similar level by ELISA, suggesting there is no antigenic competition. IgGs derived from this vaccination together with Pfs25 and Pfs25-IMX313T vaccination need to be tested in the SMFA. To justify the development of Pfs25-GP-Pfs28 vaccine, it needs to be demonstrated that the antibodies are synergistic and having additional anti-Pfs28 antibody generated by this vaccine can result in better parasite inhibition than higher antibodies to Pfs25 (induced by Pfs25-IMX313H nanoparticle. Pfs25-GP-Pfs28 failed to express together with IMX313 carrier protein, however, it is relatively easy to chemically conjugate this soluble protein to Qβ VLP and then assess its immunogenicity using an animal model. From current observations on Pfs25-Qβ VLP, it is believed Pfs25-GP-Pfs28-Qβ VLP will most likely induce more antibodies against both Pfs25 and Pfs28 and as a result, higher inhibition of parasite development in mosquitoes.

7.4 Final Remarks

An effective vaccine for malaria is still urgently needed. For transmission blocking malaria vaccines, the induction of high-titre antibodies is crucial. Work in this thesis focused on one particular TBV candidate antigen: Pfs25 and described the efforts on expression of different Pfs25-based protein/particle constructs. Most of the constructs were immunogenic and induced very high titre antigen-specific antibodies. These results are encouraging, given that

Pfs25 protein vaccine is known to generate functional antibodies in humans but lacks immunogenicity. Some of the constructs described in this thesis have huge potential as candidate TBV vaccines alone and also in combination with RTS,S. We are currently applying for funding to test Pfs25-IMX313 nanoparticle vaccine in a Phase 1 clinical trial in Oxford.

References

1. Henderson, D.A., *The eradication of smallpox – An overview of the past, present, and future.* Vaccine, 2011. **29, Supplement 4**(0): p. D7-D9.
2. John, J., *Role of injectable and oral polio vaccines in polio eradication.* Expert Review of Vaccines, 2009. **8**(1): p. 5-8.
3. Moss, W.J. and D.E. Griffin, *Global measles elimination.* Nat Rev Micro, 2006. **4**(12): p. 900-908.
4. Roper, M.H., J.H. Vandelaer, and F.L. Gasse, *Maternal and neonatal tetanus.* The Lancet, 2007. **370**(9603): p. 1947-1959.
5. Drexler, I., et al., *Modified vaccinia virus ankara for delivery of human tyrosinase as melanoma-associated antigen: Induction of tyrosinase- and melanoma-specific human leukocyte antigen A*0201-restricted cytotoxic T cells in vitro and in vivo.* Cancer Research, 1999. **59**(19): p. 4955-4963.
6. Cherry, J.D., *Pertussis: Challenges Today and for the Future.* PLoS Pathog, 2013. **9**(7): p. e1003418.
7. McAleer, W.J., et al., *Human hepatitis B vaccine from recombinant yeast.* Nature, 1984. **307**(5947): p. 178-180.
8. Medeiros, L.R., et al., *Efficacy of Human Papillomavirus Vaccines: A Systematic Quantitative Review.* International Journal of Gynecological Cancer, 2009. **19**(7): p. 1166-1176 10.1111/IGC.0b013e3181a3d100.
9. Joura, E.A., et al., *Effect of the human papillomavirus (HPV) quadrivalent vaccine in a subgroup of women with cervical and vulvar disease: retrospective pooled analysis of trial data*. Vol. 344. 2012.
10. Draper, S.J. and J.L. Heeney, *Viruses as vaccine vectors for infectious diseases and cancer.* Nat Rev Micro, 2010. **8**(1): p. 62-73.
11. Ferraro, B., et al., *Clinical Applications of DNA Vaccines: Current Progress.* Clinical Infectious Diseases, 2011. **53**(3): p. 296-302.
12. Biron, C.A., et al., *NATURAL KILLER CELLS IN ANTIVIRAL DEFENSE: Function and Regulation by Innate Cytokines.* Annual Review of Immunology, 1999. **17**(1): p. 189-220.
13. Wu, Y., et al., *Human γδ T Cells: A Lymphoid Lineage Cell Capable of Professional Phagocytosis.* The Journal of Immunology, 2009. **183**(9): p. 5622-5629.
14. Girardi, M., *Immunosurveillance and Immunoregulation by [gamma][delta] T Cells.* J Invest Dermatol, 0000. **126**(1): p. 25-31.

15. Sarma, J.V. and P. Ward, *The complement system.* Cell and Tissue Research, 2011. **343**(1): p. 227-235.
16. Akira, S., S. Uematsu, and O. Takeuchi, *Pathogen Recognition and Innate Immunity.* Cell. **124**(4): p. 783-801.
17. Tung, J.W. and L.A. Herzenberg, *Unraveling B-1 progenitors.* Current Opinion in Immunology, 2007. **19**(2): p. 150-155.
18. Pillai, S., A. Cariappa, and S.T. Moran, *MARGINAL ZONE B CELLS.* Annual Review of Immunology, 2005. **23**(1): p. 161-196.
19. Cerutti, A., M. Cols, and I. Puga, *Marginal zone B cells: virtues of innate-like antibody-producing lymphocytes.* Nat Rev Immunol, 2013. **13**(2): p. 118-132.
20. Breitfeld, D., et al., *Follicular B Helper T Cells Express Cxc Chemokine Receptor 5, Localize to B Cell Follicles, and Support Immunoglobulin Production.* The Journal of Experimental Medicine, 2000. **192**(11): p. 1545-1552.
21. van Nierop, K. and C. de Groot, *Human follicular dendritic cells: function, origin and development.* Seminars in Immunology, 2002. **14**(4): p. 251-257.
22. Romagnani, S., *Th1/Th2 cells.* Inflammatory Bowel Diseases, 1999. **5**(4): p. 285-294.
23. Manel, N., D. Unutmaz, and D.R. Littman, *The differentiation of human TH-17 cells requires transforming growth factor-[beta] and induction of the nuclear receptor ROR[gamma]t.* Nat Immunol, 2008. **9**(6): p. 641-649.
24. Dong, C., *TH17 cells in development: an updated view of their molecular identity and genetic programming.* Nat Rev Immunol, 2008. **8**(5): p. 337-348.
25. Muranski, P., et al., *Tumor-specific Th17-polarized cells eradicate large established melanoma*. Vol. 112. 2008. 362-373.
26. Aggarwal, S. and A.L. Gurney, *IL-17: prototype member of an emerging cytokine family.* Journal of Leukocyte Biology, 2002. **71**(1): p. 1-8.
27. Sakaguchi, S., et al., *Regulatory T cells: how do they suppress immune responses?* International Immunology, 2009. **21**(10): p. 1105-1111.
28. Wong, P. and E.G. Pamer, *CD8 T CELL RESPONSES TO INFECTIOUS PATHOGENS.* Annual Review of Immunology, 2003. **21**(1): p. 29-70.
29. *FDA. Complete List of Vaccines Licensed for Immunization and Distribution in the US.* http://www.fda.gov/BiologicsBloodVaccines/Vaccines/ApprovedProducts/UCM093833.
30. BREMAN, J.G., M.S. ALILIO, and A. MILLS, *CONQUERING THE INTOLERABLE BURDEN OF MALARIA: WHAT'S NEW, WHAT'S NEEDED: A SUMMARY.* The American Journal of Tropical Medicine and Hygiene, 2004. **71**(2 suppl): p. 1-15.

31. Sachs, J. and P. Malaney, *The economic and social burden of malaria.* Nature, 2002. **415**(6872): p. 680-685.
32. Weatherall, D.J., et al., *Malaria and the Red Cell.* ASH Education Program Book, 2002. **2002**(1): p. 35-57.
33. Franke-Fayard, B., et al., *Sequestration and Tissue Accumulation of Human Malaria Parasites: Can We Learn Anything from Rodent Models of Malaria?* PLoS Pathog, 2010. **6**(9): p. e1001032.
34. Trampuz, A., et al., *Clinical review: Severe malaria.* Critical Care, 2003. **7**(4): p. 1-9.
35. Doolan, D.L., C. Dobaño, and J.K. Baird, *Acquired Immunity to Malaria.* Clinical Microbiology Reviews, 2009. **22**(1): p. 13-36.
36. Baird, J.K., et al., *Age-Specific Prevalence of Plasmodium falciparum Among Six Populations with Limited Histories of Exposure to Endemic Malaria.* The American Journal of Tropical Medicine and Hygiene, 1993. **49**(6): p. 707-719.
37. Baird, J.K., et al., *Age-Dependent Acquired Protection against Plasmodium Falciparum in People Having Two Years Exposure to Hyperendemic Malaria.* The American Journal of Tropical Medicine and Hygiene, 1991. **45**(1): p. 65-76.
38. Baird, J., et al., *Onset of clinical immunity to Plasmodium falciparum among Javanese migrants to Indonesian Papua.* Ann Trop Med Parasitol, 2003. **97**(6): p. 557-64.
39. Hviid, L., *Naturally acquired immunity to Plasmodium falciparum malaria in Africa.* Acta Tropica, 2005. **95**(3): p. 270-275.
40. Kraemer, S.M. and J.D. Smith, *A family affair: var genes, PfEMP1 binding, and malaria disease.* Current Opinion in Microbiology, 2006. **9**(4): p. 374-380.
41. Fernandez, V., et al., *Small, Clonally Variant Antigens Expressed on the Surface of the Plasmodium falciparum–Infected Erythrocyte Are Encoded by the rif Gene Family and Are the Target of Human Immune Responses.* The Journal of Experimental Medicine, 1999. **190**(10): p. 1393-1404.
42. Kaviratne, M., et al., *Small Variant STEVOR Antigen Is Uniquely Located within Maurer's Clefts in Plasmodium falciparum-Infected Red Blood Cells.* Eukaryotic Cell, 2002. **1**(6): p. 926-935.
43. Udhayakumar, V., et al., *Longitudinal study of natural immune responses to the Plasmodium falciparum apical membrane antigen (AMA-1) in a holoendemic region of malaria in western Kenya: Asembo Bay Cohort Project VIII.* The American Journal of Tropical Medicine and Hygiene, 2001. **65**(2): p. 100-7.

44. Shi, Y.P., et al., *Natural immune response to the C-terminal 19-kilodalton domain of Plasmodium falciparum merozoite surface protein 1.* Infection and Immunity, 1996. **64**(7): p. 2716-23.

45. Baumann, A., et al., *Naturally acquired immune responses to malaria vaccine candidate antigens MSP3 and GLURP in Guahibo and Piaroa indigenous communities of the Venezuelan Amazon.* Malaria Journal, 2012. **11**(1): p. 46.

46. Dodoo, D., et al., *Naturally Acquired Antibodies to the Glutamate-Rich Protein Are Associated with Protection against Plasmodium falciparum Malaria.* Journal of Infectious Diseases, 2000. **181**(3): p. 1202-1205.

47. Plowe, C.V., *The evolution of drug-resistant malaria.* Transactions of the Royal Society of Tropical Medicine and Hygiene, 2009. **103**(1, Supplement): p. S11-S14.

48. Ashley, E.A., et al., *Spread of Artemisinin Resistance in Plasmodium falciparum Malaria.* New England Journal of Medicine, 2014. **371**(5): p. 411-423.

49. The mal, E.R.A.C.G.o.V., *A Research Agenda for Malaria Eradication: Vaccines.* PLoS Med, 2011. **8**(1): p. e1000398.

50. Clyde, D.F., et al., *Immunization of Man against Falciparum and Vivax Malaria by Use of Attenuated Sporozoites.* The American Journal of Tropical Medicine and Hygiene, 1975. **24**(3): p. 397-401.

51. Hoffman, S.L., et al., *Protection of Humans against Malaria by Immunization with Radiation-Attenuated Plasmodium falciparum Sporozoites.* Journal of Infectious Diseases, 2002. **185**(8): p. 1155-1164.

52. Luke, T.C. and S.L. Hoffman, *Rationale and plans for developing a non-replicating, metabolically active, radiation-attenuated Plasmodium falciparum sporozoite vaccine.* Journal of Experimental Biology, 2003. **206**(21): p. 3803-3808.

53. Hoffman, S.L., et al., *Development of a metabolically active, non-replicating sporozoite vaccine to prevent Plasmodium falciparum malaria.* Human Vaccines, 2010. **6**(1): p. 97-106.

54. Epstein, J.E., et al., *Live Attenuated Malaria Vaccine Designed to Protect Through Hepatic CD8+ T Cell Immunity.* Science, 2011. **334**(6055): p. 475-480.

55. Seder, R.A., et al., *Protection Against Malaria by Intravenous Immunization with a Nonreplicating Sporozoite Vaccine.* Science, 2013. **341**(6152): p. 1359-1365.

56. Dame, J., et al., *Structure of the gene encoding the immunodominant surface antigen on the sporozoite of the human malaria parasite Plasmodium falciparum.* Science, 1984. **225**(4662): p. 593-599.

57. Crompton, P.D., S.K. Pierce, and L.H. Miller, *Advances and challenges in malaria vaccine development.* The Journal of Clinical Investigation, 2010. **120**(12): p. 4168-4178.

58. Gordon, D.M., et al., *Safety, Immunogenicity, and Efficacy of a Recombinantly Produced Plasmodium falciparum Circumsporozoite Protein-Hepatitis B Surface Antigen Subunit Vaccine.* Journal of Infectious Diseases, 1995. **171**(6): p. 1576-1585.

59. Stoute, J.A., et al., *A Preliminary Evaluation of a Recombinant Circumsporozoite Protein Vaccine against Plasmodium falciparum Malaria.* New England Journal of Medicine, 1997. **336**(2): p. 86-91.

60. Kester, K.E., et al., *Efficacy of Recombinant Circumsporozoite Protein Vaccine Regimens against Experimental Plasmodium falciparum Malaria.* Journal of Infectious Diseases, 2001. **183**(4): p. 640-647.

61. Kester, K.E., et al., *A phase I/IIa safety, immunogenicity, and efficacy bridging randomized study of a two-dose regimen of liquid and lyophilized formulations of the candidate malaria vaccine RTS,S/AS02A in malaria-naïve adults.* Vaccine, 2007. **25**(29): p. 5359-5366.

62. Kester, K.E., et al., *Phase 2a trial of 0, 1, and 3 month and 0, 7, and 28 day immunization schedules of malaria vaccine RTS,S/AS02 in malaria-naïve adults at the Walter Reed Army Institute of Research.* Vaccine, 2008. **26**(18): p. 2191-2202.

63. Kester, K.E., et al., *Randomized, Double-Blind, Phase 2a Trial of Falciparum Malaria Vaccines RTS,S/AS01B and RTS,S/AS02A in Malaria-Naive Adults: Safety, Efficacy, and Immunologic Associates of Protection.* Journal of Infectious Diseases, 2009. **200**(3): p. 337-346.

64. Bojang, K.A., et al., *Efficacy of RTS,S/AS02 malaria vaccine against Plasmodium falciparum infection in semi-immune adult men in The Gambia: a randomised trial.* The Lancet, 2001. **358**(9297): p. 1927-1934.

65. Polhemus, M.E., et al., *Evaluation of RTS,S/AS02A and RTS,S/AS01B in Adults in a High Malaria Transmission Area.* PLoS ONE, 2009. **4**(7): p. e6465.

66. Alonso, P.L., et al., *Efficacy of the RTS,S/AS02A vaccine against Plasmodium falciparum infection and disease in young African children: randomised controlled trial.* The Lancet. **364**(9443): p. 1411-1420.

67. Alonso, P.L., et al., *Duration of protection with RTS,S/AS02A malaria vaccine in prevention of Plasmodium falciparum disease in Mozambican children: single-blind extended follow-up of a randomised controlled trial.* The Lancet, 2005. **366**(9502): p. 2012-2018.

68. Sacarlal, J., et al., *Long-Term Safety and Efficacy of the RTS,S/AS02A Malaria Vaccine in Mozambican Children.* Journal of Infectious Diseases, 2009. **200**(3): p. 329-336.

69. Bejon, P., et al., *Efficacy of RTS,S/AS01E Vaccine against Malaria in Children 5 to 17 Months of Age.* New England Journal of Medicine, 2008. **359**(24): p. 2521-2532.

70. Guinovart, C., et al., *Insights into Long-Lasting Protection Induced by RTS,S/AS02A Malaria Vaccine: Further Results from a Phase IIb Trial in Mozambican Children.* PLoS ONE, 2009. **4**(4): p. e5165.

71. *First Results of Phase 3 Trial of RTS,S/AS01 Malaria Vaccine in African Children.* New England Journal of Medicine, 2011. **365**(20): p. 1863-1875.

72. *A Phase 3 Trial of RTS,S/AS01 Malaria Vaccine in African Infants.* New England Journal of Medicine, 2012. **367**(24): p. 2284-2295.

73. Reyes-Sandoval, A., et al., *Prime-Boost Immunization with Adenoviral and Modified Vaccinia Virus Ankara Vectors Enhances the Durability and Polyfunctionality of Protective Malaria CD8+ T-Cell Responses.* Infection and Immunity, 2010. **78**(1): p. 145-153.

74. O'Hara, G.A., et al., *Clinical Assessment of a Recombinant Simian Adenovirus ChAd63: A Potent New Vaccine Vector.* Journal of Infectious Diseases, 2012. **205**(5): p. 772-781.

75. Ogwang, C., et al., *Safety and Immunogenicity of Heterologous Prime-Boost Immunisation with <italic>Plasmodium falciparum</italic> Malaria Candidate Vaccines, ChAd63 ME-TRAP and MVA ME-TRAP, in Healthy Gambian and Kenyan Adults.* PLoS ONE, 2013. **8**(3): p. e57726.

76. Cohen, S., I.A. McGregor, and S. Carrington, *Gamma-Globulin and Acquired Immunity to Human Malaria.* Nature, 1961. **192**(4804): p. 733-737.

77. Sabchareon, A., et al., *Parasitologic and Clinical Human Response to Immunoglobulin Administration in Falciparum Malaria.* The American Journal of Tropical Medicine and Hygiene, 1991. **45**(3): p. 297-308.

78. Bouharoun-Tayoun, H., et al., *Antibodies that protect humans against Plasmodium falciparum blood stages do not on their own inhibit parasite growth and invasion in vitro, but act in cooperation with monocytes.* The Journal of Experimental Medicine, 1990. **172**(6): p. 1633-1641.

79. Bull, P.C., et al., *Parasite antigens on the infected red cell surface are targets for naturally acquired immunity to malaria.* Nature Medicine, 1998. **4**(3): p. 358-360.

80. Baruch, D.I., et al., *Plasmodium falciparum erythrocyte membrane protein 1 is a parasitized erythrocyte receptor for adherence to CD36, thrombospondin, and intercellular adhesion molecule 1.* Proceedings of the National Academy of Sciences, 1996. **93**(8): p. 3497-3502.

81. Groux, H. and J. Gysin, *Opsonization as an effector mechanism in human protection against asexual blood stages of Plasmodium falciparum: Functional role of IgG subclasses.* Research in Immunology, 1990. **141**(5): p. 529-542.

82. Celada, A., A. Cruchaud, and L.H. Perrin, *Opsonic activity of human immune serum on in vitro phagocytosis of Plasmodium falciparum infected red blood cells by monocytes.* Clin Exp Immunol, 1982. **47**(9): p. 635-644.

83. Sagara, I., et al., *A randomized controlled phase 2 trial of the blood stage AMA1-C1/Alhydrogel malaria vaccine in children in Mali.* Vaccine, 2009. **27**(23): p. 3090-3098.

84. Ogutu, B.R., et al., *Blood Stage Malaria Vaccine Eliciting High Antigen-Specific Antibody Concentrations Confers No Protection to Young Children in Western Kenya.* PLoS ONE, 2009. **4**(3): p. e4708.

85. Spring, M.D., et al., *Phase 1/2a Study of the Malaria Vaccine Candidate Apical Membrane Antigen-1 (AMA-1) Administered in Adjuvant System AS01B or AS02A.* PLoS ONE, 2009. **4**(4): p. e5254.

86. Thera, M.A., et al., *A Field Trial to Assess a Blood-Stage Malaria Vaccine.* New England Journal of Medicine, 2011. **365**(11): p. 1004-1013.

87. Biswas, S., et al., *Transgene Optimization, Immunogenicity and <italic>In Vitro</italic> Efficacy of Viral Vectored Vaccines Expressing Two Alleles of Plasmodium falciparum AMA1.* PLoS ONE, 2011. **6**(6): p. e20977.

88. Draper, S.J., et al., *Enhancing Blood-Stage Malaria Subunit Vaccine Immunogenicity in Rhesus Macaques by Combining Adenovirus, Poxvirus, and Protein-in-Adjuvant Vaccines.* The Journal of Immunology, 2010. **185**(12): p. 7583-7595.

89. Sheehy, S.H., et al., *Phase Ia Clinical Evaluation of the Plasmodium falciparum Blood-stage Antigen MSP1 in ChAd63 and MVA Vaccine Vectors.* Mol Ther, 2011. **19**(12): p. 2269-2276.

90. Malkin, E., et al., *A Phase 1 trial of PfCP2.9: An AMA1/MSP1 chimeric recombinant protein vaccine for Plasmodium falciparum malaria.* Vaccine, 2008. **26**(52): p. 6864-6873.

91. Takala, S.L. and C.V. Plowe, *Genetic diversity and malaria vaccine design, testing and efficacy: preventing and overcoming 'vaccine resistant malaria'.* Parasite Immunology, 2009. **31**(9): p. 560-573.

92. Saul, A., et al., *Human phase I vaccine trials of 3 recombinant asexual stage malaria antigens with Montanide ISA720 adjuvant.* Vaccine, 1999. **17**(23–24): p. 3145-3159.

93. Genton, B., et al., *A Recombinant Blood-Stage Malaria Vaccine Reduces Plasmodium falciparum Density and Exerts Selective Pressure on Parasite Populations in a Phase 1-2b Trial in Papua New Guinea.* Journal of Infectious Diseases, 2002. **185**(6): p. 820-827.

94. Esen, M., et al., *Safety and immunogenicity of GMZ2 — a MSP3–GLURP fusion protein malaria vaccine candidate.* Vaccine, 2009. **27**(49): p. 6862-6868.

95. Mordmüller, B., et al., *Safety and immunogenicity of the malaria vaccine candidate GMZ2 in malaria-exposed, adult individuals from Lambaréné, Gabon.* Vaccine, 2010. **28**(41): p. 6698-6703.

96. Bélard, S., et al., *A Randomized Controlled Phase Ib Trial of the Malaria Vaccine Candidate GMZ2 in African Children.* PLoS ONE, 2011. **6**(7): p. e22525.

97. Druilhe, P., et al., *A Malaria Vaccine That Elicits in Humans Antibodies Able to Kill <italic>Plasmodium</italic> <italic>falciparum</italic>.* PLoS Med, 2005. **2**(11): p. e344.

98. Sirima, S.B., et al., *Safety and immunogenicity of the Plasmodium falciparum merozoite surface protein-3 long synthethic peptide (MSP3-LSP) malaria vaccine in healthy, semi-immune adult males in Burkina Faso, West Africa.* Vaccine, 2007. **25**(14): p. 2723-2732.

99. Nebie, I., et al., *Humoral and cell-mediated immunity to MSP3 peptides in adults immunized with MSP3 in malaria endemic area, Burkina Faso.* Parasite Immunology, 2009. **31**(8): p. 474-480.

100. Lusingu, J., et al., *Satisfactory safety and immunogenicity of MSP3 malaria vaccine candidate in Tanzanian children aged 12-24 months.* Malaria Journal, 2009. **8**(1): p. 163.

101. Sirima, S.B., et al., *Safety and Immunogenicity of the Malaria Vaccine Candidate MSP3 Long Synthetic Peptide in 12–24 Months-Old Burkinabe Children.* PLoS ONE, 2009. **4**(10): p. e7549.

102. Peek, L.J., et al., *A systematic approach to stabilizing EBA-175 RII-NG for use as a malaria vaccine.* Vaccine, 2006. **24**(31–32): p. 5839-5851.

103. El Sahly, H.M., et al., *Safety and Immunogenicity of a Recombinant Nonglycosylated Erythrocyte Binding Antigen 175 Region II Malaria Vaccine in Healthy Adults Living in an Area Where Malaria Is Not Endemic.* Clinical and Vaccine Immunology, 2010. **17**(10): p. 1552-1559.

104. Williams, A.R., et al., *Enhancing Blockade of <italic>Plasmodium falciparum</italic> Erythrocyte Invasion: Assessing Combinations of Antibodies against PfRH5 and Other Merozoite Antigens.* PLoS Pathog, 2012. **8**(11): p. e1002991.

105. Douglas, A.D., et al., *The blood-stage malaria antigen PfRH5 is susceptible to vaccine-inducible cross-strain neutralizing antibody.* Nat Commun, 2011. **2**: p. 601.

106. O'Brien, K.L., et al., *Efficacy and safety of seven-valent conjugate pneumococcal vaccine in American Indian children: group randomised trial.* The Lancet, 2003. **362**(9381): p. 355-361.

107. Huebner, R.E., et al., *Dose response of CRM197 and tetanus toxoid-conjugated Haemophilus influenzae type b vaccines.* Vaccine, 2004. **23**(6): p. 802-806.

108. Gwadz, R., *Successful immunization against the sexual stages of Plasmodium gallinaceum.* Science, 1976. **193**(4258): p. 1150-1151.

109. Carter, R. and D.H. Chen, *Malaria transmission blocked by immunisation with gametes of the malaria parasite.* Nature, 1976. **263**(5572): p. 57-60.

110. Saul, A., *Mosquito stage, transmission blocking vaccines for malaria.* Current Opinion in Infectious Diseases, 2007. **20**(5): p. 476-481.

111. Carter, R., K.N. Mendis, and D. Roberts, *Spatial targeting of interventions against malaria.* World Health Organization. Bulletin of the World Health Organization, 2000. **78**(12): p. 1401-11.

112. *WHO. Malaria transmission blocking vaccines: an ideal public good.* *http://www.who.int/tdr/publications/tdr-research-publications/malaria-transmission-blocking-vaccines/en/*.

113. Carter, R., *Transmission blocking malaria vaccines.* Vaccine, 2001. **19**(17–19): p. 2309-2314.

114. DA, D.F., et al., *Anti-Pfs25 Human Plasma Reduces Transmission of Diverse Plasmodium falciparum Isolates by Direct Membrane Feeding Assays.* Infection and Immunity, 2013.

115. Smith, D.L., et al., *The entomological inoculation rate and Plasmodium falciparum infection in African children.* Nature, 2005. **438**(7067): p. 492-495.

116. Sattabongkot, J., N. Maneechai, and R. Rosenberg, *Plasmodium vivax: gametocyte infectivity of naturally infected Thai adults.* Parasitology, 1991. **102**(01): p. 27-31.

117. Rosenberg, R., *Malaria: some considerations regarding parasite productivity.* Trends in Parasitology, 2008. **24**(11): p. 487-491.

118. Billingsley, P.F., et al., *Relationship Between Prevalence and Intensity of Plasmodium Falciparum Infection in Natural Populations of Anopheles Mosquitoes.* The American Journal of Tropical Medicine and Hygiene, 1994. **51**(3): p. 260-270.

119. Churcher, T.S., et al., *Measuring the blockade of malaria transmission – An analysis of the Standard Membrane Feeding Assay.* International Journal for Parasitology, 2012. **42**(11): p. 1037-1044.

120. Miura, K., et al., *Qualification of Standard Membrane-Feeding Assay with <italic>Plasmodium falciparum</italic> Malaria and Potential Improvements for Future Assays.* PLoS ONE, 2013. **8**(3): p. e57909.

121. Sinden, R., et al., *The biology of sexual development of Plasmodium: the design and implementation of transmission-blocking strategies.* Malaria Journal, 2012. **11**(1): p. 70.

122. Carter, R., et al., *Immunity to sexual stages of malaria parasites.* Progress in Allergy, 1988. **41**: p. 193-214.

123. Carter, R., et al., *Target antigens in malaria transmission blocking immunity.* Philosophical transactions of the Royal Society of London. Series B: Biological sciences, 1984. **307**(1131): p. 201-213.

124. Kaslow, D.C., *Transmission-blocking immunity against malaria and other vector-borne diseases.* Current Opinion in Immunology, 1993. **5**(4): p. 557-565.

125. Kaslow, D.C., *Transmission-blocking vaccines: Uses and current status of development.* International Journal for Parasitology, 1997. **27**(2): p. 183-189.

126. Dearsly, A.L., R.E. Sinden, and I.A. Self, *Sexual development in malarial parasites: gametocyte production, fertility and infectivity to the mosquito vector.* Parasitology, 1990. **100**(03): p. 359-368.

127. Liu, Y., et al., *The conserved plant sterility gene HAP2 functions after attachment of fusogenic membranes in Chlamydomonas and Plasmodium gametes.* Genes and Development, 2008. **22**(8): p. 1051-1068.

128. Blagborough, A.M. and R.E. Sinden, *Plasmodium berghei HAP2 induces strong malaria transmission-blocking immunity in vivo and in vitro.* Vaccine, 2009. **27**(38): p. 5187-5194.

129. Miura, K., et al., *Functional comparison of Plasmodium falciparum transmission-blocking vaccine candidates by the standard membrane-feeding assay.* Infection and Immunity, 2013.

130. van Dijk, M.R., et al., *A Central Role for P48/45 in Malaria Parasite Male Gamete Fertility.* Cell, 2001. **104**(1): p. 153-164.

131. Eksi, S., et al., *Malaria transmission-blocking antigen, Pfs230, mediates human red blood cell binding to exflagellating male parasites and oocyst production.* Molecular Microbiology, 2006. **61**(4): p. 991-998.

132. Carter, R., et al., *Properties of epitopes of Pfs 48/45, a target of transmission blocking monoclonal antibodies, on gametes of different isolates of Plasmodium falciparum.* Parasite Immunology, 1990. **12**(6): p. 587-603.

133. BOUSEMA, J.T., et al., *RAPID ONSET OF TRANSMISSION-REDUCING ANTIBODIES IN JAVANESE MIGRANTS EXPOSED TO MALARIA IN PAPUA, INDONESIA.* The American Journal of Tropical Medicine and Hygiene, 2006. **74**(3): p. 425-431.

134. Outchkourov, N.S., et al., *Correctly folded Pfs48/45 protein of Plasmodium falciparum elicits malaria transmission-blocking immunity in mice.* Proceedings of the National Academy of Sciences, 2008. **105**(11): p. 4301-4305.

135. Chowdhury, D.R., et al., *A Potent Malaria Transmission Blocking Vaccine Based on Codon Harmonized Full Length <italic>Pfs48/45</italic> Expressed in <italic>Escherichia coli</italic>.* PLoS ONE, 2009. **4**(7): p. e6352.

136. Templeton, T.J., et al., *Adherence of Erythrocytes during Exflagellation of Plasmodium falciparum Microgametes Is Dependent on Erythrocyte Surface Sialic Acid and Glycophorins.* The Journal of Experimental Medicine, 1998. **187**(10): p. 1599-1609.

137. Rener, J., et al., *Target antigens of transmission-blocking immunity on gametes of plasmodium falciparum.* The Journal of Experimental Medicine, 1983. **158**(3): p. 976-981.

138. Williamson, K.C., *Pfs230: from malaria transmission-blocking vaccine candidate toward function.* Parasite Immunology, 2003. **25**(7): p. 351-359.

139. Williamson, K.C., et al., *Recombinant Pfs230, a Plasmodium falciparum gametocyte protein, induces antisera that reduce the infectivity of Plasmodium falciparum to mosquitoes.* Molecular and Biochemical Parasitology, 1995. **75**(1): p. 33-42.

140. Vincent, A.A., et al., *Immunogenicity of malaria transmission-blocking vaccine candidate, y230.CA14 following crosslinking in the presence of tetanus toxoid.* Parasite Immunology, 1999. **21**(11): p. 573-581.

141. Tachibana, M., et al., *N-Terminal Prodomain of Pfs230 Synthesized Using a Cell-Free System Is Sufficient To Induce Complement-Dependent Malaria Transmission-Blocking Activity.* Clinical and Vaccine Immunology, 2011. **18**(8): p. 1343-1350.

142. Farrance, C.E., et al., *A Plant-Produced Pfs230 Vaccine Candidate Blocks Transmission of Plasmodium falciparum.* Clinical and Vaccine Immunology, 2011. **18**(8): p. 1351-1357.

143. Fanning, S.L., et al., *A glycosylphosphatidylinositol anchor signal sequence enhances the immunogenicity of a DNA vaccine encoding Plasmodium falciparum sexual-stage antigen, Pfs230.* Vaccine, 2003. **21**(23): p. 3228-3235.

144. Kaslow, D.C., et al., *A vaccine candidate from the sexual stage of human malaria that contains EGF-like domains.* Nature, 1988. **333**(6168): p. 74-76.

145. Vermeulen, A.N., et al., *Sequential expression of antigens on sexual stages of Plasmodium falciparum accessible to transmission-blocking antibodies in the mosquito.* The Journal of Experimental Medicine, 1985. **162**(5): p. 1460-1476.

146. Stura, E.A., et al., *Crystallization of an intact monoclonal antibody (4B7) against Plasmodium falciparum malaria with peptides from the Pfs25 protein antigen.* Acta Crystallographica Section D, 1994. **50**(4): p. 556-562.

147. Goodman, A.L., et al., *A Viral Vectored Prime-Boost Immunization Regime Targeting the Malaria Pfs25 Antigen Induces Transmission-Blocking Activity.* PLoS ONE, 2011. **6**(12): p. e29428.

148. LeBlanc, R., et al., *Markedly enhanced immunogenicity of a Pfs25 DNA-based malaria transmission-blocking vaccine by in vivo electroporation.* Vaccine, 2008. **26**(2): p. 185-192.

149. Mlambo, G., N. Kumar, and S. Yoshida, *Functional immunogenicity of baculovirus expressing Pfs25, a human malaria transmission-blocking vaccine candidate antigen.* Vaccine, 2010. **28**(43): p. 7025-7029.

150. Farrance, C.E., et al., *Antibodies to plant-produced Plasmodium falciparum sexual stage protein Pfs25 exhibit transmission blocking activity.* Human Vaccines, 2011. **7**(0): p. 191-198.

151. Gregory, J.A., et al., *Algae-Produced Pfs25 Elicits Antibodies That Inhibit Malaria Transmission.* PLoS ONE, 2012. **7**(5): p. e37179.

152. Kumar, R., et al., *Functional evaluation of malaria Pfs25 DNA vaccine by in vivo electroporation in olive baboons.* Vaccine, 2013. **31**(31): p. 3140-3147.

153. Da, D.F., et al., *Anti-Pfs25 Human Plasma Reduces Transmission of Plasmodium falciparum Isolates That Have Diverse Genetic Backgrounds.* Infection and Immunity, 2013. **81**(6): p. 1984-1989.

154. Wu, Y., et al., *Phase 1 Trial of Malaria Transmission Blocking Vaccine Candidates Pfs25 and Pvs25 Formulated with Montanide ISA 51.* PLoS ONE, 2008. **3**(7): p. e2636.

155. Malkin, E.M., et al., *Phase 1 vaccine trial of Pvs25H: a transmission blocking vaccine for Plasmodium vivax malaria.* Vaccine, 2005. **23**(24): p. 3131-3138.

156. Shimp Jr, R.L., et al., *Development of a Pfs25-EPA malaria transmission blocking vaccine as a chemically conjugated nanoparticle.* Vaccine, 2013. **31**(28): p. 2954-2962.

157. Jones, R.M., et al., *A Plant-Produced Pfs25 VLP Malaria Vaccine Candidate Induces Persistent Transmission Blocking Antibodies against <italic>Plasmodium falciparum</italic> in Immunized Mice.* PLoS ONE, 2013. **8**(11): p. e79538.

158. Duffy, P.E. and D.C. Kaslow, *A novel malaria protein, Pfs28, and Pfs25 are genetically linked and synergistic as falciparum malaria transmission-blocking vaccines.* Infection and Immunity, 1997. **65**(3): p. 1109-13.

159. Tomas, A.M., et al., *P25 and P28 proteins of the malaria ookinete surface have multiple and partially redundant functions*. Vol. 20. 2001. 3975-3983.

160. Gozar, M.M.G., V.L. Price, and D.C. Kaslow, *Saccharomyces cerevisiae-Secreted Fusion Proteins Pfs25 and Pfs28 Elicit Potent Plasmodium falciparum Transmission-Blocking Antibodies in Mice.* Infection and Immunity, 1998. **66**(1): p. 59-64.

161. Leo, O., A. Cunningham, and P.L. Stern, *Vaccine immunology.* Perspectives in Vaccinology, 2011. **1**(1): p. 25-59.

162. Garçon, N., G. Leroux-Roels, and W.F. Cheng, *Vaccine adjuvants.* Perspectives in Vaccinology, 2011. **1**(1): p. 89-113.

163. Hem, S.L. and H. HogenEsch, *Relationship between physical and chemical properties of aluminum-containing adjuvants and immunopotentiation.* Expert Review of Vaccines, 2007. **6**(5): p. 685-698.

164. O'Hagan, D.T., et al., *The mechanism of action of MF59 – An innately attractive adjuvant formulation.* Vaccine, 2012. **30**(29): p. 4341-4348.

165. Johansson, H.J., C. Jägersten, and J. Shiloach, *Large scale recovery and purification of periplasmic recombinant protein from E. coli using expanded bed adsorption chromatography followed by new ion exchange media.* Journal of Biotechnology, 1996. **48**(1–2): p. 9-14.

166. Lin, F.Y.C., et al., *The efficacy of a Salmonella typhi Vi conjugate vaccine in two-to-five-year-old children.* New England Journal of Medicine, 2001. **344**(17): p. 1263-1269.

167. Lanh, M.N., et al., *Persistent Efficacy of Vi Conjugate Vaccine against Typhoid Fever in Young Children.* New England Journal of Medicine, 2003. **349**(14): p. 1390-1391.

168. Qian, F., et al., *Conjugating recombinant proteins to Pseudomonas aeruginosa ExoProtein A: A strategy for enhancing immunogenicity of malaria vaccine candidates.* Vaccine, 2007. **25**(20): p. 3923-3933.

169. Kubler-Kielb, J., et al., *Long-lasting and transmission-blocking activity of antibodies to Plasmodium falciparum elicited in mice by protein conjugates of Pfs25.* Proceedings of the National Academy of Sciences, 2007. **104**(1): p. 293-298.

170. Donnelly, J.J., R.R. Deck, and M.A. Liu, *Immunogenicity of a Haemophilus influenzae polysaccharide-Neisseria meningitidis outer membrane protein complex conjugate vaccine.* The Journal of Immunology, 1990. **145**(9): p. 3071-9.

171. Vella, P.P., et al., *Immunogenicity of a New Haemophilus influenzae Type b Conjugate Vaccine (Meningococcal Protein Conjugate) (PedvaxHIBTM).* Pediatrics, 1990. **85**(4): p. 668-675.

172. Fan, J., et al., *Preclinical study of influenza virus A M2 peptide conjugate vaccines in mice, ferrets, and rhesus monkeys.* Vaccine, 2004. **22**(23–24): p. 2993-3003.

173. Wu, Y., et al., *Sustained high-titer antibody responses induced by conjugating a malarial vaccine candidate to outer-membrane protein complex.* Proceedings of the National Academy of Sciences, 2006. **103**(48): p. 18243-18248.

174. Ockenhouse, C.F., et al., *Phase I/IIa Safety, Immunogenicity, and Efficacy Trial of NYVAC-Pf7, a Pox-Vectored, Multiantigen, Multistage Vaccine Candidate for Plasmodium falciparum Malaria.* Journal of Infectious Diseases, 1998. **177**(6): p. 1664-1673.

175. McCurdy, L.H., et al., *Modified Vaccinia Ankara: Potential as an Alternative Smallpox Vaccine.* Clinical Infectious Diseases, 2004. **38**(12): p. 1749-1753.

176. Drexler, I., C. Staib, and G. Sutter, *Modified vaccinia virus Ankara as antigen delivery system: how can we best use its potential?* Current Opinion in Biotechnology, 2004. **15**(6): p. 506-512.

177. McShane, H., et al., *Boosting BCG with MVA85A: the first candidate subunit vaccine for tuberculosis in clinical trials.* Tuberculosis, 2005. **85**(1–2): p. 47-52.

178. McConkey, S.J., et al., *Enhanced T-cell immunogenicity of plasmid DNA vaccines boosted by recombinant modified vaccinia virus Ankara in humans.* Nature Medicine, 2003. **9**(6): p. 729-735.

179. Cosma, A., et al., *Therapeutic vaccination with MVA-HIV-1 nef elicits Nef-specific T-helper cell responses in chronically HIV-1 infected individuals.* Vaccine, 2003. **22**(1): p. 21-29.

180. Tatsis, N. and H.C.J. Ertl, *Adenoviruses as Vaccine Vectors.* Mol Ther, 2004. **10**(4): p. 616-629.

181. Xiang, Z.Q., et al., *A Replication-Defective Human Adenovirus Recombinant Serves as a Highly Efficacious Vaccine Carrier.* Virology, 1996. **219**(1): p. 220-227.

182. Casimiro, D.R., et al., *Comparative Immunogenicity in Rhesus Monkeys of DNA Plasmid, Recombinant Vaccinia Virus, and Replication-Defective Adenovirus Vectors Expressing a Human Immunodeficiency Virus Type 1 gag Gene.* Journal of Virology, 2003. **77**(11): p. 6305-6313.

183. He, Z., et al., *Viral Recombinant Vaccines to the E6 and E7 Antigens of HPV-16.* Virology, 2000. **270**(1): p. 146-161.

184. Sullivan, N.J., et al., *Accelerated vaccination for Ebola virus haemorrhagic fever in non-human primates.* Nature, 2003. **424**(6949): p. 681-684.

185. Letvin, N.L., et al., *Preserved CD4+ Central Memory T Cells and Survival in Vaccinated SIV-Challenged Monkeys.* Science, 2006. **312**(5779): p. 1530-1533.

186. Nwanegbo, E., et al., *Prevalence of Neutralizing Antibodies to Adenoviral Serotypes 5 and 35 in the Adult Populations of The Gambia, South Africa, and the United States.* Clinical and Diagnostic Laboratory Immunology, 2004. **11**(2): p. 351-357.

187. Buchbinder, S.P., et al., *Efficacy assessment of a cell-mediated immunity HIV-1 vaccine (the Step Study): a double-blind, randomised, placebo-controlled, test-of-concept trial.* The Lancet, 2008. **372**(9653): p. 1881-1893.

188. Dudareva, M., et al., *Prevalence of serum neutralizing antibodies against chimpanzee adenovirus 63 and human adenovirus 5 in Kenyan Children, in the context of vaccine vector efficacy.* Vaccine, 2009. **27**(27): p. 3501-3504.

189. Goodman, A.L., et al., *New Candidate Vaccines against Blood-Stage Plasmodium falciparum Malaria: Prime-Boost Immunization Regimens Incorporating Human and Simian Adenoviral Vectors and Poxviral Vectors Expressing an Optimized Antigen Based on Merozoite Surface Protein 1.* Infection and Immunity, 2010. **78**(11): p. 4601-4612.

190. Capone, S., et al., *Immune responses against a liver-stage malaria antigen induced by simian adenoviral vector AdCh63 and MVA prime–boost immunisation in non-human primates.* Vaccine, 2010. **29**(2): p. 256-265.

191. Draper, S.J., et al., *Effective induction of high-titer antibodies by viral vector vaccines.* Nat Med, 2008. **14**(8): p. 819-821.

192. Schwarz, A.F., et al., *CLinical evaluation of a new measles-mumps-rubella trivalent vaccine.* American Journal of Diseases of Children, 1975. **129**(12): p. 1408-1412.

193. Munoz, F.M., et al., *Safety and immunogenicity of tetanus diphtheria and acellular pertussis (tdap) immunization during pregnancy in mothers and infants: A randomized clinical trial.* JAMA, 2014. **311**(17): p. 1760-1769.

194. Singleton, R., et al., *The 13-Valent Pneumococcal Conjugate Vaccine for Invasive Pneumococcal Disease in Alaska Native Children: Results of a Clinical Trial.* The Pediatric Infectious Disease Journal, 2013. **32**(3): p. 257-263 10.1097/INF.0b013e3182748ada.

195. Dakshinamoorthy, G., et al., *Multivalent fusion protein vaccine for lymphatic filariasis.* Vaccine, 2013. **31**(12): p. 1616-1622.

196. Tarcha, E.J., et al., *Multivalent Recombinant Protein Vaccine against Coccidioidomycosis.* Infection and Immunity, 2006. **74**(10): p. 5802-5813.

197. Bachmann, M.F. and G.T. Jennings, *Vaccine delivery: a matter of size, geometry, kinetics and molecular patterns.* Nat Rev Immunol, 2010. **10**(11): p. 787-796.

198. Gerlich, W., *Medical Virology of Hepatitis B: how it began and where we are now.* Virology Journal, 2013. **10**(1): p. 239.

199. Gurramkonda, C., et al., *Purification of hepatitis B surface antigen virus-like particles from recombinant Pichia pastoris and in vivo analysis of their immunogenic properties.* Journal of Chromatography B, 2013. **940**(0): p. 104-111.

200. Suzich, J.A., et al., *Systemic immunization with papillomavirus L1 protein completely prevents the development of viral mucosal papillomas.* Proceedings of the National Academy of Sciences, 1995. **92**(25): p. 11553-11557.

201. Agnandji, S.T., et al., *First results of phase 3 trial of RTS,S/AS01 malaria vaccine in African children.* New England Journal of Medicine, 2011. **365**(20): p. 1863-1875.

202. Fifis, T., et al., *Size-Dependent Immunogenicity: Therapeutic and Protective Properties of Nano-Vaccines against Tumors.* The Journal of Immunology, 2004. **173**(5): p. 3148-3154.

203. Scheerlinck, J.-P.Y., et al., *Systemic immune responses in sheep, induced by a novel nano-bead adjuvant.* Vaccine, 2006. **24**(8): p. 1124-1131.

204. Kaslow, D.C. and J. Shiloach, *Production, Purification and Immunogenicity of a Malaria Transmission-Blocking Vaccine Candidate: TBV25H Expressed in Yeast and Purified Using Nickel-NTA Agarose.* Nat Biotech, 1994. **12**(5): p. 494-499.

205. Miura, K., et al., *Development and characterization of a standardized ELISA including a reference serum on each plate to detect antibodies induced by experimental malaria vaccines.* Vaccine, 2008. **26**(2): p. 193-200.

206. Miura, K., et al., *Transmission-blocking activity induced by malaria vaccine candidates Pfs25/Pvs25 is a direct and predictable function of antibody titer.* Malaria Journal, 2007. **6**(1): p. 107.

207. Kumar, R., E. Angov, and N. Kumar, *Potent malaria transmission blocking antibody responses elicited by Plasmodium falciparum Pfs25 expressed in E.coli after successful protein refolding.* Infection and Immunity, 2014.

208. Kaslow, D.C., et al., *Saccharomyces cerevisiae recombinant Pfs25 adsorbed to alum elicits antibodies that block transmission of Plasmodium falciparum.* Infection and Immunity, 1994. **62**(12): p. 5576-5580.

209. Zou, L., et al., *Expression of malaria transmission-blocking vaccine antigen Pfs25 in Pichia pastoris for use in human clinical trials.* Vaccine, 2003. **21**(15): p. 1650-1657.

210. Tsuboi, T., et al., *Wheat Germ Cell-Free System-Based Production of Malaria Proteins for Discovery of Novel Vaccine Candidates.* Infection and Immunity, 2008. **76**(4): p. 1702-1708.

211. Ammerer, G., et al., *PEP4 gene of Saccharomyces cerevisiae encodes proteinase A, a vacuolar enzyme required for processing of vacuolar precursors.* Molecular and Cellular Biology, 1986. **6**(7): p. 2490-2499.

212. Moehle, C.M., et al., *Protease B of Saccharomyces cerevisiae: Isolation and Regulation of the PRB1 Structural Gene.* Genetics, 1987. **115**(2): p. 255-263.

213. Sinha, J., et al., *Causes of proteolytic degradation of secreted recombinant proteins produced in methylotrophic yeast Pichia pastoris: Case study with recombinant ovine interferon-τ.* Biotechnology and Bioengineering, 2005. **89**(1): p. 102-112.

214. Wu, M., et al., *Disruption of YPS1 and PEP4 genes reduces proteolytic degradation of secreted HSA/PTH in Pichia pastoris GS115.* Journal of Industrial Microbiology & Biotechnology, 2013. **40**(6): p. 589-599.

215. Barr, P.J., et al., *Recombinant Pfs25 protein of Plasmodium falciparum elicits malaria transmission-blocking immunity in experimental animals.* The Journal of Experimental Medicine, 1991. **174**(5): p. 1203-1208.

216. Chant, A., et al., *Attachment of a histidine tag to the minimal zinc finger protein of the Aspergillus nidulans gene regulatory protein AreA causes a conformational change at the DNA-binding site.* Protein Expression and Purification, 2005. **39**(2): p. 152-159.

217. Walter, G., *Production and use of antibodies against synthetic peptides.* Journal of Immunological Methods, 1986. **88**(2): p. 149-161.

218. Khan, F., et al., *Histidine affinity tags affect MSP142 structural stability and immunodominance in mice.* Biotechnology Journal, 2012. **7**(1): p. 133-147.

219. Gupta, S., et al., *Identification of B-cell epitopes in an antigen for inducing specific class of antibodies.* Biology Direct, 2013. **8**(1): p. 27.

220. Watson, D.S., et al., *Antibody Response to Polyhistidine-Tagged Peptide and Protein Antigens Attached to Liposomes via Lipid-Linked Nitrilotriacetic Acid in Mice.* Clinical and Vaccine Immunology, 2011. **18**(2): p. 289-297.

221. Blom, A.M., B.O. Villoutreix, and B. Dahlbäck, *Complement inhibitor C4b-binding protein—friend or foe in the innate immune system?* Molecular Immunology, 2004. **40**(18): p. 1333-1346.

222. Kask, L., et al., *Structural Requirements for the Intracellular Subunit Polymerization of the Complement Inhibitor C4b-Binding Protein†.* Biochemistry, 2002. **41**(30): p. 9349-9357.

223. Dahlbäck, B., C.A. Smith, and H.J. Müller-Eberhard, *Visualization of human C4b-binding protein and its complexes with vitamin K-dependent protein S and complement protein C4b.* Proceedings of the National Academy of Sciences, 1983. **80**(11): p. 3461-3465.

224. Spencer, A.J., et al., *Fusion of the <italic>Mycobacterium tuberculosis</italic> Antigen 85A to an Oligomerization Domain Enhances Its Immunogenicity in Both Mice and Non-Human Primates.* PLoS ONE, 2012. **7**(3): p. e33555.

225. Forbes, E.K., et al., *T Cell Responses Induced by Adenoviral Vectored Vaccines Can Be Adjuvanted by Fusion of Antigen to the Oligomerization Domain of C4b-Binding Protein.* PLoS ONE, 2012. **7**(9): p. e44943.

226. Ogun, S.A., et al., *The Oligomerization Domain of C4-Binding Protein (C4bp) Acts as an Adjuvant, and the Fusion Protein Comprised of the 19-Kilodalton Merozoite Surface Protein 1 Fused with the Murine C4bp Domain Protects Mice against Malaria.* Infection and Immunity, 2008. **76**(8): p. 3817-3823.

227. Ling, L.Y., et al, *Optimization for high-level expression in Pichia pastoris and purification of truncated and full length recombinant SAG2 of Toxoplasma gondii for diagnostic use.* Southeast Asian J Trop Med Public Health, 2010. **41**(3): p. 507-513.

228. Fromm, J.R., et al., *Differences in the Interaction of Heparin with Arginine and Lysine and the Importance of these Basic Amino Acids in the Binding of Heparin to Acidic Fibroblast Growth Factor.* Archives of Biochemistry and Biophysics, 1995. **323**(2): p. 279-287.

229. Schwartz, M., et al., *Affinity and avidity of antibodies to the random polymer (T,G)-A-L and a related ordered synthetic polypeptide.* Immunochemistry, 1978. **15**(7): p. 477-481.

230. Gitlin, A.D., Z. Shulman, and M.C. Nussenzweig, *Clonal selection in the germinal centre by regulated proliferation and hypermutation.* Nature, 2014. **509**(7502): p. 637-640.

231. de Souza, V.A.U.F., et al., *Use of an Immunoglobulin G Avidity Test To Discriminate between Primary and Secondary Dengue Virus Infections.* Journal of Clinical Microbiology, 2004. **42**(4): p. 1782-1784.

232. Hedman, K. and S.A. Rousseau, *Measurement of avidity of specific IgG for verification of recent primary rubella.* Journal of Medical Virology, 1989. **27**(4): p. 288-292.

233. Baccard-Longere, M., et al., *Multicenter Evaluation of a Rapid and Convenient Method for Determination of Cytomegalovirus Immunoglobulin G Avidity.* Clinical and Diagnostic Laboratory Immunology, 2001. **8**(2): p. 429-431.

234. Ward, K.N., et al., *Use of Immunoglobulin G Antibody Avidity for Differentiation of Primary Human Herpesvirus 6 and 7 Infections.* Journal of Clinical Microbiology, 2001. **39**(3): p. 959-963.

235. Alam, M.M., et al., *Study of Avidity of Antigen-Specific Antibody as a Means of Understanding Development of Long-Term Immunological Memory after Vibrio cholerae O1 Infection.* Clinical and Vaccine Immunology, 2013. **20**(1): p. 17-23.

236. Coban, C., et al., *Effect of CpG Oligodeoxynucleotides on the Immunogenicity of Pfs25, a Plasmodium falciparum Transmission-Blocking Vaccine Antigen.* Infection and Immunity, 2004. **72**(1): p. 584-588.

237. Roeffen, W., et al., *Transmission blockade of Plasmodium falciparum malaria by anti-Pfs230-specific antibodies is isotype dependent.* Infection and Immunity, 1995. **63**(2): p. 467-71.

238. Angrisano, F., et al., *Malaria parasite colonisation of the mosquito midgut – Placing the Plasmodium ookinete centre stage.* International Journal for Parasitology, 2012. **42**(6): p. 519-527.

239. Mountford, A.P., A. Fisher, and R.A. Wilson, *The profile of IgG1 and IgG2a antibody responses in mice exposed to Schistosoma mansoni.* Parasite Immunology, 1994. **16**(10): p. 521-527.

240. Chmielewska, A.M., et al., *Combined adenovirus vector and hepatitis C virus envelope protein prime-boost regime elicits T cell and neutralizing antibody immune responses.* Journal of Virology, 2014.

241. de Cassan, S.C., et al., *The Requirement for Potent Adjuvants To Enhance the Immunogenicity and Protective Efficacy of Protein Vaccines Can Be Overcome by Prior Immunization with a Recombinant Adenovirus.* The Journal of Immunology, 2011. **187**(5): p. 2602-2616.

242. Zhao, L., et al., *Nanoparticle vaccines.* Vaccine, 2014. **32**(3): p. 327-337.

243. Figueiredo, L., et al., *Intranasal immunisation of mice against Streptococcus equi using positively charged nanoparticulate carrier systems.* Vaccine, 2012. **30**(46): p. 6551-6558.

244. Shima, F., et al., *Manipulating the antigen-specific immune response by the hydrophobicity of amphiphilic poly(γ-glutamic acid) nanoparticles.* Biomaterials, 2013. **34**(37): p. 9709-9716.

245. Link, A., et al., *Innate Immunity Mediates Follicular Transport of Particulate but Not Soluble Protein Antigen.* The Journal of Immunology, 2012. **188**(8): p. 3724-3733.

246. Aguzzi, A., J. Kranich, and N.J. Krautler, *Follicular dendritic cells: origin, phenotype, and function in health and disease.* Trends in Immunology. **35**(3): p. 105-113.

247. Foged, C., et al., *Particle size and surface charge affect particle uptake by human dendritic cells in an in vitro model.* International Journal of Pharmaceutics, 2005. **298**(2): p. 315-322.

248. Manolova, V., et al., *Nanoparticles target distinct dendritic cell populations according to their size.* European Journal of Immunology, 2008. **38**(5): p. 1404-1413.

249. Dintzis, H.M., R.Z. Dintzis, and B. Vogelstein, *Molecular determinants of immunogenicity: the immunon model of immune response.* Proceedings of the National Academy of Sciences, 1976. **73**(10): p. 3671-3675.

250. Carter, R. and D. Fearon, *CD19: lowering the threshold for antigen receptor stimulation of B lymphocytes.* Science, 1992. **256**(5053): p. 105-107.

251. Cherukuri, A., P.C. Cheng, and S.K. Pierce, *The Role of the CD19/CD21 Complex in B Cell Processing and Presentation of Complement-Tagged Antigens.* The Journal of Immunology, 2001. **167**(1): p. 163-172.

252. Jegerlehner, A., et al., *Regulation of IgG antibody responses by epitope density and CD21-mediated costimulation.* European Journal of Immunology, 2002. **32**(11): p. 3305-3314.

253. Moon, J.J., et al., *Enhancing humoral responses to a malaria antigen with nanoparticle vaccines that expand Tfh cells and promote germinal center induction.* Proceedings of the National Academy of Sciences, 2012. **109**(4): p. 1080-1085.

254. Manser, T., *Textbook Germinal Centers?* The Journal of Immunology, 2004. **172**(6): p. 3369-3375.

255. Crotty, S., *Follicular Helper CD4 T Cells (TFH).* Annual Review of Immunology, 2011. **29**(1): p. 621-663.

256. Shinall, S.M., et al., *Identification of Murine Germinal Center B Cell Subsets Defined by the Expression of Surface Isotypes and Differentiation Antigens.* The Journal of Immunology, 2000. **164**(11): p. 5729-5738.

257. Reinhardt, R.L., H.-E. Liang, and R.M. Locksley, *Cytokine-secreting follicular T cells shape the antibody repertoire.* Nat Immunol, 2009. **10**(4): p. 385-393.

258. Schwende, H., et al., *Differences in the state of differentiation of THP-1 cells induced by phorbol ester and 1,25-dihydroxyvitamin D3.* Journal of Leukocyte Biology, 1996. **59**(4): p. 555-61.

259. Daigneault, M., et al., *The Identification of Markers of Macrophage Differentiation in PMA-Stimulated THP-1 Cells and Monocyte-Derived Macrophages.* PLoS ONE, 2010. **5**(1): p. e8668.

260. Marrack, P., A.S. McKee, and M.W. Munks, *Towards an understanding of the adjuvant action of aluminium.* Nat Rev Immunol, 2009. **9**(4): p. 287-293.

261. Chang, M.-H., *Hepatitis B virus infection.* Seminars in Fetal and Neonatal Medicine. **12**(3): p. 160-167.

262. Bruss, V. and D. Ganem, *The role of envelope proteins in hepatitis B virus assembly.* Proceedings of the National Academy of Sciences, 1991. **88**(3): p. 1059-1063.

263. Krugman, S., J.P. Giles, and J. Hammond, *Viral hepatitis, type b (ms-2 strain): Studies on active immunization.* JAMA, 1971. **217**(1): p. 41-45.

264. PURCELL, R.H. and J.L. GERIN, *Hepatitis B subunit vaccine: a preliminary report of safety and efficacy tests in chimpanzees.* The American Journal of the Medical Sciences, 1975. **270**(2): p. 395-400.

265. Maupas, P., et al., *IMMUNISATION AGAINST HEPATITIS B IN MAN.* The Lancet, 1976. **307**(7974): p. 1367-1370.

266. Szmuness, W., et al., *Hepatitis B Vaccine.* New England Journal of Medicine, 1980. **303**(15): p. 833-841.

267. Valenzuela, P., et al., *Synthesis and assembly of hepatitis B virus surface antigen particles in yeast.* Nature, 1982. **298**(5872): p. 347-350.

268. Poovorawan, Y., et al., *PRotective efficacy of a recombinant dna hepatitis b vaccine in neonates of hbe antigen—positive mothers.* JAMA, 1989. **261**(22): p. 3278-3281.

269. Huovila, A.P., A.M. Eder, and S.D. Fuller, *Hepatitis B surface antigen assembles in a post-ER, pre-Golgi compartment.* The Journal of Cell Biology, 1992. **118**(6): p. 1305-1320.

270. Rutgers, T., et al., *Hepatitis B Surface Antigen as Carrier Matrix for the Repetitive Epitope of the Circumsporozoite Protein of Plasmodium Falciparum.* Nat Biotech, 1988. **6**(9): p. 1065-1070.

271. Vanloubbeeck, Y., et al., *Comparison of the immune responses induced by soluble and particulate Plasmodium vivax circumsporozoite vaccine candidates formulated in AS01 in rhesus macaques.* Vaccine, 2013. **31**(52): p. 6216-6224.

272. Bisht, H., et al., *Expression and Purification of Dengue Virus Type 2 Envelope Protein as a Fusion with Hepatitis B Surface Antigen in Pichia pastoris.* Protein Expression and Purification, 2001. **23**(1): p. 84-96.

273. Bisht, H., et al., *Recombinant dengue virus type 2 envelope/hepatitis B surface antigen hybrid protein expressed in Pichia pastoris can function as a bivalent immunogen.* Journal of Biotechnology, 2002. **99**(2): p. 97-110.

274. Hosokawa, M., et al., *Preparation of purified, sterilized, and stable adenovirus vectors using albumin.* Journal of Virological Methods, 2002. **103**(2): p. 191-199.

275. Liu, R., et al., *Expression, Purification, and Characterization of Hepatitis B Virus Surface Antigens (HBsAg) in Yeast Pichia Pastoris.* Applied Biochemistry and Biotechnology, 2009. **158**(2): p. 432-444.

276. De Genst, E.J., et al., *Structure and Properties of a Complex of α-Synuclein and a Single-Domain Camelid Antibody.* Journal of Molecular Biology, 2010. **402**(2): p. 326-343.

277. Djender, S., et al., *The Biotechnological Applications of Recombinant Single-Domain Antibodies are Optimized by the C-Terminal Fusion to the EPEA Sequence (C Tag).* Antibodies, 2014. **3**(2): p. 182-191.

278. Kashiwagi, A. and T. Yomo, *Ongoing Phenotypic and Genomic Changes in Experimental Coevolution of RNA Bacteriophage Qβ and <italic>Escherichia coli</italic>.* PLoS Genet, 2011. **7**(8): p. e1002188.

279. Kozlovska, T.M., et al., *Recombinant rna phage qβ capsid particles synthesized and self-assembled in escherichia coli.* Gene, 1993. **137**(1): p. 133-137.

280. Jegerlehner, A., et al., *Bacterially Produced Recombinant Influenza Vaccines Based on Virus-Like Particles.* PLoS ONE, 2013. **8**(11): p. e78947.

281. Brown, S.D., J.D. Fiedler, and M.G. Finn, *Assembly of Hybrid Bacteriophage Qβ Virus-like Particles.* Biochemistry, 2009. **48**(47): p. 11155-11157.

282. Freivalds, J., et al., *Assembly of bacteriophage Qβ virus-like particles in yeast Saccharomyces cerevisiae and Pichia pastoris.* Journal of Biotechnology, 2006. **123**(3): p. 297-303.

283. Yin, Z., et al., *Boosting Immunity to Small Tumor-Associated Carbohydrates with Bacteriophage Qβ Capsids.* ACS Chemical Biology, 2013. **8**(6): p. 1253-1262.

284. Cornuz, J., et al., *A Vaccine against Nicotine for Smoking Cessation: A Randomized Controlled Trial.* PLoS ONE, 2008. **3**(6): p. e2547.

285. Spohn, G., et al., *Active immunization with IL-1 displayed on virus-like particles protects from autoimmune arthritis.* European Journal of Immunology, 2008. **38**(3): p. 877-887.

286. Bachmann, M.F. and G.T. Jennings, *Therapeutic vaccines for chronic diseases: successes and technical challenges.* Philosophical Transactions of the Royal Society B: Biological Sciences, 2011. **366**(1579): p. 2815-2822.

287. Qian, F., et al., *Enhanced antibody responses to Plasmodium falciparum Pfs28 induced in mice by conjugation to ExoProtein A of Pseudomonas aeruginosa with an improved procedure.* Microbes and Infection, 2009. **11**(3): p. 408-412.

288. Wampler, D.E., et al., *Multiple Chemical Forms of Hepatitis B Surface Antigen Produced in Yeast.* Proceedings of the National Academy of Sciences of the United States of America, 1985. **82**(20): p. 6830-6834.

289. Stowers, A.W., et al., *A Region of Plasmodium falciparumAntigen Pfs25 That Is the Target of Highly Potent Transmission-Blocking Antibodies.* Infection and Immunity, 2000. **68**(10): p. 5530-5538.

290. Zhao, Q., et al., *Maturation of Recombinant Hepatitis B Virus Surface Antigen Particles.* Human Vaccines, 2006. **2**(4): p. 174-180.

291. Patil, A. and N. Khanna, *Novel membrane extraction procedure for the purification of hepatitis B surface antigen from Pichia pastoris.* Journal of Chromatography B, 2012. **898**(0): p. 7-14.

292. Cheru, L., et al., *The IC50 of anti-Pfs25 antibody in membrane-feeding assay varies among species.* Vaccine, 2010. **28**(27): p. 4423-4429.

293. Theisen, M., et al., *A multi-stage malaria vaccine candidate targeting both transmission and asexual parasite life-cycle stages.* Vaccine, 2014. **32**(22): p. 2623-2630.

294. Kubler-Kielb, J., et al., *A bicomponent Plasmodium falciparum investigational vaccine composed of protein-peptide conjugates.* Proceedings of the National Academy of Sciences, 2010. **107**(3): p. 1172-1177.

295. Hunt, J.D., et al., *Immunological parameters associated with antigenic competition in a multivalent footrot vaccine.* Vaccine, 1995. **13**(17): p. 1649-1657.

296. Daum, R.S., et al., *Magnitude of Interference after Diphtheria-Tetanus Toxoids–Acellular Pertussis/Haemophilus influenzae Type b Capsular Polysaccharide–Tetanus Vaccination Is Related to the Number of Doses Administered.* Journal of Infectious Diseases, 2001. **184**(10): p. 1293-1299.

297. Johansson, B.E. and E.D. Kilbourne, *Dissociation of influenza virus hemagglutinin and neuraminidase eliminates their intravirionic antigenic competition.* Journal of Virology, 1993. **67**(10): p. 5721-5723.

298. Berges, C., et al., *A cell line model for the differentiation of human dendritic cells.* Biochemical and Biophysical Research Communications, 2005. **333**(3): p. 896-907.